Universidade Estadual Paulista
"Júlio de Mesquita Filho"
Programa Interunidades

Doutorado

Engenharia Civil e Ambiental

ENRICO ZACCHEI

AVALIAÇÃO DA DIFUSIVIDADE DE ÍONS CLORETOS EM ESTRUTURAS DE CONCRETO ARMADO CONSIDERANDO FATORES AMBIENTAIS E DECORRENTES DAS AÇÕES EXTERNAS: UMA APLICAÇÃO NA ESTIMATIVA DETERMINÍSTICA E PROBABILÍSTICA DO TEMPO DE INÍCIO DE CORROSÃO

Bauru
2020

ENRICO ZACCHEI

AVALIAÇÃO DA DIFUSIVIDADE DE ÍONS CLORETOS EM ESTRUTURAS DE CONCRETO ARMADO CONSIDERANDO FATORES AMBIENTAIS E DECORRENTES DAS AÇÕES EXTERNAS: UMA APLICAÇÃO NA ESTIMATIVA DETERMINÍSTICA E PROBABILÍSTICA DO TEMPO DE INÍCIO DE CORROSÃO

Tese apresentada como requisito para a obtenção do título de Doutor em Engenharia Civil e Ambiental da Universidade Estadual Paulista (UNESP), Bauru, São Paulo, Brasil.

Orientador: Prof. Dr. Caio Gorla Nogueira

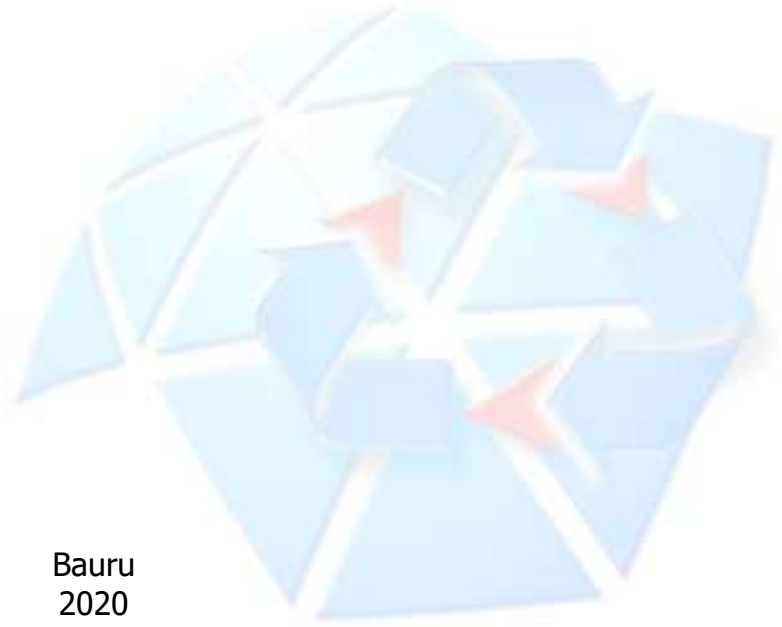

Bauru
2020

UNIVERSIDADE ESTADUAL PAULISTA

Câmpus de Bauru

ATA DA DEFESA PÚBLICA DA TESE DE DOUTORADO DE ENRICO ZACCHEI, DISCENTE DO PROGRAMA DE PÓS-GRADUAÇÃO EM ENGENHARIA CIVIL E AMBIENTAL, DA FACULDADE DE ENGENHARIA - CÂMPUS DE BAURU.

Aos 30 dias do mês de outubro do ano de 2020, às 12:30 horas, por meio de Videoconferência, realizou-se a defesa de TESE DE DOUTORADO de ENRICO ZACCHEI, intitulada **AVALIAÇÃO DA DIFUSIVIDADE DE ÍONS CLORETOS EM ESTRUTURAS DE CONCRETO ARMADO CONSIDERANDO FATORES AMBIENTAIS E DECORRENTES DAS AÇÕES EXTERNAS: UMA APLICAÇÃO NA ESTIMATIVA DETERMINÍSTICA E PROBABILÍSTICA DO TEMPO DE INÍCIO DE CORROSÃO.** A Comissão Examinadora foi constituída pelos seguintes membros: Prof. Dr. CAIO GORLA NOGUEIRA (Orientador(a) - Participação Virtual) do(a) Departamento de Engenharia Civil e Ambiental / Faculdade de Engenharia de Bauru - UNESP, Prof. Dr. EDSON DENNER LEONEL (Participação Virtual) do(a) Departamento de Engenharia de Estruturas / Universidade de São Paulo - USP, Prof. Dr. PAULO CESAR LODI (Participação Virtual) do(a) Departamento de Engenharia Civil e Ambiental / Faculdade de Engenharia de Bauru - UNESP, Professor Adjunto REYOLANDO MANOEL LOPES REBELLO DA FONSECA BRASIL (Participação Virtual) do(a) Depto. de Engenharia de Estruturas e Fundações / ESCOLA POLITÉCNICA DA USP, Prof. Dr. LIBERATO FERRARA (Participação Virtual) do(a) Dipartimento di Ingegneria Civile e Ambientale / Politecnico di Milano (Polimi). Após a exposição pelo doutorando e arguição pelos membros da Comissão Examinadora que participaram do ato, de forma presencial e/ou virtual, o discente recebeu o conceito final:_ _ _ _ _ APROVADO _ _. Nada mais havendo, foi lavrada a presente ata, que após lida e aprovada, foi assinada pelo(a) Presidente(a) da Comissão Examinadora.

Prof. Dr. CAIO GORLA NOGUEIRA

UNIVERSIDADE ESTADUAL PAULISTA
"JÚLIO DE MESQUITA FILHO"
Campus de Bauru

PROPOSTA DE ALTERAÇÃO DO TÍTULO

A COMISSÃO EXAMINADORA PROPÕE A ALTERAÇÃO DO TÍTULO DO TRABALHO DO ALUNO: **ENRICO ZACCHEI**

DE: "AVALIAÇÃO DA DIFUSIVIDADE DE ÍONS CLORETOS EM ESTRUTURAS DE CONCRETO ARMADO CONSIDERANDO FATORES AMBIENTAIS E DECORRENTES DAS AÇÕES EXTERNAS: UMA APLICAÇÃO NA ESTIMATIVA DETERMINÍSTICA E PROBABILÍSTICA DO TEMPO DE INÍCIO DE COROSÃO"

PARA: Não Houve Alteração

Bauru, 30 de outubro de 2020.

Prof. Dr Caio Gorla Nogueira
Orientador

FEB FACULDADE DE ENGENHARIA DE BAURU
Faculdade de Engenharia de Bauru – Pós-graduação
Av. Eng. Luiz Edmundo Coube, 14-01, 17033-360, Bauru - SP
tel. (14) 3103-6108, spg@feb.unesp.br, www.feb.unesp.br

Zacchei, Enrico.
Avaliação da difusividade de íons cloretos em estruturas de concreto armado considerando fatores ambientais e decorrentes das ações externas: Uma aplicação na estimativa determinística e probabilística do tempo de início de corrosão/Enrico Zacchei, 2020
153 f.

Orientador: Caio Gorla Nogueira

Tese (Doutorado)–Universidade Estadual Paulista. Faculdade de Engenharia, Bauru, 2020

1. Difusão não constante. 2. Cloretos. 3. Concreto armado. 4. Confiabilidade. 5. Análise numérica.

Resumo

Esta pesquisa estuda o processo mecânico da difusividade de íons cloretos (Cl^- íons) em estruturas de concreto armado. Quatro objetivos são definidos para obter uma melhor estimativa do coeficiente de difusão (ou difusividade), que é o parâmetro chave para calcular a concentração de íons cloretos no interior de elementos de concreto armado. Foram analisados diferentes fatores que interferem na difusão, bem como na determinação do tempo de início de corrosão. Dois tipos de abordagem foram adotados: uma de tipo determinística e outra de tipo probabilística. Esta última auxilia o processo de tomada de decisão durante a fase de projeto. As análises desenvolvidas são analíticas e numéricas. Foi introduzida uma função que considera a largura da fissuração e uma função genérica que simula as diferentes tendências da difusividade correlacionada à ação de uma carga externa. Os resultados mostram como a difusividade depende fortemente do estado de tensão-deformação do concreto e da presença das fissurações. Estas dependências são geralmente muito pouco exploradas na literatura. Além disso, o conteúdo de íons cloretos, para uma difusividade variável no tempo, assume valores mais baixos do que para uma difusividade constante. Vários cenários foram avaliados para estimar a durabilidade das estruturas, com a obtenção das estatísticas do tempo de início de corrosão para cada um desses cenários. Os resultados fornecem avanços aos trabalhos encontrados na literatura.

Abstract

This research studies the mechanical process of the chloride ions (Cl^- ions) diffusion in reinforced concrete structures. Four goals have been defined to obtain a good estimation of the diffusion coefficient (or diffusivity), which is the key parameter for calculating the concentration of chloride ions in the reinforced concrete elements. Different factors have been analysed that affect the diffusion, as well as the determination of the corrosion initiation. Two approaches have been adopted: deterministic and probabilistic approach. Probabilistic approach assists the decision-making process during the design phase. The analyses have been developed by analytical and numerical form. A function has been introduced to consider the crack width and another generic function has been introduced to simulate the different trends of the diffusivity correlated to the actions of external loads. Results show how the diffusivity strongly depends on the stress-strain state of the concrete and the presence of cracks. These dependencies are generally very little explored in the literature. In addition, the content of chloride ions, for a time-varying diffusivity, assumes lower values than for a constant diffusivity. Several scenarios have been evaluated to estimate the durability of the structures obtaining statistic parameters of the corrosion initiation for each scenario. Results provide advances with respect the papers found in the literature.

Sumário

1 INTRODUÇÃO

1.1 Generalidades

O concreto armado é um material amplamente utilizado em muitas aplicações da Engenharia Civil. Este material está sujeito a diferentes tipos de ações mecânicas, químicas e ambientais que podem afetar seu desempenho em serviço, durabilidade e segurança ao longo do tempo (WATTANAPORNPROM e ISHIDA, 2017; PELLIZZER et al., 2018).

Apesar de vários elementos químicos presentes no ambiente, a penetração de íons cloreto no concreto é o fenômeno que mais contribui diretamente para o início da corrosão das barras de aço das armaduras longitudinais e transversais dos elementos estruturais em concreto armado (MALHEIRO, 2016; WANG et al., 2017; JUNG et al., 2018).

A corrosão das barras de aço gera um estado muito prejudicial na estrutura, pois conduz ao enfraquecimento das propriedades mecânicas dos materiais, incluindo a redução da área da seção transversal das barras de aço, perda de aderência entre as barras de aço e o concreto adjacente, fissurações no cobrimento de concreto e redução da resistência e ductilidade do aço (CAPOZUCCA, 1995). A fissuração no cobrimento do concreto deve-se aos produtos corrosivos expansivos que se forma na interface entre as barras de aço e o concreto adjacente criando fissuras paralelas ao eixo axial da armadura longitudinal (STEWART e MULLARD, 2007). Esse efeito é ainda mais importante em pilares de concreto armado, uma vez que essas fissuras causam a diminuição da seção transversal de concreto, aumentando as tensões de compressão durante a vida útil do pilar. Por outro lado, a redução da seção transversal das barras da armadura longitudinal em pilares, que pode ser considerada como perda de massa de aço propriamente (VAL e STEWART, 2003; ZANG et al, 2010; NEVILLE, 2011), tem um efeito inversamente proporcional na capacidade resistente da armadura de aço. Além disso, essa perda de aço reduz o momento de inércia da armadura longitudinal e, portanto, a

carga crítica de flambagem das barras de aço, afetando o comportamento dinâmico e estático dos pilares e até da edificação. Essa perda da seção transversal das barras de aço pode produzir a ruptura física de uma ou mais barras, interrompendo sua continuidade e prejudicando o processo de transferência de forças ao longo dos elementos (CEB, 1992; BENTZ et al., 1997; KIM et al., 2010; PRINCIGALLO, 2012).

Dentre os principais fatores que afetam o início da corrosão em elementos de concreto armado estão: configurações geométricas dos elementos de concreto, como por exemplo, cobrimento insuficiente; permeabilidade do cobrimento de concreto; quantidade de cloreto na superfície externa dos elementos estruturais e sua variação ao longo do tempo; condições ambientais, como a temperatura e a umidade; o efeito do envelhecimento do concreto e o comportamento estrutural dos elementos de concreto armado que interfere na abertura e propagação de fissuras ao longo das superfícies das peças (BASTIDAS-ARTEAGA et al., 2011; FU et al., 2015).

Com relação à geometria dos elementos estruturais, o cobrimento de concreto atua como uma barreira física para proteger e isolar a armadura de agentes atmosféricos agressivos externos. A quantidade de cloretos nas superfícies das peças depende da sua exposição ao ambiente circundante, em que a penetração dos íons cloreto em direção ao aço da armadura no interior das peças é mais intensa em ambientes marinhos e em áreas costeiras, pois a formação de ciclos úmido/seco favorece o ingresso desses íons no concreto (BEM-FRAJ et al., 2012). Por outro lado, em áreas urbanas e industriais, onde a poluição ambiental tem uma concentração significativa de dióxido de carbono, a corrosão do aço das armaduras pode ser iniciada pela carbonatação (MEIRA et al., 2003).

As condições de temperatura e umidade do ambiente afetam as propriedades de difusão do concreto, excitando os íons cloretos a se moverem para o interior do concreto, bem como dentro das peças. O efeito do envelhecimento do concreto está relacionado ao processo de hidratação do cimento que também depende da proporção entre água e cimento, bem como das adições de outras substâncias como as cinzas volantes (BASTIDAS-ARTEAGA et al., 2011). A abertura e propagação das fissurações ao longo da superfície do concreto, que ocorre e se desenvolve a partir dos estados de tensão atuantes nos elementos estruturais de concreto armado também é um fator importante para criar caminhos preferenciais para a penetração dos íons cloretos para a interface com a armadura (JUNG et al., 2017; FU et al., 2010; ZACCHEI e NOGUEIRA, 2019). Todos esses fatores interferem no comportamento mecânico e na durabilidade dos elementos em concreto armado e devem ser considerados na

fase de projeto para a previsão de tempos de início de corrosão e vida útil dos sistemas estruturais.

Os íons cloreto penetram no concreto por diversos mecanismos de transporte, tais como: difusão iônica, convecção, absorção capilar (NGUYEN et al., 2017). Quando há condições saturadas do concreto, o mecanismo de transporte de íons cloreto pode ser modelado exclusivamente pelo processo de difusão iônica, sendo esse fenômeno, portanto, o mais considerado em análises de penetração de cloretos em elementos de concreto (AL-KUTTI et al., 2014; ALAFOGIANNI et al., 2019).

O processo completo, ou seja, desde a penetração dos íons cloretos no concreto até a fissuração do cobrimento pode ser dividido em quatro etapas: (i) penetração dos íons cloretos pela superfície externa do concreto em contato com o ambiente agressivo; (ii) difusão dos íons cloretos no interior estrutura; (iii) corrosão do aço que começa quando a concentração de cloretos atinge um valor crítico na interface do concreto com a armadura; (iv) fissuração do concreto em virtude dos produtos corrosivos serem expansivos. O período de difusão geralmente pode se estender por muitos anos, sendo um processo muito complexo, pois considera vários efeitos como a capilaridade e a permeabilidade do concreto. No entanto, quando a corrosão se inicia, o tempo de propagação de seus produtos (ferrugem) é significativamente menor comparado ao tempo de início da mesma, danificando o cobrimento de concreto, podendo comprometer a capacidade resistente dos elementos estruturais (EL HASSAN et al., 2010; ABABNEH e SHEBAN, 2011; MUNDRA et al., 2017).

A corrosão do aço das armaduras pode ser observada de duas formas: (i) corrosão localizada em pequenas regiões (pites) ao longo das barras e (ii) uniforme, quando a corrosão ocorre "por igual" ao redor das barras e se estende por um determinado comprimento das barras. Corrosões por cloretos ocorrem pela formação de pites, enquanto a corrosão uniforme é característica de ação da carbonatação (EL HASSAN et al., 2010).

Diante da complexidade de todo o processo de penetração dos íons cloretos no concreto até o início da corrosão, abordagens probabilísticas são recomendadas e mais realistas do que as abordagens puramente determinísticas. Os aspectos ambientais que influenciam no processo, bem como o panorama de fissuração dos elementos estruturais introduzem incertezas que não podem ser ignoradas na tentativa de desenvolver modelos mais robustos de previsão de tempo de início de corrosão (GHODS et al., 2009; NOGUEIRA et al., 2012).

Dentro desse contexto, modelos mais realistas de previsão do tempo de início de corrosão requerem a inclusão de fatores ambientais na quantificação do coeficiente de difusão de cloretos no concreto. Além disso, o processo de penetração de cloretos no concreto ocorre em meio à operação das estruturas, isto é, quando estas estão solicitadas pelas ações em serviço. Isso faz com que, nas peças de concreto armado, os estados de tensão atuantes ao longo de diversos pontos da estrutura tenham um papel importante na formação e propagação de microfissuras nos elementos, criando caminhos preferenciais para a entrada dos agentes corrosivos. Esses aspectos, portanto, afetam significativamente o coeficiente de difusão de cloretos no concreto, sendo necessária sua consideração na quantificação do referido coeficiente para a obtenção de melhores previsões de início da corrosão.

A pesquisa está embasada em três aspectos que foram considerados relevantes para o desenvolvimento de um modelo mais realista para a avaliação do coeficiente de difusão de cloretos no concreto. Após isso, o modelo é utilizado na previsão probabilística do tempo de início de corrosão para diferentes cenários ambientais. Uma breve descrição justificando cada um dos aspectos considerados na quantificação do coeficiente de difusão do concreto é apresenta a seguir.

O primeiro aspecto trata da influência de fatores ambientais e mecânicos que contribuem na composição do coeficiente de difusão de cloretos do concreto, para previsão da concentração de cloretos nos elementos em concreto armado. Dentre os fatores considerados estão: relação água-cimento e capacidade de ligação dos cloretos (fatores relativos ao material); temperatura e idade do concreto (fatores ambientais); estado de tensão-deformação (fator relacionado às ações mecânicas externas). Este último é usualmente desconsiderado na quantificação do coeficiente de difusão do concreto. Comparações entre modelos simples e esse modelo composto pelos diversos fatores apresentados nos níveis de concentração de cloretos em diferentes posições do concreto e para diferentes instantes de tempos são realizadas, para a investigação da magnitude da influência de cada fator na determinação da concentração de cloretos no interior dos elementos de concreto armado (FU et al., 2015).

O segundo aspecto considera também a fissuração na composição do coeficiente de difusão do concreto. Além das ações permanentes atuantes nas estruturas, o processo de ciclos de carregamentos e descarregamentos de ações variáveis é um importante fator que deteriora a estrutura, induzindo a formação e propagação das fissuras. As fissuras criam caminhos preferenciais de migração dos íons cloretos, acelerando o acúmulo de cloretos na superfície das armaduras e, consequentemente, o início da corrosão. Aqui, o estado de tensão-

deformação do concreto é considerado não linear e o fator umidade, como ação ambiental, é adicionado ao modelo. A análise baseia-se em expressões analíticas com valores calibrados de acordo com dados extraídos da literatura (DJERBI et al., 2008; ZHANG et al., 2011; JUNG et al., 2017; YANG et al., 2017).

O terceiro aspecto consiste em considerar na previsão da concentração de cloretos no interior de peças em concreto armado, a influência da flutuação dos íons cloretos, em função das ações externas atuantes nas estruturas. Para isso, o coeficiente de difusão é ponderado por uma função de flutuação que leva em consideração o efeito das ações externos cíclicas no processo de penetração dos íons cloretos dentro do concreto. São realizadas análises 1D (fluxo de cloretos na direção x) e 2D (fluxo de cloretos nas direções x-t e y-t) a partir da solução numérica da equação diferencial que rege o problema (BASTIDAS-ARTEAGA et al., 2011, 2013). Esta abordagem poderia ser pioneira em relação a um estudo que correlaciona cargas externas com as partículas de cloretos.

Em função das muitas incertezas relacionadas às grandezas e parâmetros envolvidos nos três aspectos descritos anteriormente, diversos parâmetros são tratados à luz da Teoria de Probabilidades, uma vez que os fatores como a temperatura, umidade e os carregamentos externos possuem caráter aleatório. A partir das análises probabilísticas, são estimados os tempos de início da corrosão para diferentes cenários, com construção das estatísticas e as curvas de probabilidade acumuladas do tempo de início da corrosão. Esse tipo de informação pode ser útil ainda na fase de projeto das estruturas, pois pode apontar os fatores mais importantes na durabilidade dos sistemas em concreto armado, bem como estimar planos de inspeção para manutenção das construções (SUO e STEWART, 2009; NOGUEIRA et al., 2012).

1.2 Objetivos

O objetivo geral desta pesquisa é desenvolver um modelo para quantificação do coeficiente de difusão de cloretos no concreto considerando fatores relativos ao material, ao ambiente e aos efeitos produzidos pelas ações externas atuantes, para utilização na previsão da concentração de íons cloretos, por meio de difusão, em elementos de concreto armado. Aliado a isso, estratégias analíticas e numéricas são adotadas para a previsão da concentração de cloretos no interior do concreto e, em seguida, combinadas a métodos probabilísticos para

previsão do tempo de início de corrosão em estruturas submetidas a diferentes classes de agressividade.

Em específico, os objetivos pontuais para atingir o objetivo geral são descritos a seguir.

- Composição do coeficiente de difusão de cloretos no concreto considerando a influência das cargas externas, a partir dos estados de tensões e deformações no concreto. A contribuição neste campo consiste em aperfeiçoar e expandir os modelos apresentados na literatura (FU et al., 2015) para diferentes valores de tensão de compressão atuante do concreto e quantificar quanto as ações externas influenciam no processo de difusão dos íons cloretos. Desta forma foi desenvolvido de forma mais completa um fator que pondera o coeficiente de difusão de cloretos no concreto, dado este que geralmente não é considerado no processo de análise da difusão.
- Composição do coeficiente de difusão de cloretos no concreto considerando um modelo não linear relacionado à fissuração do concreto. A contribuição neste campo consiste em introduzir uma nova função que leva em consideração os efeitos das fissurações no coeficiente de difusão do concreto. Isto é realizado a partir da recalibração das relações existentes na literatura (DJERBI et al., 2008; ZHANG et al., 2011; JUNG et al., 2017; YANG et al., 2017).
- Consideração da flutuação do coeficiente de difusão de íons cloretos no interior do concreto induzida pela ação das cargas externas atuantes nos elementos estruturais, a partir de métodos numéricos presentes na literatura (CRANK, 1975), em função das direções x-t e y-t. Esta análise permite quantificar no espaço e no tempo o coeficiente de difusão, e assim a concentração dos íons cloretos, e compará-lo com um coeficiente de difusão constante e unidirecional.
- Aplicação do modelo desenvolvido para quantificação do coeficiente de difusão de cloretos no concreto, com aplicação em uma análise probabilística via Teoria da Confiabilidade Estrutural para determinação de estatísticas relacionadas ao tempo de início de corrosão para diferentes cenários de agressividade.

Como anexo deste texto, são apresentados 3 (três) artigos publicados e 1 (um) artigo submetido referente aos resultados desta pesquisa sendo: um artigo em periódico indexado na *Web of Science* (fator de impacto 4,046); dois artigos apresentados e publicados em conferência internacional; um artigo submetido em periódico indexado na *Web of Science* (fator de impacto 1,515).

1.3 Organização da Tese

Depois de uma introdução que explica as generalidades do fenômeno estudado e um estado da arte que fundamenta os estudos feitos por outros autores, foram listados os quatro objetivos principais que foram alcançados. Os capítulos a seguir descrevem todo o conteúdo desenvolvido nesta pesquisa, sendo organizados da seguinte forma.

No capítulo 2 é apresentado o modelo determinístico mecânico de difusão dos íons cloretos em estruturas de concreto armado e todos os fatores considerados nesta análise que influenciam o processo de difusão.

O capítulo 3 trata do modelo probabilístico utilizado para as análises posteriores de confiabilidade estrutural. Apresenta-se de forma sucinta a "teoria da confiabilidade estrutural" e a formulação do problema para estimar o início da corrosão.

No capítulo 4 são mostrados os dados e as estratégias adotadas tanto para as análises determinísticas, quanto para as análises probabilísticas. Aqui são descritos os tipos de difusividades estudados.

O capítulo 5 traz as análises e os resultados alcançados nesta pesquisa. Os quatro grupos de resultados, mostrados em termos de efeitos na concentração de íons cloretos no concerto armado para possíveis cenários, se referem aos quatro objetivos pré-definidos.

No capítulo 6 resumem-se as conclusões sobre o trabalho. O capítulo 7 refere-se à bibliografia citada neste trabalho, enquanto o capítulo 8 reúne, em um apêndice, as publicações do autor desta tese.

2 MODELAGEM DA DIFFUSÃO DE ÍONS CLORETOS

2.1 Leis de Fick e Aspectos da Concentração de Cloretos no Processo de Difusão

A difusão dos íons cloretos em elementos de concreto armados é descrita segundo as leis de Fick. A relação constitutiva que descreve o fluxo de íons cloretos J em um elemento de concreto saturado depende do gradiente da concentração total de cloretos ∇C. Essa relação é definida como primeira lei de Fick, escrita como segue (CARRARA et al., 2016):

$$J = -D \cdot \nabla C \tag{1}$$

onde: D é o coeficiente de difusão de cloretos no concreto (ou difusividade), podendo ser assumido como um valor constante, i.e. independentemente da posição no interior do concreto e do tempo (modelo simples convencional) ou ainda podendo ser considerado como variável. Quando D é variável, este depende das características do material e das condições de exposição ao redor, que podem variar no tempo (SUN et al., 2012). O coeficiente D pode ser considerado como coeficiente de autodifusão, difusividade livre, difusividade sólida ou difusividade nos poros capilares saturados do concreto (SUN et al., 2012). Este último tipo de difusividade é o usado nas análises deste estudo, em que se assume $D = D_{cl}$.

É importante ressaltar que a Eq. (1) é uma simplificação da equação de Nernst-Plank, que considera o fluxo de difusão J_d e o fluxo de convecção J_c, sendo, portanto, expresso por $J = J_d + J_c = -D \cdot \nabla C + J_c$ (DJERBI et al., 2008; MIEN et al., 2009; ISHIDA et al., 2009; MARRIAGA e CLAISSE, 2011; ISLAM e TOSHIHARU, 2013). Na Eq. (1), o grau de saturação, porosidade, tortuosidade (caminho irregular devido à estrutura complexa de micro-poros) e constrição (presença de obstáculos devido à interação entre os poros e aos

íons) são assumidos unitários. No entanto, é importante notar que o concreto é um meio poroso com estrutura de poros finos com tortuosidade e constrição da estrutura dos poros elevadas, o que torna o fenômeno difícil de ser modelado considerando todos esses aspectos.

A Eq. (1) assume que a principal força motriz responsável pelo processo de difusão é o gradiente de concentração dos íons cloretos, o que significa que todos os outros campos potenciais, tais como campos elétricos e gradientes de potencial químico não são considerados. Derivando a Eq. (1) em relação ao tempo t e considerando as três direções de fluxo (i = x, y, z) sob condições de estado não estacionário, obtém-se a segunda lei de Fick (FU et al., 2015), que assume a forma multidirecional em i e unidirecional em x, conforme:

$$\frac{\partial C}{\partial t} = \nabla \cdot D_{cl,i} \nabla C_i = \frac{\partial}{\partial x}\left(D_{cl,x}\frac{\partial C}{\partial x}\right) + \frac{\partial}{\partial y}\left(D_{cl,y}\frac{\partial C}{\partial y}\right) + \frac{\partial}{\partial z}\left(D_{cl,z}\frac{\partial C}{\partial z}\right) \rightarrow \frac{\partial C}{\partial t} = \frac{\partial}{\partial x}\left(D_{cl,x}\frac{\partial C}{\partial x}\right) \quad (2a)$$

As condições iniciais (i.c.) e condições de contorno (b.c.) podem ser dadas por (SUN et al., 2012; FAN e WANG, 2015):

$$\begin{aligned} &\text{i.c.:} \quad C(i,0) = C_0 \\ &\text{b.c.:} \quad C(0,t_m) = C_s \\ &\qquad\quad C(\infty,t_m) = C_0 \end{aligned} \quad (2b)$$

onde: t_m é um tempo imposto em que se deseja conhecer a concentração de cloretos no interior do elemento; C_0 é a concentração inicial interna no concreto de cloretos; C_s é a concentração dos cloretos na superfície externa do concreto.

A concentração total de cloretos pode ser dividida em duas partes: concentração livre C_f (dissolvida em solução nos poros) e concentração quimicamente ligada C_b na reação dos produtos de hidratação do cimento. Essas concentrações são relacionadas com a concentração total através da seguinte equação (SUN et al., 2012; FU et al., 2010):

$$C = \omega_e C_f + C_b \quad (3)$$

onde: ω_e é o conteúdo de água evaporável determinado a partir do modelo de grau de hidratação (maturação por envelhecimento) (FAN e WANG, 2015). O termo ω_e representa uma parte do conteúdo total de água ω; a outra parte é definida por ω_n que é o conteúdo de água não evaporável. Portanto, o conteúdo total de água nos poros pode ser escrito como: $\omega = \omega_e + \omega_n$. O efeito de compactação dos poros desempenha um papel importante no processo da penetração dos cloretos no concreto, conduzindo a uma redução na difusão desses íons.

A concentração quimicamente ligada C_b depende de muitos fatores, e.g. tipo de cimento, composição dos poros, temperatura, reação com o cimento hidratado e absorção (HALAMICKOVA et al, 1995). As correlações entre íons cloretos livres e quimicamente ligados, para uma determinada temperatura, são conhecidas como curvas isotérmicas de Langmuir (KONG et al., 2002). Essas curvas são não lineares e consideram os efeitos de ligação dos cloretos com os parâmetros relacionados às propriedades do concreto. A relação entre cloretos livres e quimicamente ligados pode ser dada conforme (FU et al., 2010; CHEN et al., 2013):

$$C_b = \frac{\alpha C_f}{1+\beta C_f} \tag{4}$$

Os parâmetros α e β podem ser adotados como $\alpha = 11{,}8$ e $\beta = 4{,}0$ (FU et al., 2010; CHEN et al., 2013). Com base na Eq. (3), é possível notar que, se os efeitos de ligação dos cloretos C_b forem considerados, a concentração de cloretos é igual ao conteúdo completo de cloretos (livre + ligado) (ou seja, se $C_b \neq 0 \rightarrow C = \omega_e C_f + C_b$), enquanto que se forem desprezados, a concentração de cloretos é igual apenas à concentração de cloreto livre, i.e., $C_b = 0 \rightarrow C = \omega_e C_f$.

As correlações entre íons cloretos livres e quimicamente ligados conduzem a um processo de difusão complexo. Caso essas correlações sejam consideradas, o sistema descrito pela Eq. (3) deve ser estendido, adicionando os termos de ligação química e resolvendo um sistema acoplado.

É importante enfatizar que em este trabalho apenas o processo de difusão mecânica dos íons cloretos foi estudado. No entanto uma pequena porcentagem de íons cloretos quimicamente ligados que, portanto, não participa ao processo de difusão mecânico é quantificado na Eq. (4) quanto na Eq. (6). Isso porque é noto que os íons cloretos ligam com as outras partículas

presentes no elemento de concreto, portanto é coerente considerá-la, mas o processo de ligação químico não é objeto deste estudo.

Em virtude dessas complexidades, a Eq. (2) somente pode ser resolvida de forma analítica sob as seguintes hipóteses (GUIMARÃES e HELENE, 2009): (i) a estrutura de concreto é um meio semi-infinito; (ii) o meio semi-infinito é homogêneo; (iii) C_s é uniforme e constante ao longo do tempo; (iv) a superfície externa do elemento de concreto é plana; (v) a difusão ocorre segundo fluxo unidimensional; (vi) os íons de cloretos são transportados em um meio saturado apenas por difusão e não reagem com outros íons; (vii) a composição química das substâncias porosas do concreto é considerada em equilíbrio ao longo do processo de difusão, sendo isso admitido porque o coeficiente de difusão de cloretos no concreto é pequeno, com ordem de grandeza de 10^{-12} a 10^{-11} m^2/ s.

Portanto, respeitando as condições descritas anteriormente, a solução analítica da Eq. (2) é dada por:

$$C = C_0 + (C_s - C_0)\left(1 - \mathrm{erf}\frac{x}{2\sqrt{D_{cl}t}}\right) \tag{5}$$

onde: 1 – erf (·) descreve a evolução da difusão de íons cloretos no tempo t e na posição x; erf (·) é a função de erro Gaussiana integrada entre 0 e x / $2\sqrt{(D_{cl}\ t)}$.

A Figura 1 mostra o esquema da difusão em um elemento de concreto com geometria regular com as condições iniciais e de contorno descritas na Eq. (2b).

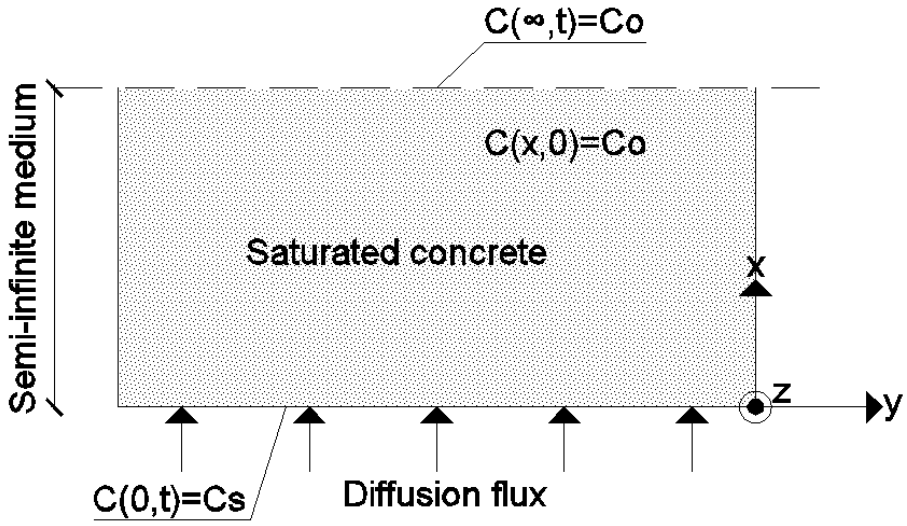

Figura 1 – Meio semi-infinito com fluxo de íons cloretos na direção x (AutoCAD, 2010) [1].

2.2 O Coeficiente de Difusão

O coeficiente de difusão D_{cl} não constante ao longo do tempo pode ser expresso pela seguinte equação modificada denominada modelo multifatorial (FU et al., 2015):

$$D_{cl} = f_{wc} \times f_1(C_b) \times f_2(T) \times f_3(t) \times F(\varepsilon_c, d) \quad (6)$$

onde: $f_{wc} = 10^{(-12{,}06+2{,}4[w/c])}$ é o valor base para a determinação do coeficiente de difusão de cloretos no concreto e depende somente do fator água-cimento w/c. Esse fator é semelhante aos modelos de mesma natureza presentes na literatura (BENTZ et al., 1996; PAPADAKIS et al., 1996), i.e. que dependem somente do fator água-cimento para a avaliação do coeficiente de difusão de cloretos no concreto. Os outros fatores, descritos a seguir, dependem da capacidade de ligação dos cloretos (f_1), da temperatura (f_2), da idade do concreto (f_3) e do estado tensão-deformação (F).

Como já explicado anteriormente o fator f_1 leva em conta os íons cloretos que interagem com as outras partículas presentes no concreto. Em este sentido, este fator corrige a

[1] Algumas figuras estão com a escrita em inglês em consonância ao programa utilizado.

difusividade D_{cl} reduzindo-o de certo valor para não considera os íons cloretos que não participam ao processo de difusão mecânica.

2.2.1 Fatores Ambientais

O fator que considera os efeitos de ligação dos íons cloretos (f_l) é definido pelas isotermas de Langmuir não lineares (KONG et al., 2002; FUN et al., 2010; CHEN et al., 2013) segundo:

$$f_1(C_b) = \left(1 + \frac{\alpha}{\omega_e[1+\beta C_f]^2}\right)^{-1} \tag{7}$$

Conforme já mencionado na Eq. (4), os íons cloretos livres (C_f) transportados pelo conteúdo de água evaporável nos poros do concreto é que são considerados nas análises.

O fator que considera a influência da temperatura é expresso pela lei de Arrhenius (KONG, et al., 2002; FU et al., 2010; DAMRONGWIRIYANUPAP et al., 2015; FU et al., 2015) sendo dado por:

$$f_2(T) = e^{\left[\frac{E_a}{R}\left(\frac{1}{T_0}-\frac{1}{T}\right)\right]} \tag{8}$$

onde: T_0 e T são as temperaturas de referência e a atuante (valor de entrada para a análise), respectivamente; E_a é a energia de ativação do processo de difusão, que depende do tipo de cimento e do fator água-cimento w/c; R é a constante universal dos gases que é correlacionada pelo potencial químico de íons cloretos, concentração molar e temperatura (ZOFIA e ADAM, 2013).

A difusividade de cloretos no concreto também é afetada pelo efeito do envelhecimento do concreto e a sua contribuição pode ser expressa conforme (FU et al., 2010; FU et al., 2015):

$$f_3(t) = \begin{cases} \frac{1}{1-m}\left(\frac{t_{ref}}{t}\right)^m & \text{in case of } t < t_r \\ \left[1 + \frac{t_r}{t}\left(\frac{m}{1-m}\right)\right]\left(\frac{t_{ref}}{t}\right)^m & \text{in case of } t \geq t_t \end{cases} \quad (9)$$

onde: t_{ref} é a idade de referência; t_r é o tempo em que a difusividade é considerada constante; t é o tempo de entrada na análise dado em anos e considerado como o tempo de exposição do elemento estrutural aos agentes externos. O índice m é usado para considerar a velocidade de redução da difusividade dos íons cloretos e depende de adições ao cimento, tais como cinzas volantes e escórias de alto forno (KIM et al., 2014).

2.2.2 Fator Relacionado à Influência do Estado de Tensão-Deformação

Conforme o trabalho publicado na literatura (FU et al., 2015) outro fator para a avaliação do coeficiente de difusão de cloretos no concreto, chamado de F, relacionado ao efeito produzido por um carregamento externo que atua nos elementos de concreto armado foi introduzido.

A ideia deste fator é de considerar a influência do carregamento através de duas parcelas. Desta forma será possível considerar a contribuição dos carregamentos no processo de difusão dos íons cloretos, aspecto este que sempre desprezado nesses tipos de análise.

A primeira parcela refere-se às deformações que se formam nos elementos de concreto armado durante a ação de um carregamento externo; a segunda parcela refere-se às micro fissurações ou danos que se criam nos elementos de concreto armado durante a ação de excessivos carregamentos externos.

Estas duas parcelas são consideradas dependentes: uma da deformação do concreto ε_c e outra do dano d. Portanto, o fator F pode ser descrito como $F = F(\varepsilon_c) + F(d) = F(\varepsilon_c, d)$. Desta forma, as duas parcelas podem ser descritas por um único fator $F(\varepsilon_c,d)$.

Considerando a expansão da série de Taylor e adotando como condições iniciais deformação nula e nenhum dano, i.e. $\varepsilon_c = 0$ e $d = 0$, F pode ser definido pela expressão seguinte:

$$F(\varepsilon_c, d) = F(0,0) + \frac{\partial F}{\partial \varepsilon_c}|_{(0,0)}\varepsilon_c + \frac{\partial F}{\partial d}|_{(0,0)}d + R_1(\varepsilon_c, d) \quad (10)$$

As derivadas representam as somatórias da série de Taylor de ε_c e d no contínuo, enquanto $R_1(\varepsilon_c,d)$ é o resto de Lagrange, em que θ varia entre 0 e 1. Assim, tem-se:

$$R_1(\varepsilon_c, d) = \frac{1}{2}\left(\varepsilon_c \frac{\partial}{\partial \varepsilon_c} + d\frac{\partial}{\partial d}\right)^2 F(\theta\varepsilon_c, \theta d) \quad (11)$$

Assumindo o primeiro, segundo e terceiro termos no lado direito da Eq. (10) como: $F(0,0) = A$; $\frac{\partial F}{\partial \varepsilon_c}|_{(0,0)} = B$ e $\frac{\partial F}{\partial d}|_{(0,0)} = C$, respectivamente, para as condições $\varepsilon_c = 0$ e d = 0, o primeiro termo A é igual a 1,0. Assim, a Eq. (10) pode ser reescrita como:

$$F(\varepsilon_c, d) = 1 + B\varepsilon_c + Cd + R_1(\varepsilon_c, d) \quad (12)$$

O fator de influência do dano f(d) que descreve o dano local no concreto pode ser descrito como (GERARD et al., 1998):

$$f(d) = 1 + \frac{D_{max}}{D_0} - \frac{D_{max}}{D_0}\left[1 + \left(\frac{d}{d_{cr}}\right)^n\right]^{-1} \quad (13)$$

onde: D_0 e D_{max} são, respectivamente, as difusividades do cloreto no concreto sólido e no concreto completamente danificado; n = 5,0 e d_{cr} = 0,4 são dois coeficientes constantes.

Finalmente, multiplicando o segundo termo da Eq. (13) por 1 + ($B_1 \times \varepsilon_c$) + ($C_1 \times d$), o fator $F(\varepsilon_c, d)$ pode ser expresso por:

$$F(\varepsilon_c, d) = 1 + \frac{D_{max}}{D_0} B_1 \varepsilon_c + \frac{D_{max}}{D_0}\left\{1 + C_1 d - \left[1 + \left(\frac{d}{d_{cr}}\right)^n\right]^{-1}\right\} \quad (14)$$

onde: $B_1 = (B \times D_0)/D_{max}$; $B = (D_{max}/D_0 - 1)/\varepsilon_{c1}$ e ε_{c1} corresponde à deformação na tensão de pico do concreto. O coeficiente C_1 será definido posteriormente. O coeficiente B é válido no estado elástico quando nenhum dano é verificado seja para cargas de tração e compressão, sendo dependente das características do material (por exemplo, relação água-cimento w/c).

Existem quatro casos relacionados à Eq. (14):

- d = 0 e $\varepsilon_c \neq 0$, quando não há danos permanentes no concreto, mas a difusividade do concreto muda em função das cargas elásticas e das deformações no esqueleto sólido;

- $\varepsilon_c = 0$ e $d \neq 0$, quando o dano ocorreu no concreto sem considerar a ação de cargas externas (por exemplo dano por variações tensionais internas tipo temperatura);
- $\varepsilon_c = 0$ e $d = 0$, quando não tem efeito de carregamento e qualquer danificação;
- $\varepsilon_c \neq 0$ e $d \neq 0$, quando o concreto é danificado sob ação de cargas externas.

Quando d = 1,0, a deformação do concreto atinge o valor final ε_{c1} e, nesse caso, o concreto é completamente danificado. Nesta condição, a Eq. (14) passa a ser definida por:

$$F(\varepsilon_{c1}, 1) = 1 + B\varepsilon_{c1} + \frac{D_{max}}{D_0}\left\{1 + C_1 - \left[1 + \left(\frac{1}{d_{cr}}\right)^n\right]^{-1}\right\} \quad (15)$$

Considerando $F(\varepsilon_{c1}, 1) = f(1)$, o coeficiente C_1 mostrado na Eq. (14) pode ser definido por:

$$C_1 = -\frac{BD_0}{D_{max}}\varepsilon_{c1} \quad (16)$$

Assim, nas análises deste trabalho, a equação que será usada apara calcular este fator F é a Eq. (14).

2.2.3 Fator Relacionado à Umidade

Com o objetivo de introduzir a influência da umidade, o coeficiente de difusão de cloretos no concreto será descrito através de outra relação. Esta relação, também não constante no tempo, considera alguns fatores já descritos anteriormente, bem como outros novos. Dessa forma, a Eq. (6) é redefinida conforme (BASTIDAS-ARTEAGA et al., 2011):

$$D_{cl} = f_{wc} \times f_2(T) \times f_3(t) \times f_4(h) \quad (17)$$

onde: o fator f_{wc} foi calculado (ver parâmetro da Eq. (6)), assumindo o valor de f_{wc} = 4,30 cm^2/ano.

No entanto, foi mostrado que esse fator é calculado através de uma relação muito simplificada, portanto é possível também adotar *a priori* um valor que pode ser muito diferente do valor calculado (ZACCHEI e NOGUEIRA, 2019(a)).

Isso significa que este fator, do qual fornece a dimensão física, pode ser bastante significativo na quantificação final de D_{cl}, mas é sujeitos a variações: o uso de uma difusividade multifatorial (ver Eq. (6) e Eq. (17)), que corrige o valor final de D_{cl} através de vários fatores, contribui a melhorar estas variações.

O novo fator introduzido é f_4 (h), função da umidade h, definido como (BASTIDAS-ARTEAGA, 2011; KIM et al., 2014; DAMRONGWIRIYANUPAP et al., 2015):

$$f_4(h) = \frac{1}{\left[1+\frac{(1-h)^n}{\left(1-h_{D_{cl}}\right)^n}\right]} \tag{18}$$

onde: h_{Dcl} é a umidade na qual D_{cl} alcança um valor médio entre seus valores máximo e mínimo calibrados através de vários estudos; adota-se igual a 0,75 para temperatura de 21,0 a 25 °C (BAŽANT e NAJJAR, 1972). O parâmetro n pode ser assumido como n = 4 (BASTIDAS-ARTEAGA, 2011; KIM et al., 2014; DAMRONGWIRIYANUPAP et al., 2015) ou $6 \leq n \leq 16$ (BAŽANT e NAJJAR, 1972).

A Figura 2 mostra algumas curvas de f_4 com diferentes valores de n. É possível notar que f_4 e, portanto, D_{cl} dependem fortemente da umidade *h*. Por exemplo, para T = 50 °C, h = 0, n = 4 e h_{Dcl} = 0,75, o fator de umidade é f_4 (h) = $3{,}89\times10^{-3}$ (BAŽANT e NAJJAR, 1972).

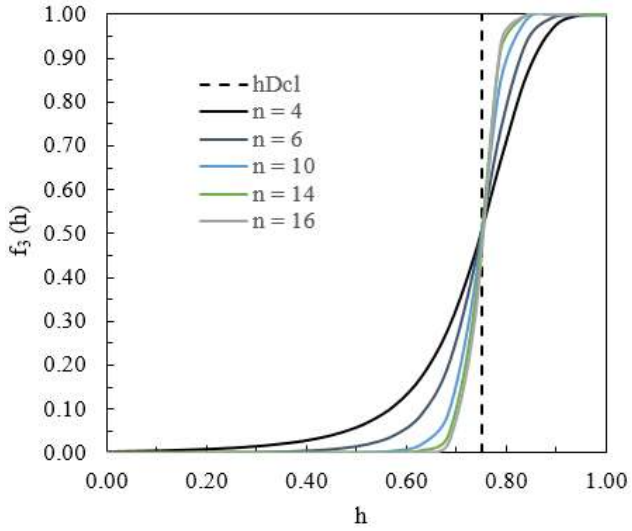

Figura 2 – Distribuição do fator $f_4(h)$[2].

2.2.4 Fator Relacionado à Fissuração do Concreto

A difusão dos íons cloretos, além de se propagar no concreto íntegro ($D = D_{cl}$), se propaga também muito mais facilmente no concreto fissurado. Nesse caso, o coeficiente de difusão D deve ser substituído por D_w. A consideração da formação de fissuras confere ao estudo um caráter altamente não linear que não será tratado com todo o rigor neste trabalho. Por simplicidade, admite-se que o processo de difusão de cloretos no concreto seja governado apenas pelo parâmetro w, que representa a largura das fissuras. Portanto, a expressão simplificada proposta para definir o novo D pode ser descrita como:

$$D_w = f(w) \times D_{cl} \tag{19}$$

onde: f(w) é uma função vinculada à fissuração e definida a partir de uma ponderação escrita com base em modelos encontrados na literatura (DJERBI et al., 2008; ZHANG et al., 2011; JUNG et al., 2017; YANG et al., 2017); D_{cl} é o coeficiente de difusão de cloretos no concreto definido pelas Eq. (6) ou Eq. (17).

[2] Segundo o formato deste trabalho foi usada a vírgula para separar os decimais, no entanto em algumas figuras aparece o ponto em consonância ao programa utilizado.

Na seção 5.2 é mostrado com mais detalhes os dados das análises deste fator. De forma qualitativa aqui será explicado o processo que levou à introdução deste novo fator.

Pela literatura foram encontradas quatros relações (DJERBI et al., 2008; ZHANG et al., 2011; JUNG et al., 2017; YANG et al., 2017) dependentes da fissuração w. Estas relações foram obtidas através de experimentações em laboratórios e análises numéricas. Essas relações permitem conhecer o comportamento de um determinado fator em função da largura das fissurações que se criam em elementos de concreto submetidos aos carregamentos externos. Este aspecto é relevante, pois é intuitivo pensar que as fissuras criam caminhos preferenciais para a difusão dos íons cloretos para o interior do concreto, aumentando a concentração desses íons nas proximidades das barras das armaduras.

Essas quatro relações da literatura foram plotadas em um intervalo pré-definido de w e foi calibrada uma nova curva como média direta das quatro. O uso da difusividade multifatorial (ver Eq. (6) e Eq. (17)), que é o objeto principal deste trabalho, permite utilizar uma série de fatores que ponderam alterando a difusividade D_{cl}. Usando a mesma lógica sistemática foi introduzido um fator f(w) como fator que altera D_{cl} levando em conta as fissurações admitindo um estado não linear do concreto.

Este fator não se encontra na literatura de forma completa. Neste sentido, aqui será proposta um modelo simplificado, mas eficaz, que leva em consideração o efeito das fissurações w na avaliação da difusividade D_{cl}.

Os comportamentos destas quatro relações e da relação calibrada para este estudo são mostrados na Fig. 6. Este aspecto faz parte de um dos quatros objetivos deste trabalho sendo, portanto, dedicada uma seção separada para comentar os resultados pertinentes a esse desenvolvimento.

3 CONFIABILIDADE ESTRUTURAL

3.1 Aspectos da Teoria da Confiabilidade

Análises probabilísticas são baseadas nas informações de parâmetros definidos como variáveis aleatórias por meio de funções de densidade de probabilidades (PDF) e seus momentos. Uma forma para estimar a probabilidade de falha de um componente é definida considerando uma função de estado limite G(X), na qual X corresponde ao vetor das variáveis aleatórias adotadas (NOGUEIRA et al., 2012), podendo ainda serem consideradas na mesma função G(X) outras variáveis como determinísticas. A probabilidade de falha é definida como a probabilidade de ocorrência de uma realização do conjunto de variáveis aleatórias no domínio de não sobrevivência quando se tem $G(X) < 0$, enquanto a probabilidade de falha em um domínio de segurança, i.e., quando ocorre $G(X) > 0$ (Fig. 3).

Já quando $G(X) > 0$ significa que a realização do conjunto de variáveis aleatórias ocorreu no domínio de sobrevivência, sendo, portanto, a região que define a probabilidade de não falha ou segurança ou ainda sobrevivência. A separação de ambos os domínios é dada quando $G(X) = 0$ que é chamado de domínio limite ou fronteira de falha. Nas análises realizadas nesta pesquisa, a palavra “falha” é usada para indicar o início da corrosão de barras de aço no interior de um elemento de concreto armado. Nesses casos, a falha pode ocorrer na interface aço-concreto pela corrosão do aço das armaduras (MICHEL et al., 2013).

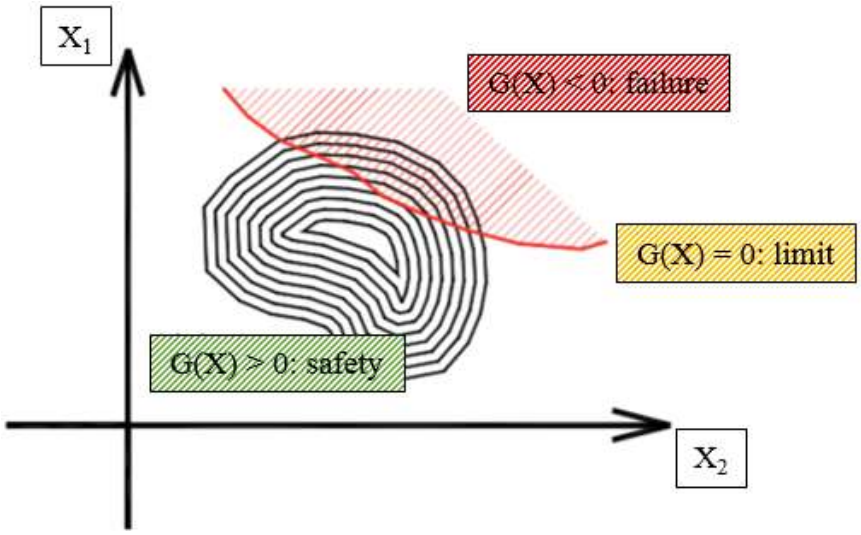

Figura 3 – Domínios de falha e de sobrevivência para um caso de duas variáveis aleatórias (adaptada de NOGUEIRA et al., 2012).

Considerando uma amostra de tamanho N_X para cada variável aleatória $X = \{x_1, x_2, \ldots, x_j\} = \{x_i\}$, para uma função de estado limite G(X), a probabilidade de falha é calculada, de forma geral, pela integral multivariada conforme:

$$p_f = P[G(X) \leq 0] = \int_{\{G(X)<0\}} f_X(x_1, x_2, \ldots, x_j)dx_1dx_2 \ldots dx_j = \int_{\{G(X)<0\}} f_X(x_i)dx_i \qquad (20)$$

onde: $f_X(x_i)$ é a função densidade conjunta de probabilidades das variáveis aleatórias x_i.

Visto que as soluções de forma fechada da Eq. (20) são difíceis de obter, três métodos alternativos foram utilizados nesta análise: (i) método de confiabilidade de primeira ordem (FORM), (ii) integração direta (DI) e (iii) método de simulação de Monte Carlo (MCS).

No FORM, a função G(X) é aproximada pela expansão em série de Taylor de primeira ordem, que é uma linearização em torno de um ponto sobre a equação de estado limite, i.e. G(X) = 0, chamado de ponto de projeto. De fato, para estimar a probabilidade de falha, é necessário encontrar a menor distância, denominada índice de confiabilidade β, entre a origem do domínio limite no espaço normal-padrão não correlacionado das variáveis aleatórias e o ponto mais provável de falha localizado na superfície de falha G(X) = 0, conforme ilustrado na Fig. 4, em que U_i equivale a X_i.

O método analítico, aqui chamado de método DI, é baseado na transformação de Rosenblatt (ROSENBLATT, 1952) e na distribuição Gaussiana, onde a média e o desvio padrão são calculados *a priori*.

Somente em poucos casos é possível encontrar a solução analítica pois é difícil conhecer *a priori* os valores esperados que satisfaz uma distribuição de probabilidades do tipo normal.

Por fim, o MCS, que gera valores pseudoaleatórios, é realizado de acordo com a seguinte formulação (PELLIZZER et al., 2015; OLIVEIRA et al., 2018):

$$P_f = \int_{\{X:\, G(X)<0\}} I(x_i) f_X(x_i) dx_i \tag{21}$$

$$I(x_i) = \begin{cases} 1, & \text{for } G(X) \leq 0 \\ 0, & \text{for } G(X) > 0 \end{cases} \tag{22}$$

$$p_f = \frac{1}{N} \sum_{i=1}^{N} I(x_i) = \frac{N_f}{N} \tag{23}$$

onde: $I(\cdot)$ é uma função indicadora; N é o número de simulações; N_f é o número de simulações para $I(x_i) \leq 0$. Assim, p_f na Eq. (23) pode ser considerado como o valor médio de $I(x_i)$, ou seja, $\bar{I}(x_i) = E\,[I(x_i)]$.

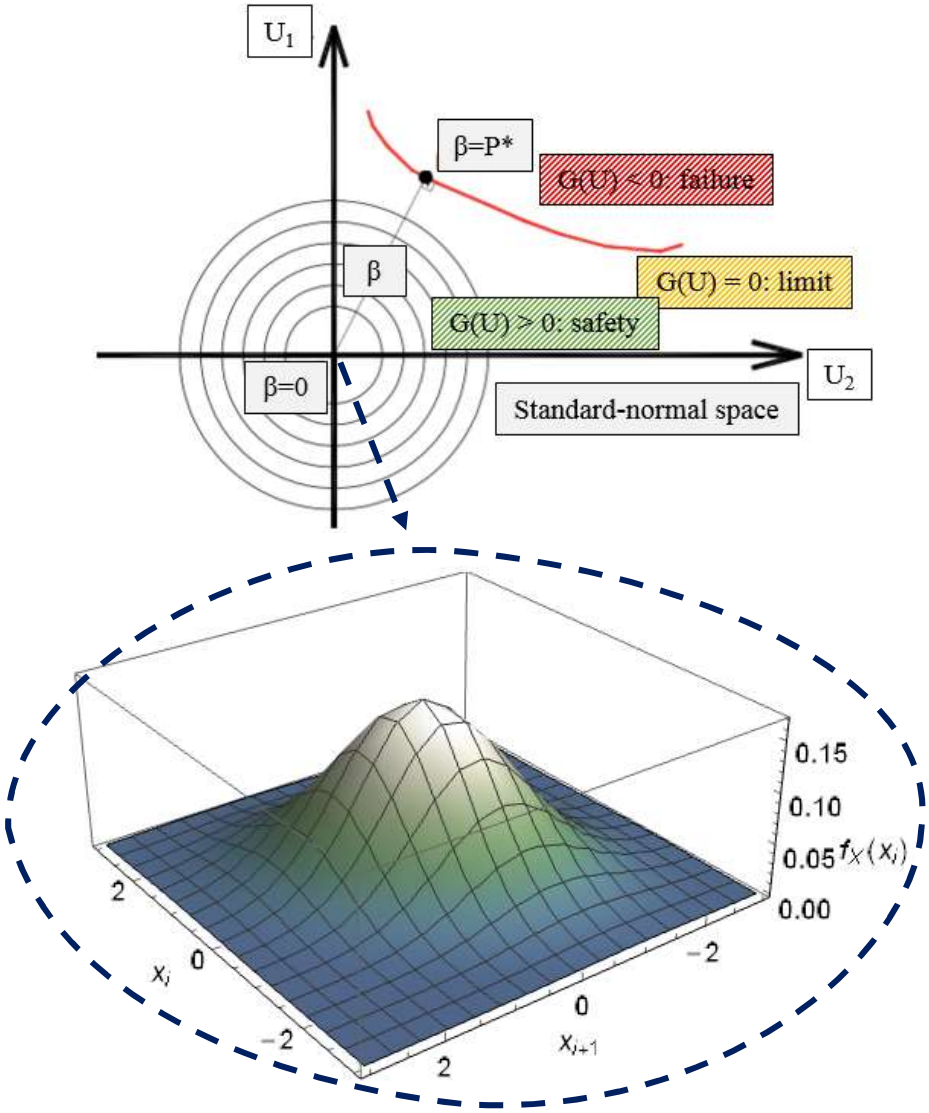

Figura 4 – Representação geométrica do FORM (adaptada de Nogueira et al., 2012).

Os resultados de p_f são exatos quando $N \rightarrow \infty$, no entanto, na prática, o número de amostras necessárias é definido por 1×10^k, onde a escolha de k depende da ordem de magnitude de p_f.

3.2 Formulação do Problema de Início da Corrosão

Neste trabalho, a função de estado limite que descreve o problema é escrita a partir da diferença entre o tempo necessário para o início da corrosão t_R e o tempo imposto como um indicativo do tempo esperado de vida útil da estrutura t_a. Assim, pode-se escrever: $G(X) = t_R(X) - t_a$.

A Eq. (5) é reescrita, para determinar o tempo $t_R(X)$ em função do cobrimento de concreto x_c e demais variáveis, conforme (EL HASSAN et al., 2010; PELLIZZER e LEONEL, 2015; PELLIZZER et al., 2018):

$$t_R(X) = \frac{x_c^2}{4D_{cl}\left(\text{erf}^{-1}\left[\frac{C-C_S}{C_0-C_S}\right]\right)^2} \approx \frac{x_c^2}{4D_{cl}\left(\text{erf}\left[\frac{C_{th}-C_S}{C_0-C_S}\right]\right)^2} \quad (24)$$

onde: C_{th} é a concentração limite de cloretos na interface da armadura que produz a despassivação do aço e que, portanto, deve ser evitada. Assim, a corrosão começa quando os íons cloretos atingem o limite de concentração na superfície das armaduras, ou seja, $C(x_c, t_R) = C_{th}$.

A Figura 5 mostra a função erro de Gauss e sua inversa $\text{erf}^{-1}(\cdot)$, onde é possível observar que os valores numéricos de $\text{erf}^{-1}(\cdot)$ são fornecidos apenas para um range de valores reais entre $-1 < \text{input} < 1$, enquanto, o intervalo da função erro $\text{erf}(\cdot)$ está entre $-\infty < \text{input} < +\infty$. Dessa forma, adota-se a função $\text{erf}(\cdot)$ ao invés de sua inversa.

Conforme já mencionado, a Eq. (24) deriva da solução exata, dentro das condições estabelecidas, que descreve a difusão no concreto dada pela Eq. (5). É importante notar que a Eq. (5) não considera o diâmetro inicial das armaduras (ZHANG et al., 2010), processos químicos e biológicos, bem como suas reações na interface aço-concreto para quantificar o tempo de início da corrosão (MICHEL et al., 2013).

No entanto, o uso da Eq. (5) fornece estimativas da concentração de cloretos a favor de segurança, o que conduz a previsões de perda de vida útil da estrutura antecipadas e, relação ao que de fato ocorre. Além disso, embora o tempo em que os efeitos dos processos mecânicos e físicos se manifestem seja da ordem de alguns meses ou poucos anos, os processos químicos e biológicos, que como mencionado não são considerados, se manifestam muito posteriormente (APOSTOLOPOULOS e PAPADAKIS, 2008).

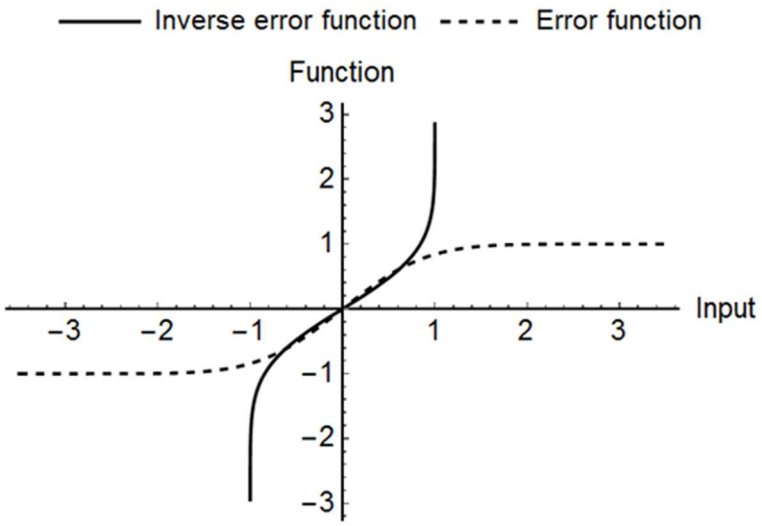

Figura 5 – Função erro de Gauss e sua inversa (MATHEMATICA, 2017).

4 ESTRATÉGIAS ANALÍTICAS E NUMÉRICAS DE SOLUÇÃO

Neste capítulo são descritas as estratégias de solução adotadas para: (i) determinação da concentração de cloretos no interior do concreto considerando o coeficiente de difusão não constante (solução analítica); (ii) efeito de flutuação na difusão dos cloretos em função de ações externas nas estruturas (solução numérica); (iii) análises de confiabilidade do tempo de início de corrosão.

4.1 Concentração de Cloretos: Difusividade Não Constante

A Figura 6 ilustra o fluxograma que descreve as etapas para a quantificação determinística da concentração de cloretos no interior do concreto, a partir da consideração do coeficiente de difusão não constante definido conforme os modelos apresentados no item 2.2 do capítulo 2.

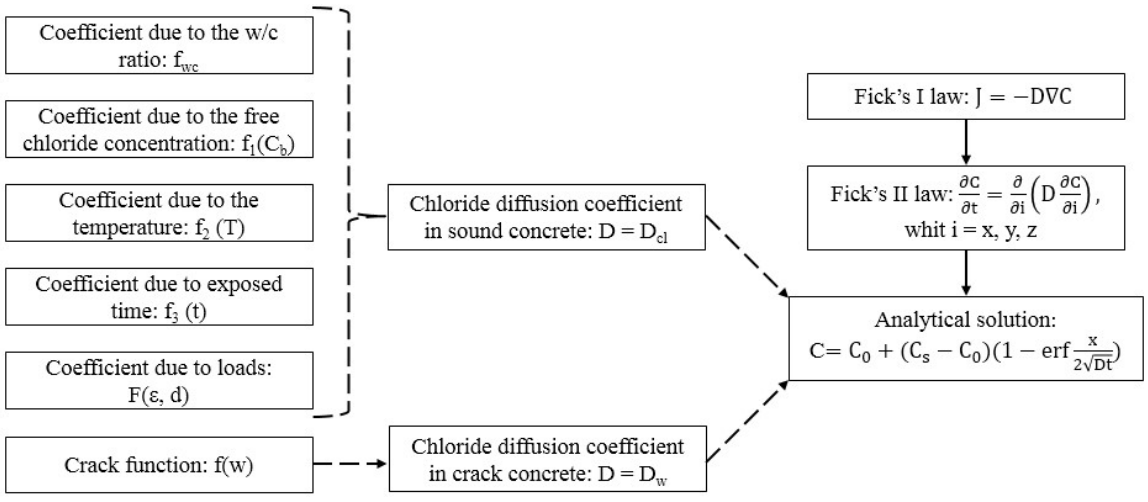

Figura 6 – Fluxograma para quantificação da concentração de cloretos no concreto.

Para a formação do gradiente de concentração de cloretos na direção do interior do concreto, admite-se que a concentração de cloretos na superfície externa dos elementos estruturais, C_s, seja geometricamente uniforme e constante no tempo. A Tabela 1 mostra os parâmetros utilizados para o cálculo da concentração de cloretos no concreto por difusão iônica.

Tabela 1 – Parâmetros de entrada para a análise.

Parâmetros	Valores
Concentração inicial de cloretos, C_o (kg/m^3)	0/5,0
Concentração superficial de cloretos, C_s (kg/m^3)	7,20
Fator água/cimento, w/c	0,40
Peso específico do concreto (kg/m^3)	2400,0
Conteúdo de água evaporável, ω_e	0,60
Concentração livre de cloretos, C_f (kg/m^3)[a]	1,50
Energia de ativação, E_a (J/mol)	41800,0
Constante universal do gás, R (J/mol K)	8,314
Temperatura de referência, T_0 (K)	293,0
Temperatura atual, T (K)	296,0
Idade de referência, t_{ref} (dia)	28,0
Tempo para difusividade constante, t_r (anos)	30,0
Tempo de exposição, t (ano)[b]	0 – 25,0

[a] O valor é definido segundo as seguintes constantes (ISHIDA et al., 2009): $\alpha = 11,8$ e $\beta = 4,0$ (conforme a Eq. (4)).

[b] Foi adotado o índice m = 0,20 [conforme Eq. (9)].

O fator w/c geralmente varia de 0,35 a 0,60. Um fator w/c entre 0,40 – 0,50 é considerado moderado (SILVA et al., 2015). O concreto com w/c mais alto (w/c > 0,60) possui uma porosidade mais alta e a sua estrutura interna é caracterizada por cavidades e vazios também maiores, formando caminhos preferenciais para a difusão. O concreto com w/c menor (w/c < 0.40) possui maior resistência à tração e à compressão podendo, portanto, suportar cargas maiores. Além disso, em regiões com maior umidade, recomenda-se ainda a utilização de fatores w/c menores, bem como maior cobrimento de concreto.

A Tabela 2 mostra os valores utilizados para definir o fator F, de acordo com a literatura (BS EN 1992-1-1:2004, 2004), considerando uma lei constitutiva à compressão para o concreto.

Tabela 2 – Parâmetros de entrada para definir o fator F. Os valores são de acordo com a literatura (BS EN 1992-1-1:2004, 2004) exceto onde indicado.

Parâmetro	Valor
Resistência caraterística à compressão do concreto, f_{ck} (MPa)	35,0
Resistência média à compressão do concreto, f_{cm} (MPa)	43,0
Modulo de elasticidade longitudinal, E_{cm} (GPa)	34,0
Deformação na tensão de pico, ε_{c1} (‰)	2,25
Deformação última à compressão, ε_{cu1} (‰)	3,50
Parâmetro, n (GERARD et al., 1998)	5,0
Parâmetro, d_{cr} (GERARD et al., 1998)	0,40
Parâmetro, C_1[a]	- 0,88

[a] O parâmetro B usado para definir C_1 foi obtido segundo a relação seguinte: $B = (D_{max}/D_0 - 1)/\varepsilon_{c1} = 3{,}11 \times 10^{-3}$, para $D_{max}/D_0 = 8$ (Eq. (16)).

A Figura 7 mostra o diagrama tensão-deformação para o concreto comprimido de acordo com um intervalo: $f_{ck} - 10 < f_{ck} < f_{ck} + 15$ MPa. Este é um intervalo comum usado para estruturas com a deformação última à compressão final igual a 3,5 ‰. A linha vertical (ε_{c1} = 2,25 ‰) separa os domínios para o efeito da determinação do coeficiente de difusão de cloretos no concreto em estado linear (antes da linha) e estado não linear (depois da linha). As equações mostradas na Figura 7 referem-se às linhas de tendência polinomiais quadráticas (linhas tracejadas) para representar o comportamento do concreto comprimido.

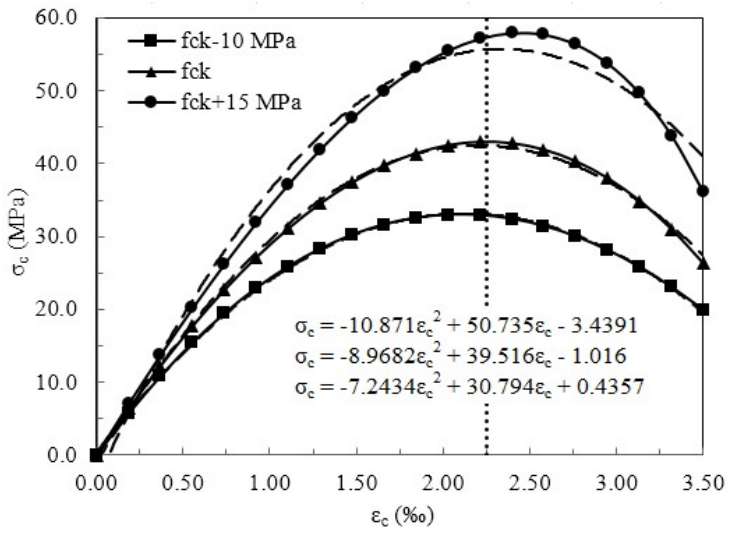

Figura 7 – Curvas tensão-deformação à compressão do concreto.

4.2 Concentração de Cloretos: Flutuação na Difusividade

A análise numérica da equação diferencial que representa o problema, segundo Eq. (2), considera como condições iniciais de concentração (i.c.) e condições de contorno (b.c.) (SUN et al., 2012; FAN e WANG, 2015; CRANK, 1975) o estabelecido a seguir:

$$\begin{aligned} \text{i.c.:} \quad & C(i,0) = C_0 \\ \text{b.c.:} \quad & C(0,t_m) = C_s \\ & C(i_m,t_m) = C_0 \end{aligned} \tag{25}$$

onde: i_m e t_m são duas variáveis definidas *a priori* e que são relacionadas à posição *i* no interior do concreto e ao tempo *t.*

A resolução da análise numérica aproximada é feita através dos polinômios de Hermite conforme a literatura (DATTOLI, 2000).

O objetivo desta parte da pesquisa é quantificar probabilisticamente o coeficiente de difusão de cloretos no concreto D_{cl} e ponderá-lo por uma função especial $f_D(i,t)$ definida a partir da consideração de tipos distintos de ação externa sobre a estrutura. Assim, essas ações externas podem influenciar o fluxo de íons de cloretos no interior do concreto, introduzindo flutuação, portanto, na concentração interna de cloretos. A função $f_D(i,t)$ considera quatro tipos de situações que podem gerar flutuação na difusividade de cloretos: constante, senoidal, gaussiana e geral. A Tabela 3 mostra os quatro tipos de funções consideradas e suas possíveis aplicações para fluxo em apenas uma direção no interior do concreto (i = x).

Tabela 3 – Funções genéricas utilizadas $f_D(x,t)$.

Tipo	**$D_{cl} \times f_D(x,t)$**	**Exemplo de aplicações**
Constante	$D_{cl} \times$ constante	- Cargas externas permanentes e de utilização
Senoidal	$D_{cl} \times$ Seno(t)	- Cargas de ondas de água
Exponencial tipo Gaussiana	$D_{cl} \times e^{-t\hat{}2}$	- Ações impulsivas, tipo ondas ou pressões impulsivas.
Geral	$D_{cl} \times \sum_{i=1,\ldots,n}$ Seno(it + ϕ)[a]	- Vento - Vibração de máquinas rotativas

[a] ϕ é a fase aleatória entre 0 e 2π, e n = 1500 (CLOUGH e PENZIEN, 1976)

Esta abordagem é puramente matemática, pois a ordem de grandeza das amplitudes das funções genéricas $f_D(x,t)$ e o tempo t de atuação não é igual para cada exemplo, i.e. uma onda impulsiva é medica em termos de pressões hidrodinâmicas. Neste sentido não é possível definir uma única função genérica $f_D(x,t)$ com uma única amplitude e um único intervalo temporal que represente de forma unívoca todos os exemplos de aplicações mostrados na Tabela 3. Portanto, este tipo de análise poderia ser abordado tanto de uma forma teórica quanto de uma forma pratica.

No entanto há alguns casos que são compatíveis com o problema mecânico da difusividade estudado neste trabalho como, por exemplo, um carregamento concentrado impulsivo ou uma oscilação produzida por máquinas rotativas que pode gerar vibrações nos elementos estruturais.

O processo de solução é resumido nas seguintes etapas: (i) definição da função da difusividade $f_D(i,t)$ que descreve o tipo de ação externa atuante; (ii) seleção das condições iniciais i.c. e de contorno b.c.; (iii) plotagem das curvas de concentração de cloretos no interior do concreto C(i,t); (iv) verificação da convergência entre as soluções exatas (indicadas com E_s), ou seja usando a Eq. (5) com D_{cl} constante, e numéricas (indicadas com N_s) usando a Eq. (25), pelo seguinte critério:

$$\left|C(i,t)_{E_s}^{k} - C(i,t)_{N_s}^{k}\right| \leq \varepsilon \tag{26}$$

onde: k representa as iterações; ε indica a tolerância de convergência ($\varepsilon = 1{,}45 \times 10^{-9}$).

Portanto, essa convergência termina quando se encontra um valor mínimo entre a diferença dos resultados analíticos com os resultados numéricos. Este tipo de convergência é possível de ser executada de forma satisfatória, pois neste estudo as soluções analíticas que fornecem as soluções exatas são conhecidas. Isso permite calibrar um modelo numérico aproximado com um modelo analítico exato. O objetivo principal dessa análise foi calibrar o modelo numérico para poder utilizá-lo com D_{cl} variável no tempo t.

Nos resultados mostrados na secção 5.3 é indicado o erro relativo calculado como $(C_{Es} - C_{Ns})/C_{Es}$. Isso permitiu em uma forma mais visual individuar um valore de convergência aceitável.

4.3 Parâmetros da Análise de Confiabilidade

As Tabelas 4 e 5 mostram as variáveis determinísticas e aleatórias, respectivamente, adotadas com as suas distribuições. O tipo de concreto considerado é composto por um cimento Portland padrão com adições de cinzas volantes e escórias de alto forno (KIM et al., 2014).

Tabela 4 – Dados dos parâmetros determinísticos adotados.

Parâmetro	Unidade	Valor
α (ZACCHEI e NOGUEIRA, 2019)	-	11,80
β (ZACCHEI e NOGUEIRA, 2019)	-	4,0
$D_{cl,ref}$*	cm^2/ano	0,40
w/c*	-	0,50
T_0 (KONG et al., 2002)	°C (K)	23,0 (296,0)
R (KONG et al., 2002)	J/mol K	8,134
t_{ref} (FU et al., 2015)	dias (anos)	28,0 (0,076)
t*	anos	25,0
t_r (FU et al., 2015)	anos	30,0
h_{Dcl} (BAŽANT e NAJJAR, 1972)	-	0,75

Nota: * = Valor estimado.

Tabela 5 – Dados das variáveis aleatorias adotadas.

Parâmetro	μ	± σ[a]	C_V (%)[b]	Distribuição	Motivo de adoção da distribuição
E_a (kJ/mol)	44,6 (KONG et al., 2002)	4,30	10,0	Normal	Parâmetro positivo truncado a 17,60 kJ/mol[c].
T (°C)	23,0*[d]	8,0	35,0	Normal	Este parâmetro pode ser positivo ou negativo.
C_f (kg/m^3)	1,50 (ZACCHEI e NOGUEIRA, 2019)	0,75	50,0	Log-normal	Este parâmetro deve ser positivo; portanto o intervalo da distribuição será (0, +∞).
ω_e	0,83*	0,1408	17,0	Beta (5, 1)	Este parâmetro é definido por $0 \leq \omega_e \leq 1$; portanto o intervalo da distribuição será [0, 1].
m	0,20 (KIM et al., 2014)	0,04	20,0	Normal	Esta distribuição permite um controle razoável da dispersão (parâmetro sensível para os resultados).
h	0,80*	0,04	5,0	Normal	
n	6,0 (BAŽANT e NAJJAR, 1972)	1,732	28,0	Normal	
x_c (cm)	5,0*[e]	1,50	30,0	Log-normal	Este parâmetro deve ser positivo; portanto o intervalo da distribuição será (0, +∞).
C_0 (kg/m^3)	0,5*	0,2886	58,0	Uniforme (0, 1)	Parâmetro contínuo e constante.
C_s (kg/m^3)	1,15 (EL HASSAN et al., 2010)[f]	0,575	50,0	Log-normal	Esse parâmetro deve ser positivo (troncado a C_0); portanto o intervalo da distribuição será (C_0, +∞).

Nota: * Valor estimado.
[a] Para as distribuições Beta e Uniforme, ±σ são calculados através da equação relativa da distribuição;
[b] C_V é o coeficiente de variação estimado por: (σ/μ) × 100.
[c] E_a = 44,6 ± 4,3 kJ/mol, para a relação w/c assumida constante e igual a 0,5. E_a alcança este valor quando os poros são livres dos fluidos (ISHIDA et al., 2009).
[d] 23,0 ± 8,0 °C → 296,0 ± 8,0 K.
[e] 50 mm, com w/c = 0,5 (STEWART e MULLARD, 2007).
[f] Para estruturas localizadas entre 0,10 km e 2,84 km respeito à costa sem contato direto com a água do mar (EL HASSAN et al., 2010).

Na distribuição Beta β(α', β'), α' e β' são chamados de parâmetros de forma. Para α' = 1, a probabilidade que X seja menor e igual a x, i.e. P (X ≤ x) é baixa, enquanto por β' = 1 essa probabilidade é alta.

A Figura 8 mostra as funções densidade de probabilidades para cada variável aleatória adotada.

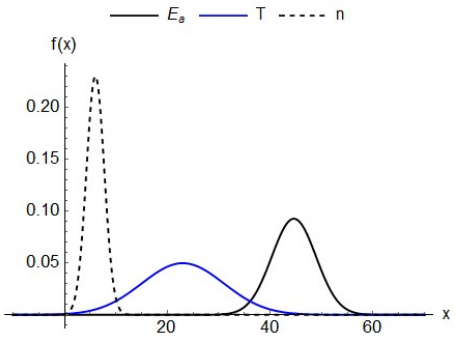

(a) Distribuição Normal N(μ, σ^2)

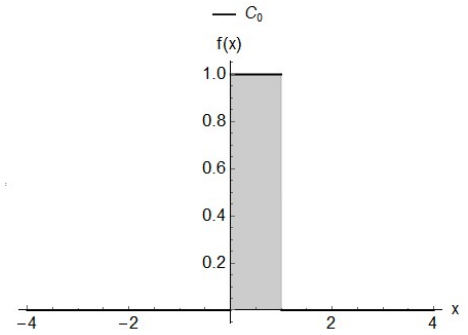

(b) Distribuição Uniforme U(x_{min}, x_{max})

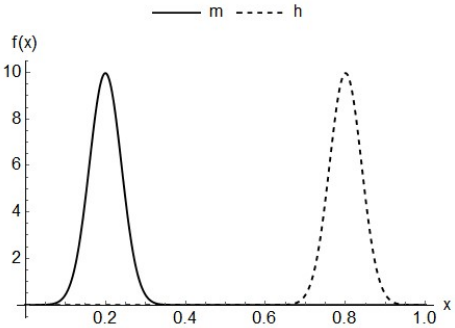

(c) Distribuição Normal N(μ, σ^2)

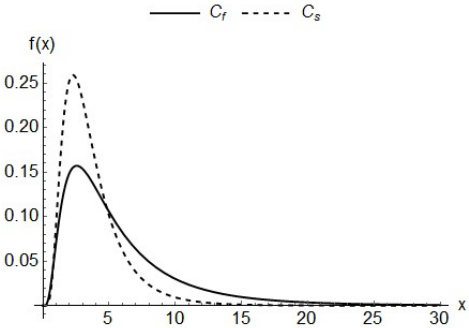

(d) Distribuição Log-normal lnX(μ, σ^2)

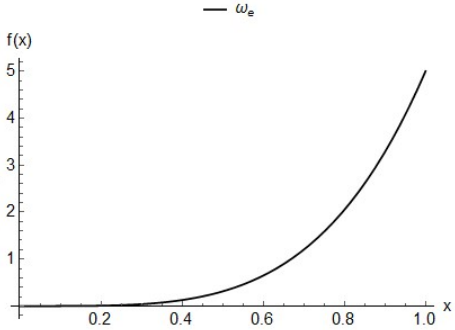

(e) Distribuição Beta (α', β')

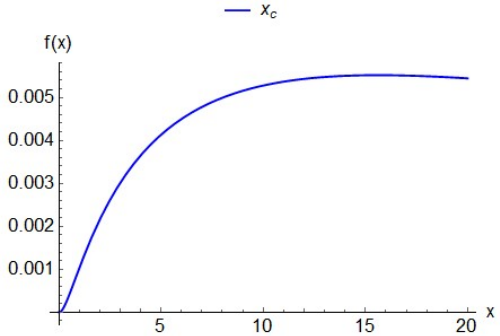

(f) Distribuição Log-normal lnX(μ, σ^2)

Figura 8 – Distribuição de probabilidades das variáveis aleatórias adotadas.

A Figura 9(a) apresenta uma visão geral das quatro variáveis aleatórias geradas, i.e., C_{th}, C_s, $t_R - t_a$ e t_R. Os parâmetros t_R e C_{th} são obtidos pela Eq. (24) considerando os valores da Tabela 5, enquanto t_a é um parâmetro que varia entre 0-55 anos.

A Figura 9(b) mostra numa escala logarítmica a variação de $t_R - t_a$ em função de t_R para um tempo fixado $t_a = 10$ anos. Na análise MCS foram geradas 1×10^6 amostras para cada variável.

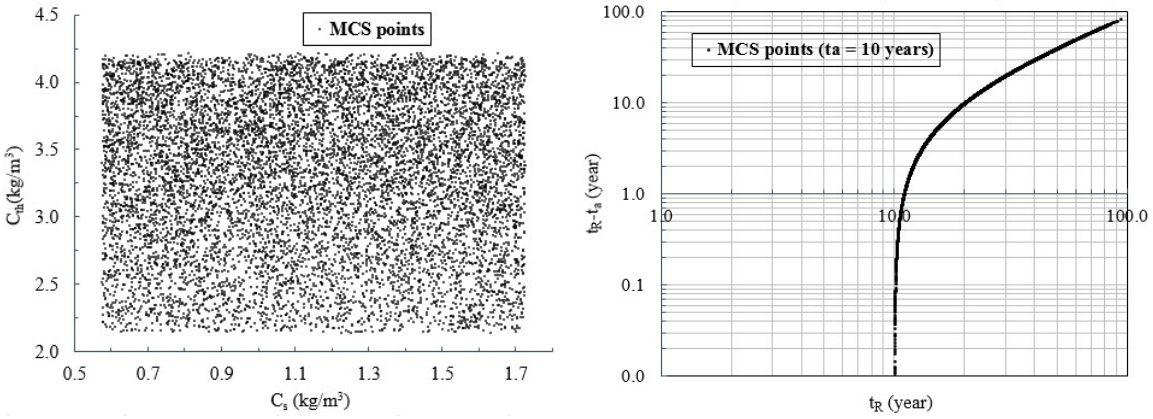

(a) (b)

Figura 9 – Pontos aleatórios dos quatro parâmetros (C_{th}, C_s, $t_R - t_a$ e t_R) gerados para uma amostra de 1×10^6 pontos.

Na Figura 10 é apresentado o fluxograma para a análise probabilística. A metodologia é dividida principalmente em duas partes e é detalhada etapa por etapa como descrito abaixo. Na parte I é definido o D_{cl} por valores determinísticos e probabilísticos, enquanto na parte II é avaliada a concentração de cloretos no interior do concreto C(i,t).

Etapa 1: são definidas a primeira e a segunda lei de Fick. São avaliados os fatores mostrados na Eq. (17) para obter o coeficiente de difusão de cloretos no concreto $D_{cl,i}$ na direção do fluxo i.

Etapa 2: são definidos os valores dos parâmetros determinísticos e aleatórios. Nesse sentido, $D_{cl,i}$ é um coeficiente que pode ser considerado como semi-probabilístico porque somente alguns parâmetros foram calculados de forma probabilística, enquanto outros de forma determinística (conforme as Tabelas 4 e 5). A precisão na determinação do início da corrosão está relacionada a uma boa estimativa de $D_{cl,i}$.

Etapa 3: são implementadas as soluções analíticas considerando fluxo de cloretos em uma direção.

Etapa 4: são implementadas as soluções numéricas considerando fluxo de cloretos em uma direção. Nesta etapa, são encontradas as soluções numéricas para um conjunto de equações diferenciais com várias funções incógnitas y_j que dependem de uma ou mais variáveis independentes x_j. As equações numéricas representam as soluções para as funções y_j através de uma função de interpolação (IF) polinomial que é uma generalização da interpolação linear (MATHEMATICA, 2017). A FI fornece as aproximações de y_j no intervalo de $x_{inicial}$ a x_{final} para as variáveis independentes x_j. O processo é iterativo iniciando com um valor de

x_j e, em seguida, variando esse valor ao longo de todo o intervalo completo de $x_{inicial}$ a x_{final}. Nesta análise é necessário definir as condições iniciais e de contorno apropriadas para y_j e suas derivadas. Essas condições definem os valores de $y_j(x_j)$ e $y_j'(x_j)$ em pontos definidos x_j.

Etapa 5: é avaliada a concentração de cloretos C(i,t). Se a convergência não for satisfeita, é necessário redefinir as condições b.c. do problema mostradas na Eq. (25). Em particular o termo que afeta mais os resultados é o parâmetro i_m.

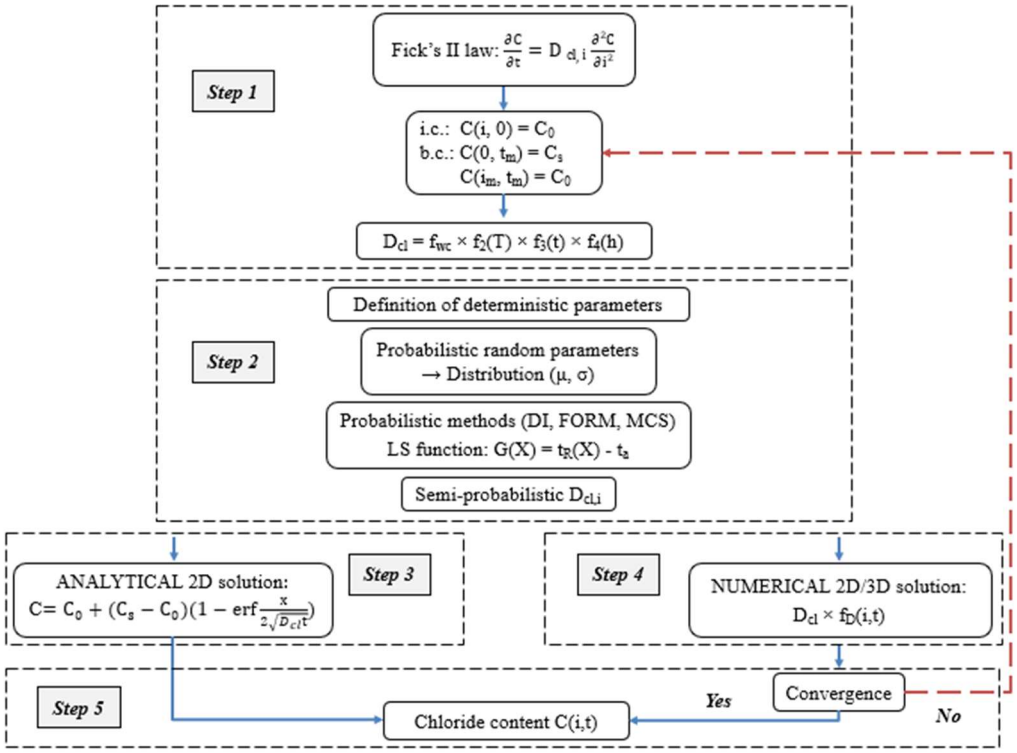

Figura 10 – Fluxograma para a análise probabilística.

5 RESULTADOS E DISCUSSÃO

A seguir, são apresentados os resultados das análises realizadas abrangendo cada um dos objetivos definidos para esta pesquisa. Todos os parâmetros necessários e modelos empregados foram discutidos nos capítulos anteriores.

5.1 Efeitos do Modelo Multifatorial e do Estado de Tensão-Deformação sobre o Coeficiente de Difusão de Cloretos no Concreto (Objetivo I)

As curvas isotérmicas definem um fenômeno complexo e não linear, que depende da concentração de íons cloretos nos poros e na composição do cimento. As reações que ligam as diferentes partículas químicas têm uma influência significativa na fase de entrada de íons cloretos no concreto (BENTZ et al., 2014). A literatura conhecida até o momento não fornece dados confiáveis sobre essa taxa de ligação entre as partículas (CARRARA et al., 2016).

A Figura 11 mostra o fator f_l em função de C definido pela Eq. (7). É possível observar que, para um valor fixo de C_f, quando ω_e aumenta o fator f_l aumenta também. Assim, acréscimos no coeficiente ω_e produzem aumentos no conteúdo de água e na concentração total de cloretos C_{tot} no interior do concreto.

Na literatura (ISHIDA et al., 2009) foi mostrada uma relação linear entre C_b e C_f sendo dada por $C_b = 2{,}5 \times C_f$. No entanto, essa relação linear subestima C_b quando $C_f > 1$, portanto isso justifica a adoção deste fator $f_l(C_b)$ neste estudo.

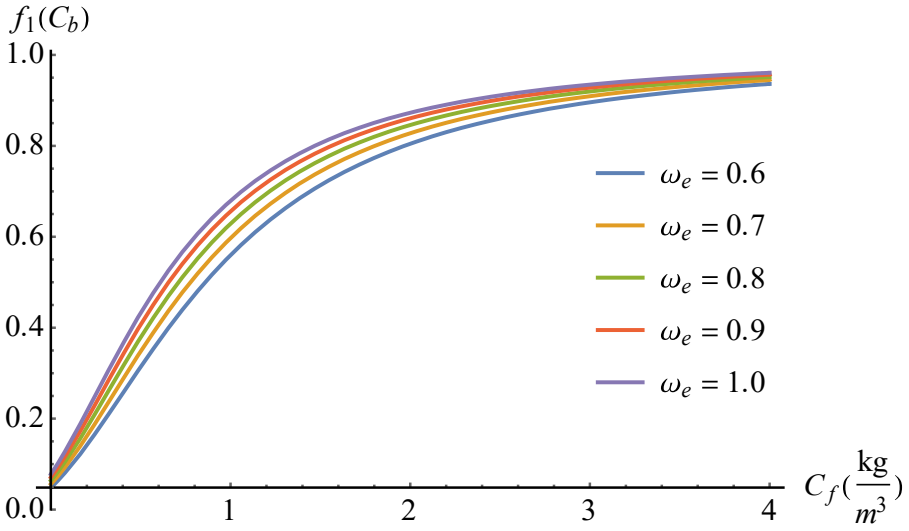

Figura 11 – Curvas isotérmicas do fator f_1.

O coeficiente de difusão de cloretos no concreto D_{cl} está relacionado aos íons livres e é obtido considerando-se o fator $f_1(C_b) < 1$, que representa uma porcentagem dos íons cloretos ligados. Na literatura, estima-se que C_f é 2,2 a 3,4 vezes C_b (SUN et al., 2012).

A Figura 12 ilustra o fator f_2 em função de T e E_a definido pela Eq. (8). Na literatura é possível encontrar valores diferentes de E_a em função do fator água-cimento w/c (KONG et al., 2002; FU et al., 2010; DAMRONGWIRIYANUPAP et al., 2015; FU et al., 2015), como por exemplo: 32,0 ± 2,4 kJ/mol para w/c = 0,6; 44,6 ± 4,3 kJ/mol para w/c = 0,5; 41,8 ± 4,0 kJ/mol para w/c = 0,4. A energia de ativação E_a também varia em função da presença da água, i.e., quando os poros estão livres de água, E_a é igual a 17,6 kJ/mol (ISHIDA et al., 2009) e, consequentemente, a concentração de cloretos no concreto diminui. Também, o aumento da variação do gradiente de temperatura aumenta o fator f_2, aumentando assim a penetração dos íons cloretos da superfície externa para o interior do elemento estrutural de concreto.

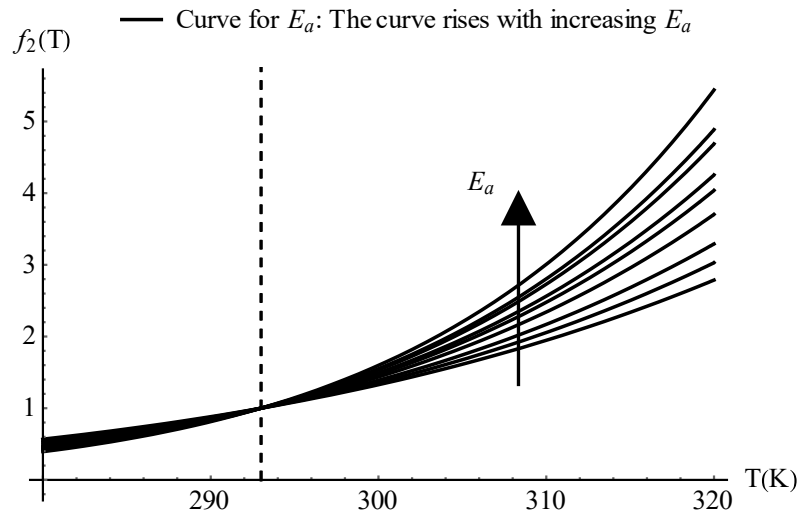

Figura 12 – Fator da temperatura f_2 vs. T (a linha vertical indica T_0 = 293 K).

A Figura 13 apresenta o efeito de envelhecimento do concreto expresso pelo fator f_3 conforme a Eq. (9). A curva é representada por dois ramos, onde é possível observar que após um determinado valor (cerca de 30 anos) a curva tende a reduzir mais rapidamente. Este valor de 30 anos se dá pelo fato de que se estima que, após 30 anos, os hidratos formados no processo de hidratação do cimento diminuam mais a porosidade, limitando a difusão dos cloretos no interior do concreto.

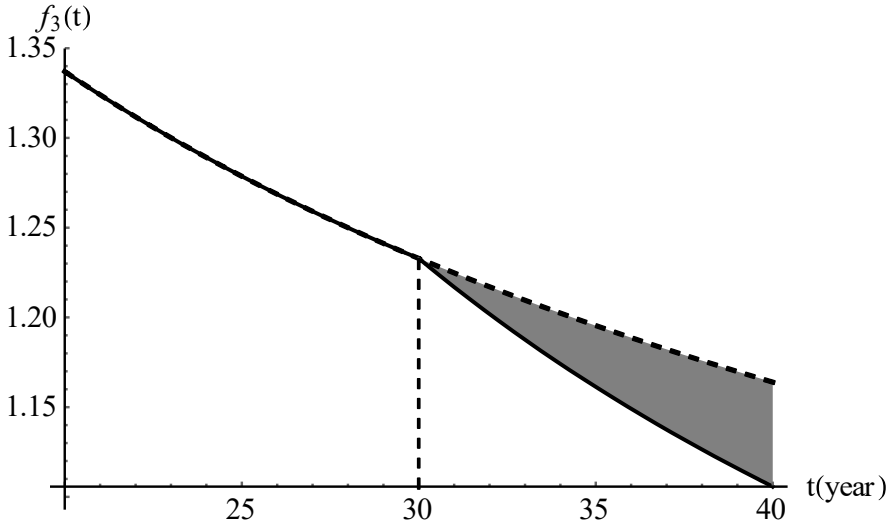

Figura 13 – Fator da idade do concreto f_3 vs. t.

Finalmente a Figura 14 ilustra o fator F em função de ε_c definido pela Eq. (14). As linhas tracejadas verticais dividem o gráfico em três partes: (i) antes de ε_c = 0,355 ‰, o fator F é igual a 1, pois não é sensível ao material ainda na fase elástica; (ii) entre 0,355 < ε_c < 1,184 ‰, o fator F é quase-linear; (iii) após ε_c = 1,184 ‰, o fator F tende a se estabilizar resultando em F ≈ constante.

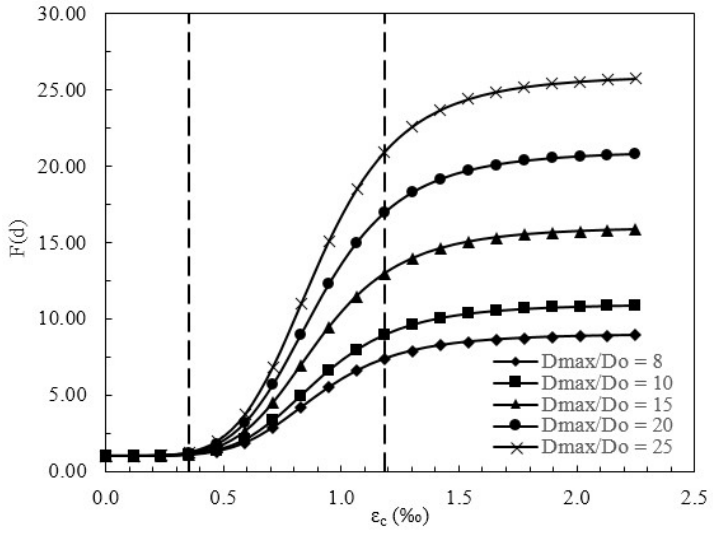

Figura 14 – Fator de carga F (adimensional) vs. ε_c para diferentes proporções D_{max}/D_0.

Na Figura 15, o coeficiente de difusão de cloretos no concreto não constante D_{cl}, i.e. considerando os efeitos de tensão-deformação e o dano (F ≠ 0), é comparado com o coeficiente D_{cl} constante, i.e. não considerando os efeitos do estado de tensão-deformação e o dano (F = 0). Todos os fatores mostrados na Eq. (6) são considerados para o cálculo de D_{cl}.

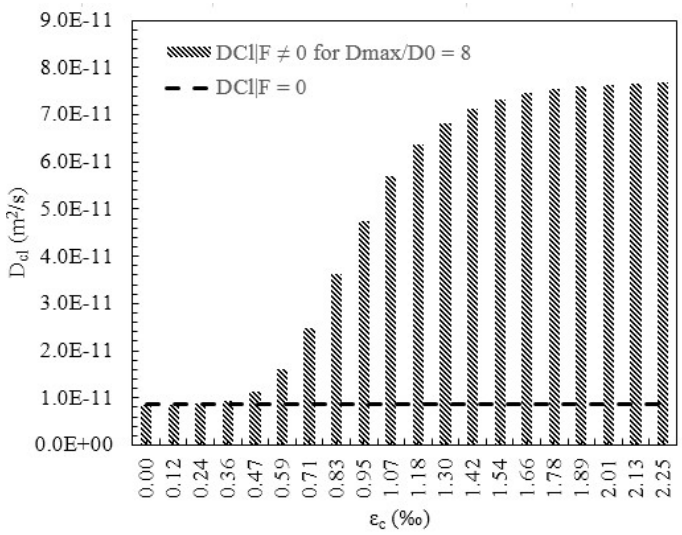

Figura 15 – Coeficiente de difusão constante e não constante.

Nesta análise, o coeficiente de difusão de cloretos no concreto $D_{cl,max|F\neq0}$ alcança um valor igual a $7{,}7 \times 10^{-11}$ m^2/s, enquanto para $D_{cl|F=0}$ é igual a $8{,}6 \times 10^{-12}$ m^2/s. A relação entre esses dois valores é 8,95. Esta relação representa a relação máxima, pois o valor $D_{cl} = 7{,}7 \times 10^{-11}$ m^2/s refere-se a uma deformação na tensão de pico $\varepsilon_{c1} = 2{,}25$ ‰.

Na literatura (SILVA et al., 2015; MORGA e MARANO, 2015; WANG et al., 2016) foram encontrados estudos que estimam a difusividade D_{cl}, e, portanto, o conteúdo de íons cloretos C, considerando o estado de tensões dentro de um elemento de concreto. Neste sentido, é possível comparar os resultados deste trabalho mostrados na Fig. 15 com a literatura.

Na literatura (WANG et al., 2016) foi mostrado que esse coeficiente de difusão varia de acordo com os níveis de tensão e deformação do concreto em que, para deformações menores que 75% da deformação última, D_{cl} é cerca de 2,24 vezes o coeficiente de difusão quando não se considera a influência do estado de tensão e deformação produzido pelos carregamentos.

Na literatura (SILVA et al., 2015), para uma resistência caraterística à compressão do concreto $f_{ck} = 35$ MPa, a difusividade D_{cl} é de cerca de $1{,}8 \times 10^{-11}$ m^2/s, ou seja, 2,10 vezes $D_{cl|F=0}$. Isso mostra como, ao se considerar o estado tensional a compressão, a difusividade D_{cl} aumenta.

Ainda na literatura (MORGA e MARANO, 2015), foi apresentado um valor indicativo da difusividade D_{cl} para w/c = 0,5 e f_{ck} = 30 a 40 MPa da ordem de $\sim 2{,}0 \times 10^{-12}$ m^2/s. Este valor é inferior ao valor calculado nesta análise, no entanto mantem a mesma ordem de grandeza.

Finalmente na literatura (WANG et al., 2018), foram calculadas as difusividades através de ensaios em laboratório considerando os carregamentos externos. A relação entre a difusividade com carregamento e sem carregamento é da ordem de 5,76.

Sendo a quantificação dos efeitos dos carregamentos externos na difusividade D_{cl} uma das novas contribuições neste trabalho, fazer uma comparação com os dados na literatura é necessário. Em particular, o conhecimento dos valores da difusividade D_{cl} obtidas mediante ação de carregamentos é útil para poder eventualmente fazer ajustes das difusividades calculadas sem carregamentos. Ou seja, é possível acrescentar o $D_{cl|F=0}$ de um certo fator para consideras as cargas.

É importante ressaltar que estes resultados são válidos para carregamentos aplicados no médio e longo prazo, ou pelo menos, para carregamentos que mantenham uma deformação constante durante o processo de difusão. Isso porque um carregamento que age num curto prazo pode não afetar o processo de difusão que precisa de períodos longos para se manifestar.

5.2 Efeitos da Fissuração sobre o Coeficiente de Difusão de Cloretos no Concreto (Objetivo II)

A difusividade de íons cloretos no concreto fissurado é fortemente influenciada pela largura das fissuras w.

A Figura 16 mostra a função de fissuração definida pela Eq. (19) calibrada usando quatro relações encontradas na literatura (DJERBI et al., 2008; ZHANG et al., 2011; JUNG et al., 2017; YANG et al., 2017). Na figura é também mostrada a relação estimada em este trabalho que segue uma forma polinomial.

Todas as quatro relações são normalizadas em relação ao valor máximo de cada uma, exceto uma equação (ZHANG et al., 2011), pois ela já assume a mesma forma da Eq. (19). A linha tracejada mostra o desenvolvimento médio dos valores das quatro relações estimado neste trabalho, onde o valor médio obtido é igual a 1,04, sendo possível definir, para este caso, que $D_w \approx D_{cl}$.

Usando um valor médio próximo de 1,0 as fissurações não interferem na difusividade de íons cloretos. Portanto, para poder ver um efeito que muda o processo de difusão é preciso considera o valor maior. O valor máximo estimado é de 1,297.

O intervalo estudado de w é de 0,1 a 0,25 mm, pois fazer uma comparação dessas relações para um *w* mais alto (w > 0,25 mm) através de uma análise analítica não é confiável. Além disso, este valor é coerente com a largura das fissuras permitida para um elemento de concreto armado que é de 0,3 mm (BS EN 1992-1-1:2004, 2004).

Vale ressaltar que este intervalo de w é representativo de micro fissurações e, portanto, as variações de f(w) = 1,04, mesmo sendo pequenas, são compatíveis com o sistema.

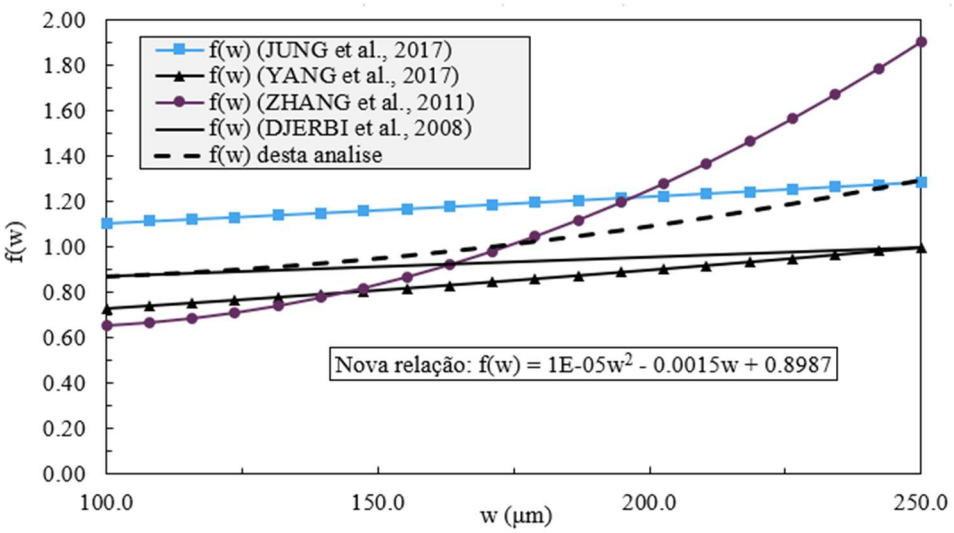

Figura 16 – Relações da função de fissuração.

É mostrado na literatura (WANG e UEDA, 2011) que, no intervalo estudado, quando w aumenta, a permeabilidade do concreto aumenta rapidamente, aumentando a concentração de cloretos. O comportamento é mútuo, i.e. aumentando o conteúdo de cloretos, a largura das fissuras se expande também (TING e YANG, 2017). Além disso, quando *w* chega a um valor que é maior do que um valor crítico, uma expansão adicional de *w* não tem influência significativa no transporte de íons cloretos para o interior do concreto (WANG e UEDA, 2011). Este valor crítico é estimado em torno de w > 0,45 mm (TING e YANG, 2017).

A relação para f(w) da literatura (JUNG et al., 2017) foi calibrada considerando também o efeito da idade, porém, nesta análise para poder fazer uma comparação mais próxima possível entre as relações, este efeito não foi considerado.

Yang et al., 2017 mostram que a penetração dos cloretos depende da profundidade da fissuração e da taxa de fissuras presentes no elemento de concreto; mas depende muito da largura da fissuração conforme a relação proposta.

A função utilizada na literatura (ZHANG et al., 2011), estudada também por outros autores (TING e YANG, 2017), mostra mais claramente que a difusividade do cloreto aumenta com o aumento de w.

O modelo mostrado na literatura (DJERBI et al., 2008), estudado também por outros autores (FU et al., 2010), é quase linear segundo um intervalo de 80 μm a ~ 250 μm. Neste modelo (DJERBI et al., 2008), a relação é dividida em duas partes: (i) em um período de transição em que a migração de íons cloretos ocorre em condições não estáveis; (ii) em um período de estado estacionário em que o aumento dos íons cloretos é constante ao longo do tempo, gerando um fluxo constante de íons cloretos no interior do concreto.

As Figuras 17 e 18 mostram a concentração de cloretos, respetivamente em x e t, para os seguintes casos: (i) concreto não fissurado sem carregamento externo C (F = 0; w = 0); (ii) concreto não fissurado com carregamento externo $C_{\varepsilon c}$ (F ≠ 0; w = 0); (ii) concreto fissurado C_w (w ≠ 0). As curvas são obtidas considerando $C_s = C_0 = 0$. As curvas referentes ao caso C_w são obtidas usando o valor $D_w = 1{,}297 \times D_{cl|F} \neq 0$, enquanto as curvas de $C_{\varepsilon c}$ são calculadas para uma deformação na tensão de pico $\varepsilon_{c1} = 2{,}25$ ‰.

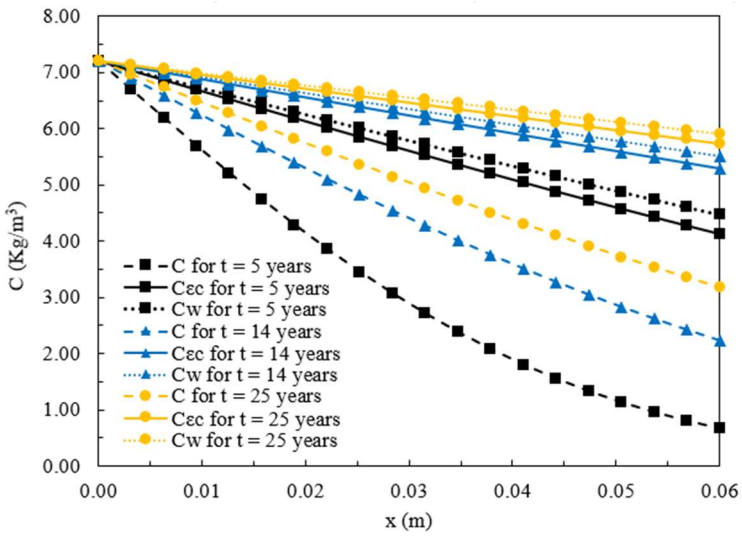

Figura 17 – Concentração de cloretos na direção x.

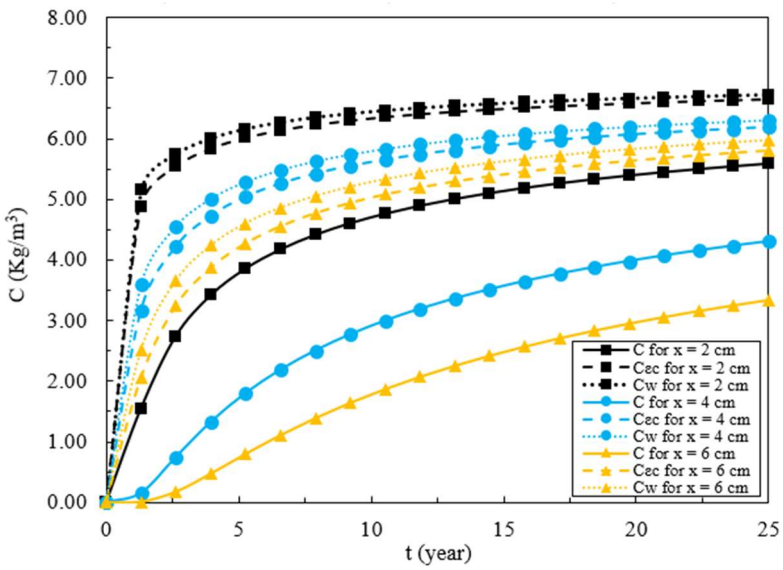

Figura 18 – Concentração de cloretos no tempo t.

Os histogramas na Figura 19 mostram a concentração média de cloretos, enquanto a Figura 20 apresenta a comparação da concentração máxima de cloretos para $C_0 = 0$ e $C_0 = 5$ kg/m^3. Os valores são expressos como porcentagem do peso específico do concreto (ver Tabela 1). A linha tracejada horizontal representa a concentração limite do cloreto (C_{th} na Eq. (24)) de acordo com a literatura (SILVA et al., 2015) (i.e. 0,30% do peso específico do concreto = 0, 003 × 2400 kg/m^3 = 7,2 kg/m^3).

Na literatura (KONG et al., 2002; ZOFIA e ADAM, 2013) estima-se que o nível de concentração de cloretos atinja o valor crítico no interior do concreto na interface das armaduras de aço num período entre 7 a 20 anos e que o intervalo de concentração limite de cloretos seja de 0,15 a 0,4% do peso específico do concreto.

No modelo desta análise, para um concreto armado convencional (BS EN 206-1:2000, 2000; NIST, 2018), os valores obtidos em x = 6 cm variam de 0,1% a 0,3% do peso específico do concreto em 7 a 20 anos.

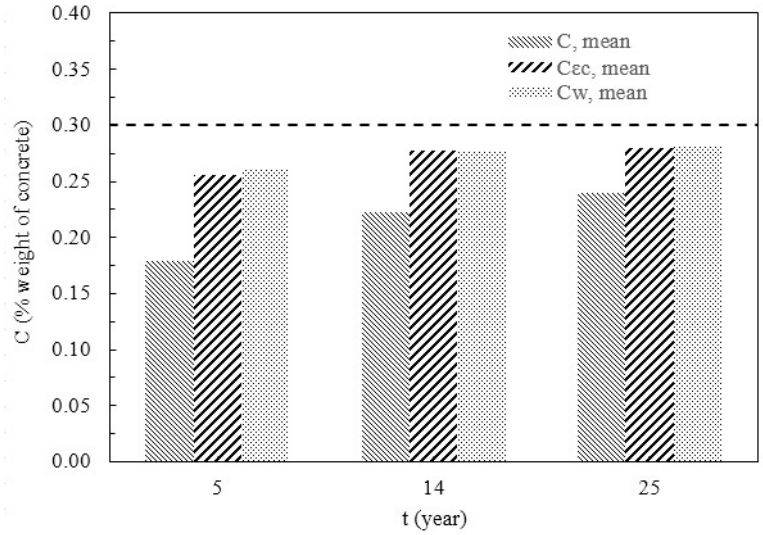

Figura 19 – Concentração média de cloretos t = {5, 14, 25} anos.

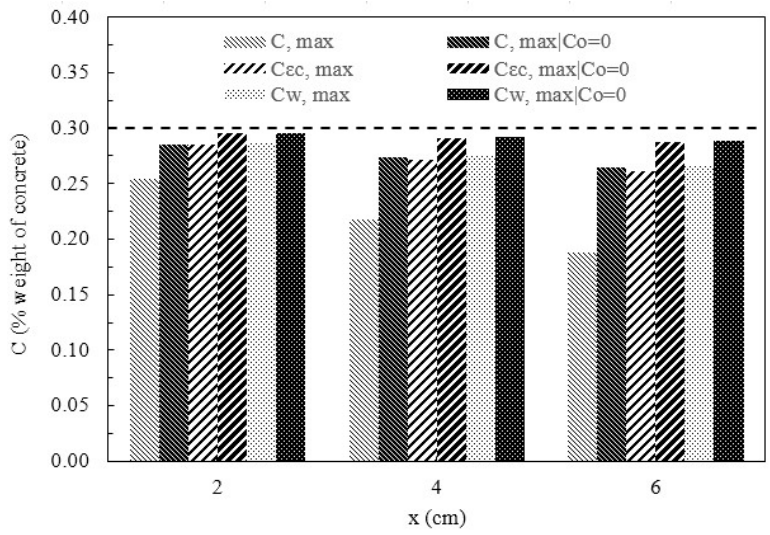

Figura 20 – Concentração máxima de cloretos com $C_0 = 0$ e $C_0 = 5$ kg/m^3 para x = {2, 4, 6} cm e t = 25 anos.

Nesta análise, foi considerado o estado não estacionário da difusividade dos cloretos. A condição do estado estacionário (i.e. Eq. (2) → $\nabla(D_{cl,i})\nabla C_i = 0$) pode ser razoavelmente assumida quando são estudados os efeitos a longo prazo. A difusividade dos cloretos para uma condição não estacionária é cerca de 10 vezes maior que na condição estacionária (HOMAN et al., 2016).

Neste estudo, apenas as deformações de compressão foram consideradas. Na literatura (YE et al., 2015), mostra-se que, para baixos valores de deformação, a tensão de compressão atua

coerentemente com os resultados mostrados neste trabalho, ou seja, influenciando positivamente o processo de acúmulo de concentração de íons cloretos, pois aumentando D_{cl}, a concentração C diminui. Mas, quando a tensão de compressão ultrapassa certo valor esta influência poderia passar a ser negativa, diminuindo D_{cl} e aumentando C. No entanto este último aspecto não foi considerado neste estudo.

Outro efeito negativo é visto também quando os elementos de concreto são sujeitos a carregamento por tração, como mostrado pela literatura (YE et al., 2015), no entanto este efeito não é objeto deste estudo.

5.3 Efeitos da Flutuação das Ações Externas na Concentração de Íons Cloretos (Objetivo III)

A Figura 21 mostra as soluções exatas analíticas e numéricas obtidas considerando o modelo para $f_D(x,t)$ constante, i.e. $f_D(x,t) = 1,0$ (ver Tabela 3). São mostrados os gráficos completos (C, x, t) e as seções transversais (C vs. x e C vs. t) para cada t e x pré-definido.

Utilizando este tipo de função, a difusividade D_{cl} não é dependente do tempo t, portanto será possível fazer uma comparação dos dois modelos de forma coerente. Isso porque a solução analítica tradicional considera a difusividade D_{cl} constante no tempo t.

Para todas as análises numéricas o valor da difusividade é $D_{cl} = 24,28$ cm^2/ano que corresponde ao valor máximo mostrado na Fig. 15 considerando os carregamentos. Os parâmetros usados para obter este valor estão na Tabela 1.

A solução exata de C(x,t), dada pelas Eq. (2) e Eq. (5) é calculada dentro de um intervalo $0 \leq t \leq t_{final}$ e $0 \leq x \leq x_{final}$; enquanto a solução numérica de C(x,t), dada pela Eq. (2) e Eq. (25), é calculada dentro de um intervalo $0 \leq t_m \leq t_{m,final}$ e $0 \leq x_m \leq x_{m,final}$. Os intervalos utilizados são: $t_{final} = t_{m,final} = 2\pi$ anos e $x_{final} = x_{m,final} = 6$ cm.

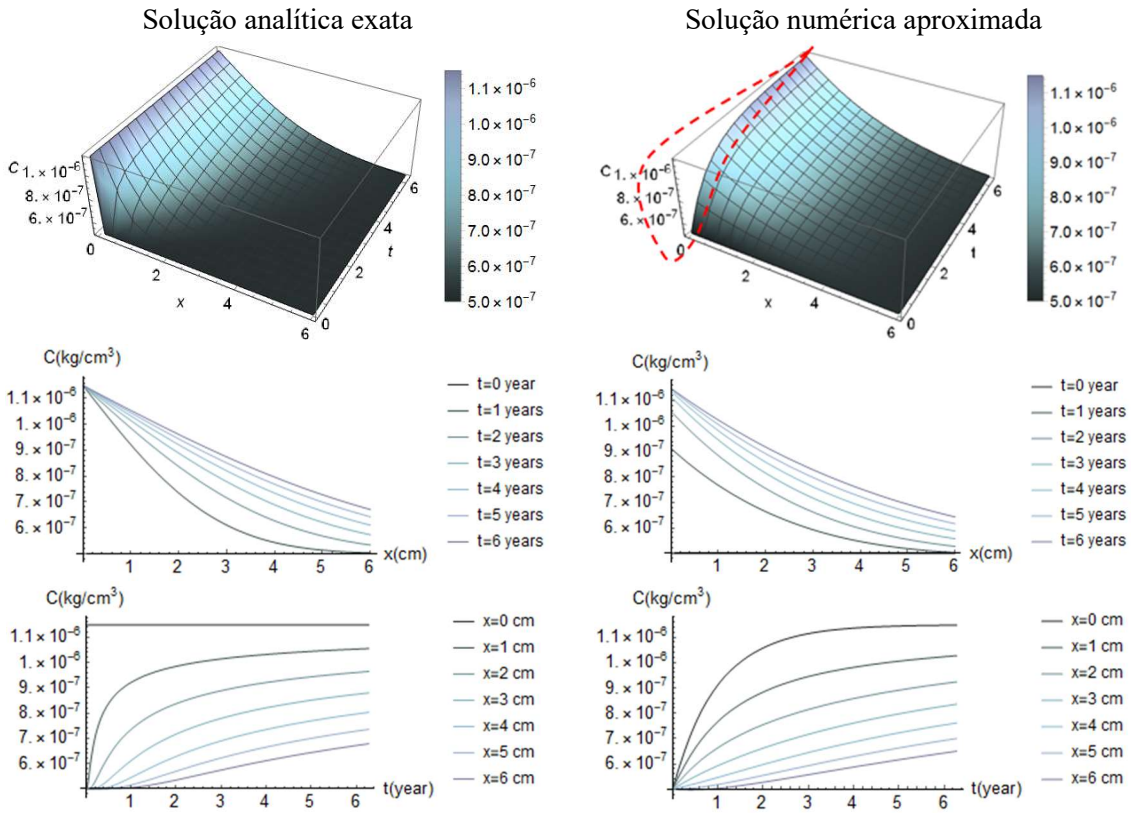

Figura 21 – Solução exata analítica e numérica para $f_D(x,t)$ constante. As curvas variam segundo o intervalo adotado: $\{0 \leq t \leq 2\pi$ anos, com passo de tempo dt = 1 ano$\}$ e $\{0 \leq x \leq 6$ cm, com passo de posição dx = 1 cm$\}$.

Para obter a solução numérica, é necessário definir o b.c. (ver Eq. (25)) em $C(x_m, t_m) = C_0$; em particular é necessário definir *a priori* o termo x_m. Com uma distância máxima de $x_m = 20 \times x_{m,final}$, foi obtida uma boa convergência conforme as metodologias mostrada na seção 4.2.

Comparando as duas análises é possível notar algumas diferenças e fazer algumas considerações. A primeira consideração é que os comportamentos das curvas nos resultados numéricos aproximados, tanto na curva C vs. x quanto na curva C vs. t, são parecidas aos resultados analíticos exatos. No entanto há algumas diferenças que podem ser explicadas nos pontos a seguir.

- Na análise numérica aproximada, nas curvas C vs. x, em x = 0, a concentração C não coincide com C_s. Isso está ligado ao fato de que nas curvas C vs. t a análise numérica fornece uma curva para todos os valores de x definidos deixando uma região vazia (marcada em vermelho pontilhado) entre t = 0 – 3 anos. Outro fator que contribui para acentuar esta diferença está ligado às condições de contorno b.c. que vinculam as

curvas nas duas extremidades fixadas: a interpolação numérica começa em x_{final} e termina em x = 0, restringindo o espaço para poder gerar números que representam as curvas (PELLIZZER, 2019).

- Em virtude do ponto precedente, a análise numérica aproximada não é vantajosa para uma representação C vs. x para t = 0 – 3 anos. No entanto, resulta mais precisa para t > 3 anos quando $C \approx C_s$ (ver Fig. 25) e resulta vantajosa para uma representação C vs. t para x = 0 cm. De fato a análise exata fornece uma única linha horizontal coerente com a Eq. (5), pois para x = 0, $C(x, t) = C_s$, mas sem conseguir mostrar as variações que C tem no tempo t acumulando íons cloretos nas superfícies externas do concreto. A análise exata não mostra a curva C vs. x para t = 0, pois para t = 0, erf $(\infty) \rightarrow 1$ e $C(x, t) = C_0$. Isso é coerente com a Eq. 5, no entanto não permite quantificar uma curva no tempo t; aspeto que uma análise numérica permitiria.

- Finalmente, uma análise numérica permite calcular com boa aproximação em termos de comportamento das curvas C vs. t e C vs. t e em termos de valores, as concentrações de íons cloretos C com uma difusividade que depende do tempo t. Isso torna possível quantificar de forma mais completa o processo de difusão e considera eventuais ações externas que afetam a difusividade. Esta forma poderia permitir evitar estimações imprecisas e/ou subestimadas de D_{cl} e, consequentemente, de C.

As Figuras 22, 23 e 24 mostram as soluções analíticas exatas para $f_D(x,t)$ constante e as soluções numéricas aproximadas para $f_D(x,t)$ no caso de assumir uma forma senoidal, gaussiana ou geral, respetivamente. O valor da difusividade de pico é $D_{cl} = 24{,}28$ cm^2/ano como mostrado na Fig. 15.

Solução analítica exata | Solução numérica aproximada

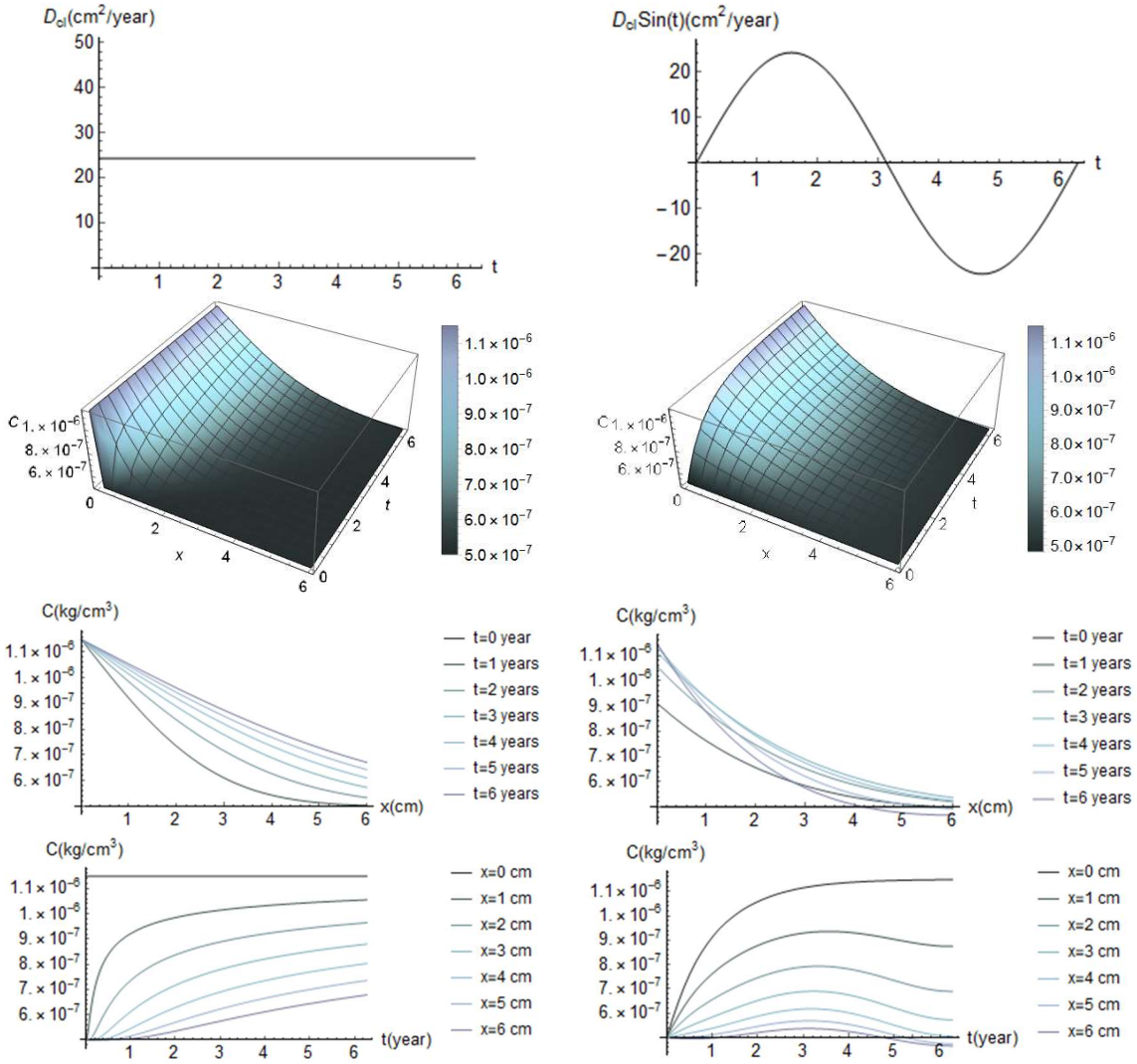

Figura 22 – Solução exata para $f_D(x,t)$ constante e numérica para $f_D(x,t)$ senoidal. Acima é mostrado o andamento da difusividade D_{cl} considerado. Curvas que variam no intervalo adotado: $\{0 \leq t \leq 2\pi$ anos, com passo de tempo dt = 1 ano$\}$ e $\{0 \leq x \leq 6$ cm, com passo de posição dx = 1 cm$\}$.

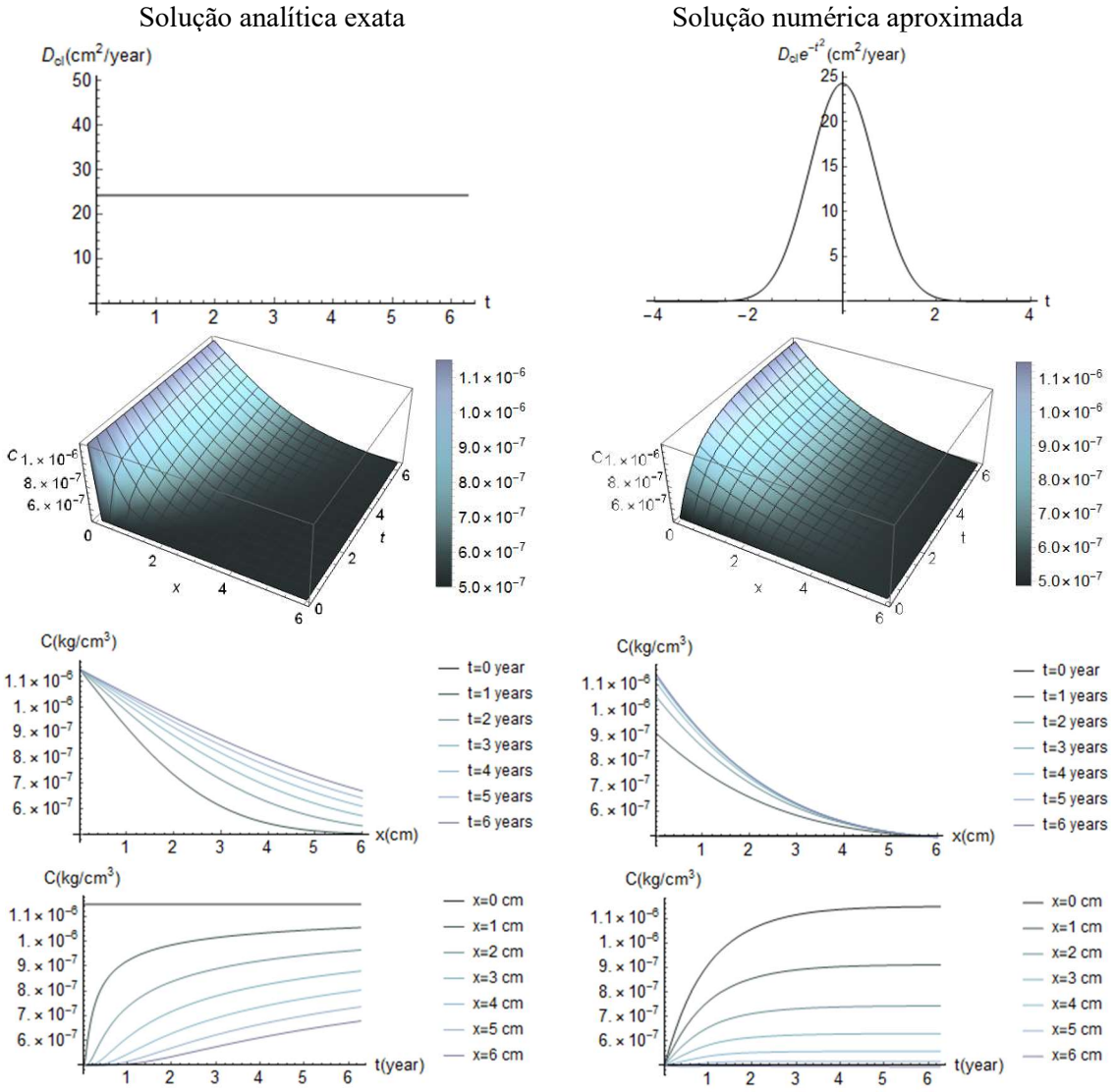

Figura 23 – Solução exata para $f_D(x,t)$ constante e numérica por $f_D(x,t)$ Gaussiano. Acima é mostrado o andamento da difusividade D_{cl} considerado. Curvas que variam no intervalo adotado: $\{0 \leq t \leq 2\pi$ anos, com passo de tempo dt = 1 ano$\}$ e $\{0 \leq x \leq 6$ cm, com passo de posição dx = 1 cm$\}$.

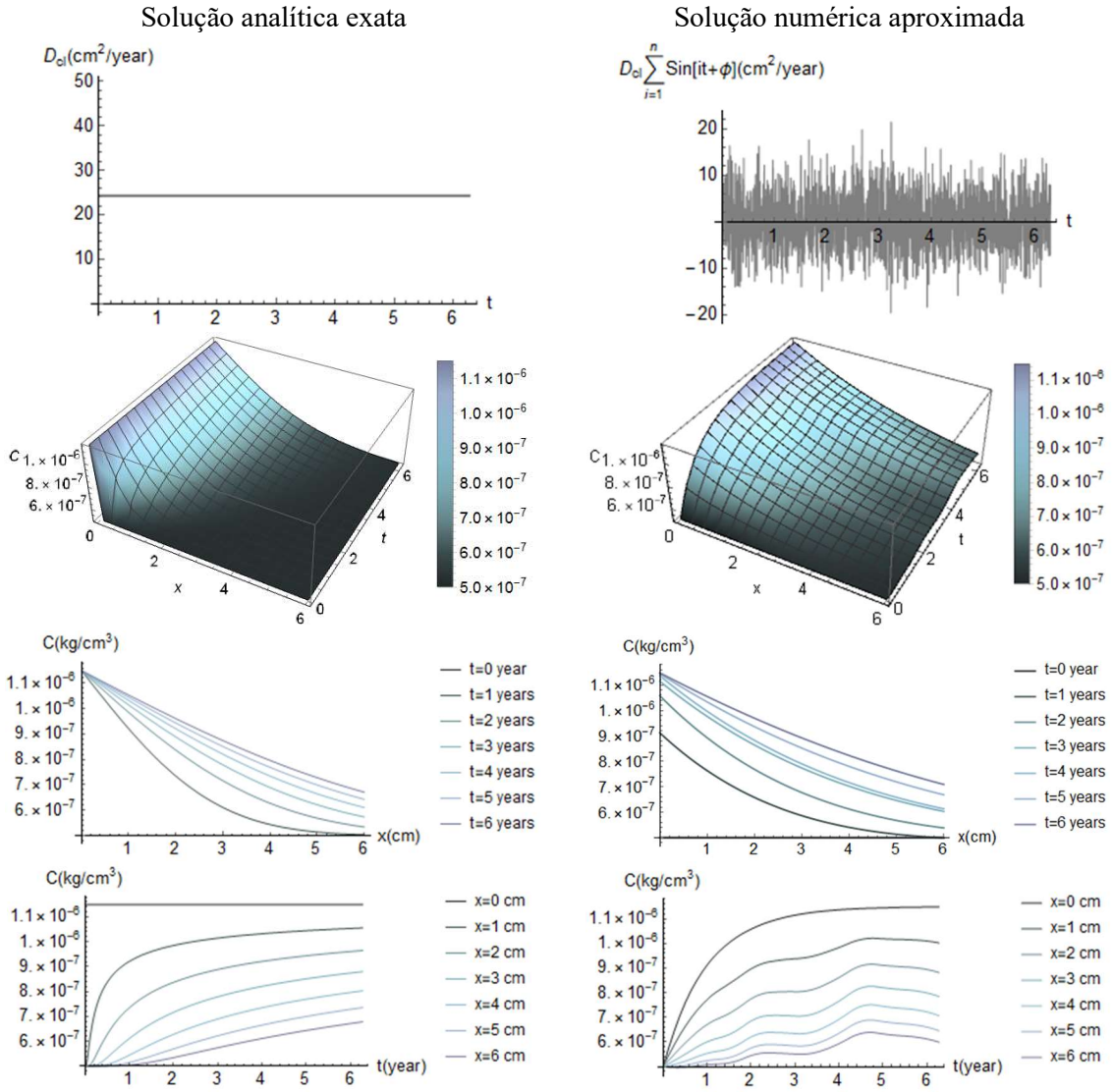

Figura 24 – Solução exata para $f_D(x,t)$ constante e numérica por $f_D(x,t)$ geral. Acima é mostrado o andamento da difusividade D_{cl} considerado. Curvas que variam no intervalo adotado: $\{0 \leq t \leq 2\pi$ anos, com passo de tempo dt = 1 ano$\}$ e $\{0 \leq x \leq 6$ cm, com passo de posição dx = 1 cm$\}$

Na Fig. 25 é mostrado o erro relativo calculado como a concentraçao dos cloretos obtidos pela soluçao analítica menos a concentraçao dos cloretos obtidos pela soluçao numérica. Esta diferencia foi dividida por esta última concentraçao para fornecer os valores em temos percentuais. Portanto a relação é: $(C_{Es} - C_{Ns})/C_{Es}$. São mostrados os erros relativos por cada t e cada x nos casos com f_D constante e geral. Os resultados mostram como as duas soluções se aproximam muito para t > 3 anos e que para x = 6 cm o erro é muito baixo e inferior a 5%.

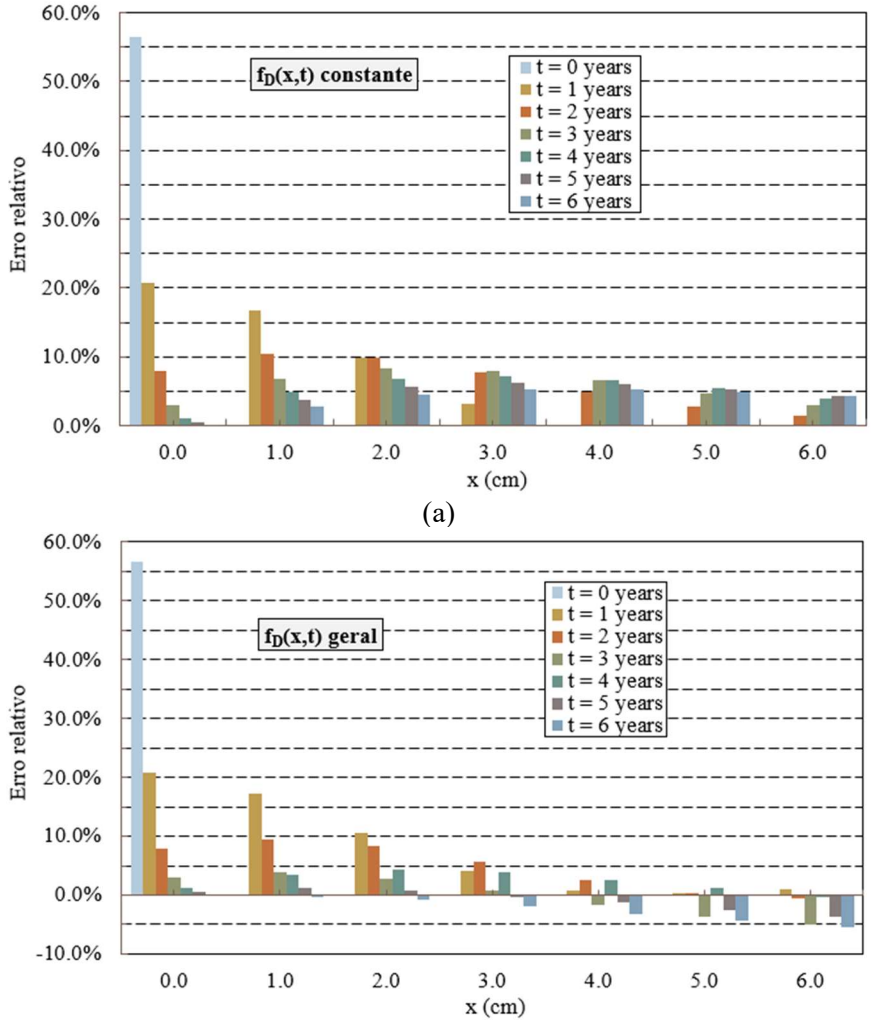

Figura 25 – Erro relativo entre as análises exata e numérica para $f_D(x,t)$ constante (a) e geral (b).

Comparando as soluções numéricas aproximadas com as soluções analíticas exatas, para vários D_{cl} mostrados nas Figuras 22, 23 e 24, é possível fazer as seguintes considerações.

- As flutuações D_{cl} impostas são funções dependentes do tempo t e isso afeta as flutuações de C, que é função tanto da posição x quanto do tempo t. Isso é mais evidente nas curvas C vs. t, mas também nas curvas C vs. x, pois em alguns casos as curvas podem cruzar uma com outra exatamente por essa variabilidade do tempo t. Além disso, as curvas C vs. t assumem um comportamento coerente com as flutuações D_{cl} impostas. Isso é visível nas curvas C vs. t.

- Devido as variabilidades do tempo t na difusividade D_{cl}, a concentração de íons cloretos C pode assumir valores mais baixos em relação à concentração de íons cloretos C com difusividade constante. Este é uma vantagem das elaborações através de soluções numéricas, pois permitem estimar de forma mais completa a contribuição da difusividade D_{cl} no tempo t. Isso é mostrado em todos os casos e representa uma redução do processo de acúmulo dos íons cloretos C dentro dos elementos de concreto que leva, portanto, a um aumento no tempo de início de corrosão, pois C atinge as armaduras em tempos maiores.

Até aqui foram feitas análises mostrando resultados para poder quantificar de uma forma mais completa a difusividade D_{cl}. Foi usada a equação multifatorial (ver Eq. (6)) para considerar os fatores que dependem da capacidade de ligação dos cloretos, da temperatura, da idade do concreto e do estado de tensão-deformação. Foi considerada também a umidade numa outra equação multifatorial (ver Eq. (17)).

Depois, na Eq. (19), foi introduzido um novo fator que leva em conta as fissurações w na difusividade.

Considerando estes aspetos sobre a estimação da difusividade, na análise numérica foi possível otimizar D_{cl} para quantificar uma baixa concentração de íons cloretos C.

Uma vez obtidos todos esses resultados que definem de forma mais abrangente a difusividade D_{cl}, torna-se possível estimar cenários de início de corrosão de uma forma mais geral, considerando aspectos probabilísticos. Os resultados a seguir apresentam a análise probabilística, para diferentes cenários, do tempo de início de corrosão considerando as informações sobre a difusividade D_{cl} obtidas até aqui.

5.4 Coeficiente de Difusão de Cloretos no Concreto Probabilístico (Objetivo IV)

A Figura 26 apresenta quatro cenários usando os três métodos adotados nesse trabalho: MCS, DI e FORM. Nesta análise probabilística a difusividade D_{cl} foi calculada segundo a Eq. (17) para poder estimar a contribuição de alguns parâmetros mais impactantes na difusividade como T, C_f, h. De fato, este último fator, a umidade h, não é um fator incluído na Eq. (6). Desta forma foram considerados todos os fatores existentes que influenciam a difusividade D_{cl}.

Como já escrito, o valor de referência f_{wc} da Eq. (17) é definido por uma relação analítica muito simplificada, portanto é possível para este fator adotar um parâmetro obtido pela literatura. Nesta análise probabilística foi usado o valor de f_{wc} = 41,0 mm^2/ano (NOGUEIRA et al., 2012).

Vale ressaltar que na difusividade D_{cl} calculada pela Eq. (17) também não inclui carregamentos.

O cenário I é calculado usando os valores mostrados nas Tabelas 4 e 5. No cenário II, apenas a temperatura T foi alterada; no cenário III, os parâmetros alterados são T e C_f; no cenário IV a umidade h sofreu a variação. Relembrando alguns parâmetros chaves, é necessário definir que os cenários analisados se referem a uma distância x = 5,0±1,5 cm com um C_{th} = 3,75 kg/cm^3 calculado de forma semi-probabilística, pois foi obtido pelas Eqs. (3)-(4) e inserido na Eq. (24).

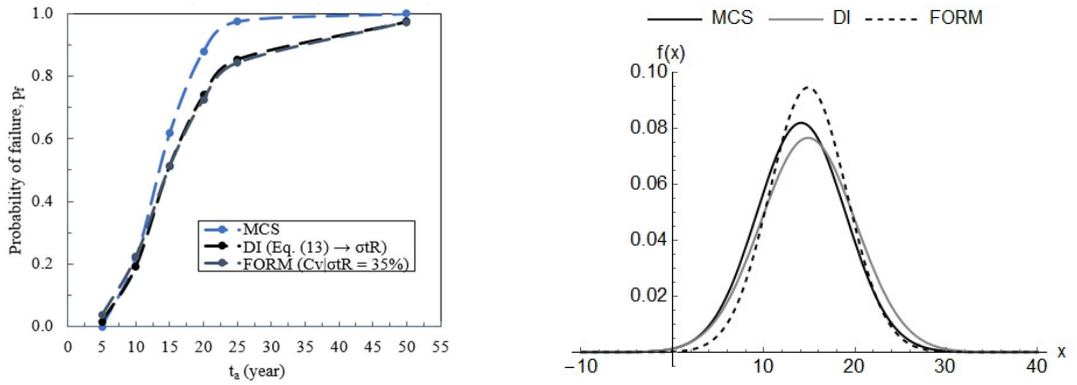

Cenário I: Valores da Tabela 5. D_{cl} = 49,36 mm²/ano.

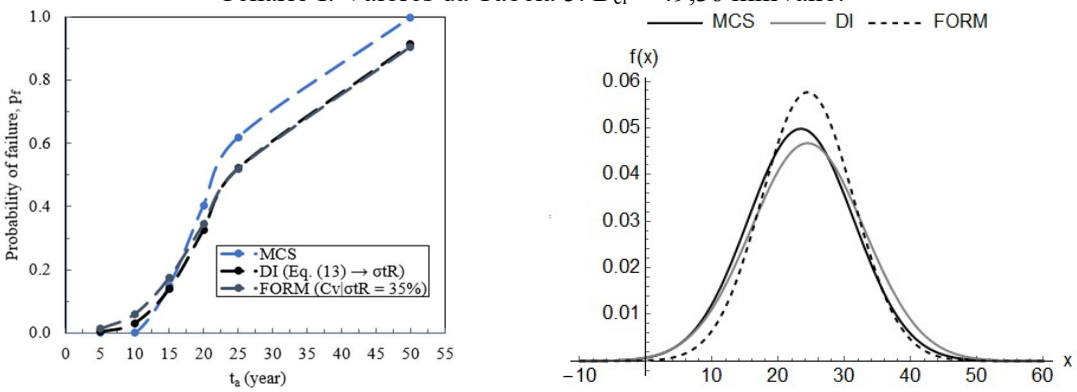

Cenário II: Valores da Tabela 5, porém com T = 288±8 K. D_{cl} = 29,99 mm²/ano.

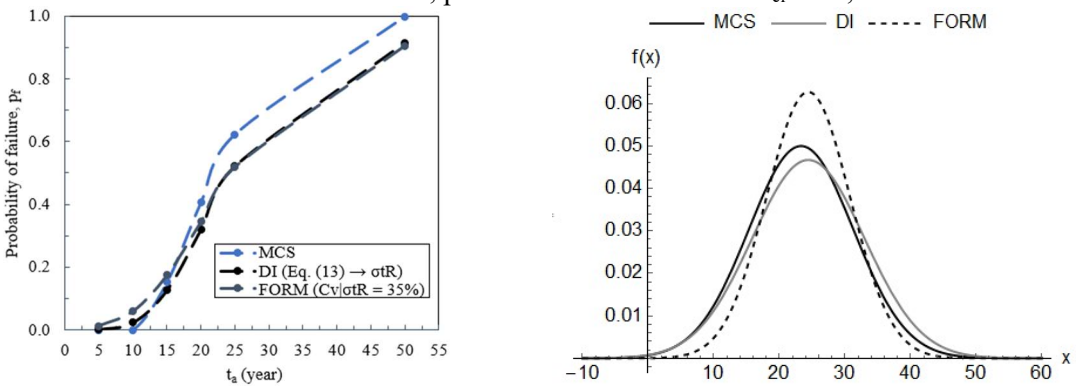

Cenário III: Valores da Tabela 5, porém com T = 288±8 K e C_f = 2,25 kg/m³. D_{cl} = 29,99 mm²/ano.

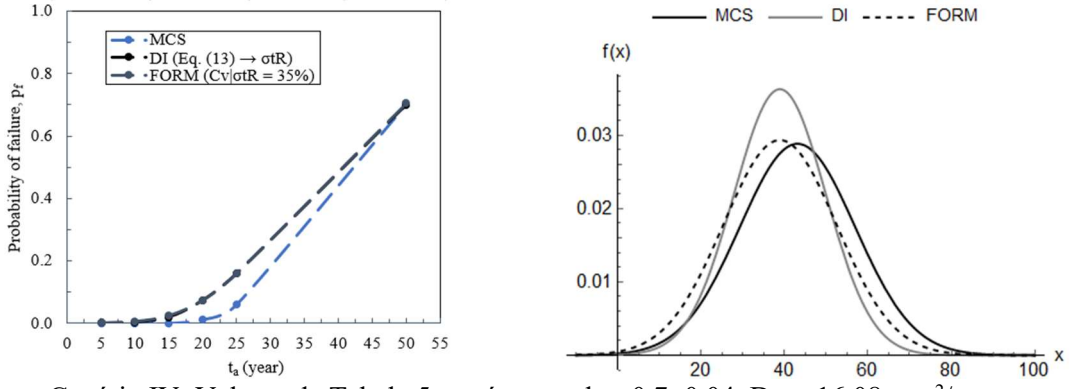

Cenário IV: Valores da Tabela 5, porém com h = 0,7±0,04. D_{cl} = 16,08 mm²/anos.

Figura 26 – Resultados dos quatro cenários em x = 5,0±1,5 cm com um C_{th} = 3,75 kg/cm³. Probabilidade de falha em função de t_a (esquerda) e PDFs dos valores médios (ver Tabela 6) dos três métodos (direita).

Os dados de entrada, na análise MCS, para plotar as curvas p_f em função de t_a são obtidos diretamente pela Eq. (23), enquanto nas análises via FORM e DI é necessário definir μ_{tR} e σ_{tR} para estimar o índice de confiabilidade β e depois quantificar p_f. Em DI, as estatísticas do tempo de início de corrosão t_R, i.e. μ_{tR} e σ_{tR} são obtidos pela Eq. (24) usando os valores das Tabelas 4 e 5.

Já no FORM, μ_{tR} é o mesmo do DI, mas σ_{tR} é considerado como 34,13% → 35% de μ_{tR} (i.e. $CV|\sigma_{tR} = 35\%$). Esse valor de coeficiente de variação foi obtido a partir das estatísticas da função de variáveis aleatórias que definem $t_R(X)$.

Como já escrito, foi escolhido um único fator, $t_R(X)$ dado pela Eq. (24), que une os parâmetros calculados de forma determinística e probabilística o qual representa o tempo necessário para o início da corrosão. Portanto este $t_R(X)$ é uma função de variáveis aleatórias que inclui um conjunto de parâmetros, sendo descrito na forma Gaussiana. Assim, este é o termo chave da análise probabilística.

Esta metodologia de fornecer um único termo através de uma única curva PDF foi também adotada na literatura (WANG et al., 2018).

A Tabela 6 mostra os valores médios e seu desvio padrão, $\mu_{tR} \pm \sigma_{tR}$, dos três métodos utilizados para cada cenário. As curvas foram mostradas na Fig. 26 (direita).

Tabela 6 – Parâmetros das PDFs.

	$\mu_{tR} \pm \sigma_{tR}$ (anos)		
Cenário	MCS	FORM	DI
I	13,77±4,57	12,35±4,32	12,35±3,49
II	23,39±8,01	20,83±7,29	20,83±5,89
III	23,32±7,98	20,83±7,29	20,83±5,43
IV	43,09±13,84	38,87±13,60	38,87±11,0

É possível observar que, para uma previsão em longo prazo (i.e. $t_a > 30$ anos) é mais difícil estimar a probabilidade de falha. Portanto, as três curvas tendem a se afastar uma com a outra. A partir de $t_a = 15$ anos, a curva MCS tende a se afastar em relação à curva DI, que deveria representar a solução analítica. No entanto, a curva obtida pelo método DI é muito

sensível aos valores de μ_{tR} e σ_{tR} adotados (ver Tabela 6) que, *a priori*, são desconhecidos e, consequentemente, pode superestimar ou subestimar os resultados.

Para o método MCS, o formato das PDFs depende do número de amostras usadas: quanto menor os números de amostras, maior será a dispersão. Além disso, os resultados do MCS estão estritamente correlacionados com a escolha do valor de CV adotado para cada variável: se o CV for grande, a dispersão também será grande.

Em geral, os pontos onde há proximidade entre as curvas, indicam que os dados tendem a ser próximos da média e, portanto, a estimativa tem uma boa calibração (ZACCHEI e MOLINA, 2018).

Ainda na Figura 26, para os cenários II e III, é possível observar que a p_f é menor que o valor de p_f do cenário I: as curvas dos cenários II e III são mais achatadas. Isso mostra a importância da variação da temperatura. Ao contrário, a variação de C_f não é tão influente.

Finalmente, a Figura 27 mostra a probabilidade de falha pare os três tipos de coeficientes de difusão. Um deles é aquele calculado de forma probabilística usada na Figura 26, enquanto os outros dois foram calculados de forma determinística, conforme mostrado na Figura 15. Para essas análises, somente os métodos MSC e FORM foram adotados.

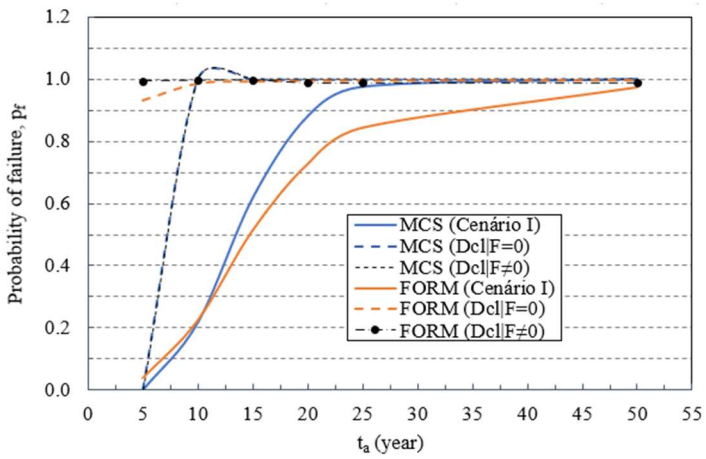

p_f com a difusividade do cenário I (Fig. 26) vs. difusividades da Fig. 15.

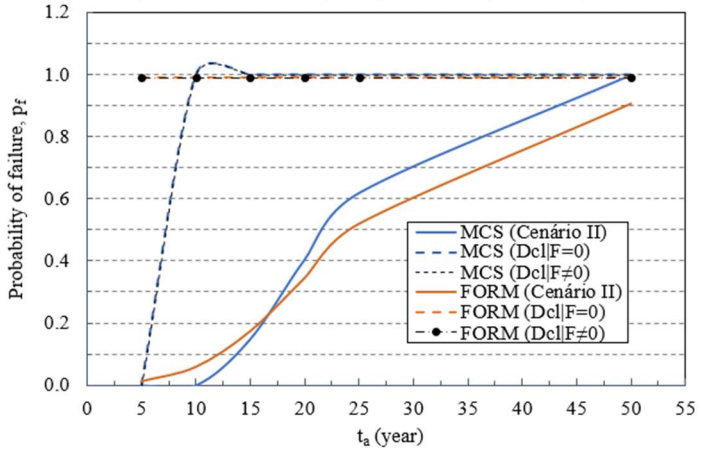

p_f com a difusividade do cenário II (Fig. 26) vs. difusividades da Fig. 15.

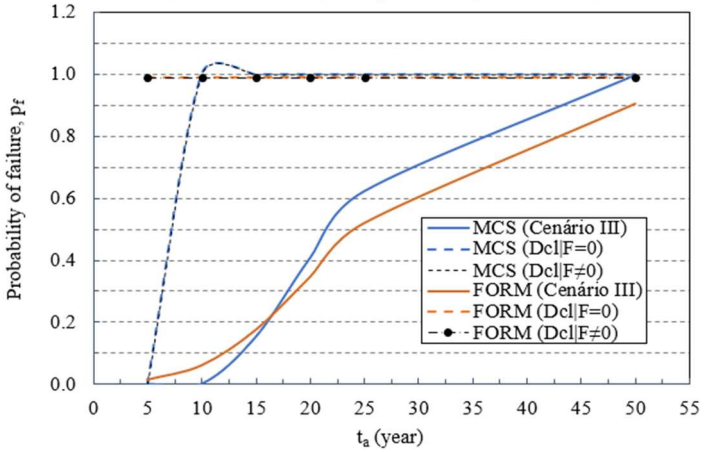

p_f com a difusividade do cenário III (Fig. 26) vs. difusividades da Fig. 15.

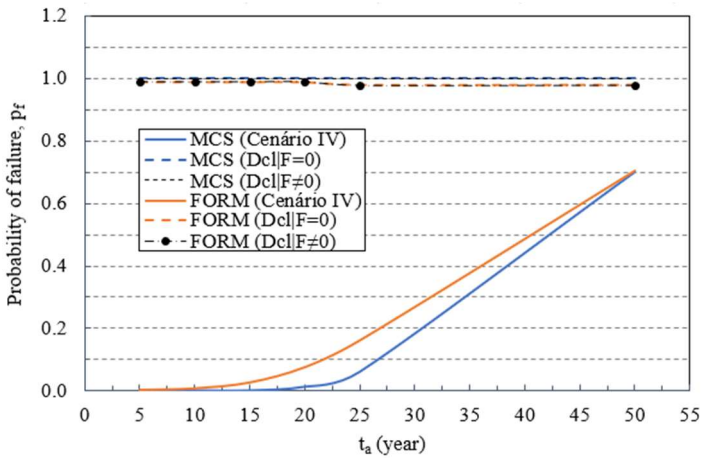

p_f com a difusividade do cenário IV (Fig. 26) vs. difusividades da Fig. 15.

Figura 27 – Comparação da probabilidade de falha usando três tipos de coeficientes de difusão: um D_{cl} para cada cenário usado na Figura 26 e dois D_{cl} mostrados na Figura 15. Cálculo em x = 5,0±1,5 cm com um C_{th} = 3,75 kg/cm^3

O comportamento das curvas na Figura 26 é similar ao comportamento das curvas obtidas na Figura 25. Os resultados na Figura 26 mostram que a probabilidade de falha p_f para $D_{cl|F\neq0}$ assume o valor igual a 1,0 já a partir de t_a = 5 anos. Isso porque este coeficiente de difusão, como já mostrado, considera os efeitos de tensão-deformação e o efeito do dano que contribuem a aumentar muito a concentração de cloretos no interior do concreto.

No caso da probabilidade de falha p_f para $D_{cl|F=0}$ as curvas chegam rapidamente ao valor de 1,0. Isso pode ser atribuído ao fato que este fator é obtido por uma análise determinística que sobrestima o valor do coeficiente de difusão.

Na literatura (WANG et al., 2018) foi estimada, através de experimentos em laboratórios, a probabilidade de falha p_f em função do tempo de início de corrosão t_a para difusividade que leva em conta os carregamentos externos e para uma difusividade sem carregamentos. Há diferença de até 6 anos conforme o cenário I, que representa o cenário pior, na Fig. 27. No presente estudo esta diferença pode ser maior que 6 anos, por exemplo no cenário III, isso porque a relação máxima entre a difusividade com carregamento e sem carregamento é da ordem de 9 enquanto na literatura (WANG et al., 2018) foi usado uma única relação de 1.76.

É importante ressaltar que os resultados são puramente teóricos, pois não foram confeccionados modelos de vigas reais, nem foram realizados testes em laboratório. No entanto, os valores de entrada (valores mostrados no Capítulo 4) e de saída (valores mostrados no Capítulo 5) poderiam ser utilizados para qualquer estrutura de concreto, desde que respeitadas às condições impostas nos Capítulos 2 e 3.

6 CONCLUSÕES

Este trabalho avaliou a difusividade de íons cloretos em estruturas de concreto armado, considerando diversos aspectos na composição do coeficiente de difusão de cloretos no concreto. As conclusões acerca dos quatro objetivos propostos estão listadas abaixo.

1) A teoria clássica de Fick, que adota D_{cl} constante, conduz a uma estimativa da concentração de íons cloretos que não representa a dependência que há entre diversos fatores interligados que variam no tempo e no espaço. Conforme mostrado, o coeficiente de difusão de cloretos no concreto D_{cl} depende fortemente do estado de tensão-deformação do concreto, sendo que essa dependência é geralmente ignorada. Nas análises realizadas, foi estimado que a razão $D_{cl|F=0}/D_{cl,max|F\neq0} = 1/8{,}95 = 0{,}112$. Estes resultados indicam que o coeficiente de difusão de cloretos no concreto pode ser muito maior do que o valor constante normalmente adotado.

2) Nas construções reais, as solicitações de cargas externas induzem, durante a execução e ao longo da vida útil da estrutura, panoramas de fissuração. As fissuras reduzem a durabilidade dos elementos de concreto, pois criam caminhos preferenciais para a penetração dos íons cloretos. Para quantificar a difusão de cloretos considerando a presença de fissuras, foi introduzida uma função que considera a largura da fissura *w*. Os resultados mostraram que o coeficiente de difusão de cloretos no concreto relacionado à fissuração é $D_w \approx (0{,}872 - 1{,}297) \times D_{cl|F\neq0}$. A diferença observada do conteúdo de cloretos considerando o efeito dos carregamentos e desprezando o efeito dos carregamentos em x = 6 cm por 5, 14 e 25 anos foi de 3,2; 2,32 e 1,85 kg/m^3, respectivamente. Esses resultados mostram um grande aumento do conteúdo de cloretos devido à influência dos carregamentos externos. Além disso, a difusão dos cloretos é muito mais rápida em um intervalo de 0 a 5 anos; por exemplo, em x = 2 cm o conteúdo de cloretos atinge 0,20% do peso específico do concreto (ver Fig. 18). Estes resultados foram obtidos comparando o que se obteve neste trabalho com os estudos

encontrados na literatura (DJERBI et al., 2008; ZHANG et al., 2011; JUNG et al., 2017; YANG et al., 2017).

3) Foram encontradas soluções numéricas para estudar o comportamento de $D_{cl,i}$ para diferentes carregamentos. As funções que representam uma difusividade flutuante são de tipo senoidal, gaussiana e geral. Uma comparação entre o coeficiente de difusão constante e não constante é realizada através da introdução de uma função genérica $f_D(x,t)$. Isso é possível através do desenvolvimento de uma solução numérica com condições de contorno pré-definidas. Desta forma, é possível simular diferentes tendências de movimento de uma única partícula de íon cloreto correlacionada a uma carga externa para o interior do concreto. Esta análise pode quantificar melhor um acúmulo em excesso de íons cloretos. Os resultados mostraram que um D_{cl} constante pode subestimar a difusividade, portanto, pode sobrestimar o conteúdo de cloretos nas estruturas. De fato, o conteúdo de íons cloretos, variando no tempo, assume valores mais baixos do que para coeficiente de difusão constante. Aqui o D_{cl} varia entre $1{,}1 \times 10^{-6}$ kg/cm^3 em x = 0 cm e $5{,}0 \times 10^{-7}$ kg/cm^3 em x = 6 cm. Neste sentido estes resultados poderiam fornecer uma contribuição em relação aos trabalhos na literatura (BASTIDAS-ARTEAGA et al., 2011; 2013).

4) A análise de confiabilidade foi realizada usando 1×10^6 simulações para cada variável aleatória. Os resultados são apresentados em termos de conteúdo de cloretos e de probabilidade de falha. O parâmetro estudado é a previsão do início da corrosão, pois é um fator importante nas previsões de danos, estimativa de vida útil e redução das resistências em elementos estruturais de concreto armado. Nesta análise, a função de estado limite é escrita como a diferença entre o tempo para o início da corrosão t_R e o tempo de vida estrutural esperada no projeto t_a como $G(X) = t_R(X) - t_a$. O parâmetro t_R é estimado usando três métodos: MCS, FORM e DI. Novos dados determinísticos e probabilísticos foram fornecidos para as análises realizadas neste trabalho (ver Tabelas 4 e 5). Esses dados foram coletados na literatura conforme citado e foram reajustados para realizar uma análise mais apropriada. Os valores esperados e seu desvio padrão dos quatro cenários são mostrados na Tabela 6. O μ_{tR} e o σ_{tR} dos cenários II e III são superiores a 39% e 51-71%, respetivamente, em relação ao cenário I. Nesse sentido, esses três cenários mostram a importância da variação de temperatura e C_f. O cenário IV mostra, em vez, uma significativa oscilação com pequenas variações de umidades. Finalmente, a probabilidade de falha é calculada em um intervalo de 0 a 50 anos,

mostrando uma boa calibração entre os métodos em um intervalo de 5 a 20 anos. Nestes sentidos estes resultados fornecem uma contribuição aos trabalhos encontrados na literatura (NOGUEIRA et al., 2012; 2012). Em particular, a Tabela 6 reuniu as medidas de tendência central e dispersão da variável aleatória tempo de início de corrosão para cada cenário analisado. Essas estatísticas permitem, para os dados considerados neste estudo, avaliar diretamente e de forma muito simples a probabilidade do tempo de início de corrosão para um dado tempo de vida útil da estrutura. É importante ressaltar que tais resultados foram obtidos considerando o modelo multifatorial descrito, com o coeficiente de difusão do concreto calibrado com base na análise numérica apresentada. Assim, foi possível considerar todos os fatores ambientais na análise probabilística, a partir da segunda lei de Fick, com um coeficiente de difusão "equivalente". Essa metodologia pode ser usada com os dados de interesse de uma determinada região em que se executará a edificação, para obter as estatísticas do tempo de início de corrosão e fazer as previsões probabilísticas de início do fenômeno, considerando o tempo de vida desejado para a estrutura.

7 BIBLIOGRÁFIA

ABABNEH, A.; SHEBAN, M. Impact of mechanical loading on the corrosion of steel reinforcement in concrete structures. Mat. Stru., v. 44, p. 1123-1137, 2011.

ALAFOGIANNI, P.; DASSIOS, K.; TSAKIROGLOU, C. D.; MATIKAS, T. E.; BARKOULA, N. M. Effect of CNT addition and dispersive agents on the transport properties and microstructure of cement mortars. Constr. Build. Mat., v. 197, p. 251-261, 2019.

AL-KUTTI, W. A.; RAHMAN, M. K.; SHAZALI, M. A.; BALUCH, M. H. Enhancement in chloride diffusivity due to flexural damage in reinforced concrete beams. J. Mater. Civ. Eng., v. 26, p. 658-667, 2014.

APOSTOLOPOULOS, C. A.; PAPADAKIS, V. G. Consequences of steel corrosion on the ductility properties of reinforcement bar. Constr. Build. Mat., v. 22, p. 2316-2324, 2008.

AutoCAD. Version 2010, Autodesk, Inc., 2010.

BASTIDAS-ARTEAGA, E.; CHATEAUNEUF, A.; SÁNCHEZ-SILVA, M.; BRESSOLETTE, P.; SCHOEFS, F. A comprehensive probabilistic model of chloride ingress in unsaturated concrete. Eng. Struct., v. 33, p. 720-730, 2011.

BASTIDAS-ARTEAGA, E.; SCHOEFS, F.; STEWART, M. G.; WANG, X. Influence of global warning on durability of corroding RC structures: a probabilistic approach. Engineering Structures, v. 51, p. 259-266, 2013.

BAŽANT, Z. P.; NAJJAR, L. J. Nonlinear water diffusion in nonsaturated concrete. Matériaux et Constructions, v. 5, p. 3-20, 1972.

BEN-FRAJ, A.; BONNET, S.; KHELIDJ, A. New approach for coupled chloride/moisture transport in non-saturated concrete with and without slag. Construction and Building Materials, v. 35, p. 761–771, 2012.

BENTZ, D. P.; DETWILER, R.J.; GARBOCZI, E.J.; HALAMICKOVA, P.; SCHWARTZ, L.M. In: Nilsson, L. O.; Ollivier, J. P. (Edit.). Proceedings of Chloride Penetration into Concrete. Rilem, 1997, p. 1-6.

BENTZ, D. P.; GUTHRIE, W. S.; JONES, S. Z. Jones; MARTYS, N. S. Predicting service life of steel-reinforced concrete exposed to chlorides. Conc. Int., v. 36, p. 55-64, 2014.

CAPOZUCCA, R. Damage to reinforced concrete due to reinforcement corrosion. Construction and Building Materials, v. 9, p. 295-303, 1995.

CARRARA, P.; DE LORENZIS, L.; BENTZ, D. P. Chloride diffusivity in hardened cement paste from microscale analyses and accounting for binding effects. Model. Simul. Mat. Sci. Eng., v. 24, p. 1-44, 2016.

CHEN, W.; ZHANG, J.; ZHANG, J. A variable-order time-fractional derivative model for chloride ions sub-diffusion in concrete structures. Fract. Calc. Appl. Anal., v. 16, p. 76-92, 2013.

CLOUGH, R.W.; PENZIEN, J. Dynamics of Structures, 1. ed. New York: McGraw-Hill, 1976.

COMITE EURO-INTERNATIONAL DU BETON (CEB). Durable Concrete Structures, Bulletin d'Information, No. 183, 1992.

CRANK, J. The Mathematics of Diffusion, 2. ed. Oxford: Clarendon Press, 1975.

DAMRONGWIRIYANUPAP, N.; LIMKATANYU, S.; XI, Y. thermo-hygro-coupled model for chloride penetration in concrete structures. Hind. Publis. Corp., v. 2015, p. 1-10, 2015.

DATTOLI, G. Generalized polynomials, operational identities and their applications. Journal of Computational and Applied Mathematics, v. 118, p. 111-123, 2000.

DJERBI, A.; BONNET, S.; KHELIDJ, A.; BAROGHEL-BOUNY, V. Influence of traversing crack on chloride diffusion into concrete. Cem. Concr. Resea., v. 38, p. 877-883, 2008.

EL HASSAN, J.; BRESSOLETTE, P.; CHATEAUNEUF, A.; EL TAWIL, K. Reliability-based assessment of the effect of climatic conditions on the corrosion of RC structures subject to chloride ingress. Eng. Struct., v. 32, p. 3279-3287, 2010.

EUROPEAN COMMITTEE FOR STANDARDIZATION (CEN). Concrete - Part 1: Specification, performance, production and conformity, BS EN 206-1:2000, Brussels, Belgium, 2000.

EUROPEAN COMMITTEE FOR STANDARDIZATION (CEN). Design of concrete structures - Part 1–1: General rules and rules for buildings, BS EN 1992-1-1:2004, Brussels, Belgium, 2004.

FAN, W. J.; WANG, X.Y. Prediction of Chloride Penetration into Hardening Concrete. Hind. Publis. Corp., v. 2015, p. 1-8, 2015.

FU, C.; JIN, X.; JIN, N. Modeling of chloride ions diffusion in cracked concrete. In: Earth and Space 2010: Engineering, Science, Construction, and Operations in Challenging Environments, 14-17 March, 2010, Honolulu, Hawaii, USA, 2010, p. 3579-3589.

FU, C.; JIN, X.; YE, H.; JIN, N. Theoretical and experimental investigation of loading effects on chloride diffusion in saturated concrete. J. Adv. Conc. Techn., v. 13, 30-43, 2015.

FU, C.; YE, H.; JIN, X.; JIN, N.; GONG, L. A reaction-diffusion modelling of carbonation process in self-compacting concrete. Comp. Struct., v. 15, p. 847-864, 2015.

GERARD, B.; PIJAUDIER-CABOT, G.; LABORDERIE, C.; Coupled diffusion-damage modelling and the implications on failure due to strain localisation. Int. J. Solids Structures, v. 35, p. 4107-4120, 1998.

GHODS, P.; KARADAKIS, K.; ISGOR, O. B.; MCRAE, G. Modeling the chloride-induced corrosion initiation of steel rebar in concrete. In: COMSOL Conference 2009, 8-10 October, 2009, Boston, MA, USA, 2009, p. 1-4.

GUIMARÃES, A. T. C.; HELENE, P. R. L. Model to predict the chloride penetration in concrete with profile forming peak: verification of its precision. Rev. Mat., v. 14, p. 983-992, 2009.

HALAMICKOVA, P.; DETWILER, R.J.; BENTZ, D.P.; GARBOCZI, E.J. Water permeability and chloride ion diffusion in Portland cement mortars: relationship to sand content and critical pore diameter. Cement and Concrete Research, v. 25, p. 790-802, 1995.

HOMAN, L.; ABABNEH, A. N.; XI, Y. The effect of moisture transport on chloride penetration in concrete. Constr. Buil. Mat., v. 125, p. 1189-1195, 2016.

ISHIDA, T.; IQBAL, P. O. N.; ANH, H. T. L. Modeling of chloride diffusivity coupled with non-linear binding capacity in sound and cracked concrete. Cem. Conc. Resea., v. 39, p. 913-923, 2009

ISLAM, M. S.; TOSHIHARU, K. Proposal of analysis methods based on stagnation of chloride ion in concrete. J. Adv. Conc. Techn., v. 11, p. 374-382, 2013.

JUNG, S. H.; RYU, H. S.; KARTHICK, S.; KWON, S. J. Time and crack effect on chloride diffusion for concrete with fly ash. Int. J. Conc. Struct. Mat., v. 12, p. 1-10, 2017.

JUNG, S. H.; YANG, H. M.; YANK, K. H.; KWON, S. J. Maintenance for repaired RC column exposed to chloride attack based on probability distribution of service life. Int. J. Conc. Struct. Mat., v. 12, p. 1-9, 2018.

KIM, D. H.; SHIMURA, K.; HORIGUCHI, T. Effect of tensile loading on chloride penetration of concrete mixed with granulated blast furnace slag. J. Adv. Conc. Techn., v. 8, p. 27-34, 2010.

KIM, Y. Y.; LEE, B. J., KWON, S. J. Evaluation technique of chloride penetration using apparent diffusion coefficient and neural network algorithm. Adv. Mat. Sci. Eng., v. 2014, p. 1-13, 2014.

KONG, J. S.; ABABNEH, A. N.; FRANGOPOL, D. M.; XI, Y. Reliability analysis of chloride penetration in saturated concrete. Prob. Eng. Mech., v. 17, p. 305-315, 2002.

MALHEIRO, R.; MEIRA, G. R.; LIMA, M. Experimental study of chloride transport into double layered components with concrete and rendering mortar. Rev. Constr., v. 15, p. 119-132, 2016.

MARRIAGA, J. L.; CLAISSE, P. The influence of the blast furnace slag replacement on chloride penetration in concrete. Ing. Invest., v. 31, p. 38-47, 2011.

MEIRA, G. R.; PADARATZ, I. J.; ALONSO, C.; ANDRADE, C. Effect of distance from sea on chloride aggressiveness in concrete structures in brazilian coastal site. Mater. Construcc., v. 53, p. 179-189, 2003.

MEIRA, G.R.; ANDRADE, M.C.; PADARATZ, I.J.; ALONSO, M.C.; BORBA Jr., J.C. Measurements and modelling of marine salt transportation and deposition in a tropical region in Brazil. Atmospheric Environment, v. 40, p. 5596-5607, 2006.

MICHEL, A.; SOLGAARD, A. O. S.; PEASE, B. J.; GEIKER, M. R.; STANG, H.; OLESEN, J. F. Experimental investigation of the relation between damage at the concrete-steel interface and initiation of reinforcement corrosion in plain and fibre reinforced concrete. Corrosion Science, v. 77, p. 308-321, 2013.

MIEN, T. V.; STITMANNAITHUM, B.; NAWA, T. Simulation of chloride penetration into concrete structures subjected to both cyclic flexural loads and tidal effects. Comp. Conc., v. 6, p. 421-435, 2009.

MORGA, M.; MARANO, G. C. Chloride penetration in circular concrete columns. Int. J. Con. Struct. Mat., v. 9, p. 173-183, 2015.

MUNDRA, S.; CRIADO, M.; BERNAL, S. A.; PROVIS, J. L. Chloride-induced corrosion of steel rebars in simulated pore solutions of alkali-activated concretes. Cement Con. Research, v. 100, p. 385-397, 2017.

NATIONAL INSTITUTE OF STANDARDS AND TECHNOLOGY (NIST). Disponível em: https://concrete.nist.gov/ciks/menu0002.html. Acesso em maio 2018.

NEVILLE, A. M. Properties of Concrete, 5. ed. England: Pearson Education, 2011.

NGUYEN, P.T.; BASTIDAS-ARTEAGA, E.; AMIRI, O.; EL SOUEIDY, C.P. An efficient chloride ingress model for long-term lifetime assessment of reinforcement concrete structures under realistic climate and exposure conditions. International Journal of Concrete Structures and Materials, v. 11, p. 199-213, 2017.

NOGUEIRA, C. G.; LEONEL, E. D.; CODA, H. B. Probabilistic failure modelling of reinforced concrete structures subjected to chloride penetration. Int. J. Adv. Struct. Eng., v. 4, p. 10-23, 2012.

NOGUEIRA, C. G.; LEONEL, E. D.; CODA, H. B. Reliability algorithms applied to reinforced concrete structures durability assessment. Ibra. Struct. Mat. J., v. 5, p. 440-450, 2012.

OLIVEIRA, H. L.; CHATEAUNEUF, A.; LEONEL, E. D. Probabilistic mechanical modelling of concrete creep based on the boundary element method. Advances in Structural Engineering, v. 00, p. 1-12, 2018.

PELLIZZER, G.P. Sobre a modelagem numérica da difusão de cloretos no concreto: Uma abordagem pelo método dos elementos de contorno com aplicação de modelos de

confiabilidade e otimização. Tese (Doutorado) – Escola de Engenharia de São Carlos, Universidade de São Paulo, São Carlos, Brasil, 2019.

PELLIZZER, G. P.; LEONEL, E. D. Avaliação da integridade mecânica de estruturas em concreto armado submetidas à corrosão de armaduras: abordagem via método dos elementos finitos, mecânica do dano e lei de Fick. In: Proceedings of the XXXVI Latin-American Congress on Computational Methods in Engineering, CILAMCE 2015, 22-25 November, 2015, Rio de Janeiro, Brazil, 2015, p. 1-15.

PELLIZZER, G. P.; LEONEL, E. D.; NOGUEIRA, C. G. Influence of reinforcement's corrosion into hyperstatic reinforced concrete beams: a probabilistic failure scenarios analysis. Ibracon Structures and Materials Journal, v. 8, p. 479-490, 2015.

PELLIZZER, G. P.; LEONEL, E. D.; NOGUEIRA, C. G. Numerical approach about the effect of the corrosion on the mechanical capacity of the reinforced concrete beams considering material nonlinear models. Rev. Ibr. Estr. Mat., v. 11, p. 26-51, 2018.

PRINCIGALLO, A. Estimating the chloride transport in cement paste. Mat. Constr., v. 62, p. 151-161, 2012.

ROSENBLATT, M. Remarks on a multivariate transformation. The Annals of Mathematical Statistics, v. 23, p. 470-472, 1952.

SILVA, R. V.; DE BRITO, J.; NEVES, R.; DHIR, R. Prediction of chloride ion penetration of recycled aggregate concrete. Mat. Resea., v. 18, p. 427-440, 2015.

SIVA, C.A.; GUIMARÃES, A. T. C. Evaluation of the diffusion model considering the variation in time of the chloride content of the concrete surface. Rev. Mat., v. 19, p. 81-93, 2014.

STEWART, M. G.; MULLARD, J. A. Spatial time-dependent reliability analysis of corrosion damage and the timing of first repair for RC structures. Engineering Structures, v. 29, p. 1457-1464, 2007.

SUN, Y. M.; LIANG, M. T.; CHANG, T. P. Time/depth dependent diffusion and chemical reaction model of chloride transportation in concrete. App. Math. Mod., v. 36, p. 1114-1122, 2012.

SUO, Q.; STEWART, M. G. Corrosion cracking prediction updating of deteriorating RC structures using inspection information. Reliability Engineering and System Safety, v. 94, p. 1340-1348, 2009.

TING, S.; YANG, L. Chloride ion erosion experiment research in cracked concrete. IOP Conference Series: Earth and Environmental Science, v. 81, p. 1-7, 2017.

VAL, D. V.; STEWART, M. G. Life-cycle cost analysis of reinforced concrete structures in marine environments. Struct. Saf., v. 25, p. 343-362, 2003.

WAGN, L.; UEDA, T. Mesoscale modelling of the chloride diffusion in cracks and cracked concrete. J. Adv. Conc. Techn., v. 9, p. 241-249, 2011.

WANG, J.; BASHEER, P. A. M.; NANUKUTTAN, S. V.; LONG, A. E.; BAI, Y. Influence of service loading and the resulting micro-cracks on chloride resistance of concrete. Constr. Buil. Mat., v. 108, p. 56-66, 2016.

WANG, X. H., BASTIDAS-ARTEAGA, E., GAO, Y. Probabilistic analysis of chloride penetration in reinforced concrete subjected to pre-exposure static and fatigue loading and wetting-drying cycles. Engineering Failure Analysis, v. 84, p. 205-219, 2018.

WANG, Y.; NANUKUTTAN, S.; BAI, Y.; BASHEER, P. A. M. Influence of combined carbonation and chloride ingress regimes on rate of ingress and redistribution of chlorides in concretes, Const. Buil. Mat., v. 140, p. 173-183, 2017.

WATTANAPORNPROM, R.; ISHIDA, T. Modeling of chloride penetration into concrete under airborne chloride environmental conditions combined with washout effects. J. Adv. Conc. Techn., v. 15, p. 126-142, 2017.

Wolfram Mathematica. Version 11 Student Edition, Wolfram Research, Inc., 2017.

YANG, K. H.; SINGH, J. K.; LEE, B. Y.; KWON, S. J. Simple technique for tracking chloride penetration in concrete based on the crack shape and width under steady-state conditions. Sust., v. 9, p. 282-295, 2017.

YE, H.; FU, C.; JIN, N.; JIN, X. Influence of flexural loading on chloride ingress in concrete subjected to cyclic drying-wetting condition. Comp. Conc., v. 15, p. 183-199, 2015.

ZACCHEI, E.; MOLINA, J. L. Shape optimization of double-arch dams by using parameters obtained through Bayesian estimators. Iranian Journal of Science and Technology, Transactions of Civil Engineering, v. 2018, p. 1-14, 2018.

ZACCHEI, E.; NOGUEIRA, C. G. Chloride diffusion assessment in RC structures considering the stress-strain sate effects and crack width influences. Construction and Building Materials, v. 201, p. 100-109, 2019.

ZACCHEI, E.; NOGUEIRA, C. G. Numerical solutions for chloride diffusions using stochastic inputs. In: 3rd International Conference on Recent Advances in Nonlinear Design, Resilience and Rehabilitation of Structures, CoRASS 2019, 16-18 October, 2019, Coimbra, Portugal, 2019(a), p. 1-9.

ZANG, R.; CASTEL, A.; FRANÇOIS, R. Concrete cover cracking with reinforcement corrosion of RC beam during chloride-induced corrosion process. Cem. Conc. Resea., v. 40, p. 415-425, 2010.

ZHANG, R.; CASEL, A.; FRANÇOIS, R. Concrete cover cracking with reinforcement corrosion of RC beam during chloride-induced corrosion process. Cement and Concrete Research, v. 40, p. 415-425, 2010.

ZHANG, S. F.; LU, C. H.; LIU, R.G. Experimental determination of chloride penetration in cracked concrete beams. Proc. Eng., v. 24, p. 380-384, 2011.

ZOFIA, S.; ADAM, Z. Theoretical model and experimental tests on chloride diffusion and migration processes in concrete. Proc. Eng., v. 57, p. 1121-1130, 2013.

8 APÊNDICES (PUBLICAÇÕES)

Construction and Building Materials 201 (2019) 100–109

Contents lists available at ScienceDirect

Construction and Building Materials

journal homepage: www.elsevier.com/locate/conbuildmat

Chloride diffusion assessment in RC structures considering the stress-strain state effects and crack width influences

Enrico Zacchei [a,*], Caio Gorla Nogueira [b]

[a] Higher Polytechnic School of Ávila, University of Salamanca (USAL), 50 Hornos Caleros Avenue, 05003 Ávila, Salamanca, Spain
[b] School of Civil Engineering of Bauru, São Paulo State University (UNESP), 14-01 Eng. Luís Edmundo Carrijo Coube Avenue, 17033-360 Bauru, SP, Brazil

HIGHLIGHTS

- Chloride ions diffusion in sound/cracked RC under non-steady-state conditions.
- Effects of the loads for the linear and non-linear material states are analysed.
- Modified governing equations to account the no-constant diffusion are used.
- Classic results (constant diffusion) vs. new ones (no-constant diffusion).
- Chloride transport in damaged concrete, experimental and numerical aspects.

ARTICLE INFO

Article history:
Received 20 July 2018
Received in revised form 21 December 2018
Accepted 22 December 2018

Keywords:
Chloride diffusion
No-constant chloride coefficient
Stress-strain effects
Cracked concrete diffusivity

ABSTRACT

The aim of this study is to investigate the chloride ions diffusion in sound and cracked concrete under compressive loads. The model includes the analytical setup and data analyses. The governing equations are modified to account for the no-constant chloride diffusion coefficient. With this condition it is possible to define several terms in the time domain to predict the service life of structures. The material is a saturated and hardened cement paste under non-steady-state conditions. Loads are studied for linear and non-linear material states. The predicted values at the depth of steel reinforcement ranges from 0.1 to 0.3% in 7–20 years. The ratio of the chloride diffusion coefficient under loading and no-loading is 9, whereas the chloride diffusivity coefficient in cracks is 0.9–1.3 times the chloride diffusion coefficient under loading.

1. Introduction

Corrosion damage of reinforcement in concrete elements due to chloride ions attack is a major problem for long term durability of reinforced concrete (RC) structures and, if unvalued, it can put the whole or part of the structural system at risk, including people's lives [1–4].

Chloride ions tend to migrate into the concrete cementitious matrix from the external environment until the reinforcement surface where start the corrosion, after the depassivation of the steel reinforcement.

After the initiation of corrosion process, there is a large loss of resistance observed in the structural elements, in function of the reinforcement cross section area reduction and concrete cracking. The aesthetic of the structure is also affected by corrosion degradation.

Structures situated in aggressive environments such as industrial zones, up to 200 m from seacoasts [5,6] are much more exposed to chloride ions penetration than others situated far from the sea or in non-aggressive regions.

There are two main exposure environments: a local climate and a microclimate. The former is represented by ambient temperature, relative humidity and wind speed. The latter is determined by the interaction of the concrete with its local climate.

These expositions affect the chloride penetration rate in concrete, in particular, in humid environments, the water is transported inside concrete by a vapor density gradient, whereas when the concrete surface is directly subjected to water (rainfall, structures sea-side) the concrete absorbs water due to the capillary mechanism.

The whole process (from penetration to cracking) can be divided in four phases: (i) the penetration of chloride during which chloride ions diffuse through concrete cover toward the steel

* Corresponding author.
E-mail addresses: enricozacchei@usal.es (E. Zacchei), caio.nogueira@unesp.br (C.G. Nogueira).

https://doi.org/10.1016/j.conbuildmat.2018.12.166
0950-0618/

rebars; (ii) the corrosion of steel which begins when the chloride concentration reaches a critical value at rebars surface; (iii) the rust expansion in the steel-concrete interface zone; (iv) cracking, spalling and its propagation in concrete.

The penetration phase usually takes a long time and is a very complex process because depends on the capillarity and permeability. Once the corrosion starts, it will take only a few years to increase the cracking advance in the concrete cover [10,11].

In literature, there are several studies about the diffusivity of chloride ions and its concentration assessment inside concrete, with applications in: a circular reinforced concrete column [14–16]; chloride diffusion with the presence of double layers and rendering mortar [16]; chloride diffusion by considering the real-world aspects [17]; chloride penetration test under tensile loading [18]; and long-term chloride concentration in bridges treated [55].

The chloride diffusion has also been studied by using statistical approaches for water-cement ratio and curing time [19]. Other probabilistic approaches are studied in literature [20,21], where the probability of corrosion initiation along time considering different environment aggressiveness, several combinations of cover depth and water-cement ratio has been carried out. In [22] a probabilistic approach applied to the evaluation of the service life has been developed, justified by the fact that several parameters that describe the diffusion have random, therefore increase uncertainties on results.

The focus of this paper is to predict the evolution of the chloride concentration inside the sound and damaged concrete by the diffusion process. The paper focus on chloride transport in damaged concrete, experimental and numerical aspects taken from the literature.

The choice of using only diffusion process is justified by the fact that the analysis in this paper is based on the first and second Fick's law. The Fick's first law is a simplification of the Nernst-Plank equation, which considers beside the diffusion flux, also the convention flux [28,30,31,32,33]. From the Nernst-Plank equation, neglecting the degree of saturation, porosity, tortuosity (i.e. irregular paths due to the complex micro-pore cement matrix structure) and constrictivity (i.e. presence of hindrances and path width due to the interaction between pore structure and ion transport), the Fick's first law only considers the diffusion flux. The Fick's second law provides an analytical solution, which only describes the diffusion process, i.e. it considers the mechanical and physical aspects.

The used values are consistent to the literature and NIST software [23]. Here, the chloride diffusion coefficient is defined by several effects such as: water-cement ratio, chloride binding, influence of the temperature, aging effect and linear and nonlinear stress-strain states produced by loads. In the nonlinear state, the presence of cracks was considered.

Other important aspects to define the chloride diffusivity that have not been studied in this paper can be the relative humidity [24], carbonation reaction [25], interaction of carbonation with the chloride penetration [26], composite material comprising cement past and aggregates [19,27].

Many previous researches have focused on predicting chloride ingress not subjected to any external loads. Few studies related to this subject have been carried out yet, but it is possible to see some as the calculation of a function, which depends on the applied and fracture load ratio for cyclic flexural loads [28]; modelling of the influence of micro-cracks due to structural loads and stress levels [29]; calculation of a diffusivity factor which accounts the influence of the concrete strain [24]; effects of compressive loading on the chloride diffusion [60].

Regarding to cracks, concrete structures are not crack-free and in the real situations, cracks cannot be avoided. Cracks, which may have different widths (from very small internal micro-cracks to quite large cracks) and different depths, reduce the cover thickness and speed up the migration of the chloride ions in ideal channels to reach the surface of the steel.

Many micro-cracks can contribute to facilitate the ions penetration [56], therefore, it is important to consider such phenomenon and its effects to perform better predictions of the chloride concentrations in concrete along time.

Finally, in this paper we do not want to recommend a diffusivity model with load effects over other ones, but rather to point out possible factors that influence the chloride concentration inside concrete to more accurate analytical predictions.

2. Models and algorithms

Due to the concentration gradient between the chloride ions in the exposed surface of the concrete and the internal pore solution in the cement matrix, chloride ions enter in the concrete by diffusion. Therefore, the principal driving force responsible for the diffusion process is the ions concentration gradient neglecting all other potential fields, e.g. electrical fields and chemical potential gradients.

The constitutive relation, which describes the flux of chloride ions (J) in saturated concrete depending on the total chloride concentration gradient (∇C), is described by the Fick's first law as follows [12]:

$$J = -D(\nabla C) \tag{1}$$

where D is the diffusivity parameter, which can be assumed constant in a conventional simple model (i.e., independent from the position, concentration and time) or variable by more than one order of magnitude. When D is variable, it depends on the material characteristics, as well as surrounding exposure conditions and it is defined in a time-depth diffusion model [13]. In accordance to literature [12], D can be distinguished between self-diffusion coefficient, free diffusivity, solid diffusivity and diffusivity in saturated capillary pores (D_{cl}). The latter type of diffusivity is used in the analyses of this paper, which means that $D = D_{cl}$.

Generally, Eq. (1) can be derived considering the general mass balance principle along the time t in the three directions (i = x, y, z) under non-steady-state conditions by the Fick's kinetic second law [25]:

$$\frac{\partial C}{\partial t} = \nabla(D_{cl,i}\nabla C_i) = \frac{\partial}{\partial x}\left(D_{cl,x}\frac{\partial C}{\partial x}\right) + \frac{\partial}{\partial y}\left(D_{cl,y}\frac{\partial C}{\partial y}\right) + \frac{\partial}{\partial z}\left(D_{cl,z}\frac{\partial C}{\partial z}\right) \tag{2}$$

Eq. (2) establishes the chloride concentration (C) at a specific position x, y and z along time t. The solution of this equation is obtained under the following hypotheses: (1) the concrete structure is a semi-infinite medium; (2) the medium is homogeneous; (3) the chloride concentration at external surface is uniform and constant; (4) the external surface of the concrete is plane; (5) the diffusion front is a mono-dimensional model, therefore, the loss of chloride in other directions has not been considered [34]; (6) the chloride ions are transported into a water-saturated concrete only via diffusion and do not interact/react with the other ions; (7) the chemical composition of substances in concrete pore is considered to be in equilibrium throughout the entire diffusion process, since the chloride diffusion coefficient is slow with an order of 10^{-12} to 10^{-11} m^2/s.

Under aforementioned hypotheses, the closed form analytical solution of the Eq. (2) for the flux only in x direction can be given by:

$$\begin{gathered} C(x,t) = C_0 + (C_s - C_0)\left[1 - \operatorname{erf}\left(\frac{x}{2\sqrt{D_{cl}t}}\right)\right] \\ \text{i.c.} : C(x,0) = C_0 \\ \text{b.c.} : C(0,t) = C_s \; ; C(\infty,t) = C_0 \end{gathered} \tag{3}$$

where i.c. and b.c. are the initial and boundary conditions, respectively [13,35] in which C_0 is the initial chloride concentration; C_s is the concrete exposed surface concentration. The term $\left[1 - \operatorname{erf}\left(\frac{x}{2\sqrt{D_{cl}t}}\right)\right]$ describes the evolution of the chloride diffusion front in the direction x at a time t, with erf(.) is the Gaussian error function integrated between 0 and $\frac{x}{2\sqrt{D_{cl}t}}$. Fig. 1 shows an example of the semi-infinite concrete medium considered to represent the Eq. (3) with ions flux only in the x direction.

The diffusion coefficient (D_{cl}) is not constant in time and can be expressed by the following multifactor equation [37]:

$$D_{cl} = f_{wc} \times f_1(C_b) \times f_2(T) \times f_3(t) \times F(\varepsilon_c, d) \tag{4}$$

where f_{wc} is the constant part of the concrete diffusion coefficient depending on only the water-cement ratio (w/c) and given by: $f_{wc} = 10^{(-12.06+2.4\times[w/c])}$ m^2/s [37]. The factors f_1, f_2, f_3 and F are specific contributions according to each considered effect on the diffusion coefficient and will be explained in the next sections.

The used algorithm is shown in Fig. 2. In the left-hand side there are the design parameters (factors) and in the middle, there are the two types of the chloride diffusion coefficient. In the right-hand side there are the governing equations and the analytical solution under aforementioned seven hypothesis.

The hypothesis of water saturated occur in many real-world cases due to the limited thickness of the concrete cover (typical thickness of concrete cover is about 3, 4 and 5 cm).

The hypothesis of chloride concentration at external surface C_s as uniform and constant may be applied (i) when the effects of the environment variations are negligible [9] and (ii) when there is no frequent washing for example by rain. Moreover, C_s can be considered constant because increases with increasing the time, up to a certain value where it begins to stabilize [45].

However, it is important to know that C_s also depends on the chloride binding capacity of the concrete and its porosity at the surface [54]. It is not independent to the C(x,t) and time t, therefore the results can be underestimated [53,57]. In fact, in Eq. (3) erf(·) accounts the underestimating of the C_s [9].

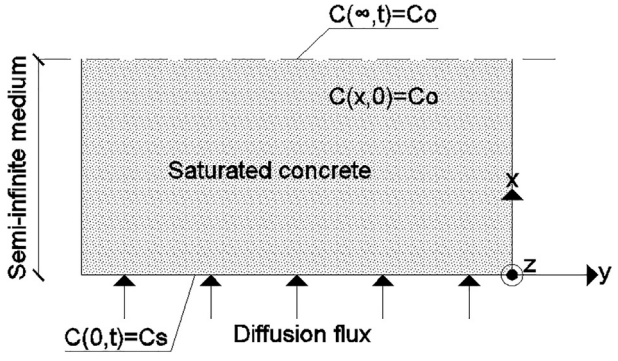

Fig. 1. Semi-infinite concrete medium and diffusion flux only in x direction [36].

3. Chloride diffusivity modelling in sound concrete

3.1. Factor due to chloride binding

The total chloride concentration is divided in two parts: free (C_f) and bound (C_b) chloride concentration. The free chlorides are dissolved in the pore solution and the remainder is permanently bound to the solid mass of the cement paste (called binding effect). Therefore, only free chlorides are responsible for initiating the corrosion process in RC elements. Regarding to the bound chlorides, they can be chemically and physically bounded. Chemically bound chlorides react with the cement past in the solid structure of concrete, whereas physically bound chloride is attracted and trapped in the pore surfaces. Physically, bound chlorides are due to the mutual attraction between charged particles (i.e., Van der Waals forces) and are strongly related to the external surface area of ions [12]. In fact, when the total chloride content (free + bound) is considered to perform the corrosion assessment in the diffusion models, the prediction causes an underestimation of the service life [13]. In this regard, to achieve better predictions of the chloride concentration inside concrete, it is necessary to consider the chloride ions amount which reacts with the concrete matrix components. These chemical reactions are also important because they can produce deleterious products and especially start the concrete cracking process even in cases of lower load levels.

The correlations between free and bound chloride ions at a given temperature are known as the chloride binding isotherms. The chloride binding effect factor (f_1) is defined by nonlinear Langmuir isotherm [8,19,38,39] which is given by:

$$f_1(C_b) = \left(1 + \frac{\alpha}{\omega_e[1 + \beta C_f]^2}\right)^{-1} \tag{5}$$

where ω_e is the evaporable water content which can be determined from hydration model [35], α and β are constant values, C_b and C_f are correlated through the following relation [13,38]: $C_{tot} = \omega_e C_f + C_b$, with the total chloride concentration C_{tot}. The free chloride ions are transported through the evaporable water content and are considered in the calculations.

If the chloride binding effect is neglected, the chloride concentration is substituted by the total chloride content, whereas if it is considered, the chloride concentration is substituted with the free chloride concentration. The coupled diffusion-binding interactions lead to anomalous diffusion of chloride ions which no longer obeys the Eq. (2).

3.2. Factor due to temperature

The variation of the temperature changes the velocity of the chloride diffusion. The factor that considers the temperature is expressed by Arrhenius' law [19,25,27,37,38] and is given by:

$$f_2(T) = e^{\left[\frac{E_a}{R}\left(\frac{1}{T_0} - \frac{1}{T}\right)\right]} \tag{6}$$

where T_0 and T are the reference and current temperature, respectively; E_a is the activation energy of the diffusion process, which depends on the type of cement and w/c ratio; R is the universal gas constant which is correlated by chemical potential of ions, molar concentration and temperature [40].

3.3. Factor due to aging effect

The diffusivity is affect by the aging effect and its contribution can be expressed by [37,38]:

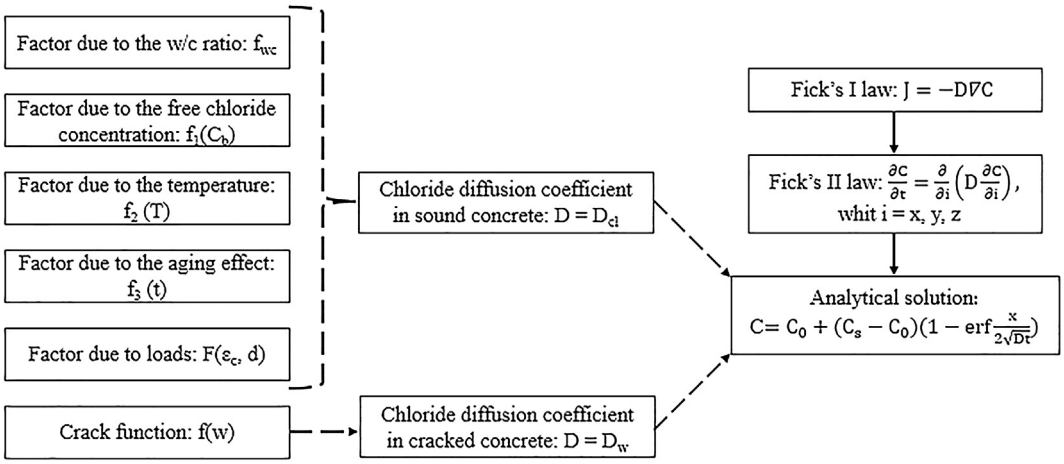

Fig. 2. Algorithm for establishing the predictive chloride diffusion.

$$f_3(t) = \begin{cases} \frac{1}{1-m}\left(\frac{t_{ref}}{t}\right)^m & \text{in case of } t < t_r \\ \left[1 + \frac{t_r}{t}\left(\frac{m}{1-m}\right)\right]\left(\frac{t_{ref}}{t}\right)^m & \text{in case of } t \geq t_t \end{cases} \quad (7)$$

where t_{ref} is the reference age; t_r is the time when diffusivity is assumed to be constant. The time t expressed in year is considered as the "exposed time". The index m is used to express the reducing speed of chloride diffusivity and depends on the fly ash and slag added to the cement [41].

3.4. Factor due to acting loads

The loading effect factor F can be considered as two parts: one depends on the concrete compressive strain ε_c and another depends on the damage variable d. The factor F can be defined through the new model proposed in literature [37], in which $F = F(\varepsilon_c) + F(d) = F(\varepsilon_c, d)$. When $\varepsilon_c = 0 \text{and} d = 0$, F is expressed by the Taylor expansion as:

$$F(\varepsilon_c, d) = F(0,0) + \frac{\partial F}{\partial \varepsilon_c}|_{(0,0)}\varepsilon_c + \frac{\partial F}{\partial d}|_{(0,0)}d + R_1(\varepsilon_c, d) \quad (8)$$

where $R_1(\varepsilon_c, d)$ is the Lagrange remainder which is defined, for θ varying between 0 and 1, as:

$$R_1(\varepsilon_c, d) = \frac{1}{2}\left(\varepsilon_c\frac{\partial}{\partial \varepsilon_c} + d\frac{\partial}{\partial d}\right)^2 F(\theta\varepsilon_c, \theta d) \quad (9)$$

Assuming the first, second and third terms on the right side of Eq. (8) as: $F(0,0) = A$, $\frac{\partial F}{\partial \varepsilon_c}|_{(0,0)} = B$ and $\frac{\partial F}{\partial d}|_{(0,0)} = C$, respectively, under the conditions $\varepsilon_c = 0 \text{and} d = 0$, the first term A is equal to 1. Thus, Eq. (8) can be rewritten as:

$$F(\varepsilon_c, d) = 1 + B\varepsilon_c + Cd + R_1(\varepsilon_c, d) \quad (10)$$

The damage influence factor f(d) that describes the concrete local damage can be written as [37]:

$$f(d) = 1 + \frac{D_{max}}{D_0} - \frac{D_{max}}{D_0}\left[1 + \left(\frac{d}{d_{cr}}\right)^n\right]^{-1} \quad (11)$$

where D_0 and D_{max} are, respectively, the chloride diffusivity in sound concrete and in completely damaged concrete; n and d_{cr} are constant values that are derived from the mechanical model proposed by literature [7].

In order to obtain, from a function that only depends on one parameter d to a function that depends on two parameters ε_c and d (i.e. $f(d) \rightarrow F(\varepsilon_c, d)$) through an unique equation, the method consists to multiply the second term of the Eq. (11) by $(1 + B_1\varepsilon_c + C_1 d)$ to obtain:

$$F(\varepsilon_c, d) = 1 + \frac{D_{max}}{D_0}B_1\varepsilon_c + \frac{D_{max}}{D_0}\left\{1 + C_1 d - \left[1 + \left(\frac{d}{d_{cr}}\right)^n\right]^{-1}\right\} \quad (12)$$

where the coefficient C_1 is defined later; B_1 is defined by $B_1 = BD_0/D_{max}$. The coefficient B is valid in the elastic state when no damage occurs for tensile and compressive loads and depends on the material characteristic (e.g. w/c ratio).

There are four cases related to the Eq. (12): (i) $d = 0$, when there is no permanent damage in concrete, but the chloride diffusivity changes with elastic loads and deformations in solid skeleton; (ii) $\varepsilon_c = 0$, when the damage has occurred in concrete without sustained loads; (iii) $\varepsilon_c = 0$ and $d = 0$, when there is no loading effect; (iv) $\varepsilon_c \neq 0$ and $d \neq 0$, when the concrete is damaged with sustained loads.

When $d = 1$, the concrete strain reaches the ultimate value ε_{c1} and, in such case, the concrete is completely damaged. Then, Eq. (12) becomes:

$$F(\varepsilon_{c1}, 1) = 1 + B\varepsilon_{c1} + \frac{D_{max}}{D_0}\left\{1 + C_1 - \left[1 + \left(\frac{1}{d_{cr}}\right)^n\right]^{-1}\right\} \quad (13)$$

By considering $F(\varepsilon_{c1}, 1) = f(1)$, the coefficient C_1 can be defined by:

$$C_1 = -\frac{BD_0}{D_{max}}\varepsilon_{c1} \quad (14)$$

4. Chloride diffusivity modelling in cracked concrete

The chloride diffusion, besides propagates in sound concrete ($D = D_{cl}$), it propagates in concrete affected by cracks. In such cases, the diffusion coefficient D must be replaced by $D = D_w$ due to the fact that the analytical solution (Eq. (3)) approximates well the chloride diffusion even in cracked concrete as shown in [58], where a comparison between experimental and numerically analysis has been carried out.

The formation of cracks implies the study in a nonlinear analysis. It is assumed that the diffusion process is governed by only the crack width parameter w as shown in the experimental analyses in literature [58,59]. Therefore, the expression to define the new D can be described by:

$$D_w = f(w)D_{cl} \quad (15)$$

where f(w) is a crack function, which has been studied in the literature [33,42–44] to understand the relationship between chloride diffusion and concrete cracks.

Table 1
Input parameters to the analyses.

Parameter	Value
Initial chloride concentration, C_o (kg/m^3)	0.0/5.0*
Superficial chloride concentration, C_s (kg/m^3)	7.20*
Water to cement ratio, w/c[a]	0.40*
Mass density of the concrete (kg/m^3)	2400*
Evaporable water content, ω_e	0.6*
Free chloride concentration, C_f (kg/m^3)[b]	1.5*
Activation energy, E_a (J/mol) [38]	41,800
Universal gas constant, R (J/mol K) [38]	8.314
Reference temperature T_0 (K) [25]	293.0
Current temperature, T (K)	296.0*
Reference age, t_{ref} (dd) [37]	28
Time for constant diffusivity, t_r (year) [38]	30
Exposed time, t (year)[c]	0–25*

Note:
* = Value adopted to carry out this analysis.
[a] w/c ratio refers to a standard composition (i.e. no additives, fly ashes, limestone or slag particles).
[b] This value is correlated by following constants: $\alpha = 11.8$ and $\beta = 4.0$ [31] (see Eq. (5)).
[c] In the aging effect, index m = 0.20 has been adopted [41] (see Eq. (7)).

5. Research data

Table 1 lists the key parameters for predicting chloride diffusion.

The w/c ratio, which includes the concrete properties, usually ranges 0.35–0.60. A w/c ratio between 0.40 and 0.50 is considered moderate [46]. Concrete with a higher w/c ratio (w/c > 0.60) has a higher porosity and its "alveolar" structure is characterized by large cavities and voids forming preferential pathways for the diffusion. Concrete with a lower w/c (w/c < 0.40) has a higher strength, and hence higher tensile resistance, therefore can support higher loads. Moreover, in regions with higher humidity it is recommended to use lower w/c ratio and large concrete cover.

Table 2 shows the values for the stress-strain analysis to define the F factor.

Fig. 3 shows the used stress-strain curve into the range: $f_{ck} - 10 < f_{ck} < f_{ck} + 15$ MPa. This is common range used for structures whit the ultimate compressive strain is equal to 3.5‰. Dotted vertical line ($\varepsilon_{c1} = 2.25$‰) divides the adopted linear state from the non-linear state. The fitting functions refer to the polynomial trend lines of order two (dashed lines).

6. Analytical analyses

6.1. Sound concrete

The chloride binding isotherm is a complicated phenomenon, depending on the Cl^- ions concentration in the pore solution as well as the composition of the cement. Binding reaction has a significant influence on the ingress of chloride ions into concrete [17]. The literature available to date does not provide reliable data on the binding rate [12]. Fig. 4 shows the non-linear f_1 factor in function of C_f. It is possible to see that for C_f fixed, when ω_e increases the factor f_1 increases. And by increasing ω_e, the water content ω_e and C_{tot} increases too. A linear relationship between C_b and C_f has been estimated in the literature [31]: $C_b = 2.5C_f$. However, this linear approach overestimates C_b when $C_f > 1$.

Fig. 5 shows the factor f_2 which mainly depends on T and E_a. In literature is possible to find different values of E_a as a function of w/c [19,27,37,38] e.g. 32.0 ± 2.4 kJ/mol for w/c of 0.6;

Table 2
Input parameters to define the F factor.

Parameter	Value
Characteristic compressive strength, f_{ck} (MPa) [47]	35.0
Mean compressive strength, f_{cm} (MPa) [47]	43.0
Modulus of elasticity, E_{cm} (GPa) [47]	34.0
Strain at peak stress, ε_{c1} (‰) [47]	2.25
Ultimate compressive strain, ε_{cu1} (‰) [47]	3.5
Parameter, n [7]	5.0
Parameter, d_{cr} [7]	0.40
Parameter, C_1[a] (Eq. (14))	−0.88

[a] The B parameter used to define C_1 is obtained by following relation: $(D_{max}/D_0 - 1)/\varepsilon_{c1} = 3.11 \times 10^{-3}$, for $D_{max}/D_0 = 8$.

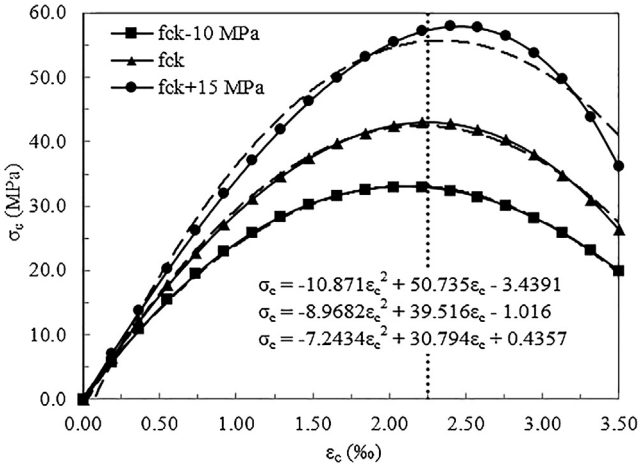

Fig. 3. Concrete stress-strain curves [47].

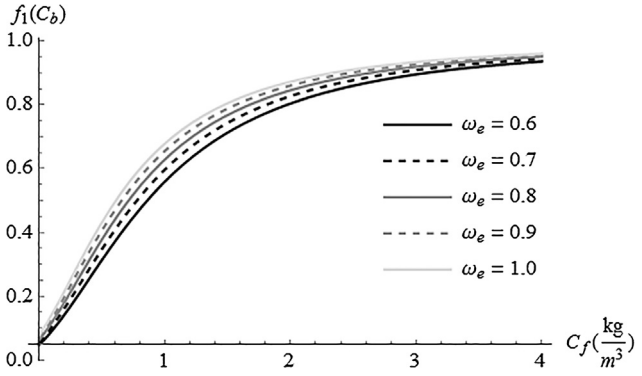

Fig. 4. Nonlinear chloride binding isotherm.

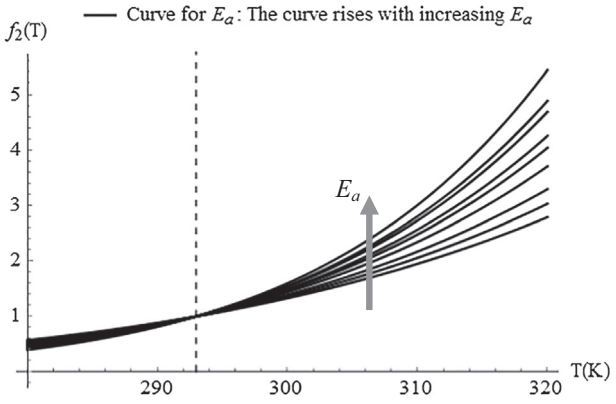

Fig. 5. Temperature factor: the vertical dashed line indicates $T_0 = 293$ K.

44.6 ± 4.3 kJ/mol for w/c of 0.5 and 41.8 ± 4.0 kJ/mol for w/c of 0.4. The activation energy E_a also varies in function of the liquid presence: when the pores are fluid free E_a is equal to 17.6 kJ/mol [31] and consequently the rate of chloride content decreases. The increasing of the temperature gradient variation accelerates the f_2 factor, thus the chloride ions penetration from the edge to the inside of the concrete increases.

Fig. 6 shows the aging effect expressed by f_3 factor represented with two branches, where it is possible to see that after a certain value (about 30 years) the curve is more reduced. It is estimated that after 30 years the cement hydrates further decrease the porosity, limiting the chloride diffusion inside concrete. A real concrete has an adjustment and improvement in the time (grey solid area). Curves in Figs. 4–6 are implemented by software [52].

Fig. 7 shows F factor in function of the elastic strain by using Eq. (12). The vertical dashed lines divide the graphic in three parts: (i) before $\varepsilon_c = 0.355‰$ the F factor is not influenced by the elastic strains (F = 1); (ii) between $0.355‰ < \varepsilon_c < 1.184‰$, the F factor is quasi-linear (F/ε_c = constant); (iii) after $\varepsilon_c = 1.184‰$ the F factor stabilizes (F = constant).

In Fig. 8, the non-constant (with the effects of stress-strain state and damage: F≠0) diffusion coefficient $D_{cl}\left(\frac{w}{c}, C_b, T, t, \varepsilon_c, d\right)$ is compared with the constant (without the effects of stress-strain state and damage: F = 0) diffusion coefficient $D_{cl}\left(\frac{w}{c}, C_b, T, t\right)$.

In this analysis, $D_{cl,max|F\neq0}$ equal to 7.7×10^{-11} m^2/s, whereas $D_{cl|F=0}$ is equal to 8.6×10^{-12} m^2/s (the ratio between these two values of D_{cl} is 8.95). This value is high because $D_{cl,max|F\neq0}$ is calculated for ε_{c1}. In the literature [29], it was shown that the chloride diffusion coefficient varies according to the stress levels and e.g., the chloride diffusion coefficient under 75% of the ultimate stress is around 2.24 times of that with no considered loading. In [46], for f_{ck} = 35MPa the chloride diffusion coefficient is about 1.8×10^{-11} m^2/s, that is 2.10 times $D_{cl|F=0}$. A characteristic value of the diffusion coefficient for w/c = 0.5 and f_{ck} = 30–40 MPa can be 2.0×10^{-12} m^2/s [14]. Defining these ratios is useful to adjust the chloride diffusion coefficient for acting loads. It is also important to consider that short-time loading might not cause a lasting detrimental effect on the chloride penetration resistance of concrete structures. The coefficient D_{cl} refers to the free ions and is obtained by considering the factor $f_1(C_b) < 1$, which accounts a percentage of bound chloride ions. In the literature, it is estimated that the total diffusion coefficient is 2.2–3.4 times the free diffusion coefficient [13].

6.2. Cracked concrete

The chloride diffusion coefficient in cracked concrete is based on one parameter: crack width w. Fig. 9 shows the crack function

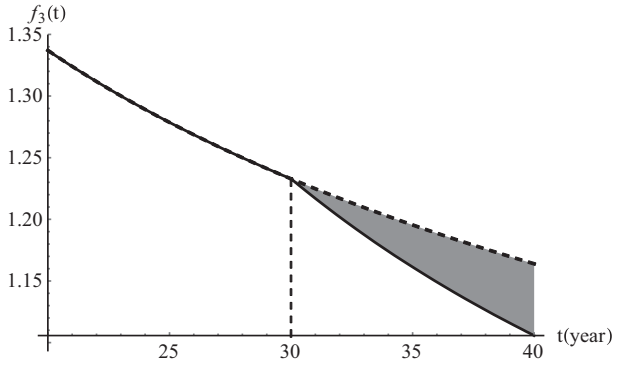

Fig. 6. Factor of aging effect.

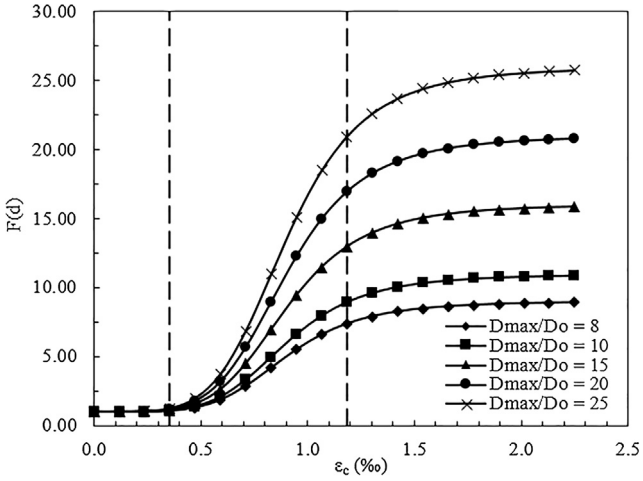

Fig. 7. Loading factor in the elastic state for different D_{max}/D_0 ratios.

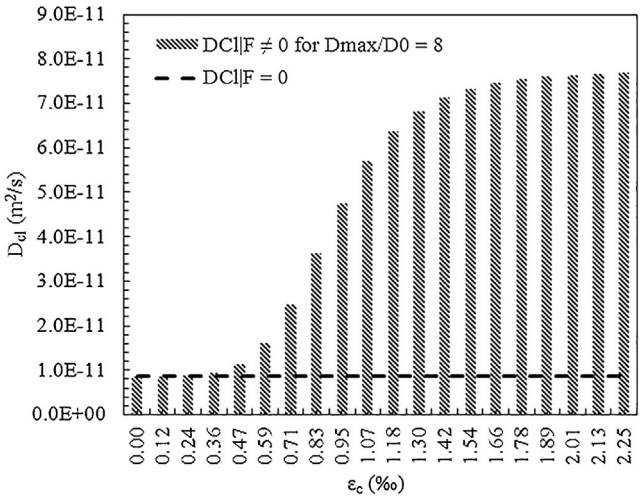

Fig. 8. Constant and non-constant chloride diffusion coefficient.

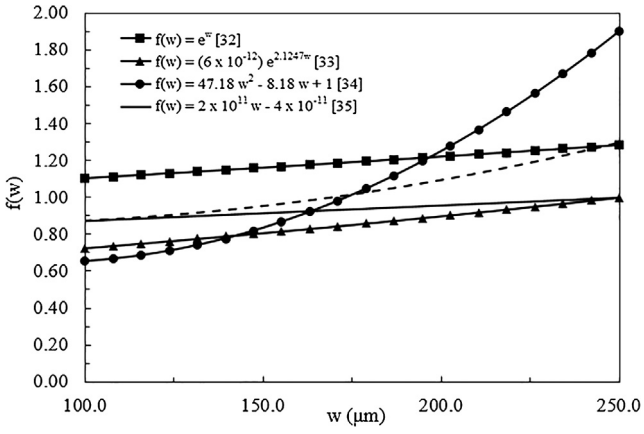

Fig. 9. Crack function versus crack width w.

by using four equations [33,42–44]. All equations are normalized with respect to own maximum value, except for equation given by [44]. The dashed line is the mean trend of the four equations. The mean value is 1.04 and we can define, in such case, that $D_w \approx D_{cl}$.

The studied range of w is 0.1–0.25 mm because authors believe that the comparation of these equations for higher w by analytical analysis is not much reliable. Also, it is in accordance with the allowed crack width for reinforced concrete member, which is 0.3 mm [47].

It is shown in the literature [48] that, in the studied range, when w increases, cracked concrete permeability increases rapidly, thus chloride content increases too. The behaviour is mutual: increasing the content of ions, crack width expands [49]. Moreover, when w is larger than a critical value, the expanding of the w has no significant influence on the transportation of chloride ions [48]; this value is estimated as w > 0.45 mm [49].

The equation for f(w) adopted by [42] has been calibrated considering also the age and crack effect on diffusion, but in this analysis to compare this equation to the others one, both effects have not been considered.

The [43] shows, by using the representative element volume theory, that chloride penetration depends on crack depth and crack density, but it heavily depends on crack width, as considered by the equation proposed in [43]. The quadratic function used by [44], defined by the double-porosity model and studied also in [49], shows more clearly that the chloride diffusion coefficient increases with the increasing of w.

The model showed by [33], studied also in [38,58,59], is slightly linear from 80 μm to ~250 μm. This equation is divided in two parts: (i) transition period where the migration of chloride ions is under non-steady-state conditions; (ii) steady-state period where the increase of chloride ions is constant with elapsed time, providing a constant flux of chloride.

7. Results and discussion

Figs. 10 and 11 show the chloride content in the cases: (i) undamaged concrete C (for $F = 0; w = 0$) and $C_{\varepsilon c}$ ($F \neq 0; w = 0$); (ii) cracked concrete C_w ($w \neq 0$) in x direction and a t domain, respectively. The curves are obtained with C_s constant and $C_0 = 0$. The curves of C_w are obtained by using the chloride coefficient $D_w = 1.297 D_{cl|F\neq 0}$.

The results are consistent to the experimental results in literature – in order to validate the model and the used data (see Tables 1 and 2) – where in [58] it is shown that the chloride content in cracked concrete is greater than in sound concrete, whereas in [60] it is shown the influence of the compressive loading on the chloride diffusion.

$C_{\varepsilon c}$ is calculated according to only one concrete strength defined in Table 2. However, in literature it is shown that the diffusion coefficient decreases with an increase of concrete strength at lower crack width values [59].

The histograms in Fig. 12 show the mean chloride content, whereas in Fig. 13 show the comparison of the maximum chloride content for $C_0 = 0$ and $C_0 = 5$ kg/m^3. The values are expressed as

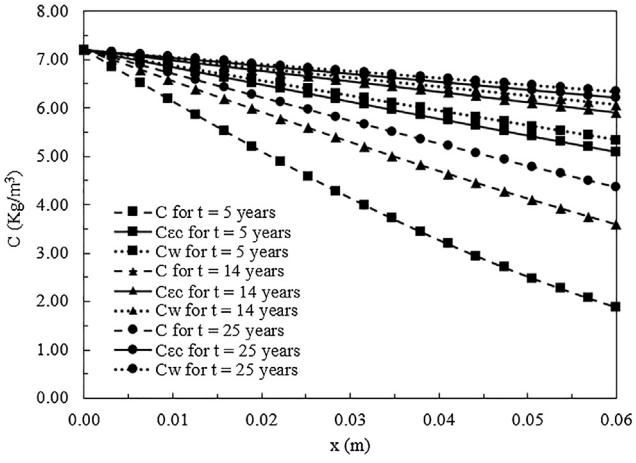

Fig. 10. Chloride content in x direction.

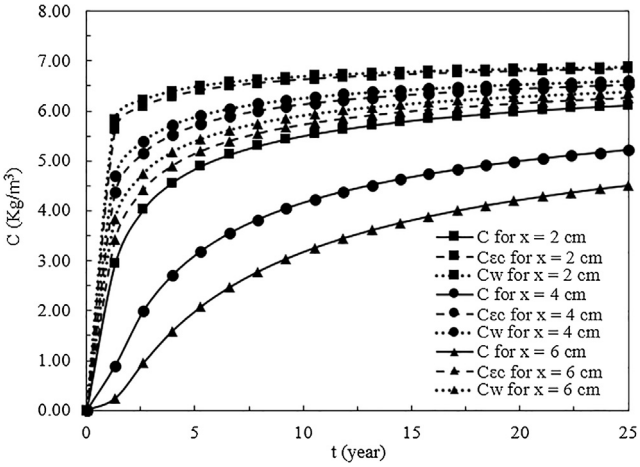

Fig. 11. Chloride content in the time t.

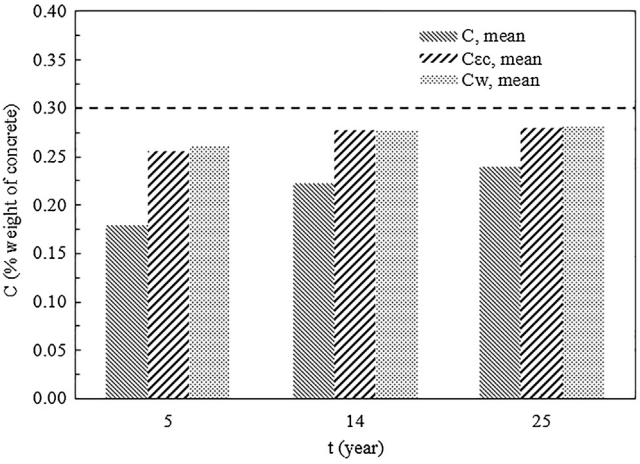

Fig. 12. Mean chloride content t = {5, 14, 25} years.

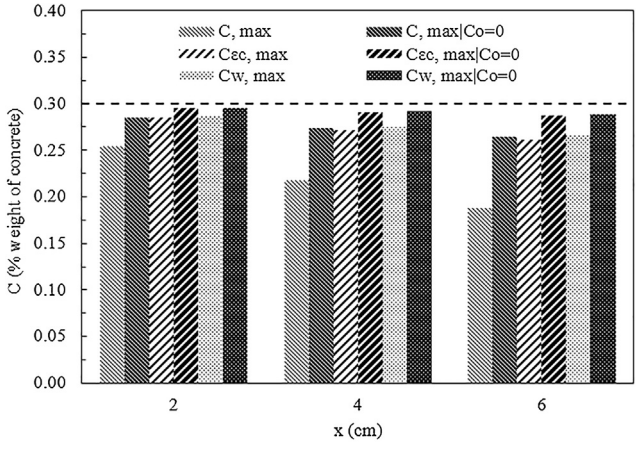

Fig. 13. Maximum chloride content with $C_0 = 0$ and $C_0 = 5$kg/m^3 for x = {2, 4, 6} cm and t = 25 years.

Table 3
Comparison between analytical and computational results.

Used value	Analytical results	Computational results by NIST [23]
Analysis: Predict the chloride ion diffusivity of a concrete based on mixture parameters (m^2/s)		
- w/c = 0.4	7.9×10^{-12}	2.5×10^{-12}[a]
Analysis: Predict the service life of a reinforced concrete structure exposed to chlorides (year)		
- C_s = 7.2 kg/m^3	6.6	4.4[b]
- Reinforcement depth = 6 cm		
- D = 8.6×10^{-12} m^2/s		
Analysis: Predict the chloride ion penetration profile of a concrete after a specific time (mol/L)		
- C_s = 0.198 mol/L (≈ 7.2 kg/m^3)	0.0519	0.0418[c]
- Maximum exposed time = 9125 days (=25 years)		
- w/c = 0.4		
- For t = 1825 days (=5 years)		
- For × = 6 cm		
- D = 8.6×10^{-12} m^2/s		
Analysis: Predict the chloride ion penetration profile of a concrete after a specific time with temperature effects (mol/L)		
- T = 23 °C (=296 K)	0.0519	0.0168c
- C_s = 0.198 mol/L		
- Maximum exposed time = 9125 days		
- For t = 1825 days		
- For × = 6 cm		
- w/c = 0.4		
- D = 8.6×10^{-12} m^2/s		
- E_a = 41.8 kJ/mol		

[a] Volume fraction of aggregate = 66.84%. Degree of hydration = 0.6.
[b] Chloride concentration needed at reinforcement to start corrosion = 2.613 kg/m3. Standard deviation in reinforcement depth = 0.008 m.
[c] Member thickness = 0.5 m. Degree of hydration = 0.6. Volume fraction of aggregate = 66.84%. Chloride binding = 1.67 Cf/(1 + 4.08 Cf). Rate constant for binding = 1 × 10–7 s^{-1}.

percentage of the concrete weight. The horizontal dashed line is an allowed chloride content of concrete in accordance to literature [46] (0.30% of concrete weight = 7.2 kg/m^3).

In the literature, it has been estimated that the chloride concentration level reaches the critical value at the depth of steel bars in about 7–20 years and the critical chloride concentration range 0.15–0.4% of the concrete weight [19,40].

These time and chloride concentration ranges refer to a concrete use containing steel reinforcement or other embedded metal [50]. The predicted values of our model at the x = 6 cm ranges 0.1–0.3% in 7–20 years.

It is important to emphasize that Eq. (3) provides no consideration for the physical presence of steel reinforcements in concrete. However, this aspect can be neglected because the typically used diameters are small [17]. Moreover, the chloride diffusivity is usually analysed up to the concrete cover depth. In [17], it is illustrated that the service life models that do not explicitly account for the physical presence of steel reinforcement bars could over predict service life by up to 25% or even more.

In this analysis the non-steady-state of the chloride diffusivity is considered. The condition of the steady-state [Eq. (2) $\rightarrow \nabla(D_{cl,i}\nabla C_i) = 0$] can be reasonably assumed when the long-term effects are investigated. The chloride diffusivity for the non-steady-state condition is about 10 times higher than that the steady-state condition [51].

In this study, only the compression strains have been considered. In the literature [24], it is shown that, at low strain value, the compressive strain has a positive influence on chloride transportation, but when the compressive strain overpasses the critical value, it has a negative influence.

Finally, Table 3 shows the comparison between the analytical results and computational results with NIST software [23] in order to validate some parameters used in this paper. Four analyses have been carried out: (1) predict the chloride ion diffusivity of a concrete based on mixture parameters, (2) predict the service life of a reinforced concrete structure exposed to chlorides, (3) predict the chloride ion penetration profile of a concrete after a specific time, and (4) predict the chloride ion penetration profile of a concrete after a specific time with temperature effects.

8. Conclusions

This paper presents an analytical procedure to analyse the chloride transport in concrete. The sound and cracked concrete has been considered as well as the linear and non-linear behaviour of the material. The order of magnitude of the results are consistent to the experimental and numerical results in the literature.

The mains conclusions of this paper are listed below:

1) The classic Fick's theory (with D = constant) leads to an estimation of the chloride content that cannot depict the time factors dependence and their interconnection. In particular, as it can be seen in this paper, D_{cl} strongly depends on the stress-strain state and this dependence is often missed in literature (in this analysis $D_{cl|F=0}/D_{cl,max|F\neq0} \cong 0.112$). Moreover, real structural members are not semi-infinite homogeneous elements, therefore the adopted assumptions in the Fick's theory are inadequate for real elements.
2) In real constructions, the poor maintenance and the service loads during the service life induce cracks. Cracks decrease the durability of RC structures by creating preferential paths for the chloride ions penetration. To quantify the chloride diffusion in cracks, four experimental equations have been used considering the crack width, which is directly responsible for the diffusion. The results shown that $D_w \approx (0.872 - 1.297)D_{cl|F\neq0}$.
3) The difference of the chloride content under loading and no-loading at x = 6 cm for 5, 14, and 25 years is 3.2, 2.32 and 1.85 kg/m^3, respectively. These results show a great increase of chloride content due to the loads, which reduces along time. Moreover, the chloride diffusivity result is very fast in an interval of 0–5 years, for example at x = 2 cm, the chloride content reaches 0.20% weight of concrete.

Finally, the literature does not report, to date, enough information to allow for an exact calibration of diffusion parameters accounting for all the possible phenomena: there are always discrepancies between the published results. Future work is needed to further improve mathematical models to effectively schedule the maintenance, repair and rehabilitation program. Chloride diffusion is usually measured by analytical, numerical and experimentally methods, but there is a lack of systematic experimental data for chloride diffusion into concrete.

Conflict of interest

None.

Acknowledgements

The first author acknowledges the "Servicios Informáticos CPD" of the University of Salamanca for the Wolfram Mathematica license and the University of Salamanca to pay the rights (when applicable) to completely download all papers in the references. The first author also acknowledges the Professor Dale P. Bentz for providing the software NIST.

Funding

The study was funded by Support Program for Foreign Students of Doctorate (PAEDEX), Ibero-American University Postgraduate Association (AUIP) and São Paulo State University (UNESP) (reference number: 3.224.803.003.569).

References

[1] Comite Euro-International du Beton (CEB), Durable Concrete Structures, Bulletin D'Information N. 183 (1992).
[2] C.A. Apostolopoulos, V.G. Papadakis, Consequences of steel corrosion on the ductility properties of reinforcement bar, Constr. Build. Mater. 22 (2008) 2316–2324, https://doi.org/10.1016/j.conbuildmat.2007.10.006.
[3] R. Zang, A. Castel, R. François, Concrete cover cracking with reinforcement corrosion of RC beam during chloride-induced corrosion process, Cem. Concr. Res. 40 (2010) 415–425, https://doi.org/10.1016/j.cemconres.2009.09.026.
[4] E. Bastidas-Arteaga, A. Chateauneuf, M. Sánchez-Silva, P. Bressolette, F. Schoefs, A comprehensive probabilistic model of chloride ingress in unsaturated concrete, Eng. Struct. 33 (2011) 720–730, https://doi.org/10.1016/j.engstruct.2010.11.008.
[5] R. Wattanapornprom, T. Ishida, Modeling of chloride penetration into concrete under airborne chloride environmental conditions combined with washout effects, J. Adv. Concr. Technol. 15 (2017) 126–142, https://doi.org/10.3151/jact.15.126.
[6] G.R. Meira, I.J. Padaratz, C. Alonso, C. Andrade, Effect of distance from sea on chloride aggressiveness in concrete structures in Brazilian coastal site, Mater. Constr. 53 (2003) 179–189, https://doi.org/10.3989/mc.2003.v53.i271-272.302.
[7] B. Gerard, G. Pijaudier-Cabot, C. Laborderie, Coupled diffusion-damage modelling and the implications on failure due to strain localisation, Int. J. Solids Struct. 35 (1998) 4107–4120, https://doi.org/10.1016/S0020-7683(97)00304-1.
[8] B. Martín-Pérez, H. Zibara, R.D. Hooton, M.D.A. Thomas, A study of the effect of chloride binding on service life predictions, Cem. Concr. Res. 30 (2000) 1215–12223, https://doi.org/10.1016/S0008-8846(00)00339-2.
[9] O.T. De Rincón, P. Castro, E.I. Moreno, A.A. Torres-Acosta, O.M. De Bravo, I. Arrieta, C. García, M. Martínez-Madrid, Chloride profiles in two marine structures-meaning and some predictions, Build. Environ. 39 (2004) 1065–1070, https://doi.org/10.1016/j.buildenv.2004.01.036.
[10] J. El Hassan, P. Bressolette, A. Chateauneuf, K. El Tawil, Reliability-based assessment of the effect of climatic conditions on the corrosion of RC structures subject to chloride ingress, Eng. Struct. 32 (2010) 3279–3287, https://doi.org/10.1016/j.engstruct.2010.07.001.
[11] G.P. Pellizzer, E.D. Leonel, C.G. Nogueira, Numerical approach about the effect of the corrosion on the mechanical capacity of the reinforced concrete beams considering material nonlinear models, Rev. Ibr. Estr. Mat. 11 (2018) 26–51, https://doi.org/10.1590/S1983-41952018000100003.
[12] P. Carrara, L. De Lorenzis, D.P. Bentz, Chloride diffusivity in hardened cement paste from microscale analyses and accounting for binding effects, Model. Simul. Mater. Sci. Eng. 24 (2016) 1–44, https://doi.org/10.1088/0965-0393/24/6/065009.
[13] Y.M. Sun, M.T. Liang, T.P. Chang, Time/depth dependent diffusion and chemical reaction model of chloride transportation in concrete, App. Math. Mod. 36 (2012) 1114–1122, https://doi.org/10.1016/j.apm.2011.07.053.
[14] M. Morga, G.C. Marano, Chloride penetration in circular concrete columns, Int. J. Concr. Struct. Mater. 9 (2015) 173–183, https://doi.org/10.1007/s40069-014-0095-y.
[15] A. Princigallo, Estimating the chloride transport in cement paste, Mater. Constr. 62 (2012) 151–161, https://doi.org/10.3989/mc.2012.02011.
[16] R. Malheiro, G.R. Meira, M. Lima, Experimental study of chloride transport into double layered components with concrete and rendering mortar, Rev. Constr. 15 (2016) 119–132, https://doi.org/10.4067/S0718-915X2016000300012.
[17] D.P. Bentz, W.S. Guthrie, S.Z. Jones, N.S. Martys, Predicting service life of steel-reinforced concrete exposed to chlorides, Concr. Int. 36 (2014) 55–64.
[18] D.H. Kim, K. Shimura, T. Horiguchi, Effect of tensile loading on chloride penetration of concrete mixed with granulated blast furnace slag, J. Adv. Concr. Technol 8 (2010) 27–34.
[19] J.S. Kong, A.N. Ababneh, D.M. Frangopol, Y. Xi, Reliability analysis of chloride penetration in saturated concrete, Prob. Eng. Mech. 17 (2002) 305–315, https://doi.org/10.1016/S0266-8920(02)00014-0.
[20] C.G. Nogueira, E.D. Leonel, H.B. Coda, Probabilistic failure modelling of reinforced concrete structures subjected to chloride penetration, Int. J. Adv. Struct. Eng. 4 (2012) 10–23, https://doi.org/10.1186/2008-6695-4-10.
[21] C.G. Nogueira, E.D. Leonel, H.B. Coda, Reliability algorithms applied to reinforced concrete structures durability assessment, Ibra. Struct. Mater. J. 5 (2012) 440–450, https://doi.org/10.1590/S1983-41952012000400003.
[22] S.H. Jung, H.M. Yang, K.H. Yang, S.J. Kwon, Maintenance for repaired RC column exposed to chloride attack based on probability distribution of service life, Int. J. Conc. Struct. Mater. 12 (2018) 1–9, https://doi.org/10.1186/s40069-018-0259-2.
[23] National Institute of Standards and Technology (NIST), U.S. Department of Commerce. <https://concrete.nist.gov/ciks/menu0002.html> (accessed May 2018).
[24] H. Ye, C. Fu, N. Jin, X. Jin, Influence of flexural loading on chloride ingress in concrete subjected to cyclic drying-wetting condition, Comput. Concr. 15 (2015) 183–199, https://doi.org/10.12989/cac.2015.15.2.183.
[25] C. Fu, H. Ye, X. Jin, N. Jin, L. Gong, A reaction-diffusion modelling of carbonation process in self-compacting concrete, Comput. Struct. 15 (2015) 847–864, https://doi.org/10.12989/cac.2015.15.5.847.
[26] Y. Wang, S. Nanukuttan, Y. Bai, P.A.M. Basheer, Influence of combined carbonation and chloride ingress regimes on rate of ingress and redistribution of chlorides in concretes, Constr. Build. Mater. 140 (2017) 173–183, https://doi.org/10.1016/j.conbuildmat.2017.02.121.
[27] N. Damrongwiriyanupap, S. Limkatanyu, Y. Xi, A thermo-hygro-coupled model for chloride penetration in concrete structures, Hind. Publis. Corp. 2015 (2015) 1–10, https://doi.org/10.1155/2015/682940.
[28] T.V. Mien, B. Stitmannaithum, T. Nawa, Simulation of chloride penetration into concrete structures subjected to both cyclic flexural loads and tidal effects, Comput. Concr. 6 (2009) 421–435, https://doi.org/10.12989/cac.2009.6.5.421.
[29] J. Wang, P.A.M. Basheer, S.V. Nanukuttan, A.E. Long, Y. Bai, Influence of service loading and the resulting micro-cracks on chloride resistance of concrete, Constr. Build. Mater. 108 (2016) 56–66, https://doi.org/10.1016/j.conbuildmat.2016.01.005.
[30] M.S. Islam, K. Toshiharu, Proposal of analysis methods based on stagnation of chloride ion in concrete, J. Adv. Concr. Technol. 11 (2013) 374–382, https://doi.org/10.3151/jact.11.374.
[31] T. Ishida, P.O.N. Iqbal, H.T.L. Anh, Modeling of chloride diffusivity coupled with non-linear binding capacity in sound and cracked concrete, Cem. Concr. Res. 39 (2009) 913–923, https://doi.org/10.1016/j.cemconres.2009.07.014.
[32] J.L. Marriaga, P. Claisse, The influence of the blast furnace slag replacement on chloride penetration in concrete, Ing. Invest. 31 (2011) 38–47.
[33] A. Djerbi, S. Bonnet, A. Khelidj, V. Baroghel-bouny, Influence of traversing crack on chloride diffusion into concrete, Cem. Concr. Res. 38 (2008) 877–883, https://doi.org/10.1016/j.cemconres.2007.10.007.
[34] A.T.C. Guimarães, P.R.L. Helene, Model to predict the chloride penetration in concrete with profile forming peak: verification of its precision, Rev. Mater. 14 (2009) 983–992, https://doi.org/10.1590/S1517-70762009000300010.
[35] W.J. Fan, X.Y. Wang, Prediction of chloride penetration into hardening concrete, Hind. Publis. Corp. 2015 (2015) 1–8, https://doi.org/10.1155/2015/616980.
[36] AutoCAD, Version 2010, Autodesk, Inc. (2010).
[37] C. Fu, X. Jin, H. Ye, N. Jin, Theoretical and experimental investigation of loading effects on chloride diffusion in saturated concrete, J. Adv. Concr. Technol. 13 (2015) 30–43, https://doi.org/10.3151/jact.13.30.
[38] C. Fu, X. Jin, N. Jin, Modeling of chloride ions diffusion in cracked concrete, Earth and Space 2010: Engineering, Science, Construction, and Operations in Challenging Environments (2010) 3579–3589, 14–17 March, Honolulu, Hawaii, USA.
[39] W. Chen, J. Zhang, J. Zhang, A variable-order time-fractional derivative model for chloride ions sub-diffusion in concrete structures, Fract. Calc. Appl. Anal. 16 (2013) 76–92, https://doi.org/10.2478/s13540-013-0006-y.
[40] S. Zofia, Z. Adam, Theoretical model and experimental tests on chloride diffusion and migration processes in concrete, Proc. Eng. 57 (2013) 1121–1130, https://doi.org/10.1016/j.proeng.2013.04.141.
[41] Y.Y. Kim, B.J. Lee, S.J. Kwon, Evaluation technique of chloride penetration using apparent diffusion coefficient and neural network algorithm, Adv. Mater. Sci. Eng. 2014 (2014) 1–13, https://doi.org/10.1155/2014/647243.

[42] S.H. Jung, H.S. Ryu, S. Karthick, S.J. Kwon, Time and crack effect on chloride diffusion for concrete with fly ash, Int. J. Concr. Struct. Mater. 12 (2018) 1–10, https://doi.org/10.1186/s40069-018-0230-2.
[43] K.H. Yang, J.K. Singh, B.Y. Lee, S.J. Kwon, Simple technique for tracking chloride penetration in concrete based on the crack shape and width under steady-state conditions, Sustainability 9 (2017) 282–295, https://doi.org/10.3390/su9020282.
[44] S.F. Zhang, C.H. Lu, R.G. Liu, Experimental determination of chloride penetration in cracked concrete beams, Proc. Eng. 24 (2011) 380–384, https://doi.org/10.1016/j.proeng.2011.11.2661.
[45] C.A. Silva, A.T.C. Guimarães, Evaluation of the diffusion model considering the variation in time of the chloride content of the concrete surface, Rev. Mater. 19 (2014) 81–93, https://doi.org/10.1590/S1517-70762014000200003.
[46] R.V. Silva, J. De Brito, R. Neves, R. Dhir, Prediction of chloride ion penetration of recycled aggregate concrete, Mater. Res. 18 (2015) 427–440, https://doi.org/10.1590/1516-1439.000214.
[47] European Committee for Standardization (CEN), Design of concrete structures – Part 1–1: General rules and rules for buildings (2004) BS EN 1992-1-1:2004, Brussels, Belgium.
[48] L. Wang, T. Ueda, Mesoscale modelling of the chloride diffusion in cracks and cracked concrete, J. Adv. Concr. Technol. 9 (2011) 241–249, https://doi.org/10.3151/jact.9.241.
[49] S. Ting, L. Yang, Chloride ion erosion experiment research in cracked concrete, MSETEE, IOP Conf. Ser.: Earth Environ. Sci. 81 (2017) 1–7, https://doi.org/10.1088/1755-1315/81/1/012134.
[50] European Committee for Standardization (CEN), Concrete – Part 1: Specification, performance, production and conformity (2000) BS EN 206-1:2000, Brussels, Belgium.
[51] L. Homan, A.N. Ababneh, Y. Xi, The effect of moisture transport on chloride penetration in concrete, Constr. Build. Mater. 125 (2016) 1189–1195, https://doi.org/10.1016/j.conbuildmat.2016.08.124.
[52] Wolfram Mathematica, Version 11 Student Edition, Wolfram Research, Inc. (2017).
[53] I. Othmen, S. Bonnet, F. Schoefs, Statistical investigation of different analysis methods for chloride profiles within a real structure in a marine environment, Ocean Eng. 157 (2018) 96–107, https://doi.org/10.1016/j.oceaneng.2018.03.040.
[54] A. Da Costa, M. Fenaux, J. Fernández, E. Sánchez, A. Moragues, Modelling of chloride penetration into no-saturated concrete: case study application for real marine offshore structures, Constr. Build. Mater. 48 (2013) 217–224, https://doi.org/10.1016/j.conbuildmat.2013.02.009.
[55] M.D. Pritzl, H. Tabatabai, A. Ghorbanpoor, Long-term chloride profiles in bridge decks treated with penetrating sealer or corrosion inhibitors, Constr. Build. Mater. 101 (2015) 1037–1046, https://doi.org/10.1016/j.conbuildmat.2015.10.158.
[56] P.P. Win, M. Watanabe, A. Machida, Penetration profile of chloride ion in cracked reinforced concrete, Cem. Concr. Res. 34 (2004) 1073–1079, https://doi.org/10.1016/j.cemconres.2003.11.020.
[57] L. Pang, Q. Li, Service life prediction of RC structures in marine environment using long term chloride ingress data: comparison between exposure trials and real structure surveys, Constr. Build. Mater. 113 (2016) 979–987, https://doi.org/10.1016/j.conbuildmat.2016.03.156.
[58] E. Kato, Y. Kato, T. Uomoto, Development of simulation model of chloride ion transportation in cracked concrete, J. Adv. Concr. Technol. 3 (2005) 85–94, https://doi.org/10.3151/jact.3.85.
[59] S.Y. Jang, B.S. Kim, B.H. Oh, Effect of crack width on chloride diffusion coefficients of concrete by steady-state migration tests, Cem. Concr. Res. 41 (2011) 9–19, https://doi.org/10.1016/j.cemconres.2010.08.018.
[60] A.D. Tegguer, S. Bonnet, A. Khelidj, V. Baroghel-Bouny, Effect of uniaxial compressive loading on gas permeability and chloride diffusion coefficient of concrete and their relationship, Cem. Concr. Res. 52 (2013) 131–139, https://doi.org/10.1016/j.cemconres.2013.05.013.

3rd International Conference on International Conference on Recent Advances in Nonlinear Design, Resilience and Rehabilitation of Structures, CoRASS 2019
H. Barros, C. Ferreira, José M. Adam and Norb Delatte (Eds)

CHLORIDE DIFFUSIVITY ACCOUNTING FOR SHORTENING STRAIN EFFECTS IN RC STRUCTURES

ENRICO ZACCHEI* **AND CAIO G. NOGUEIRA**

School of Civil Engineering
São Paulo State University (UNESP)
14-01 Eng. Luís Edmundo Carrijo Coube Avenue, 17033-360, Bauru-SP, Brazil
e-mail: e.zacchei@unesp.br (Eng. Dr. Enrico Zacchei)
e-mail: caio.nogueira@unesp.br (Prof. Dr. Caio Gorla Nogueira)

Key words: Chloride ions diffusion, Loading effect factor, Cracked concrete, RC structures.

Summary. In the last decade, Reinforced Concrete (RC) (steel bar + concrete, and/or additives) in structures has been widely studied. Structures are subjected to internal and external actions affecting their performance, serviceability and safety. Moreover, RC structures are subjected to degradations by chemical (e.g. corrosion), physical and/or mechanical processes (e.g. diffusion of chloride ions). The aim of this study is to investigate the chloride ions diffusion in sound and cracked concrete under compressive loads in accordance to Eurocode. The governing equations are modified to account for the non-constant chloride diffusion coefficient. With this condition it is possible to define several terms in the time-domain to predict the service life of structures. The considered material is a saturated and hardened cement paste under non-steady-state conditions. Loads are studied for linear and non-linear states, whereas the model is developed by analytical and computational analyses. A satisfactory calibration between the observations and modelling output has been obtained. Results show that the predicted values at the depth of the steel reinforcement ranges from 0.1% to 0.3% of concrete weight in 7-20 years; the ratio of the chloride diffusion coefficient under loading and no-loading is about 9, whereas the chloride diffusivity coefficient in cracks is 0.9-1.3 times the chloride diffusion coefficient under loading.

1 INTRODUCTION

The durability of civil engineering constructions is affected by chloride ingress inducing corrosion of steel reinforcement. If the corrosion process is well unvalued it can put several parts of the structural system (e.g. structural and non-structural elements) at risk including people's lives.

The durability is a prerequisite for the normal function of a structure and coupled to the study of the characteristics of the Reinforced Concrete (RC) are of high interest in research[1,14,15,17].

A parameter that significantly influences the chloride ingress into concrete is the diffusion coefficient, which serves as an input into the developing of the analysis.

The focus of this paper is to predict the evolution of the chloride concentration inside the sound and damaged RC by the diffusion process. The choice of using diffusion process in sound RC is justified by the fact that the analysis in this paper is based on the first and second Fick's

law. On the other side, the analyse of the chloride diffusion in damaged RC is justified because the structures in the real situations are not crack-free. In this second case, Fick's laws are complemented by semi-empirical equations.

Cracks, which may have different widths and different depths, reduce the cover thickness and increase the migration of the chloride ions in channels to reach the surface of the steel.

Many micro-cracks can contribute to facilitate the ions penetration; therefore, it is important to consider such phenomenon and its effects to perform better predictions of the chloride concentrations in concrete.

The contribute of this paper is to point out possible factors that influence the chloride concentration inside concrete for more accurate analytical and numerical predictions.

2 CHLORIDE DIFFUSIVITY MODELS

2.1 Sound concrete

The model that describes the flux of chloride ions (J) in saturated concrete depending on the total chloride concentration gradient (∇C) is defined by the Fick's first law as follows[5]

$$J = -D(\nabla C) \tag{1}$$

where: D is the diffusivity parameter, which can be assumed constant (traditional condition) or variable (i.e. when it is defined in a time-depth diffusion model).

In this analysis D is variable and it is considered as the diffusivity in saturated capillary pores, called D_{cl}.

Equation (1) can be derived considering the general mass balance principle along the time t in the all directions (i = x, y, z) under non-steady-state conditions by the Fick's second law[7], which calculates the chloride concentration (C) at a specific position i along time t:

$$\frac{\partial C}{\partial t} = \nabla\left(D_{cl,i}\nabla C_i\right) = \frac{\partial}{\partial x}\left(D_{cl,x}\frac{\partial C}{\partial x}\right) + \frac{\partial}{\partial y}\left(D_{cl,y}\frac{\partial C}{\partial y}\right) + \frac{\partial}{\partial z}\left(D_{cl,z}\frac{\partial C}{\partial z}\right) \tag{2}$$

The solution of Eq. (2) is obtained if several hypotheses are respected: (i) the medium is semi-infinite and homogeneous; (ii) the superficial chloride concentration, C_s, is uniform and constant; (iii) the external surface of the concrete is plane; (iv) the diffusion front is a mono-dimensional model; (v) the chloride ions are transported into a water-saturated concrete only via diffusion and do not react with the other particles; (vi) the chemical composition of substances in concrete pore is considered to be in equilibrium throughout the entire diffusion process.

Under these hypotheses, the analytical solution of the Eq. (2) in x and t is given by

$$C(x,t) = C_0 + (C_s - C_0)\left[1 - erf\left(\frac{x}{2\sqrt{D_{cl}t}}\right)\right] \tag{3}$$

$$i.c.: C(x,0) = C_0$$
$$b.c.: C(0,t) = C_s\,;\, C(\infty,t) = C_0$$

where: i.c. and b.c. are the initial and boundary conditions, respectively, and C_0 is the initial chloride concentration. The term in square brackets describes the evolution of the C in the direction x at a time t, with $\mathrm{erf}(\cdot)$ that represents the Gaussian error function.

The hypothesis of the water saturated occur in many real-world cases due to the limited thickness of the concrete cover (typical dimension is ~3-5 cm). The hypothesis of C_s uniform and constant may be applied when the effects of the environment variations are negligible, e.g. when there is no frequent washing by rain. C_s also depends on the concrete porosity at the surface and it is not independent to the C(x,t)[18].

Figure 1 shows the model described by Eq. (3).

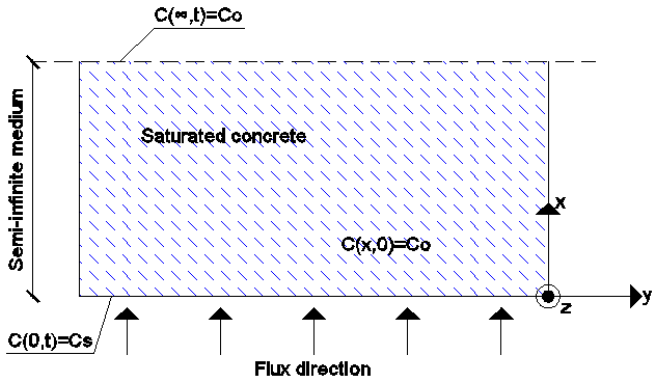

Figure 1: Diffusion flux in a semi-infinite concrete medium[8]

The diffusion coefficient (D_{cl}) is expressed by the following multifactor equation[2]

$$D_{cl} = f_0 \times f_1(C_b) \times f_2(T) \times f_3(t) \times F(\varepsilon_c, d) \tag{4}$$

where: f_0 is the constant factor, f_1 depends on bound chloride concentration C_b, f_2 depends on the temperature T and f_3 depends on the age t. More details regarding these factors are provided in the literature[2,9].

F is the loading effect factor, which is divided in two parts: one depends on the concrete compressive strain ε_c and another depends on the damage variable d (i.e. $F = F(\varepsilon_c) + F(d) = F(\varepsilon_c, d)$). When $\varepsilon_c = 0$ and $d = 0$, F is expressed by the Taylor expansion as

$$F(\varepsilon_c, d) = F(0,0) + \frac{\partial F}{\partial \varepsilon_c}|_{(0,0)}\varepsilon_c + \frac{\partial F}{\partial d}|_{(0,0)}d \tag{5}$$

Assuming the first, second and third term on the right side of Eq. (5) as 1, B and C, respectively, under the conditions $\varepsilon_c = 0$ and $d = 0$, Eq. (5) can be rewritten as

$$F(\varepsilon_c, d) = 1 + B\varepsilon_c + Cd \tag{6}$$

Introducing the damage influence factor $f(d)$ consistent to the literature[10], which describes the concrete local damage with

$$f(d) = 1 + \frac{D_{max}}{D_0} - \frac{D_{max}}{D_0}\left[1 + \left(\frac{d}{d_{cr}}\right)^n\right]^{-1} \tag{7}$$

it is possible to obtain, from a function with one parameter d, a function with two parameters ε_c and d (i.e. $f(d) \rightarrow F(\varepsilon_c, d)$). Finally, multiplying $(1 + B_1\varepsilon_c + C_1 d)$ in the second term of the Eq. (7) the final relations is

$$F(\varepsilon_c, d) = 1 + \frac{D_{max}}{D_0} B_1\varepsilon_c + \frac{D_{max}}{D_0}\left\{1 + C_1 d - \left[1 + \left(\frac{d}{d_{cr}}\right)^n\right]^{-1}\right\} \tag{8}$$

where: D_0 and D_{max} are the chloride diffusivity in sound concrete and in completely damaged concrete, respectively, n and d_{cr} are constant values, $C_1 = (-B \times D_0 \times \varepsilon_{c1})/D_{max}$ and $B_1 = (B \times D_0)/D_{max}$.

There are four cases related to the Eq. (8): (1) $d = 0$, when there is no damage in concrete, but the chloride diffusivity changes with the elastic load and deformation; (2) $\varepsilon_c = 0$, when the concrete is damaged without sustained loads; (3) $\varepsilon_c = 0$ and $d = 0$, when there are no loading effects; (4) $\varepsilon_c \neq 0$ and $d \neq 0$, when the concrete is damaged with sustained loads.

Figure 2 shows the diffusion coefficient vs. ε_c used in this analysis for constant and non-constant value.

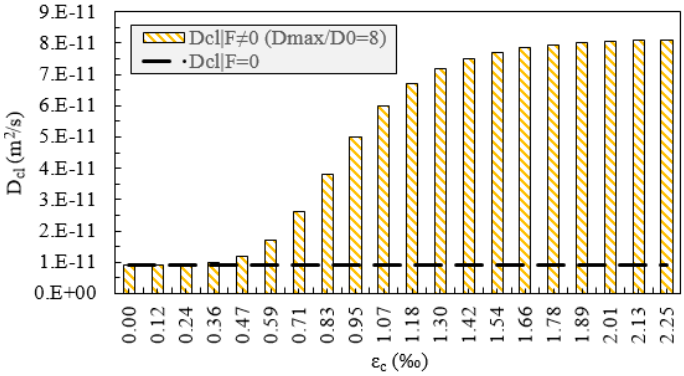

Figure 2: Chloride diffusion coefficient (constant and non-constant)

It is possible to see that D_{cl} under loadings ($Dcl|_{F\neq0}$) increases from 0.47‰ and stabilizes from 1.89 ‰. This is due to the fact that for small ε_c the cracks are of the order of the size of

the voids, therefore there are no variations, whereas for large ε_c a chloride ion is no longer affected by the edge of the crack.

2.2 Cracked concrete

In cracked concrete the diffusion coefficient D is replaced by D_w because the analytical solution (Eq. (3)) does not account the crack width, w[4,11,12].

It is assumed that the diffusion process is governed by a crack function f(w) to create a relationship between chloride diffusion and concrete cracks as:

$$D_w = f(w) D_{cl} \tag{9}$$

Figure 3 shows the curves obtained by relationships retrieved from the literature[13,14,15,16] and their mean curve (dashed black line). f(w) varies between 0.6-1.9 for w between 0.1-0.25 mm.

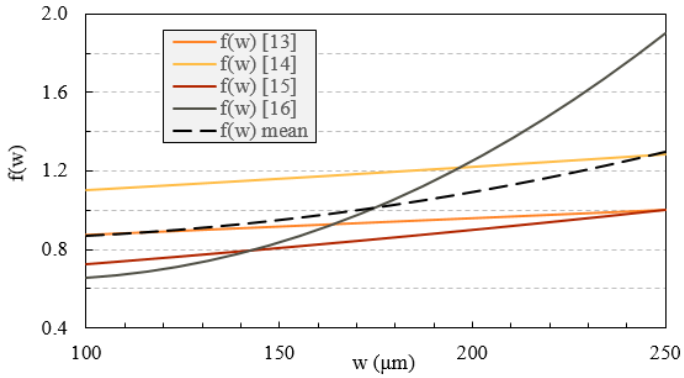

Figure 3: Crack function by four semi-empirical equations

3 MATERIALS AND METHODS

Here the used data (15 + 9 parameters) and methodology (3 principal steps) are explained. Table 1 lists the values for the stress-strain analysis to define the F(ε_c, d) factor[6,10].

Parameter	Value	Unit
Characteristic compressive strength, f_{ck}	35.0	MPa
Mean compressive strength, f_{cm}	43.0	
Elasticity modulus, E_{cm}	34000	
Strain at peak stress, ε_{c1}	2.25	‰
Ultimate compressive strain, ε_{cu1}	3.5	
Concrete density	24.0	kN/m^3
Constant value, n	5.0	-
Constant value, d_{cr}	0.40	-
Constant value, C_1	-0.88	-

Table 1: Input parameters regarding F(ε_c,d) factor

Table 2 lists the adopted parameters to predict the chloride ions diffusion. For each parameter is indicated its dependence (see Eqs. (3)-(4)).

Dependence	Parameter	Value	Unit
C(x,t)	Initial chloride concentration, C_o	0 and 5.0	kg/m^3
	Superficial chloride concentration, C_s	7.2	
f_0	Water/cement ratio for standard composition, w/c	40.0	%
$f_1(C_b)$	Free chloride concentration, C_f	1.5	kg/m^3
	Constant value, α	11.8	-
	Constant value, β	4.0	-
	Evaporable water content, ω_e	60.0	%
$f_2(T)$	Activation energy, E_a	41.80	kJ/mol
	Gas constant, R	8.314	J/(mol × K)
	Reference temperature, T_0	293.0	K
	Current temperature, T	296.0	
$f_3(t)$	Reference age, t_{ref}	28.0	dd
	Time for constant diffusivity, t_r	30.0	year
	Exposed time (age), t	from 0 to 25	
	Index value, m	0.20	-

Table 2: Input parameters[9]

To define C_1, the B parameter is obtained by following relation: $(D_{max}/D_0 - 1)/\varepsilon_{c1} = 3.11 \times 10^{-3}$, for $D_{max}/D_0 = 8$.

The used algorithm is shown in Figure 4. In the left-hand side there are the design parameters (factors) and in the middle there are the two types of the chloride diffusion coefficient. In the right-hand side there are the governing equations and the analytical solution. The algorithm steps go from left side to right side.

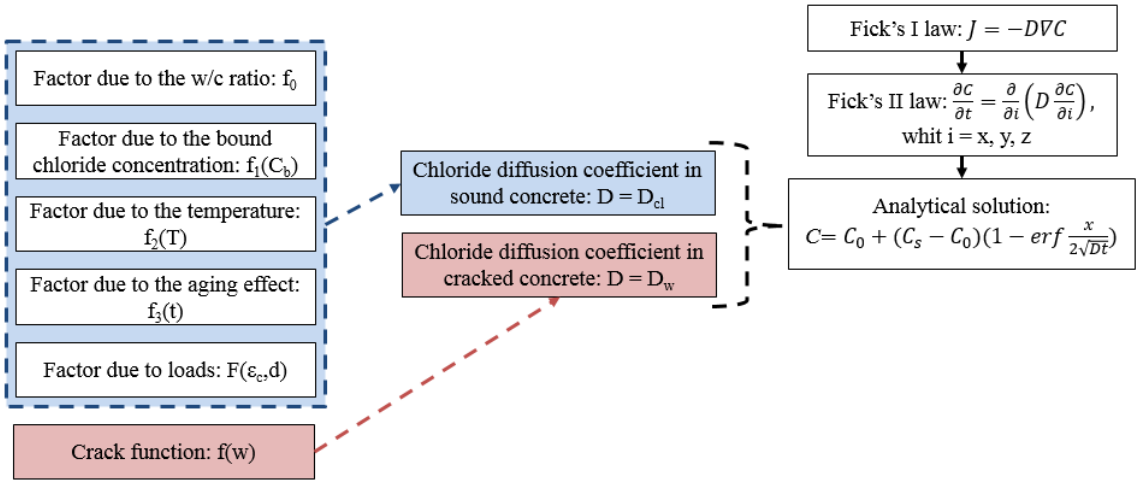

Figure 4: Algorithm to predictive chloride ions diffusion

4 ANALYSES AND RESULTS

Results are expressed in terms of chloride ions content. It is common to express this content in kg/m^3 or respect to the percentage of the weight of concrete.

Figure 5 shows the chloride content in x direction and t domain, for the following three cases:

- Sound concrete without loadings, C (F = 0, w = 0).
- Sound concrete with loadings, $C_{\varepsilon c}$ (F ≠ 0, w = 0).
- Cracked concrete, C_w (w≠0).

Curves are obtained with C_s constant and C_0 = 0. For the curves of C_w, the chloride coefficient $D_w = 1.3 \times D_{cl|F\neq0}$ is used.

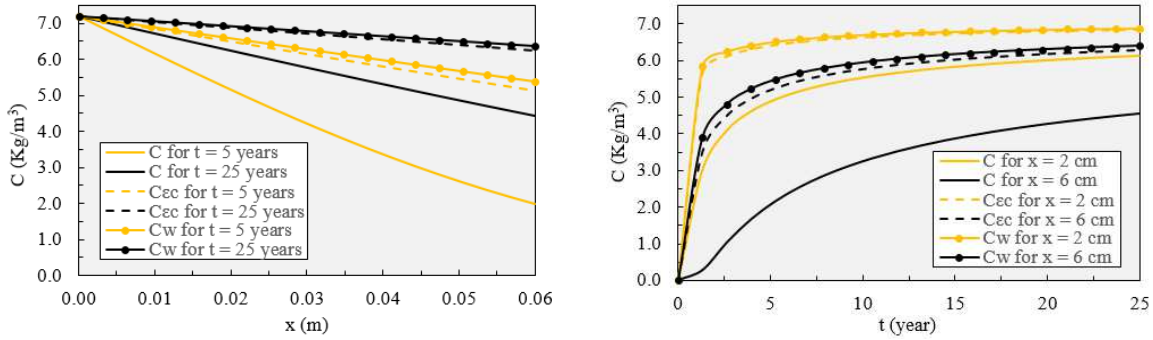

Figure 5: Chloride content in x and t

The chloride content under loadings is greater than the chloride content without loadings, shown the effect of the stress on the diffusion. Moreover, it is possible to see that the chloride content C, for t = 5 years and x = 6 cm, calculated by traditional relation (without loadings and cracks) is very underestimated[3].

The bubble chart with 3D effects in Figure 6 shows the mean chloride content and the comparison of the maximum chloride content for C_0 = 0 and C_0 = 5 kg/m^3.

An allowed chloride content of concrete could be equal to 7.2 kg/m^3 (i.e. 0.30% of concrete weight). The predicted values in this model at the x = 6 cm ranges 0.1–0.3% in 7–20 years.

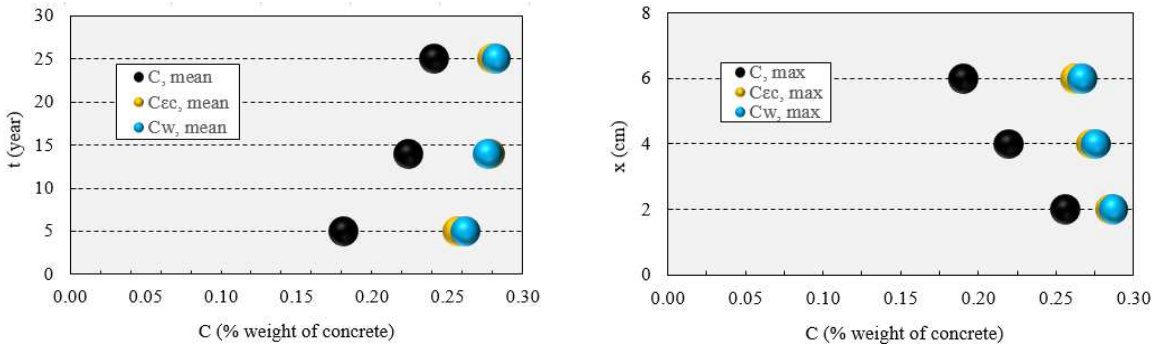

Figure 6: Mean and maximum chloride content expressed in % by weight of concrete

The chloride content $C_{\varepsilon c}$ and C_w are overlapped because $C_{\varepsilon c}$ is calculated for ε_c = 2.25‰, that is when the strain reaches the peak and the material moves from the elastic state to plastic

state.

5 CONCLUSIONS

The mains conclusions of this paper are summarized below.

- Real structures are not composed by semi-infinite homogeneous elements, therefore the adopted assumptions in the Fick's equations are inadequate for real elements. This must incentive the research about these issues.
- Fick's equations, with the constant diffusivity coefficient D, leads to an estimation of the chloride content that cannot depict the time factors dependence and their interconnection. In this paper, it is possible to see that D_{cl} strongly depends on the stress-strain state. In particular, in this analysis $D_{cl|F=0} \approx 10\%\ D_{cl,max|F\neq0}$.
- In real constructions, the service loadings induce cracks, which decrease the durability of RC structures by creating preferential paths for the chloride ions penetration. To quantify the chloride diffusion in cracks, it is possible to consider a crack width that is directly responsible for the diffusion. The results shown that D_w ranges between $0.9 \times D_{cl|F\neq0}$ and $1.3 \times D_{cl|F\neq0}$.
- The difference of the chloride content under loading and no-loading at x equal to 6 cm for 5 years, 14 years and 25 years is 3.1 kg/m^3, 2.2 kg/m^3 and 1.7 kg/m^3, respectively. These results show a great increase of chloride content due to loadings. Moreover, the chloride diffusivity result is very fast in an interval of 0-5 years, for example at x = 2 cm, the chloride content reaches 0.20% of the concrete weight.

REFERENCES

[1] W.A. Al-Kutti, M.K. Rahman, M.A. Shazali, M.H. Baluch, "Enhancement in chloride diffusivity due to flexural damage in reinforced concrete beams", *J. Mater. Civ. Eng.*, **26**, 658-667 (2014).

[2] C. Fu, X. Jin, H. Ye, N. Jin, "Theoretical and experimental investigation of loading effects on chloride diffusion in saturated concrete", *J. Adv. Conc. Tech.*, **13**, 30-43 (2015).

[3] J. Wang, P.A.M. Basheer, S.V. Nanukuttan, A.E. Long, Y. Bai, "Influence of service loading and the resulting micro-cracks on chloride resistance of concrete", *Const. Build. Mater.*, **108**, 56-66 (2016).

[4] R. Zhang, A. Castel, R. François, "Concrete cover cracking with reinforcement corrosion of RC beam during chloride-induced corrosion process", *Cem. Conc. Resear.*, **40**, 415-425 (2010).

[5] P. Carrara, L. De Lorenzis, D.P. Bentz, "Chloride diffusivity in hardened cement paste from microscale analyses and accounting for binding effects", *Model. Simul. Mat. Sci. Eng.*, **24**, 1-44 (2016).

[6] European Committee for Standardization (CEN), Design of concrete structures - Part 1–1: General rules and rules for buildings, EN 1992-1-1:2004, Brussels, Belgium, (2004).

[7] C. Fu, H. Ye, X. Jin, N. Jin, L. Gong, "A reaction-diffusion modelling of carbonation process in self-compacting concrete", *Comp. Struct.*, **15**, 847-864 (2015).

[8] AutoCAD, Version 2010, Autodesk, Inc. (2010).

[9] E. Zacchei, C.G. Nogueira, "Chloride diffusion assessment in RC structures considering the stress-strain effects and crack width influences", *Const. Build. Mater.*, **201**, 100-109 (2019).
[10] B. Gerard, G. Pijaudier-Cabot, C. Laborderie, "Coupled diffusion-damage modelling and the implications on failure due to strain localisation", *Int. J. Solids Struct.*, **35**, 4107-4120 (1998).
[11] E. Kato, Y. Kato, T. Uomoto, "Development of simulation model of chloride ion transportation in cracked concrete", *J. Adv. Conc. Techn.*, **3**, 85-94 (2005).
[12] S.Y. Jang, B.S. Kim, B.H. Oh, "Effect of crack width on chloride diffusion coefficients of concrete by steady-state migration tests", *Cem. Concr. Resea.*, **41**, 9-19 (2011).
[13] A. Djerbi, S. Bonnet, A. Khelidj, V. Baroghel-bouny, "Influence of traversing crack on chloride diffusion into concrete", *Cem. Concr. Resea.*, **38**, 877-883 (2008).
[14] S.H. Jung, H.S. Ryu, S. Karthick, S.J. Kwon, "Time and crack effect on chloride diffusion for concrete with fly ash", *Int. J. Conc. Struct. Mat.,* **12**, 1-10 (2018).
[15] K.H. Yang, J.K. Singh, B.Y. Lee, S.J. Kwon, "Simple technique for tracking chloride penetration in concrete based on the crack shape and width under steady-state conditions", *Sust.*, **9**, 282-295 (2017).
[16] S.F. Zhang, C.H. Lu, R.G. Liu, "Experimental determination of chloride penetration in cracked concrete beams", *Proc. Eng.*, **24**, 380-384 (2011).
[17] Im, D., Sancharoen, P., Julnipitawong, P., Tangtermsirikul, S., Effects of chloride content on thermal properties of concrete, International Journal of Geomate 14 (2018), 135-142.
[18] A. Da Costa, M. Fenaux, J. Fernández, E. Sánchez, A. Moragues, "Modelling of chloride penetration into no-saturated concrete: case study application for real marine offshore structures", *Constr. Build. Mater.*, **48**, 217–224 (2013).

3rd International Conference on International Conference on Recent Advances in Nonlinear Design, Resilience and Rehabilitation of Structures, CoRASS 2019
H. Barros, C. Ferreira, José M. Adam and Norb Delatte (Eds)

NUMERICAL SOLUTIONS FOR CHLORIDE DIFFUSIONS USING STOCHASTIC INPUTS

ENRICO ZACCHEI* **AND CAIO G. NOGUEIRA**

School of Civil Engineering
São Paulo State University (UNESP)
14-01 Eng. Luís Edmundo Carrijo Coube Avenue, 17033-360, Bauru-SP, Brazil
e-mail: e.zacchei@unesp.br (Eng. Dr. Enrico Zacchei)
e-mail: caio.nogueira@unesp.br (Prof. Dr. Caio Gorla Nogueira)

Key words: Chloride ions diffusion, Diffusivity fluctuation, MCS, Failure probability.

Summary. Corrosion damage of reinforcement in concrete elements due to chloride attack is a major problem for long term durability of Reinforced Concrete (RC) structures and, if unvalued, it can put the whole or part of the structural system at risk, including the environment and people's lives. The diffusion of the chloride ions in RC structures varies in time (days, years) and space (two dimensions and three dimensions) and depends on many uncertain factors, such as the composition of the concrete and its properties, temperature, aging and humidity. Moreover, each of these factors have a several uncertain intrinsic sub-factors that are difficult to be defined. In this work two aspects have been studied: the content of chloride ions in concrete and the fluctuation of the diffusivity. The first aspect by using stochastic randomness parameters helps to estimate the service life of the structure, whereas the second one calls attention to the fact that the real nature of the diffusion process is random. Numerical analyses have been carried out. The governing equations were modified to account for the non-constant diffusion coefficient in hardened cement paste under non-steady-state condition. This paper's aim is to develop a new probabilistic analysis. Results show that the expected time for corrosion initiation is around of 40 years, whereas the more probability of failure is around 50 years. Finally, the fluctuation of the diffusivity in 2D/3D model is carried out showing a reduction of the chloride content.

1 INTRODUCTION

This work analyses the diffusion of chloride ions in Reinforced Concrete (RC) constructions. The effects of this diffusion increase the probability that the reinforced steel can be corroded, affecting the long-term durability of the construction elements. This issue is studied by specialists and researchers in different part of the world to minimize the failure risk and the negative impact of the project on the environment[4,5,10,11,12].

Here, two alternative approaches are carried out, in this sense, this paper incentives at providing some points of innovation. The first approach is a probabilistic approach, whereas the second one is a numerical computational approach. The main goals regarding both approaches are to estimate the time for corrosion initiation of the steel reinforcement by chloride

ions diffusion and to define the influence of the fluctuating chloride diffusivity in two and three dimensions.

The contributions of the temperature, aging and humidity on the chloride diffusivity are taken into account.

In order to validate and compare the results, the analytical solution is adopted, and three different probabilistic techniques are used. Using several approaches (probabilistic, analytical and numerical) improves the understanding of processes, given that the real conditions are very irregular and aleatory.

2 CHLORIDE DIFFUSIVITY MECHANICAL MODELS

2.1 Governing equations

The flux of chloride ions, J, depends on its concentration gradient, ∇C, by the Fick's first law[5]:

$$J = -D_{cl}(\nabla C) \tag{1}$$

where: D_{cl} is the diffusivity in saturated capillary pores in the concrete.

Considering the mass balance principle along the time t in the three directions i = {x, y, z} under non-steady-state conditions, Eq. (1) becomes[7]:

$$\frac{\partial C}{\partial t} = \nabla\left(D_{cl,i}\nabla C_i\right) = \frac{\partial}{\partial x}\left(D_{cl,x}\frac{\partial C}{\partial x}\right) + \frac{\partial}{\partial y}\left(D_{cl,y}\frac{\partial C}{\partial y}\right) + \frac{\partial}{\partial z}\left(D_{cl,z}\frac{\partial C}{\partial z}\right) \tag{2}$$

Equation (2) is known as the Fick's second law, which calculates the chloride concentration, C, at a specific position i along time t.

The analytical solution of Eq. (2) is obtained if two main hypotheses are respected: the medium is homogeneous and the diffusion front is mono-dimensional.

Other mechanical and chemical limitations can be considered to further simplify the analytical solution.

Regarding the mechanical limitations, there are: (i) the superficial chloride concentration, C_s, is uniform and constant; (ii) the concrete structure is a semi-infinite medium; and (iii) the external surface of the concrete is plane.

Regarding the chemical limitations: (i) the chloride ions are transported into a water-saturated concrete only via diffusion and do not react with the other ions; and (ii) the chemical composition of substances in the concrete pores is in equilibrium during the entire diffusion process.

2.2 Analytical equation

The analytical solution of the Eq. (2) in x and t is given by[4]:

$$C(x,t) = C_0 + (C_s - C_0)\left[1 - erf\left(\frac{x}{2\sqrt{D_{cl}t}}\right)\right]$$
$$Initial\ condition: C(x,0) = C_0$$
$$Boundary\ conditions: C(0,t) = C_s;\ C(\infty,t) = C_0 \tag{3}$$

where: C_0 is the initial chloride concentration and erf(·) is the Gaussian error function.

The diffusivity, D_{cl}, in this analysis, is expressed by the following multi-factors equation[2]:

$$D_{cl} = D_{cl,ref} \times f_1(T) \times f_2(t) \times f_3(h) \tag{4}$$

where: $D_{cl,ref}$ is a constant factor, f_1 depends on temperature T, f_2 depends on the concrete age t and f_3 depends on the humidity h. More details regarding these factors are provided in the literature[2,9].

2.3 Numerical equation

The numerical analysis is considered by solving the system of partial differential equations described by Eq. (2) plus the following conditions:

$$Initial\ condition: C(i,0) = C_0$$
$$Boundary\ conditions: C(0,t_m) = C_s;\ C(i_m,t_m) = C_0 \tag{5}$$

where: i_m and t_m are two defined variables related to the position i (= x,y,z) and time, respectively.

To carry out the numerical analyses, the initial and boundary conditions must be pre-determined, in an explicit way, to not generate the arbitrary constants that represent the degrees of freedom associated with the calculation of the integrals to solve Eq. (2).

The used conditions are: $0 \leq t_m \leq 2\pi$ years and $0 \leq x_m \leq 6$ cm. At the maximum distance in direction x of $x_m = 120$ cm, the boundary condition is restored, i.e. $C(x_m,t_m) = C_0$.

3 MATERIALS AND METHODS

3.1 Materials

The data used in this analysis are divided in two categories: probabilistic and deterministic data. The parameters that have not variations so influent have been chosen as deterministic, therefore are defined a-priori.

Table 1 shows both types of data indicating their value and the coefficient of variation C_V, as $C_v = 100 \times$ (standard deviation/mean value). The adopted distribution for all probabilistic parameters is Gaussian.

The parameters without asterisk are retrieved from literature as quoted, whereas those with the asterisk are estimated by authors (e.g. $x_c = 50$ cm, which means that the analysis is carried

out at this depth; w/c = 0.5 is between a common range of a standard concrete[14]; $D_{cl,ref}$ is usually calculated through equations depending on only a w/c ratio [2], but the authors believe that this dependency is very simplify, therefore this factor has been taken a priori).

Probabilistic parameter	Mean value	C_V (%)	Deterministic parameter	Value
Initial chloride concentration, C_o (kg/m^3)	0.5[15]	58	Reference temperature, T_0 (K)	293[9]
Superficial chloride concentration, C_s (kg/m^3)	1.15[11]	50	Reference age, t_{ref} (year)	0.077[2]
Activation energy, E_a (kJ/mol)	44.6[10]	10	Time for constant diffusivity, t_r (year)	30[2]
Reinforcement cover depth, x_c (cm)	50*	30	Exposed time (age), t (year)	25[9]
Temperature, T (K)	296[9]	35	Humidity, h	0.80[13]
m-value	0.2[9]	20	Humidity at D_{cl}, h_{Dcl}	0.75[13]
n-value	6.0[13]	29	Water/cement ratio for an ordinary Portland cement, w/c	0.5*
			Gas constant, R (J/mol × K)	8.314[9]
			$D_{cl,ref}$ (mm^2/year)	40.0*
			Chloride threshold concentration, C_{th} (kg/m^3)	3.35[1]

Table 1: Probabilistic/deterministic input parameters

Some parameters shown in Table 1 have been already mentioned. The other parameters are correlated to the factors defined in Eq. (4) in the following schematic way consistent to the literature[2,9]:

- $D_{cl,ref} \rightarrow \{w/c\}$
- $f_1(T) \rightarrow \{T, T_0, E_a, R\}$
- $f_2(t) \rightarrow \{t, t_{ref}, t_r, m\}$
- $f_3(h) \rightarrow \{h, h_{Dcl}, n\}$

3.2 Stochastic method

The probabilistic analysis treats the parameters as Random Variables (RVs) by using Probability Density Functions (PDFs) with respect to the time t and direction i. Several techniques exist to estimate the probability of failure of the corrosion initiation time. Figure 1 show the more used techniques among which, the chosen Monte Carlo simulation (MCS).

A specific failure mode is defined through the Limit State (LS) function G(X) for each RV. The probability of failure occurs when G(X) < 0; otherwise it does not occur.

Considering N samples of each RV expressed by the $X = \{x_1, x_2, \ldots, x_j\} = \{x_i\}$, the general probability of failure p_f is defined by[6]:

$$p_f = P[G(X) < 0] = \int_{X:\, G(X)<0} f_X(x_1, x_2, \ldots, x_j)\, dx_1 dx_2 \ldots dx_j = \int_{X:\, G(X)<0} f_X(x_i)\, dx_i \tag{6}$$

where: $f_X(x_i)$ is the joint PDF of the random variables x_i. This equation represents the area of the PDF between a predefined interval. This area defines the probability that G(X) to be less than 0.

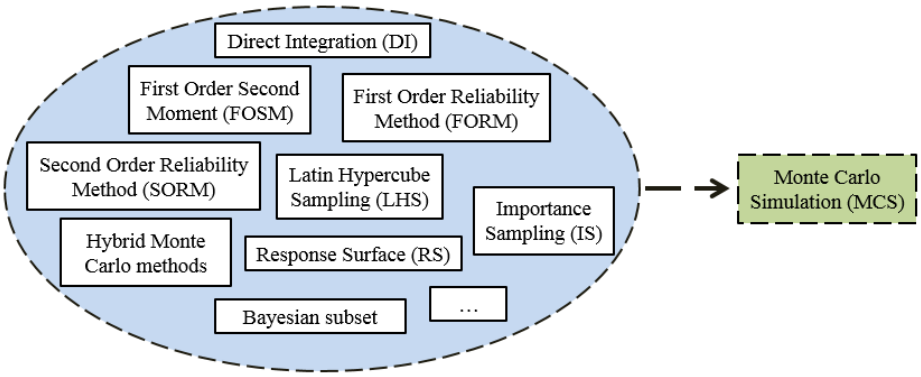

Figure 1: Choose of the methodology ("fishing")

The method used in this analysis is:

- MCS, which generates pseudo-random values, is performed according the following formulations:

$$P_f = \int_{X:\, G(X)<0} I(x_i) f_X(x_i) dx_i \tag{7}$$

$$I(x_i) = \begin{cases} 1, & for\ G(X) \le 0 \\ 0, & for\ G(X) > 0 \end{cases} \tag{8}$$

$$p_f = \frac{1}{N}\sum_{i=1}^{N} I(x_i) = \frac{N_f}{N} \tag{9}$$

where: $I(\cdot)$ is the indicator function and N_f is the number of simulations with $I(x_i) \le 0$.

LS function is written as the difference between the time for corrosion initiation t_R and the lifetime expected of the construction t_a, as: $G(X) = t_R(X) - t_a$. When $G(X) = 0$, $t_R = t_a$ and the failure begins.

From Eq. (3), $t_R(X)$ is obtained as a function of the reinforcement cover depth x_c, as follows:

$$C(x,t) = C_0 + (C_s - C_0)\left(1 - erf\frac{x}{2\sqrt{D_{Cl}\, t}}\right) \rightarrow t_R(X) = \frac{x_c^2}{4D_{Cl}\left(erf\left[\frac{C_{th} - C_s}{C_0 - C_s}\right]\right)^2} \tag{10}$$

where: C_{th} is the chloride threshold concentration. The corrosion begins when the chloride ions $C(x,t)$ reach the value C_{th} at x_c: $C(x_c,t_R) = C_{th}$. This justify the introduction in Eq. (3) of C_{th}.

In order to compare the results obtained by using MCS, others two techniques are used:

- First Order Reliability Method (FORM). In this method, the function G(X) is approximated by the first order Taylor expansion, which is a linearization around a design point. To estimate the probability of failure it is necessary to find a distance, called reliability index β, between the origin of the LS and the most probable point located at the failure surface G(X) = 0[6].
- Direct Integration (DI), which is based on Gaussian distribution and Rosenblatt transformation[3] where the mean value and standard deviation are calculated analytically a-priori.

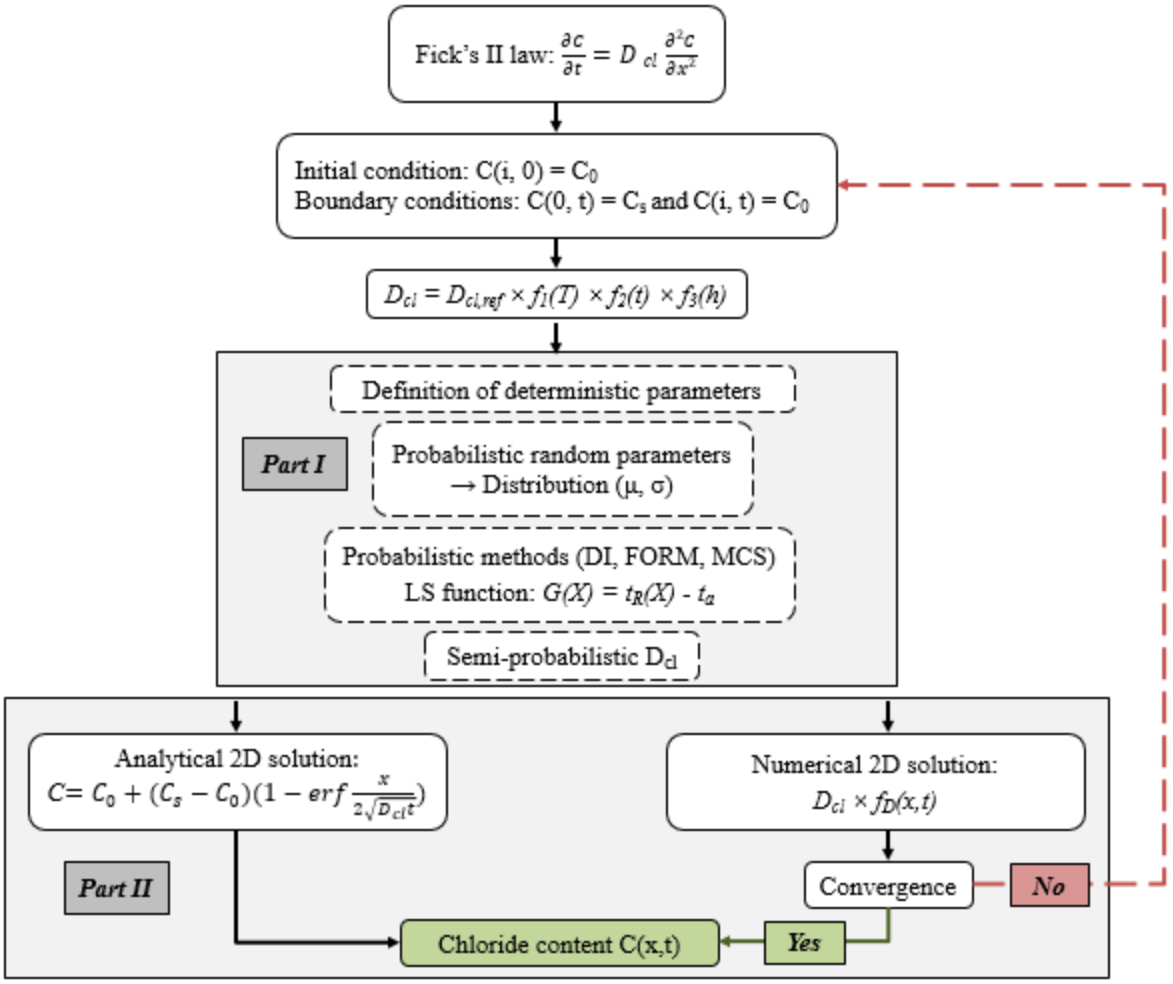

Figure 2: Algorithm of the analysis

Figure 2 shows the algorithm used to estimate the probability of failure of RC structures and the fluctuation of the chloride diffusivity.

The algorithm is mainly divided in two parts. In the first part, the D_{cl} is defined by probabilistic approach, whereas in the second part, the chloride concentration C(i,t) is found.

The convergence procedure is summarized in the following steps: (i) definition of the chloride coefficient function $f_D(x,t)$ that describe the fluctuation (constant and general); (ii)

selection of the boundary conditions of the numerical analysis; (iii) plotting of the chloride content 2D curves C(x,t); and (iv) verification of the convergence between the analytical (exact) and numerical solutions up to find a minimum difference.

4 ANALYSIS AND RESULTS

Figure 3 shows the results in terms of probability of failure p_f in relation to t_a and the PDFs of the expected value. One scenario is defined by using the three methodologies where PDFs can be considered as "static results" (independent on t_a), whereas p_f can be considered as a "dynamic results" (dependent on t_a).

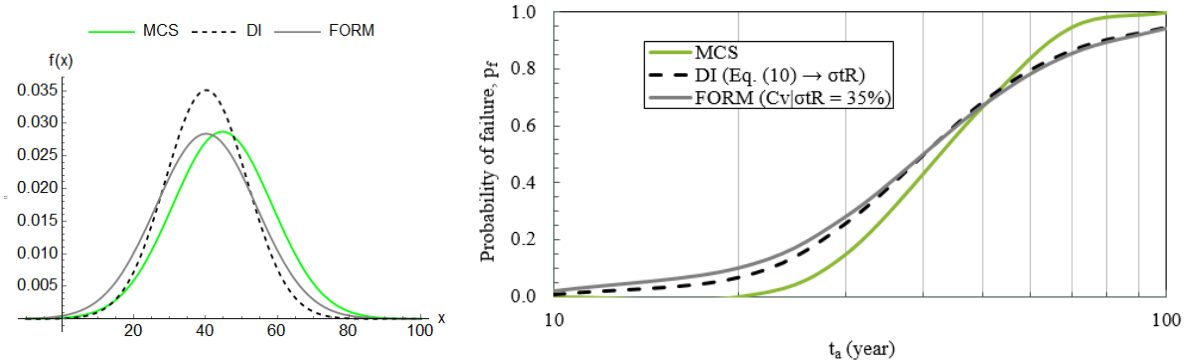

Figure 3: PDFs (left) and probability of failure (right)

The mean μ_{tR} and the standard deviation σ_{tR} of the t_R, for DI, is calculated by using Eq. (10), whereas for FORM, μ_{tR} is the same with respect to DI but the deviation standard is calculated by considering $\sigma_{tR}/\mu_{tR} = 35\%$.

From the comparison among the three different methods, it is possible to see that at $t_a = 50$ years the probability of failure is the same and it is equal to 67%. The curves of the probability of failure for DI and FORM are closer to each other, due to the fact that their parameters are chosen a-priori. For the MCS, the shape of the PDF depends on the number of samples that are used (1×10^6 samples for each variable): the lesser the samples, the largest the dispersion is. Moreover, the results are strictly correlated to the choice of C_V: if C_V is large, the dispersion will be also large. The proximity among the curves indicate that the data tend to be close to the mean value providing a good calibration.

Finally, Figure 4 shows the chloride ions content by using the iterative numerical analysis (linear interpolation) by software[8]. The fluctuation of D_{cl} is calculated for general diffusivity, which has a non-conventional trend with respect to the trends with D_{cl} constant. The amplitude of the D_{cl} comes from the stochastic analysis. The fluctuations are defined by a function $f_D(x,t)$ that are multiplied for D_{cl}.

It is possible to see that the trend of the C(t) is consistent to the adopted fluctuation because it is in function of the time, therefore in x it does not act. This shows a minor accumulation in the case of general fluctuation in some points, for instance for about t = 2.7 years.

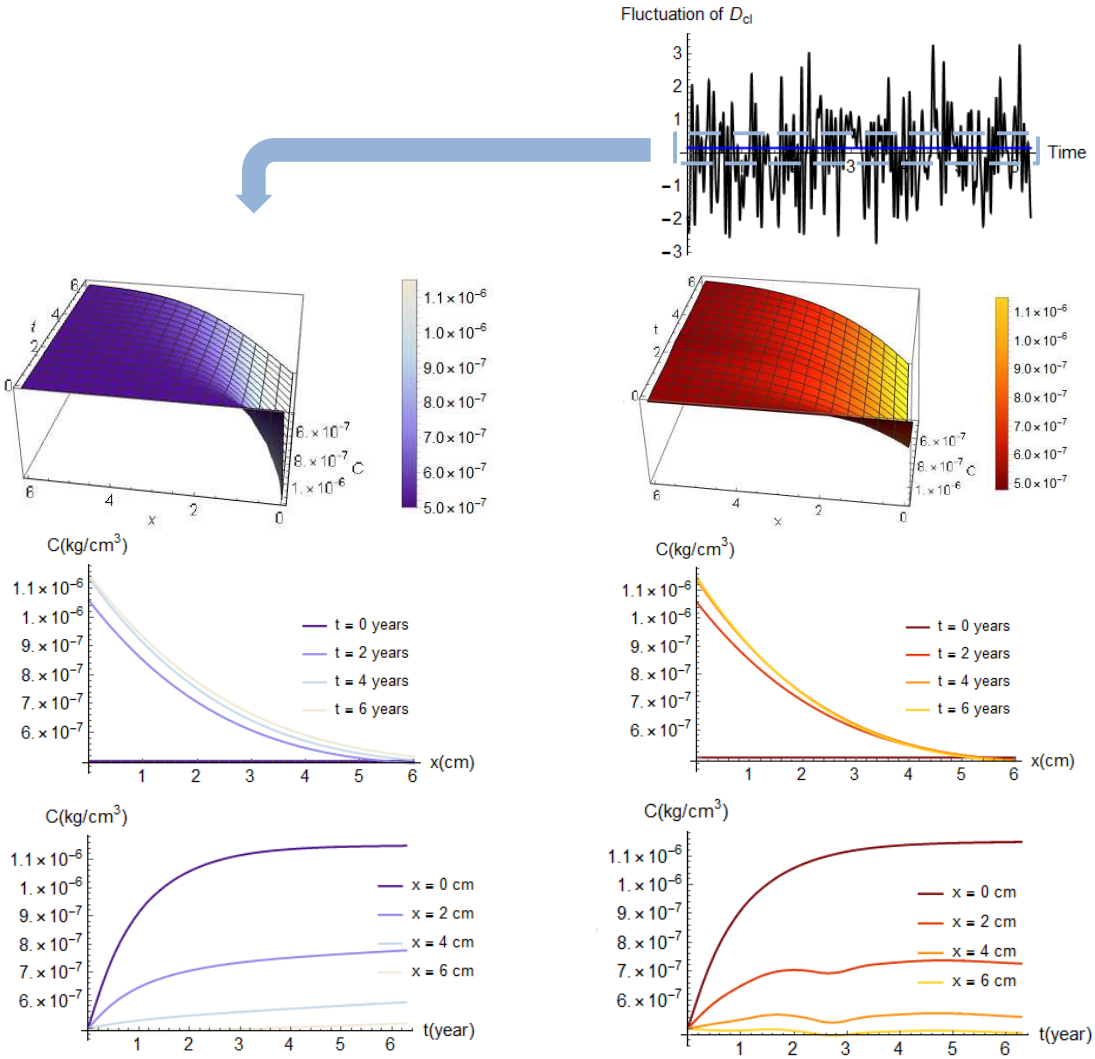

Figure 4: Fluctuation of the chloride ions for a D_{cl} constant (left) and D_{cl} general (right)

5 CONCLUSIONS

The mains conclusions of this paper are:

- Fick's equations, in a traditional form, cannot represent the fluctuation of the diffusivity that can be correlated to the temperature, aging, humidity and other factors interconnected with each other.
- The probabilistic analysis shows that, with the considered parameters, the expected value and its standard deviation is for DI ~ N(40.16, 11.37), FORM ~ N(40.16 14.05) and MCS ~ N(44.68, 13.90). Moreover, this analysis estimates a diffusivity D_{cl} equal to 15.56 mm^2/year
- The probability of failure is calculated in an interval 0 – 100 years, showing a good calibration among the methods in an interval 40 – 60 years. For instance, by the three methods in t_a = 50 years p_f is 0.67.
- The chloride ions content varies between 1.1 × 10^{-6} and 5 × 10^{-7} kg/cm^3. For D_{cl}

general, it is possible to see that D_{cl} is slightly overestimated with some reduction in an interval between 2-3 years. This shows a minor accumulation that reduce the probability of the corrosion of the steel reinforcement.

REFERENCES

[1] D.V. Val, G. Mark, G. Stewart, "Life-cycle cost analysis of reinforced concrete structures in marine environments", *Struct. Saf.*, **25**, 343-362 (2003).

[2] C. Fu, X. Jin, H. Ye, N. Jin, "Theoretical and experimental investigation of loading effects on chloride diffusion in saturated concrete", *J. Adv. Conc. Tech.*, **13**, 30-43 (2015).

[3] M. Rosenblatt, "Remarks on a multivariate transformation", *Ann. Math. Stat.*, **23**, 470-472 (1952).

[4] Y.M. Sun, M.T. Liang, T.P. Chang, "Time/depth dependent diffusion and chemical reaction model of chloride transportation in concrete", *App. Math. Mod.*, **36**, 1114-1122 (2012).

[5] P. Carrara, L. De Lorenzis, D. P. Bentz, "Chloride diffusivity in hardened cement paste from microscale analyses and accounting for binding effects", *Model. Simul. Mat. Sci. Eng.*, **24**, 1-44 (2016).

[6] C.G. Nogueira, E.D. Leonel, H.B. Coda, "Probabilistic failure modelling of reinforced concrete structures subjected to chloride penetration", *Int. J. Adv. Struct. Eng.*, **4**, 10-23 (2012).

[7] C. Fu, H. Ye, X. Jin, N. Jin, L. Gong, "A reaction-diffusion modelling of carbonation process in self-compacting concrete", *Comp. Struct.*, **15**, 847-864 (2015).

[8] Wolfram Mathematica, Version 11 Student Edition, Wolfram Research, Inc. (2017).

[9] E. Zacchei, C.G. Nogueira, "Chloride diffusion assessment in RC structures considering the stress-strain effects and crack width influences", *Constr. Build. Mat.*, **201**, 100-109 (2019).

[10] J.S. Kong, A.N. Ababneh, D.M. Frangopol, Y. Xi, "Reliability analysis of chloride penetration in saturated concrete", *Prob. Eng. Mech.*, **17**, 305-315 (2002).

[11] El Hassan, J., Bressolette, P., Chateauneuf, A., El Tawil, K., "Reliability-based assessment of the effect of climatic conditions on the corrosion of RC structures subject to chloride ingress", *Eng. Struct.*, **32**, 3279-3287 (2010).

[12] S.Y. Jang, B.S. Kim, B.H. Oh, "Effect of crack width on chloride diffusion coefficients of concrete by steady-state migration tests", *Cem. Conc. Rese.*, **41**, 9-19 (2011).

[13] Z.P. Bažant, L.J. Najjar, "Nonlinear water diffusion in nonsaturated concrete", *Mat. Constr.*, **5**, 3-20 (1972).

[14] R.V. Silva, J. De Brito, R. Neves, R. Dhir, "Prediction of chloride ion penetration of recycled aggregate concrete", *Mater. Res.*, **18**, 427–440 (2015).

[15] E. Zacchei, C.G. Nogueira, "Stochastic and numerical solutions applied to chloride ions diffusion in reinforced concrete", Encontro Regional de Matematica Aplicada e Computacional, VI ERMAC, Bauru, São Paulo, Brazil, 1-7, 17-19 June, 2019.

VI ERMAC
ENCONTRO REGIONAL DE MATEMÁTICA APLICADA E COMPUTACIONAL

Stochastic and numerical solutions applied to chloride ions diffusion in reinforced concrete

Enrico Zacchei
São Paulo State University (UNESP); Faculty of Civil Engineering
e.zacchei@unesp.br

Caio Gorla Nogueira
São Paulo State University (UNESP); Faculty of Civil Engineering
caio.nogueira@unesp.br

Abstract: The diffusion of the chloride ions in reinforced concrete constructions varies in time and space and depends on many uncontrolled factors, such as material properties, temperature, aging and humidity. Moreover, each of these factors have others intrinsic uncertainties. The aim of this paper to estimate the time for corrosion onset and the influence of the chloride diffusion coefficient in general dynamic loadings. The first goal helps estimating the service life and devising a maintenance plan, whereas the second aim deals with random loads. The governing equations are modified to consider variations of the diffusion coefficient under non-steady-state conditions. We develop a probabilistic analysis providing new scenarios. Numerical iterations have been implemented.

Keywords: Mathematics Applied to Engineering. Numerical and Stochastic Analyses. Probability of Failure. Chloride Ions Diffusion.

Introduction

This paper studies the diffusion of chloride ions in reinforced concrete (RC) structures. This diffusion increases the corrosion damage of reinforced steel in concrete elements, which is a major issue for long term durability of structures. For this reason, it is much studied by specialists and researchers (CARRARA et al., 2016; KONG et al, 2002; KIM et al., 2014; EL HASSAN et al., 2010; OLIVEIRA et al., 2018; SUN et al., 2012; PELLIZZER, 2015).

We follow two alternative approaches that are seldom carried out. In this sense, this paper incentives at providing some points of innovation about this topic.

The first one is a probabilistic approach, whereas the second one is a numerical approach. The main goals are (i) to estimate the time for corrosion onset of the steel reinforcement by chloride ions diffusion and (ii) to define the influence of the chloride diffusion coefficient for general dynamic loadings.

Probabilistic models are used to minimize the failure risk, which is strictly correlated to the impact that the project has on the environment and on the planning of the maintenance schedules. The project economics is also affected.

Usually, to model the chloride diffusion, analytical solutions are adopted. The advantage is correlated to the low computational cost, but they do not represent accurately chloride diffusion under real conditions.

Defining the time of the corrosion onset is necessary to estimate the service life of the whole structure and its elements. The chloride diffusion coefficient is the most important parameter to predict chloride diffusion in concrete structures subjected to temperature, aging and humidity. Analysing the chloride diffusion coefficient through several approaches (e.g., probabilistic, analytical and numerical) improves our understanding of the processes, because real conditions are very irregular and aleatory.

Mechanical model

The mechanical model by using two principal relations, I and II Fick's law, which describe the chloride diffusion in concrete is introduced in this section, according to Carrara et al. (2016).

The flux of chloride ions, denoted by J in saturated concrete (i.e. when the gas volume is zero and all pores are filled with water) depends on the total chloride concentration gradient, ∇C, and is defined by I Fick's law:

$$J = -D_{Cl}\nabla C, \tag{1}$$

where D_{Cl} is the diffusivity (either constant or variable in time and space). In this work, it is assumed to depend on temperature, concrete aging and humidity. Considering the general mass balance principle under non-steady-state conditions, Equation (1) can be derived obtaining the II Fick's law:

$$\frac{\partial C}{\partial t} = \nabla \cdot (D_{Cl}\,\nabla C_i) = \frac{\partial}{\partial i}\left(D_{Cl}\frac{\partial C}{\partial i}\right), \tag{2}$$

where t denotes time and i is a Cartesian coordinate. We use Einstein's notation, where a repeated index denotes summation over it.

Stochastic methods

The probabilistic analysis is based on the estimation of random variables (RVs), through the statistical distributions of probability density functions (PDFs) (NOGUEIRA et al., 2012).

Several likely failure modes are defined through the limit state (LS) function G(X) for each RV. The probability of failure occurs when $G(X) < 0$ (failure domain), whereas the probability of non-failure occurs when $G(X) > 0$ (safety domain). The separation of both domains is given when $G(X) = 0$ (limit domain).

Considering N samples of each RV expressed by the vector $X = \{x_1, x_2, \ldots, x_j\} = \{x_i\}$, the general probability of failure p_f is estimated by:

$$p_f = P[G(X) < 0] = \int_{\{X:\, G(X)<0\}} f_X(x_1, x_2, \ldots, x_j)dx_1 dx_2 \ldots dx_j = \int_{\{X:\, G(X)<0\}} f_X(x_i)dx_i, \tag{3}$$

where $f_X(x_i)$ is called joint PDF of the random variables x_i.

Equation (3) represents the area of the PDF between a predefined interval. This area defines the probability that G(X) to be less than 0.

The failure can occur at any time and position of the reinforced concrete. Given that the closed-form solutions of the Equation (3) are quasi-impossible to obtain, in this paper three methods have been used to solve this issue (PELLIZZER, 2015) as:

(1) First order reliability method (FORM) that derives from the fact that the function G(X) is approximated by the first order Taylor expansion, which is a linearization around a design point. In order to estimate the probability of failure it is necessary to find a distance, called reliability index β, between the origin of the LS and the most probable point located at the failure surface $G(X) = 0$.

(2) Direct integration (DI), which is based on Gaussian distribution and Rosenblatt transformation (ROSENBLATT, 1952). If G(X) is a linear combination of normal random variables x_i then, G(X) also follows a normal distribution, therefore its mean and standard deviation can be calculated analytically.

(3) Monte Carlo simulation (MCS), which generates pseudo-random values, is performed according the following formulation (OLIVEIRA et al., 2018):

$$P_f = \int_{\{X:\, G(X)<0\}} I(x_i) f_X(x_i) dx_i, \tag{4}$$

$$I(x_i) = \begin{cases} 1, & \text{for } G(X) \le 0, \\ 0, & \text{for } G(X) > 0, \end{cases} \tag{5}$$

$$p_f = \frac{1}{N}\sum_{i=1}^{N} I(x_i) = \frac{N_f}{N}, \tag{6}$$

where $I(\cdot)$ is an indicator function and N_f is the number of simulations with $I(x_i) \le 0$. Equation (6) is the mean value of $I(x_i)$.

LS function is written as the difference between the time for corrosion initiation t_R and the structural lifetime expected in design t_a as: $G(X) = t_R(X) - t_a$. When $G(X) \to 0$, $t_R = t_a$ and the failure is achieved.

From the known analytical solution (SUN et al., 2012) of the Equation (2), $t_R(X)$ has been obtained as a function of the reinforcement cover depth x_c, as follows:

$$C = C_0 + (C_s - C_0)\left(1 - \operatorname{erf}\frac{x}{2\sqrt{D_{Cl}\, t}}\right) \rightarrow t_R(X) = \frac{x_c^2}{4D_{Cl}\left(\operatorname{erf}\left[\frac{C_{th} - C_s}{C_0 - C_s}\right]\right)^2}, \tag{7}$$

where C_0 is the internal chloride concentration, C_s is the superficial chloride concentration, x is the direction and erf is the error function. Moreover, C_{th} is the concentration of the chloride threshold, which is introduced considering that the corrosion begins when the chloride ions reach C_{th} at x_c. This justify the transformation from C to C_{th}: $C(x_c, t_R) = C_{th}$.

The analytical solution, at the left hand in Equation (7), comes from Equation (2) under the following fundamental hypothesis: (i) D_{Cl}, C_o and C_s are constant, (ii) the medium is semi-infinite and (iii) diffusion occurs in one dimension.

Numerical applications

The numerical analysis is carried out by solving simultaneously the system of the partial differential equations (PDEs), with initial (i.c.) and boundary (b.c.) conditions (SUN et al., 2012):

$$\frac{\partial C}{\partial t} = D_{cl}\frac{\partial^2 C}{\partial x^2}, \tag{8}$$

$$\begin{aligned} \text{i.c.:} \quad & C(x, 0) = C_0 \\ \text{b.c.:} \quad & C(0, t_m) = C_s \\ & C(x_m, t_m) = C_0, \end{aligned} \tag{8a}$$

where x_m and t_m are two defined variables correlated to position and time, respectively. To carry out the numerical analyses by using PDEs, i.c. and b.c. must be a-priori determined.

In the next section these conditions will be defined. The key value that influence the trend of the chloride ions distribution is the x_m. In fact, its value imposes the conditions at downstream that influence the condition at upstream. By a convergence respect to the analytical results a maximum distance of x_m = 120 cm is adopted.

Analyses and results

The analysis is carried out following the three main steps shown in Figure 1. First, it is necessary to define the mechanical model, then D_{cl} by a semi-probabilistic combination is obtained, finally, chloride ions content is estimated and plotted.

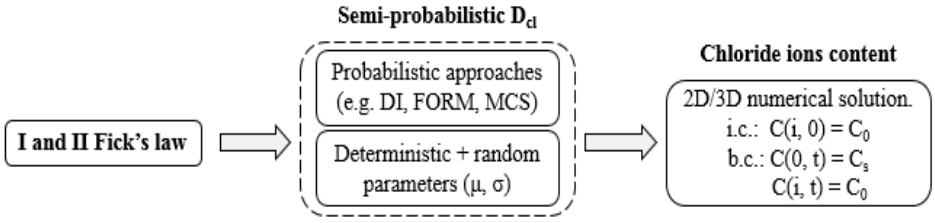

Figure 1: Methodology.

The probabilistic analysis treats the parameters as RVs in respect to the time t and space i. Stochastic models that do not include spatial variability cannot adequately describe the performance of RC structures, therefore they can oversimplify the analysis underestimating the failure probabilities. Table 1 lists the group of the adopted deterministic and RVs, indicating their distributions. The distributions and the values with the asterisk are estimated by authors whereas those without asterisk have retrieved from literature (KONG et al, 2002; KIM et al., 2014; ZACCHEI and NOGUEIRA, 2019; EL HASSAN et al., 2010; BAŽANT and NAJJAR, 1972). Figure 2 shows the generating points by using MCS and some PDFs.

Table l: Used data.

Parameter	Unit	Symbol	μ	±σ	σ/μ (%)	Distribution type
Internal chloride	kg/m^3	C_0	0.5*	0.2886	58	Uniform (0,1)
Superficial chloride	kg/m^3	C_s	1.15	0.575	50*	Log-normal
Free chloride	kg/m^3	C_f	1.50	0.75	50*	Log-normal
Reinforced depth	cm	x_c	5.0*	1.5	30*	Log-normal
Activation energy	kJ/mol	E_a	44.6	4.3	10*	Normal
Temperature	°C (K)	T	23 (296)*	8.0	35*	Normal
Evaporable water	-	ω_e	0.83*	0.1408	17	Beta (5,1)
Humidity	-	h	0.80*	0.1632	20	Beta (4,1)
m-value	-	m	0.2	0.1632	82	Beta (1,4)
n-value	-	n	6	3.4641	58	Uniform (0,12)

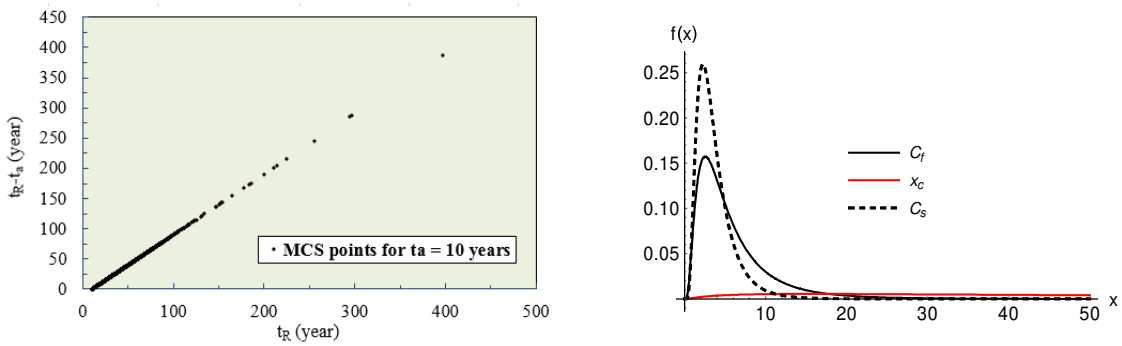

Figure 2: MCS points (left) and PDFs (right).

Figure 3 shows the results in terms of probability of failure in relation to t_a. DI is calculated by using Equation (7) to estimate σ_{tR}. FORM is calculated for σ_{tR}/μ_{tR} = 35%. Following two cases are considered:

a) T = 296 K and C_f = 1.15 kg/cm^3,

b) T = 288 K and C_f = 2.25 kg/cm^3.

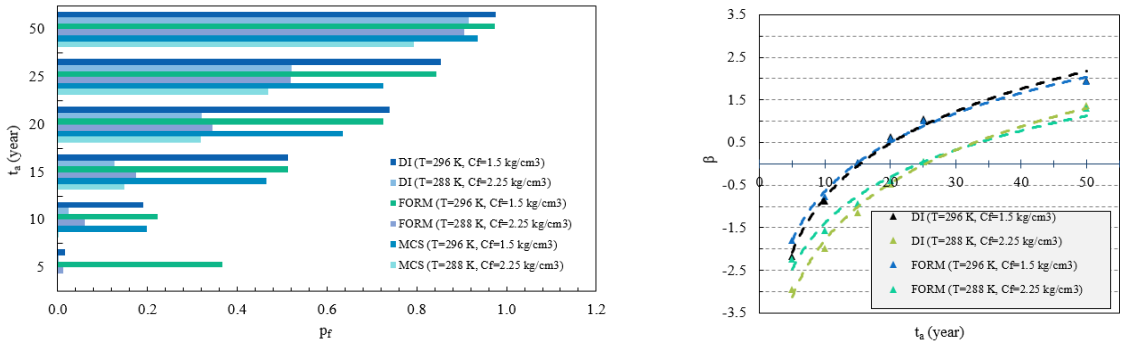

Figure 3: Probability of failure (left) and reliability index β vs. t_a (right).

In Figure 3, it is possible to see two scenarios by using the adopted three methodologies. For a prevision at long period, where it is more difficult to estimate the probability of failure, values from MCS (with N = 10000) tend to the valued from DI. This comparation shows the importance of C_f and T variations - T variations are predominant with respect to variations of C_f.

Finally, Figure 4 shows the chloride ions content by using the iterative numerical analysis by software (WOLFRAM MATHEMATICA, 2017). The trend of the curves is non-conventional respect to the trends with constant D_{Cl}. The loading is considered as a general dynamic load (CLOUGH and PENZIEN, 2003), whit the values that correspond to the abovementioned first scenario and a range of: $0 \leq t \leq 2\pi$ years (with steps dt = 1 year); $0 \leq x \leq 6$ cm (with steps dx = 1 cm).

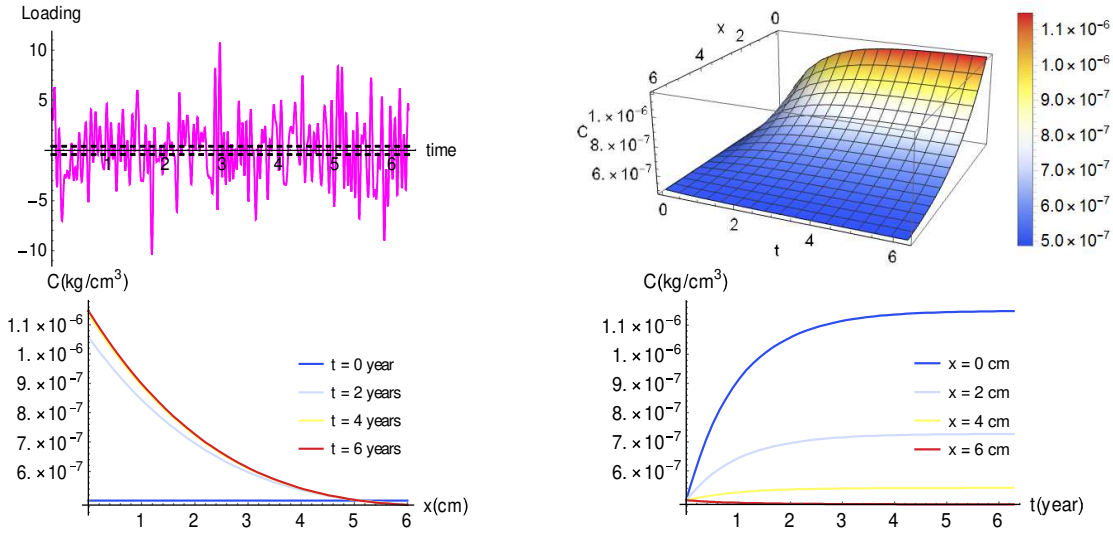

Figure 4: Chloride ions concentration for general dynamic loads.

The ions chloride content varies between 5.0 × 10^{-7} kg/cm^3 and 1.1 × 10^{-6} kg/cm^3. These values correspond to the key values C_{th} = 3 × 10^{-6} kg/cm^3 and D_{Cl} = ±0.5 cm^2/year.

Conclusions

This paper treats the diffusion of the chloride ions in reinforces concrete structures. Considering that there are many variables that influence the diffusion, a probabilistic analysis is more adequate. In this sense, three different techniques by using several simulations and probability density functions have been carried out to estimate the probability of failure, as a function of the time of corrosion onset. Two scenarios have been estimated. Also, numerical solutions have been found to study the trend of D_{Cl} when it is not constant. The outcomes are presented in terms of the chloride content and probability of failure.

Results show that the mean probability of failure for the first case at $t_a = 10$ years is $\bar{p}_f = 0.2034$ whereas for the second case is $\bar{p}_f = 0.0281$. At $t_a = 25$ years, $\bar{p}_f = 0.807$ in the first case, whereas for the second case is $\bar{p}_f = 0.5033$. The ions chloride content varies between $5 \times 10^{-7} - 1 \times 10^{-6}$ kg/cm^3 with $C_{th} = 3 \times 10^{-6}$ kg/cm^3 and $D_{Cl} = \pm 0.5$ cm^2/year.

The prediction of the diffusion time can indicate the beginning of the strength reduction of the structural elements. Therefore, the research about the time to corrosion initiation is an important factor in future damage predictions, because the end of the service lifetime of the structure could be earlier than estimated.

Acknowledgements

The first author acknowledges the “Servicios Informáticos CPD” of the University of Salamanca (USAL) for the Wolfram Mathematica license and USAL to pay the rights (when applicable) to download all papers in the references. The first author also acknowledges the funding from the Coordination of the Improvement of Graduated Professionals (CAPES), Support Program for Foreign Students of Doctorate (PAEDEX) and Iberian-American University Postgraduate Association (AUIP) (reference number: 3.224.803.003.569).

References

BAŽANT, Z.P.; NAJJAR, L.J. Nonlinear water diffusion in nonsaturated concrete. **Matériaux et Constructions**, v. 5, p. 3-20, 1972.

CARRARA, P.; DE LORENZIS, L; BENTZ, D.P. Chloride diffusivity in hardened cement paste from microscale analyses and accounting for binding effects. **Modelling and Simulation in Materials Science and Engineering**, v. 24, p. 1-44, 2016.

CLOUGH, R.W.; PENZIEN, J. **Dynamics of Structures**. Berkeley, USA: Computers & Structures, Inc., 2003.

EL HASSAN, J.; BRESSOLETTE, P.; CHATEAUNEUF, A.; EL TAWIL, K. Reliability-based assessment of the effect of climatic conditions on the corrosion of RC structures subject to chloride ingress. **Engineering Structures**, v. 32, p. 3279-3287, 2010.

KIM, Y.Y.; LEE, B.J.; KWON, S.J. Evaluation technique of chloride penetration using apparent diffusion coefficient and neural network algorithm. **Advances in Materials Science and Engineering**, v. 2014, p. 1-13, 2014.

KONG, J.S.; ABABNEH, A.N.; FRANGOPOL, D.M.; XI, Y. Reliability analysis of chloride penetration in saturated concrete. **Probabilistic Engineering Mechanics**, v. 17, p. 305-315, 2002.

NOGUEIRA, C.G.; LEONEL, E.D.; CODA, H.B. Probabilistic failure modelling of reinforced concrete structures subjected to chloride penetration. **International Journal of Advanced Structural Engineering**, v. 4, p. 10-23, 2012.

OLIVEIRA, H.L.; CHATEAUNEUF, A.; LEONEL, E.D. Probabilistic mechanical modelling of concrete creep based on the boundary element method. **Advances in Structural Engineering**, v. 00, p. 1-12, 2018.

PELLIZZER, G. P. **Análise mecânica e probabilística da corrosão de armaduras de estruturas de concreto armado submetidas à penetração de cloretos**. 2015. 247 f. Dissertação (Mestrado em Engenharia de Estruturas)-USP, São Carlos, 2015.

ROSENBLATT, M. Remarks on a multivariate transformation. **The Annals of Mathematical Statistics**, v. 23, p. 470-472, 1952.

SUN, Y.M.; LIANG, M.T.; CHANG, T.P. Time/depth dependent diffusion and chemical reaction model of chloride transportation in concrete. **Applied Mathematical Modelling**, v. 36, p. 1114-1122, 2012.

WOLFRAM MATHEMATICA, Version 11, Student Edition, Wolfram Research, Inc., 2017.

ZACCHEI, E.; NOGUEIRA, C.G. Chloride diffusion assessment in RC structures considering the stress-strain sate effects and crack width influences. **Construction and Building Materials**, v. 201, p. 100-109, 2019.

KSCE Journal of Civil Engineering

2D/3D numerical analyses of corrosion initiation in RC structures for fluctuations of chloride ions by external actions

--Manuscript Draft--

Manuscript Number:	KSCE-D-20-01242
Full Title:	2D/3D numerical analyses of corrosion initiation in RC structures for fluctuations of chloride ions by external actions
Article Type:	Research Paper
Corresponding Author:	Enrico Zacchei PORTUGAL
Corresponding Author Secondary Information:	
Corresponding Author's Institution:	
Corresponding Author's Secondary Institution:	
First Author:	Enrico Zacchei, PhD
First Author Secondary Information:	
Order of Authors:	Enrico Zacchei, PhD
	Caio Gorla Nogueira, Professor
Order of Authors Secondary Information:	
Funding Information:	Asociación Universitaria Iberoamericana de Postgrado (3.224.803.003.569) — Dr. Enrico Zacchei
Abstract:	The diffusion of chloride ions in reinforced concrete (RC) varies in space and time, depending on many uncertain factors as material properties, temperature, aging, humidity and external loadings. In this research, the goals are to provide different scenarios of data to probabilistic assessing of the corrosion initiation time and chloride ions content inside concrete considering different fluctuations. For the former, stochastic analyses helps to estimate the service life in RC; for the latter, the focus is on the nature of loading variation due to location, architectural specifications and structural constraints that usually are not considered. The innovative approach is to study the trend of a single particle of chloride ion regarding the action of the external loadings by incorporating a proposed function f D , which can assume constant or random values. The governing equations are modified to account for the non-constant diffusivity under transient conditions. Results show that the chloride content for random diffusivity assumes lower values than for constant diffusivity. Moreover, in 2D analysis the chloride content is lesser of about 78% than in 3D analysis.
Author Comments:	Dear Editor, We would like to submit an original research article entitled “2D/3D numerical analyses of corrosion initiation in RC structures for fluctuations of chloride ions by external actions”. We believe that this manuscript is appropriate for publication by your journal. We confirm that this work has not been published and currently it is not under consideration for publication elsewhere. Authors declare they have downloaded and read completely all papers in the references and have respected the “scientific ethics”. The focus of the paper is to investigate the diffusion of the chloride ions in RC structures. The diffusion varies in time and space and depends on many uncertain factors, e.g. material properties, temperature, aging, humidity, loadings. Moreover, each of these factors have others intrinsic uncertainties. The objectives of this paper induce at estimating of: (i) the time of corrosion initiation; (ii) the influence of a single

	particle of a chloride ion with respect to the external loadings. First point by using stochastic analysis helps to estimate the service life and maintenance plan, the second point puts the attention on the fact that the nature of loadings can be random. Numerical solutions with defined boundary conditions are proposed in 2D and 3D approaches. The governing equations were modified to account the non-constant diffusivity under non-steady-state condition. Several new scenarios are provided. In this paper, authors believe that this research should provide the engineers and scientists with a powerful and reliable methodology of analysis aimed to improve the knowledge on structures' safety. In the last years, authors studied this theme providing some important results published in journals: 1. Zacchei and Nogueira: https://doi.org/10.1016/j.conbuildmat.2018.12.166 2. Nogueira et al.: https://doi.org/10.1016/j.engfailanal.2014.09.006 3. Nogueira et al.: https://doi.org/10.1016/j.engfailanal.2013.01.023 Best, Enrico Zacchei and Caio Gorla Nogueira

2D/3D numerical analyses of corrosion initiation in RC structures for fluctuations of chloride ions by external actions

Enrico Zacchei, Ph.D., Researcher (a)
enricozacchei@gmail.com (corresponding author)

Caio Gorla Nogueira, Ph.D., Professor (b)
caio.nogueira@unesp.br

(a) Itecons - Institute for Research and Technological Development in Construction, Energy, Environment and Sustainability, Pedro Hispano Avenue, 3030-289 Coimbra, Portugal

(b) School of Civil Engineering, São Paulo State University (UNESP), 14-01 Eng. Luís Edmundo Carrijo Coube Avenue, 17033-360, Bauru-SP, Brazil.

Abstract. The diffusion of chloride ions in reinforced concrete (RC) varies in space and time, depending on many uncertain factors as material properties, temperature, aging, humidity and external loadings. In this research, the goals are to provide different scenarios of data to probabilistic assessing of the corrosion initiation time and chloride ions content inside concrete considering different fluctuations. For the former, stochastic analyses helps to estimate the service life in RC; for the latter, the focus is on the nature of loading variation due to location, architectural specifications and structural constraints that usually are not considered. The innovative approach is to study the trend of a single particle of chloride ion regarding the action of the external loadings by incorporating a proposed function f_D, which can assume constant or random values. The governing equations are modified to account for the non-constant diffusivity under transient conditions. Results show that the chloride content for random diffusivity assumes lower values than for constant diffusivity. Moreover, in 2D analysis the chloride content is lesser of about 78% than in 3D analysis.

Keywords. Chloride ions diffusion; differential numerical analysis; MCS; diffusivity fluctuation; reliability analysis.

1 Introduction

Reinforced concrete (RC) has been widely used in many applications of civil engineering in the last decade and especially nowadays. As a construction material applied to design and builds RC structures, it is subjected to different types of mechanical and environmental actions affecting their performance, durability and safety along time. Despite several environmental sources of degradation, the chloride

ingress is the most important phenomenon, which is responsible to initiate the reinforcement steel bars corrosion (Pellizzer et al. (2018)).

Regarding the structural performance of the RC systems, corrosion is a very harmful state because it leads to mechanical and material properties deterioration, including cross-section area reduction of the steel bars, bond strength loss between steel bars and surrounding concrete, cracking of concrete cover and reduction of the steel yield, ultimate strength and ductility of the RC elements. The cracking of concrete cover, known as the spalling phenomenon (Stewart and Mullard (2007)), is due to the expansive corrosion products formed at the interface steel bar-concrete, leading to the longitudinal cracks along the main reinforcement direction. This effect is still more important in RC columns because the spalling causes the cross-section concrete loss and increases compression stresses in service. On the other hand, the reduction of the reinforcement cross-section, which can be deduced as a loss of steel mass (Zhang et al. (2010)), has a proportional effect on yield and ultimate steel strength, as well as on the structural element ductility.

Moreover, it reduces the reinforcement moment of inertia and, hence, the maximum buckling load of the steel bars, affecting dynamic and static behaviour of the RC elements and systems. This loss of the reinforcement cross-section may even produce the physical rupture of a steel bar, interrupting its continuity and harming the forces transference process along the elements (Capozucca (1995)).

The main factors that affect the corrosion initiation at the reinforcement bars surface inside concrete are: geometrical characteristics of concrete elements, which means insufficient cover; concrete cover permeability; amount of chloride at the surface of the concrete elements and its variation along time; environmental conditions, such as temperature and humidity; the concrete aging effect and the structural behaviour of the RC elements which affects and is affected by opening and propagation of cracks (Fu et al. (2015); Bastidas-Arteaga et al. (2011)).

Concrete cover acts as a physical barrier to protect and isolate the reinforcement from the atmospheric direct contact. The quality of the concrete cover affects directly the diffusion process, representing high or low permeability to the chloride ions ingress from the external to steel bars surface. The amount of chloride at the surface of the concrete elements depends on its exposure to the surrounding environment and the corresponding aggressiveness. Thus, the chloride penetration towards to the embedded reinforcement steel is still more intensive in marine environments, in coastal areas and in regions with use of the de-icing salt (Meira et al. (2006)). In urban and industrial areas, where the environmental pollution has a significant concentration of carbon dioxide, carbonation-initiated reinforcement corrosion prevails.

Temperature and humidity conditions affect the concrete diffusion properties accelerating or slowing the chloride penetration inside concrete. The concrete aging effect is related to the continuum cement hydration process along time, which also depends on the water-cement ratio and the material additions to the cement like fly ash and others (Bastidas-Arteaga et al. (2011)). Finally, the opening and propagation of cracks along the concrete surface is also an important factor to create preferential paths to the chloride ions penetration, increasing the chloride concentration at the steel bars surface and decreasing the corrosion time initiation (Zacchei and Nogueira (2019)). All these factors interfere at the RC durability and must be considered in the design phase of the structural systems.

Chloride ions penetrate the concrete by several different transport mechanisms such as: ionic diffusion, convection, capillary absorption, advection, permeation, dispersion and chemical activity (Nguyer et al. (2017)). However, when saturated conditions are observed in concrete elements, the transport mechanism of chloride ions can be exclusively modelled by the ionic diffusion process. It is worth to mention that in tidal zones, the chloride ions ingress is affected by other phenomena, like the capillary absorption than ionic diffusion only because of the presence of wet/dry cycles on the concrete elements surface (Ben-Fraj et al. (2012)).

Physically, the reinforcement corrosion can be observed in two forms: (i) pitting, when the corrosion is localized is small regions (concentrated holes) along the bars and/or (ii) uniform, when the corrosion is considered homogeneous around and along the bars. They initiate by the loss of the passive protecting film of steel which is formed in contact with the alkaline concrete, as a function of the excessive concentration of chloride ions at the steel surface (El Hassan et al. (2010)).

Regarding all the discussed themes above, many studies have been carried out in order to consider the environmental and mechanical effects on the concrete diffusivity and how it influences on the time of corrosion initiation: (i) loading effects which induces damage and concrete cracks (Al-Kutti et al. (2014); Xie et al. (2016); Wang et al. (2018); Yuan et al. (2015)); (ii) climate factors such as chloride binding, temperature, humidity, water activity (Nguyer et al. (2017)). After the corrosion initiation, there are also studies to understand how the strength and stiffness of the RC elements are affected by the corrosion products (Ortega and Robles (2016)).

In parallel to the theoretical developments, experimental alternative approaches have been carried out to model the chloride penetration in concrete by using electrical voltage to describe the flux of several ionic species under diffusion and migration (Lizarazo-Marriaga and Claisse (2011)); to study the chloride content when the concrete has a several layers of mortar rendering at external surface (Malheiro et al. (2011)); to estimate the effects of the chloride content in concrete regarding to the distance from sea (Meira et al. (2006); Bastidas-Arteaga et al. (2013)).

Although the expressive efforts to modelling the chloride ions ingress into concrete have been conducted by theoretical approaches, all the involved parameters and assumptions are governed by many uncertainties. Especially those regarding the environmental phenomena and the concrete diffusivity, they strongly influence the time initiation corrosion and the dynamics of the diffusion process. For this reason, probabilistic approaches to RC structures durability are recommended in the corrosion predictions (Nogueira et al. (2012)). Therefore, it was observed that there are three main focuses addressed in recent researches: (i) quantification and reduction of the uncertainties about materials, models and specific environmental conditions, in order to better estimate the probability of corrosion initiation and predict the RC structures durability; (ii) studying the long-term effect of climate change on RC durability, which depends on the initial mixture of the concrete constituents, physical components to protection of the reinforcement bars and chloride external exposure, including different scenarios and variations along time; (iii) analysing of the diffusivity by considering extreme natural hazards.

In this paper, the assessment of the corrosion initiation time when RC structures are subjected to different scenarios of chloride exposure is addressed by using a probabilistic approach. The study compares classic analytical solutions (Fick's law (Carrara et al. (2016))) and numerical predictions in order to consider more realistic paths of the chloride ions ingress into concrete. The impact of several environmental factors on the concrete diffusivity is also studied and combined with the numerical approaches and chloride exposure scenarios to improve the prediction chloride concentration inside concrete and the corrosion initiation time. Defining the time of the corrosion initiation is useful to estimate the service life of the whole structure and its elements. Moreover, the probabilistic models are used to better consider the uncertainties of the real parameter, which has advantages on the economic project and on the planning of the maintenance schedules.

The introducing of numerical solutions is because the analytical models cannot represent accurately chloride diffusivity under real conditions. The innovative approach is to simulate the trend of a single particle of a chloride ion inside of a RC element subjected to external loadings. To carry out this analysis, the diffusivity, which is a key to define a diffusion process, has been modified. Analysing this phenomenon by considering a fully coupled technique (probabilistic, numerical, different scenarios of chloride exposure and more embracing model to the diffusivity), the predictions can be improved in order to develop a more realistic model to RC structures durability previsions.

2 Mechanical model

2.1 Fick's law

The mathematical relation that describes the chloride ions flux J in saturated concrete elements at the macroscopic scale depends on the total chloride concentration gradient ∇C and is defined by the Fick's first law as follows (Carrara et al. (2016)):

$$J = -D_{cl} \nabla C \tag{1}$$

Where: D_{cl} is the diffusivity or also called as diffusion coefficient of the concrete and can be interpreted as a measure of the relative permeability of the concrete against the chloride ions ingress. The diffusivity can be described by several models, in which the simplest one is constant and does not depend on the position inside concrete or time (Andrade (2002)). On the other hand, there are many external (environmental) and internal (e.g. concrete moisture) factors that can influence the diffusion coefficient and can be incorporated to make a better description of the flux process inside concrete along time.

It is an important issue to be considered when corrosion studies are performed because the flux and, therefore, the chloride concentration at the interface reinforcement bars-surrounding concrete depend on directly of the concrete diffusion coefficient. Among the factors that interfere on the concrete diffusivity are: chloride type available in the concrete pores (binding effects), temperature, humidity, concrete aging, stress-strain states and cracks (Fu et al. (2015); Zacchei and Nogueira (2019)).

Eq. (1) can be derived considering the general mass balance principle along the time t in the direction i under transient conditions, obtaining the Fick's kinetic second law (or modified heat equation), which is a parabolic linear second order partial differential equation (PDE):

$$\frac{\partial C}{\partial t} = \nabla\left(D_{cl,i} \nabla C_i\right) = \frac{\partial}{\partial i}\left(D_{cl} \frac{\partial C}{\partial i}\right) \tag{2}$$

The total chloride concentration C can be divided in two parts: free (dissolved in pore solution) C_f and chemically bound to the reaction of hydration products of cement C_b, which are correlated through the following relation (Sun et al. (2012); Fu et al. (2010)):

$$C = \omega_e C_f + C_b \tag{3}$$

Where: ω_e is the evaporable water content that can be determined from degree of hydration (aging maturing) model (Fan and Wang (2015)). The term ω_e is a part of the total water content ω; the other part is defined by ω_n that is non-evaporable water content. Therefore, the total water content at the concrete pores can be written as: $\omega = \omega_e + \omega_n$. The pore compaction effect plays a dominant role leading to a reduction in chloride diffusion. The term C_b depends on many factors, e.g. type of cement, composition of pore solution and temperature (Halamickova et al. (1995)).

The correlations between free and bound chloride ions, expressed by Eq. (4), at a given temperature are known as the chloride binding isotherms. The nonlinear Langmuir isotherms consider the chloride binding effects, in which the parameters related to the concrete properties are: $\alpha = 11.8$ and $\beta = 4.0$ (Kong et al. (2002); Fu et al. (2010); Chen et al. (2013)).

$$C_b = \frac{\alpha C_f}{1+\beta C_f} \tag{4}$$

From Eq. (3), it is possible to see that if the chloride binding effects are considered the chloride concentration is equal to the complete chloride content (free + bound) which means $C_b \neq 0 \rightarrow C = \omega_e C_f + C_b$, whereas if they are neglected the chloride concentration is equal only to the free chloride concentration and $C_b = 0 \rightarrow C = \omega_e C_f$. The coupled diffusion-binding interactions lead to anomalous diffusion of chloride ions. Eq. (2) will still describe the diffusion part, but if binding is accounted for, the system should be extended adding the binding isotherms and solving a coupled system.

2.2 Analytical solution

From Eq. (2), the differential equation (chloride concentration at *C(i,t)* in which *i* indicates the position of the analysed flux direction inside concrete and *t* is the chosen time to measure *C*) can be described for x-direction with initial condition (i.c.) and Dirichlet's boundary (b.c.) condition (Sun et al. (2012); Fan and Wang (2015)) as:

$$\frac{\partial C}{\partial t} = D_{cl} \frac{\partial^2 C}{\partial x^2} \tag{5}$$

$$\begin{aligned} \text{i.c.:} \quad & C(x,0) = C_0 \\ \text{b.c.:} \quad & C(0,t) = C_s \\ & C(\infty,t) = C_0 \end{aligned} \tag{5a}$$

Where: C_0 is the inner chloride concentration which is already present in the concrete; C_s is the chloride concentration at the external concrete surface. The initial condition is considered equal to the boundary condition to infinity, i.e. $C = C_o$ independently on the time and position. If there is no chloride ions inside concrete at the initial time, the C_0 is equal do zero.

Eq. (5) describes a 1D model where *x* represents the position inside concrete in the chloride flux direction, which depends on their concentration gradient between the external surface and the position *x*.

The most classical set up involves a hardened cement paste, in which at one face a chloride concentration is applied (C_s), while the opposite face is in contact with a solution with concentration C_0. However, Eq.

(5) can be applied under the following main hypothesis: (i) when the material can be considered homogeneous and (ii) when the diffusion takes place mainly in a single direction.

There are many other limitations for adopting this model of which different solution and extensions are available and well-established in literature.

For instance, some of them are described below: (1) the concrete must be saturated (when the gas volume is zero and all pores are filled with water), extended in literature (Da Costa et al. (2013)) where the non-saturate concrete is considered; (2) the concrete structure must be a semi-infinite medium, extended in literature (Pang and Li (2016)) where Eq. (5) is applied for real and so finite structure; (3) the chloride concentration at external surface must be uniform and constant (in time and in space), extended in literature (Silva and Guimarães (2014)) where C_s is divided in a variable and constant part; (4) the external surface of the concrete is plane, extended in literature (Morga and Marano (2015)) where the diffusion is studied in circular concrete columns; (5) the chloride ions must be transported into a water-saturated concrete only via diffusion and do not interact/react with the other ions, extended in literature (Ishida et al. (2009)) where the chemical reactions are considered.

About the latter condition, it is valid because the diffusion coefficient represents a very slow rate (about 10^{-12} to 10^{-11} m^2/s), indicating that the chemical compositions of substances in concrete pore remain almost in equilibrium throughout the entire diffusion process at any time. The reason of this slowness is that chloride penetration takes place in totally or partly water-filled pores and not via air-filled pores.

The closed-form analytical solution of the Eq. (5) is:

$$C = C_0 + (C_s - C_0)\left(1 - \mathrm{erf}\frac{x}{2\sqrt{D_{cl}\, t}}\right) \quad (6)$$

Where: *1 – erf(·)* describes the evolution of the chloride diffusion front in the time *t* and position *x*. The *erf(·)* is the Gaussian error function, that adjust the equation, integrated between 0 and $x/\left(2\sqrt{D_{cl}\, t}\right)$.

In some studies, *x* is decreased Δ_x from the depth of the surface convection regions of concrete cover, thus the C_s maximum is not calculated at immediately inner surface, but a little more inside in the element (i.e. at Δ_x) (Zhang et al. (2011); Rahimi and Gehlen (2018); Pang and Li (2016)). Moreover, the influence of the mesoscopic structure of the concrete, i.e. the presence of aggregates and interfacial transition zone play an important role regarding the achievement of the maximum value of C_s (Bentz et al. (1997); Park and Choi (2012)).

2.3 Numerical solution

In the numerical analysis, the used differential equation (Eq. 5) is the same of the analytical solution given by Eq. (6), whereas the initial (i.c.) and Dirichlet's boundary (b.c.) conditions (Sun et al. (2012); Fan and Wang (2015)) are:

$$\begin{aligned} &\text{i.c.:} \quad C(i,0) = C_0 \\ &\text{b.c.:} \quad C(0,t_m) = C_s \\ &\qquad C(i_m,t_m) = C_0 \; or \; C_m \end{aligned} \tag{7}$$

Where: i_m and t_m are two predefined variables related to position and time, respectively, which will be quantified later. The C_m refers to any value of chloride concentration at the i_m position inside concrete and t_m time. For the time to corrosion initiation assessment, C_m is assumed as the threshold chloride concentration to depassivation of the reinforcement. To carry out the numerical analyses by using PDEs, the i.c. and b.c. must be determined, *a priori*, so that they are not generated the arbitrary constants which represent the degrees of freedom associated with i.c. and b.c. Thus, it is necessary to give, explicitly, both conditions (show after) to find the solution (Wolfram Mathematica (2017)).

2.4 Chloride ions diffusivity

In this analysis, the chloride diffusion coefficient is not constant and is modified considering all the following multi-factors (Bastidas-Arteaga et al. (2011)), as described by the Eq. (8):

$$D_{cl} = D_{cl,ref} \times f_1(T) \times f_2(t) \times f_3(h) \tag{8}$$

Where: the factors f_1, f_2, f_3 are represented by correction expressions for temperature, concrete aging and humidity, respectively. The $D_{cl,ref}$ is called reference diffusion because is based on particular time, temperature and relative humidity for fully saturated concrete (Fu et al. (2015); El Hassan et al. (2010)). This factor usually is calculated through a very simple model based on only the *w/c* ratio (Fu et al. (2015)). Therefore in this analysis, $D_{cl,ref}$ has been taken *a priori* from previous studies ($D_{cl,ref}$ = 0.4 cm^2/year as presented in Table 2) (Zacchei and Nogueira (2019)).

The factor that considers the temperature *T*, which is expressed in kelvin, comes from the Arrhenius' law (Fu et al. (2015); Kong et al. (2002); Fu et al. (2010); Damrongwiriyanupap et al. (2015)) and is given by:

$$f_1(T) = e^{\left[\frac{E_a}{R}\left(\frac{1}{T_0}-\frac{1}{T}\right)\right]} \tag{9}$$

Where: T_0 is the chosen reference temperature (T_0 = 296 K → 23 °C); E_a is the activation energy (enthalpy) of the diffusion process, which depends on *w/c* ratio (Zacchei and Nogueira (2019)). Assuming water vapour as an ideal gas, the universal gas constant *R* is introduced, which is correlated by chemical potential of ions, molar concentration and temperature (R = 8.314 J/(mol K)) (Zofia and

Adam (2013)). The concrete coefficient of diffusion decreases over time due to the continuous cement hydration and depends on the aging effect by (Fu et al. (2015); Fu et al. (2010); Wang et al. (2018)):

$$f_2(t) = \begin{cases} \frac{1}{1-m}\left(\frac{t_{ref}}{t}\right)^m & \text{in case of } t < t_r \\ \left[1 + \frac{t_r}{t}\left(\frac{m}{1-m}\right)\right]\left(\frac{t_{ref}}{t}\right)^m & \text{in case of } t \geq t_t \end{cases} \quad (10)$$

Where: t_{ref} is the reference concrete age (t_{ref} = 28 days → 0.076 years); t_r is the time when the diffusivity is assumed to be constant (t_r = 30 years). The time t expressed in years is considered as the "exposed time" (t = 25 years). The parameter m (defined later) is used to express the reducing speed of chloride diffusivity and depends on the fly ash and slag added to the cement (Kim et al. (2014)) as well as on the *w/c* ratio.

The factor concerns the humidity h is shown by (Bastidas-Arteaga et al. (2011); Damrongwiriyanupap et al. (2015); Mien et al. (2009)):

$$f_3(h) = \frac{1}{\left[1 + \frac{(1-h)^n}{\left(1-h_{D_{cl}}\right)^n}\right]} \quad (11)$$

Where: h_{Dcl} is the humidity at which D_{cl} drops half-way between its maximum and minimum values. In other words, it is basically a mean value calibrated with several studies. It is assumed equal to 0.75 (75%) at 21 - 25 °C (Bažant and Najjar (1972)). The parameter n is a value that characterize the spread of the drop in D_{cl} (n = 4 (Bastidas-Arteaga et al. (2011); Damrongwiriyanupap et al. (2015); Mien et al. (2009))) or $6 \leq n \leq 16$ (Bažant and Najjar (1972)). Figure 1 shows some curves with different n values. As it can be seen, the D_{cl} strongly depends on pore humidity h. As an example, for T = 50 °C, h = 0, n = 4 and h_{Dcl} = 0.75 the humidity factor is $f_3(h)$ = 3.89 × 10^{-3} (Bažant and Najjar (1972)).

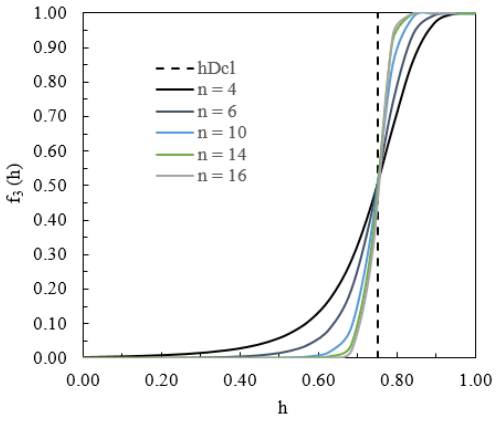

Figure 1 – Humidity factor distribution.

3 Methodologies

3.1 General techniques for failure probability assessments

The procedures used in this study to achieve the proposed goals are: (i) probabilistic analysis to define the probability of failure considering the time for corrosion initiation; (ii) numerical analysis to study the chloride content inside concrete for different diffusion coefficients defined by particular functions. Table 1 lists some techniques to estimate the probability of failure for possible scenario of the corrosion initiation time. In this table there is a short description of the respective technique and the type of analysis used in this study.

Table 1 – Techniques for probability of failure assessment.

Technique	Brief description	Type of analysis
DI (Pellizzer (2015))	This is the direct solution of the probability of failure. This multivariate integral is defined at the failure domain and evaluated considering the joint density function. Such approach is exact, but it requires the joint knowledge of the variables behaviour, which in practical terms is very difficult to obtain. However, when the random variables are statistically independent, the joint density function can be obtained by simple multiplication of all the marginal density distributions of the random variables.	X
FOSM (Pellizzer (2015))	It is based on a linearization of the limit state function (LS) at the design point given by a hyperplane tangent. The data to define the joint density function are only the mean and standard deviation of the random variables (RV). The information about the RV, such as the individual density functions and correlation between pares of RV are not considered. The solution is exact only when the limit state function is linear and the RV are uncorrelated and Gaussian.	-
FORM (Hariri-Ardebili (2018))	The description of the FOSM is the same here, but FORM is broader then FOSM because the information of the individual density functions and correlation between pares of the RV are considered in the reliability analysis. It is a transformation method since the reliability problem is solved at the uncorrelated normal standard space and probabilistic transformations are required to convert the information from the physical space to the uncorrelated normal standard space. The solution is very accurate when linear LS functions describe the physical problem and the non-Gaussian random variables are used. However, for high nonlinear LS functions, the hyperplane tangent at the design point may over or under estimate the probability of failure leading to inaccurate solutions.	X
SORM (Hariri-Ardebili (2018))	The description of the FORM is the same here, except for the approximation at the design point. Instead of a linearization, it is considered a quadratic function given by a paraboloid with its vertex positioned at the design point. For nonlinear LS functions, SORM provides a more accurate solution when compared to FORM, but the numerical costs to achieve the solution are higher than FORM.	-
MCS pure (Pellizzer (2015))	It is based on the pseudo-random generation of numbers to describe the probabilistic behaviour of the RV along the domain of the analysed problem. The random generation of the sample can incorporate the non-Gaussian and correlated variables. This technique is exact when the number of samples generation tends to infinity (a very large sample). But this is the restriction of this method, which can be prohibitive when the probability of failure is too small, requiring a very large number of simulations, especially in cases of numerical solution necessary to describe the response of the problem.	X
MCS IS (Hariri-Ardebili (2018))	The description of the MCS pure is the same here. However, MCS IS reduces the variance and computational cost in MCS because it concentrates the sampling function centre at the design point instead of the origin (mean values) in uncorrelated normal standard space. Therefore, the design point information is required to perform MCS IS.	-
Response surface (Pellizzer (2015))	The LS function is defined by a polynomial (with low or high order; with or without cross terms) constructed from a deterministic design experiments at the design point to represent analytically the limit state function. To solve the reliability problem, an adaptive procedure is required in which a new response surface is defined for each iteration of the algorithm solution.	-

Note: X = Technique used in this analysis; DI = Direct Integration; FOSM = First Order Second Moment; FORM = First Order Reliability Method; SORM = Second Order Reliability method; MCS = Monte Carlo Simulation; IS = Importance Sampling.

3.2 Strategy of solution to concrete diffusivity and chloride concentration

The adopted methodology to study the chloride content inside concrete is mainly divided in two parts, which are depicted in Figure 2. In the first part (steps 1 and 2), the D_{cl} (Eq. 8) is defined considering deterministic and random values, whereas in the second part (steps 3 and 4) the chloride concentration $C(i,t)$ is assessed. The two parts are explained in the following steps.

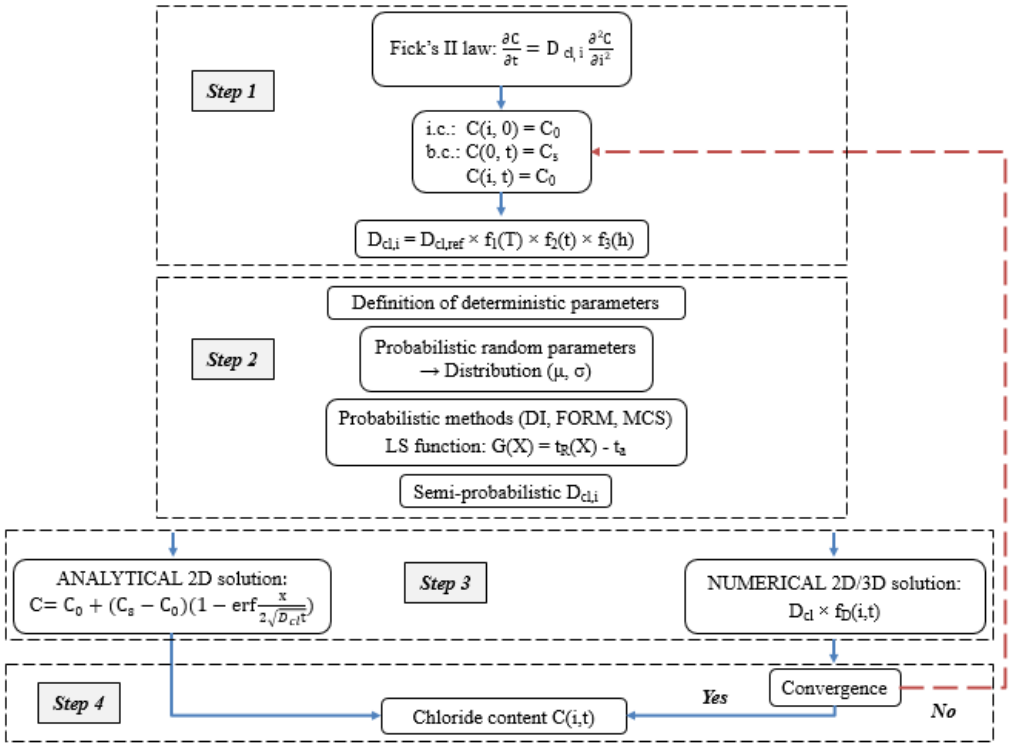

Figure 2 – Flowchart of the adopted methodology.

Step 1: Definition of the first and second Fick's law. Evaluation of the factors ($D_{cl,ref}$, f_1, f_2, f_3) to obtain the final coefficient of diffusion $D_{cl,i}$. Both laws are the basis of the 2D and 3D models;

Step 2: Definition of deterministic and random values. In this sense, $D_{cl,i}$ is a semi-probabilistic coefficient because only five independent random parameters (E_a, T, m, h, n) have been used (El Hassan et al. (2010)); the other parameters are calculated deterministically ($D_{cl,ref}$, w/c, T_0, R, t_{ref}, t, t_r, h_{Dcl}). All parameters will be better explained later. The accuracy of the depassivation time and corrosion initiation depends on strongly to the good estimation of $D_{cl,i}$;

Step 3: Implementation of the 2D analytical solutions and 2D / 3D numerical solutions. In order to carry out a numerical analysis, a generic function $f_D(i,t)$ is proposed (this function will be explained later). Here, the numerical solutions to set of differential equations with several unknown functions y_j that depend on one or more independent variables x_j are found. Numerical differential equations represent solutions for the functions y_j by "interpolating function" (IF), which is a polynomial interpolation

defined as a generalization of linear interpolation (Wolfram Mathematica (2017)). The IF provides approximations to the y_j over the range of values $x_{initial}$ to x_{final} for the independent variables x_j. The process is iterative: it starts at a value of x_j and then takes a sequence of steps, trying to cover the whole range $x_{initial}$ to x_{final}. It is necessary to define an appropriate initial and boundary conditions for the y_j and their derivatives. These conditions specify values for $y_j(x_j)$ and $y_j'(x_j)$ at particular points x_j;

Step 4: Evaluation of the chloride content $C(i,t)$. If the convergence is not satisfied it is necessary to redefine the i.c. and b.c.

4 Probabilistic analysis

4.1 Formulation of the problem: corrosion initiation time

The probabilistic analysis is based on the information of the random variables through the probability density functions (PDFs). Then, a potentially failure mode is defined considering a limit state (LS) function G(X), in which X is a vector of the adopted random variables (Nogueira et al. (2012)). The probability of failure happens for a domain G(X) < 0 (failure/undesired domain), whereas the probability of non-failure happens for a domain G(X) > 0 (safety domain). The boundary of both domains is given when G(X) = 0 (limit domain). In this context, it is used the word "failure" to indicate the corrosion initiation.

Considering N_X samples of each random variable vector $X = \{x_1, x_2, \ldots, x_j\} = \{x_i\}$, for a LS function G(X), the general probability of failure is calculated by:

$$p_f = P[G(X) < 0] = \int_{\{X:\, G(X)<0\}} f_X(x_1, x_2, \ldots, x_j)\, dx_1 dx_2 \ldots dx_j = \int_{\{X:\, G(X)<0\}} f_X(x_i)\, dx_i \qquad (12)$$

Where: $f_X(x_i)$ are the joint PDF of the random variables x_i.

Since closed-form solutions of the Eq. (12) are difficult to obtain, three methods have been used in this analysis: (i) First Order Reliability Method (FORM), (ii) direct integration (DI) and (iii) pure Monte Carlo simulation (MCS). DI is based on the Rosenblatt's transformation with the mean and standard deviation calculated a priori (Rosenblatt (1952)). FORM and MCS are performed according the classical formulation (Pellizzer et al. (2015); Oliveira et al. (2018)).

In this analysis, the LS function is written as the difference between the time for corrosion initiation t_R and the structural life-time expected in design t_a as: $G(X) = t_R(X) - t_a$. When $G(X) \rightarrow 0$, i.e. when $t_R = t_a$, the failure is achieved. The Eq. (6) is rewritten for determining the time $t_R(X)$ as a main function of the cover depth x_c and coefficient of diffusion D_{cl} as follows (Pellizzer et al. (2018); Pellizzer and Leonel (2015); El Hassan et al. (2010)):

$$t_R(X) = \frac{x_c^2}{4D_{cl}\left(\text{erf}^{-1}\left[\frac{C-C_s}{C_0-C_s}\right]\right)^2} \approx \frac{x_c^2}{4D_{cl}\left(\text{erf}\left[\frac{C_{th}-C_s}{C_0-C_s}\right]\right)^2} \quad (13)$$

Where: C_{th} is the concentration of the chloride threshold, which must not be formed at the surface of the reinforcement bars to avoid the destruction of the steel passive layer (limit chloride concentration to star the corrosion process). Therefore, the corrosion begins when the chloride ions reach the chloride concentration threshold at the reinforcement surface (x_c), i.e. $C(x_c,t_R) = C_{th}$.

Figure 3 shows the error function and its inverse erf^{-1} (·), where it is possible to see that explicit numerical values of erf^{-1} (·) are given only for real values between -1 < input < 1. The interval of the error function erf (·) is between - ∞ < input < + ∞, but the real values less than 1 are given only between - 3.5 < input < +3.5. In this analysis the input values have a large range; therefore, it was adopted erf (·) instead of its inverse.

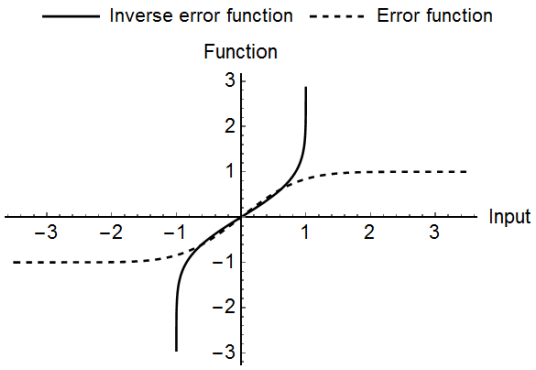

Figure 3 – Error function and its inverse.

As already mentioned, Eq. (13) derives from the solution that describes the diffusion inside concrete given by Eq. (6). It is important to note that Eq. (6) does not consider the initial rebar diameter (Zhang et al. (2010)), the chemical and biological process, as well as their reactions at concrete-reinforcement interface to quantify the corrosion initiation (Michel et al. (2013)). Moreover, there is a porous zone around the steel reinforcing bar in which the corrosion products must first fill before they start to induce internal pressure on the surrounding concrete. However, the use of this equation is more pessimistic and it is an advantage for the service life prediction because the time of appearance of the mechanical and physical processes is of the order of some months, whereas for the chemical and biological processes is years or century (Apostolopoulos and Papadakis (2008)).

4.2 Prediction scenarios results: analytical 2D solution

The probabilistic analysis developed in this paper treats the parameters as statistically independent random variables in the time *t* and space *i*. Stochastic models that do not include time and spatial

variability cannot adequately describe the performance of RC structures and can oversimplify the analysis underestimating the failure probabilities (Suo and Stewart (2009)). Tables 2 and 3 list the group of the adopted deterministic and random variables with their statistic information (mean value, coefficient of variation and marginal probabilistic density function). The type of concrete is made by an Ordinary Portland Cement with fly ash and slag that are account in the variation of *m*-parameter (Kim et al. (2014)).

Table 2 – Deterministic data.

Parameter	Unit	Value
α (Zacchei and Nogueira (2019))	-	11.8
β (Zacchei and Nogueira (2019))	-	4.0
$D_{cl,ref}$*	cm^2/year	0.4
w/c*	-	0.5
T_0 (Kong et al. (2002))	°C (K)	23 (296)
R (Kong et al. (2002))	J/(mol K)	8.134
t_{ref} (Fu et al. (2015))	days (years)	28 (0.076)
t*	years	25
t_r (Fu et al. (2015))	years	30
h_{Dcl} (Bažant and Najjar (1972))	-	0.75

Note: * = Estimated value

Table 3 – Random variables data.

Parameter	μ	± σ[a]	C_V (%)[b]	Distribution	Reason of distribution
E_a (kJ/mol)	44.6 (Kong et al. (2002))	4.3	10	Normal	Positive parameter truncated at 17.6 kJ/mol[c].
T (°C)	23*[d]	8.0	35	Normal	This parameter can be positive or negative.
C_f (kg/m^3)	1.50 (Zacchei and Nogueira (2019))	0.75	50	Log-normal	This parameter must be positive; therefore the interval distribution is (0, +∞).
ω_e	0.83*	0.1408	17	Beta(5, 1)	This parameter is defined in $0 \leq \omega_e \leq 1$, therefore the interval distribution is [0, 1].
m	0.2 (Kim et al. (2014))	0.04	20	Normal	A common distribution is used to control the dispersions (sensible parameter for results).
h	0.80*	0.04	5	Normal	A common distribution is used to control the dispersions (sensible parameter for results).
n	6 (Bažant and Najjar (1972))	1.732	28	Normal	A common distribution is used to control the dispersions (sensible parameter for results).
x_c (cm)	5.0*[e]	1.5	30	Log-normal	This parameter must be positive; therefore the interval distribution is (0, +∞).
C_0 (kg/m^3)	0.5*	0.2886	58	Uniform(0, 1)	Continuous and constant parameter.
C_s (kg/m^3)	1.15 (El Hassan et al. (2010))[f]	0.575	50	Log-normal	This parameter must be positive (truncated at C_0), therefore the interval distribution is (C_0, +∞).

Note: * Estimated value.

[a] For the beta and uniform distributions, ±σ is calculated by the relative distribution equations.

[b] C_V is the coefficient of variation estimated by: $(\sigma/\mu) \times 100$.

[c] E_a = 44.6±4.3 kJ/mol, for w/c ratio assumed constant and equal to 0.5. E_a reaches this value when the pores are fluid free (Ishida et al. (2009)).

[e] 50 mm, with w/c = 0.5, is considered a fair cover (Stewart and Mullard (2007)).

[d] 23±8 °C corresponds to 296±8 K.

[f] For structures located between 0.1 km and 2.84 km from the coast without direct contact with seawater (El Hassan et al. (2010)).

In the Beta distribution B (α', β'), α' and β' are the shape parameters. For α' = 1 the probability P(X ≤ x) is low, whereas for β' = 1 is high. For example, the evaporable water content ω_e is more probable that is higher than 0.6 (up to 1.0), therefore the Beta distribution more appropriate is for α' >> β'.
Figure 4 shows the probabilistic distribution function for each random variable.

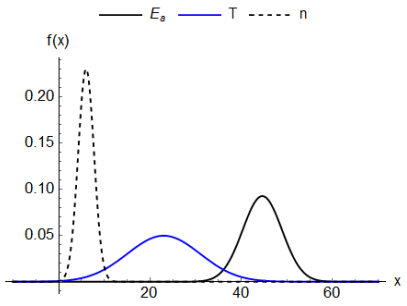

(a) Normal distribution N(μ, σ^2)

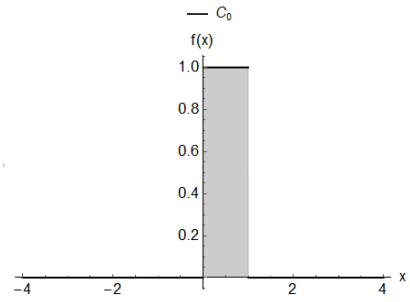

(b) Uniform distribution U(x_{min}, x_{max})

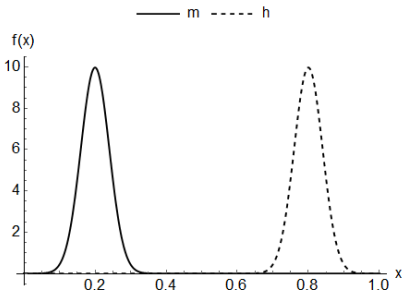

(c) Normal distribution N(μ, σ^2)

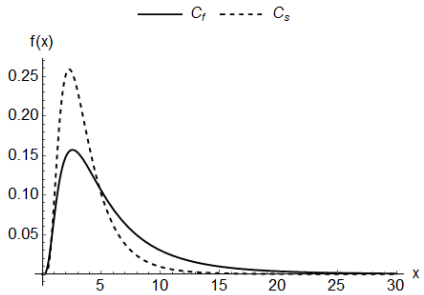

(d) Log-normal distribution logX(μ, σ^2)

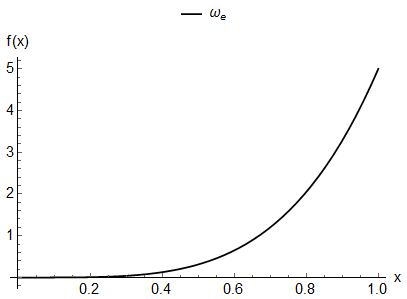

(e) Beta distribution B(α', β')

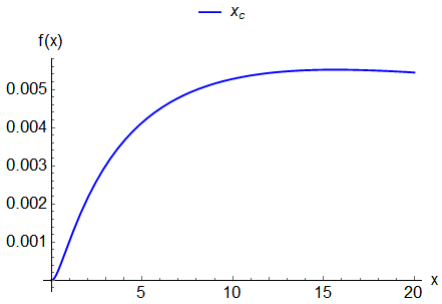

(f) Log-normal distribution logX(μ, σ^2)

Figure 4 Used probability distributions.

Figure 5 gives an overview of the four random variables randomly generated: C_{th}, C_s, $t_R - t_a$ and t_R, in which the right figure is on logarithmic scale. In this analysis, for MCS, 1×10^6 samples have been probabilistically generated.

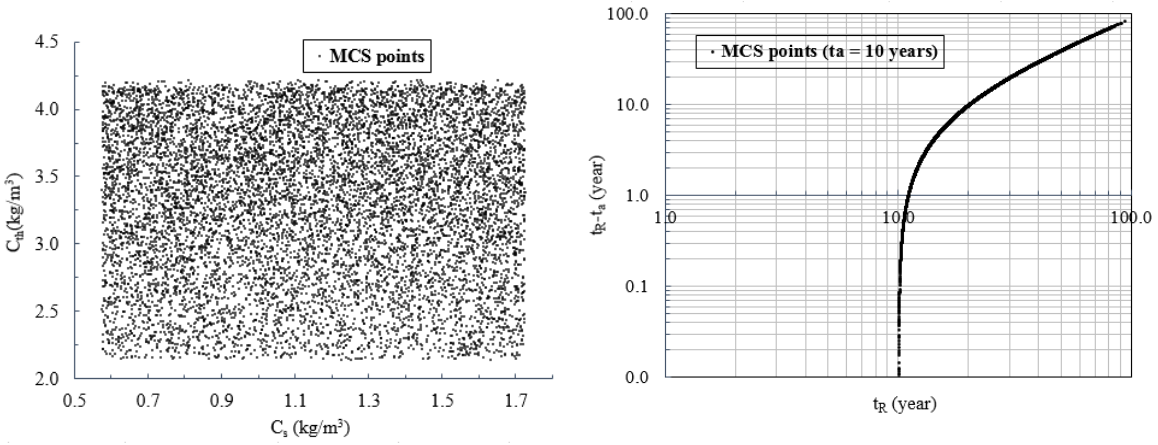

Figure 5. Random points for four parameters (C_{th}, C_s, $t_R - t_a$ and t_R) generated by MCS (1×10^6 points).

Figure 6 shows three scenarios for the probability of failure (corrosion initiation time) by using the adopted three methodologies (DI, FORM and MCS). Scenario I is calculated by using the values shown in Table 2 and 3. In scenario II only the temperature T changes, whereas in scenario III T and C_f change. The time t_a was adopted as 5, 10, 15, 20, 25 and 50 years.

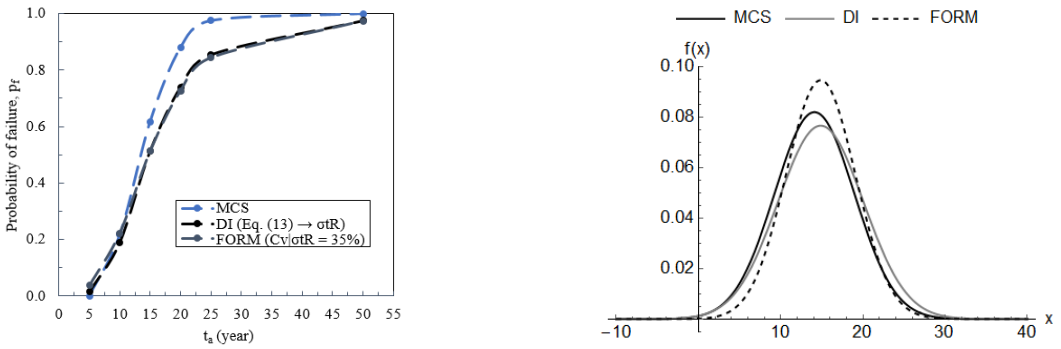

(I) Values of the Table 3.

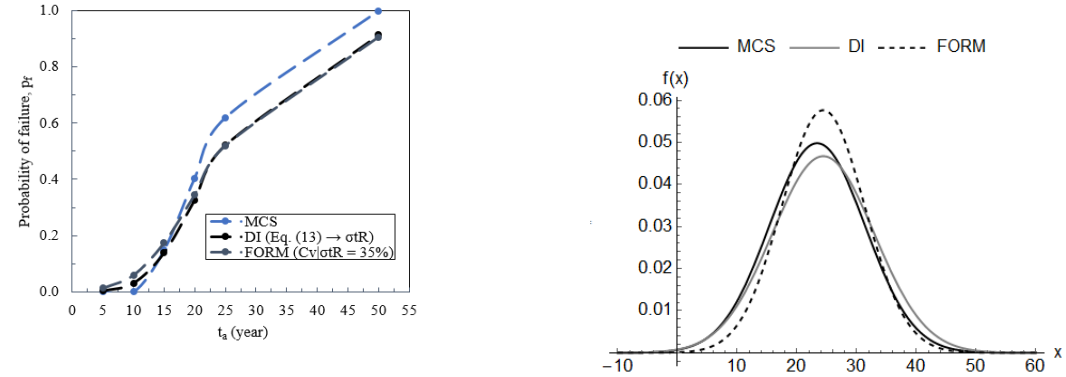

(II) Values of the Table 3, except T = 15 °C.

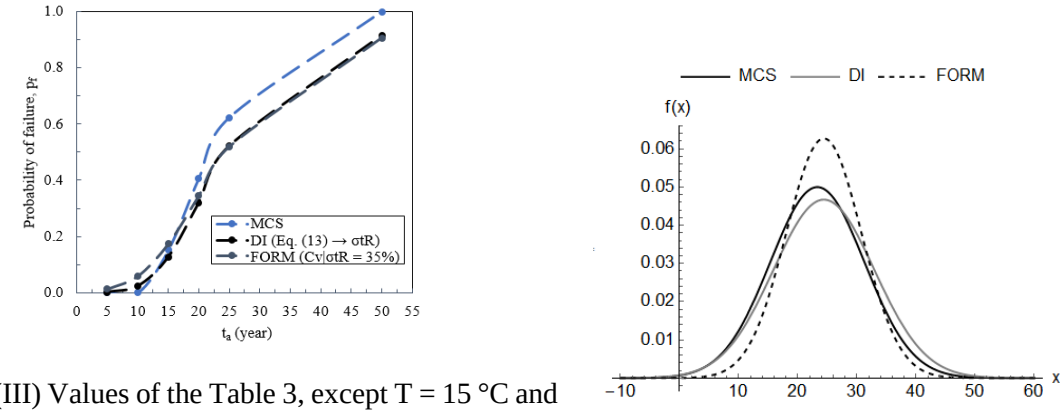

(III) Values of the Table 3, except T = 15 °C and C_f = 2.25 kg/m^3.

Figure 6. Results of the three scenarios I, II, and III. Probability of failure × t_a (left) and PDFs with mean μ_{tR} by three methodologies (right).

For MCS, the input data to plot the curves $P_f \times t_a$ (Figure 6) are obtained directly by the frequentist probability definition given by $P_f = \frac{NF}{N}$ (total number of failures/total number of simulations), in which the LS function is written as $G(X) = t_R - t_a$. In case of FORM approach, the corrosion initiation time is considered as a random variable function, in which the μ_{tR} and σ_{tR} must be estimated from the data showed in Tables 2 and 3. The mean value and the standard deviation of t_R were defined considering the

first order approximation of the Taylor's series applied to Eq. (13). Table 4 shows the mean values and the standard deviation of the corrosion initiation time for the three analysed scenarios obtained by MCS and FORM.

D_{cl} and C_b come from Eqs. (8) and (4), respectively; whereas C_{th} comes from both Eqs. (6) and (13) combined. In DI, μ_{tR} and σ_{tR} are obtained by Eq. (13) using the values in Table 2 and 3.

Table 4. Scenarios of the t_R (in years).

	Scenario I $D_{cl} = 0.423$ cm^2/year $C_b = 2.50 \times 10^{-6}$ kg/cm^3 $C_{th} = 3.75 \times 10^{-6}$ kg/cm^3		Scenario II $D_{cl} = 0.257$ cm^2/year $C_b = 2.50 \times 10^{-6}$ kg/cm^3 $C_{th} = 3.75 \times 10^{-6}$ kg/cm^3		Scenario III $D_{cl} = 0.257$ cm^2/year $C_b = 2.65 \times 10^{-6}$ kg/cm^3 $C_{th} = 4.51 \times 10^{-6}$ kg/cm^3	
	μ_{tR}	σ_{tR}	μ_{tR}	σ_{tR}	μ_{tR}	σ_{tR}
MCS	14.11	4.68	23.39	8.01	23.31	7.98
FORM	14.87	4.21	24.41	6.92	24.41	6.36
DI	14.87	5.20	24.41	8.54	24.41	8.54

It is possible to see that, the differences between the predicted values of the probability of failure considering MCS and FORM tend to be higher for long periods when compared to short periods. It is important to realize that the LS function is highly nonlinear for all the adopted parameters and the FORM may lose accuracy in such cases. In the three scenarios, the t_R coefficient of variation is 34% for MCS and 28% for FORM, which indicates the differences on the variability of the corrosion initiation time.

MCS curve tends to depart respect to DI curve, which should represent the exact solutions. However, DI is very sensitive to the used μ_{tR} and σ_{tR} (that *a priori* are unknown), a consequently, can over- or under-estimate the results.

In Figure 6, for scenarios II and III, it is possible to observe that P_f is lesser that P_f of scenario I. This shows the importance of the temperature variation. On the other hand, the variation of C_f is not so influent on the results of the probability of corrosion initiation time. The final PDFs for t_R in MCS and FORM are also depicted in Figure 6. As described before, the MCS has provided lower dispersion than FORM. However, considering the obtained mean values and the standard-deviation for t_R, it was observed a good agreement between the two reliability methods. The importance of this approach is the construction of the statistical data for the corrosion initiation time from the available data. This information (μ_{tR} and σ_{tR}) can be very useful in the RC structures design phase because it allows the designer to change some controllable parameters, such as concrete cover and w/c ratio to predict the inspection periods of the concrete structure, in order to avoid the corrosion initiation.

5 Numerical results for the chloride concentration assessment

5.1 Convergence criterion

The analysis is carried out in 2D and 3D by software (Wolfram Mathematica (2017)). In this section it was studied the chloride content inside concrete implementing numerically a generic function $f_D(i,t)$ multiplied by D_{cl} obtained in the previous probabilistic analysis. The function $f_D(i,t)$ is introduced to study two types of fluctuation of the chloride concentration: constant and general random. These functions can be seen as the influence of mechanical loadings on the diffusion process. In this analysis, a convergence criterion is necessary because de PDE is numerically solved. The convergence procedure is summarized in the following steps: (i) definition of the chloride coefficient function $f_D(i,t)$ that describe the type of loading influence; (ii) selection of the boundary conditions of the numerical analysis; (iii) plotting of the chloride content 2D and 3D curves $C(i,t)$; and (iv) verification of the convergence between the exact (subscript E_s) and numerical solutions (subscript N_s) by following criterion:

$$\left|C(i,t)_{E_s}^{k} - C(i,t)_{N_s}^{k}\right| \leq \varepsilon \tag{14}$$

Where: k represents the iterations; ε denotes a tolerance to reach the convergence ($= 1.45 \times 10^{-9}$). This convergence is therefore found by minimizing the difference between the analytical and numerical results.

Since the chloride content can be expressed in 3D, in alternative, considering separately the variables i = x or y and t, the convergence between an exact solution and numerical solutions can be evaluated using the sum of square errors (SSE) expression described below:

$$SSE = \sum_{k=1}^{n}\left[\left(C(i)_{E_s}^{k} - C(i)_{N_s}^{k}\right)^2 + w\left(C(t)_{E_s}^{k} - C(t)_{N_s}^{k}\right)^2\right] \tag{15}$$

Where: w is a weighting factor indicating the relative importance of the errors (a possible value for w is 1). The convergence is stopped when $SSE|_{k+1} < SSE|_k$ stabilizes.

5.2 2D chloride ions diffusion

Design loads act on a structure in complex manner due to their random histories. Here, the idea is to simulate how the external acting loads influence the movement of a single particle of chloride ion entering concrete in the diffusion process. In this sense, a simulation of the interaction effects between the macro-system actions (external loadings) with the micro-system actions (diffusion phenomenon) is performed. In order to carry out this simulation, a generic function that acts directly on the diffusivity is introduced (external loads on the structure ↔ fluctuation of a single particle of chloride ion). The proposed generic function $f_D(x,t)$ will be represented by constant and random general forms. Table 5 lists two types of considered loads and their applications.

Table 5. Proposed generic function $f_D(x,t)$ and some applications.

Type	$D_{cl} \times f_D(x,t)$	Example of applications of the function
Constant	$D_{cl} \times$ constant	- Temperature and humidity. They usually are considered constant because it is quite complicated to define the real humidity and temperature after early-age concrete. It is assumed that humidity and temperature be stable when subjected to the external climate conditions. - Loads: dead load, accidental loads, hydrostatic loads, pseudo-static and pseudo-dynamic accelerations, uplifts.
General	$D_{cl} \times \sum_{i=1,...,n} \text{Sin}(\omega i t + \phi)$	- Earthquake. Shear waves, compressive and vertical waves, seismic amplification. - Wind action. - Vibration of machines. - All-natural aleatory actions.

The Figure 7 shows the chloride concentration *C* with the exact (a) and numerical (b) solutions for $f_D(x,t)$ constant and equal to 1.0. All data refer to the scenario I. Only in this case it is possible the comparison. The exact solution of $C(x,t)$, given by Eqs. (5) and (6), is calculated within an interval $0 \leq t \leq t_{final}$ and $0 \leq x \leq x_{final}$; whereas the numerical solution of $C(x,t)$, given by Eq. (7), is calculated within an interval $0 \leq t_m \leq t_{m,final}$ and $0 \leq x_m \leq x_{m,final}$. The used intervals are: $t_{final} = t_{m,final} = 2\pi$ years and $x_{final} = x_{m,final} = 6$ cm.

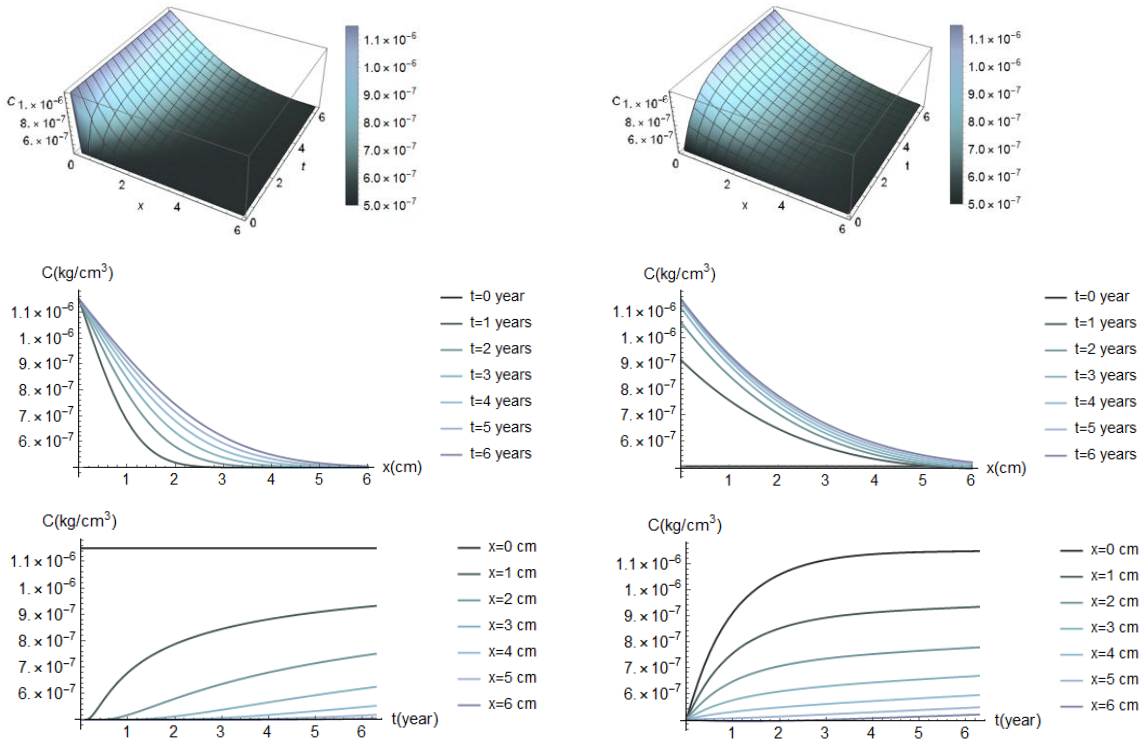

(a) (b)

Figure 7. Exact (a) and numerical (b) solution for $f_D(x,t)$ constant and equal to 1.0. Curves vary regarding to the adopted range: $\{0 \leq t \leq 2\pi$ years, with steps dt = 1 year$\}$ and $\{0 \leq x \leq 6$ cm, with steps dx = 1 cm$\}$.

Moreover, to obtain the numerical solution it is necessary to define the b.c.: $C(x_m,t_m) = C_0$ (see Eq. 7). In particular, it is necessary to define a priori the term x_m. With a maximum distance of $x_m = 20\ x_{m,final}$, a good convergence has been obtained. In Figure (7b), it is possible to see that for x = 0, C is different for each curve. This is due to the boundary conditions that block the extremities and the interactive process is forced. Moreover, the interaction stars from $x_{m,final}$, therefore in x = 0 the approximation is more visible with low accuracy. However, from the curve with t = 3 years on, a good agreement between the exact and numerical solution is achieved, in which for x = 0, $C \approx C_s$. The horizontal line in the exact solution in Figure 7(a) comes from the Eq. (6): when x = 0, $C(x,t) = C_s$.

Figure 8 shows the same analysis depicted in Figure 7 but considering $f_D(x,t)$ random general. In this sense, a comparison between $f_D(x,t)$ random general and constant is made. The general function is defined by several sum of sinusoid (i = 1,…,n) where ωi is the circular frequency in rad/s, t is the time in seconds, ϕ is the angular phase among the sinusoid functions, which is chosen as an uniform random value between 0 and 2π.

The horizontal line in Figure 8(c) is because when t = 0, $\text{erf}(\infty) \rightarrow 1$, thus $C(x,t) = C_0$ (see Eq. 6). From t = 3 years on, a good agreement was achieved in comparison with the exact solution.

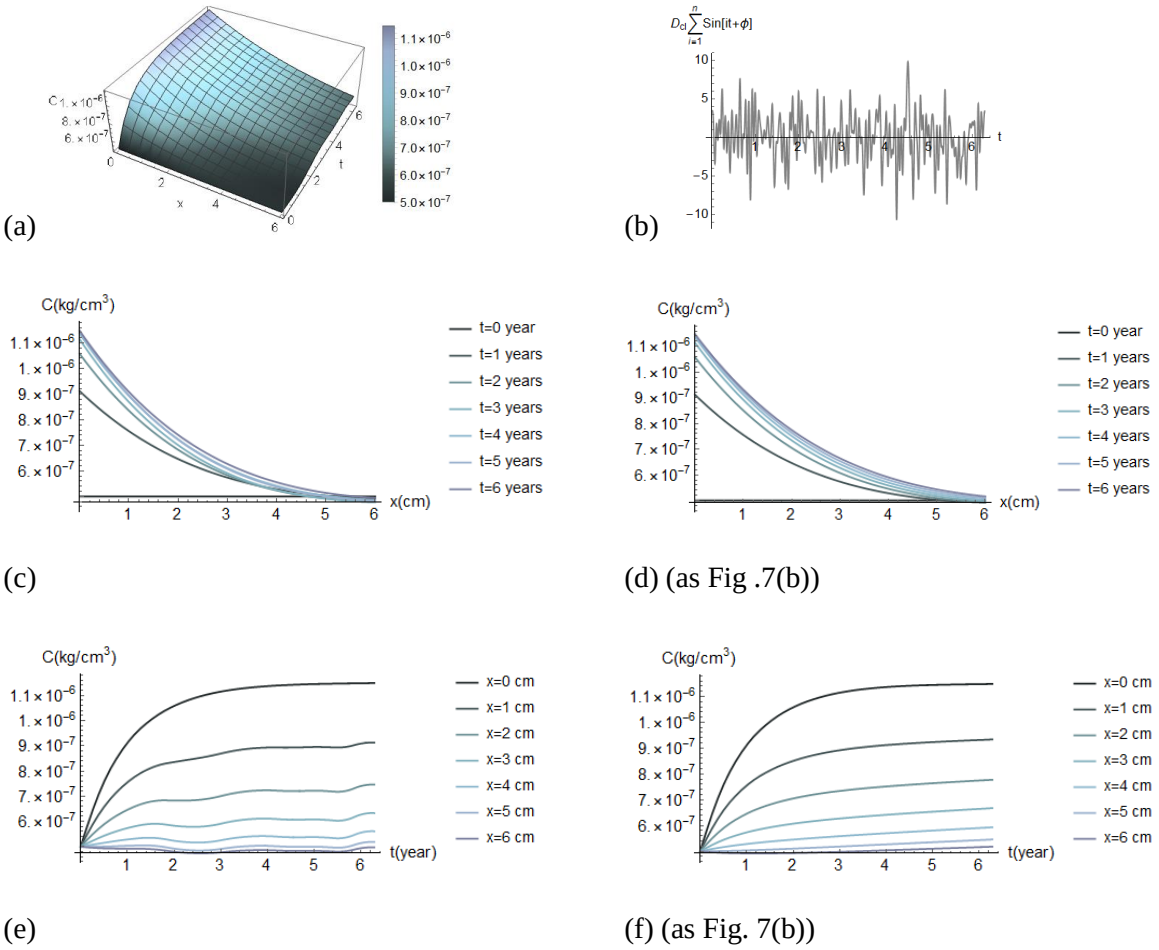

Figure 8. Numerical solution for $f_D(x,t)$ random general (a, c, e) and for $f_D(x,t)$ constant and equal to 1.0 (d, f). General load (b). Curves vary regarding to the adopted range: $\{0 \leq t \leq 2\pi$ years, with steps dt = 1 year$\}$ and $\{0 \leq x \leq 6$ cm, with steps dx = 1 cm$\}$.

By comparing Fig. 8(e) and Fig. 8(f) it is possible to note that, due to the oscillations of the solutions for general random, the chloride content can assume lower values with respect the constant diffusivity. This is evident, for instance, at about 2.5 years and 4.5 years.

5.3 3D chloride ions diffusion

Considering the Eq. (7), the chloride content passes from *C(x,t)* to *C(x,y,t)*, which means that, the analysis passes from a 2D system to a 3D system.

An approach to estimate C(x,y,t) by summing a contribution of C in x and y directions in function of t, is proposed. It is important to note that the variation of C is defined by the changes during the diffusion process. This means that at time t, the concentration C that comes from x direction and the concentration

C that comes from y direction is different due to the changing of ∇C. However, results show that C in 3D analysis increases with respect in 2D analysis as expected, therefore the approximation can be considered acceptable.

Therefore, the boundary conditions increase to consider the flux in *y* direction. *C(x,y,t)* is calculated within an interval $t_m = 2\pi$, $0 \leq x_m \leq 6$ cm and $0 \leq y_m \leq 6$ cm. The values x_m and y_m of the b.c. $C(x_m,y_m,t_m) = C_0$ are assumed: $x_m = 20\ x_{m,final}$ and $y_m = 20\ y_{m,final}$. Here, a good convergence has been obtained. Figure 9 shows the numerical solution of the 3D chloride diffusion. The chlorides concentration at each point is the sum of the values obtained at x and y directions. Figure 10 shows the chloride diffusion in 3D model for different t_m: 1, 3 and 12 years, respectively.

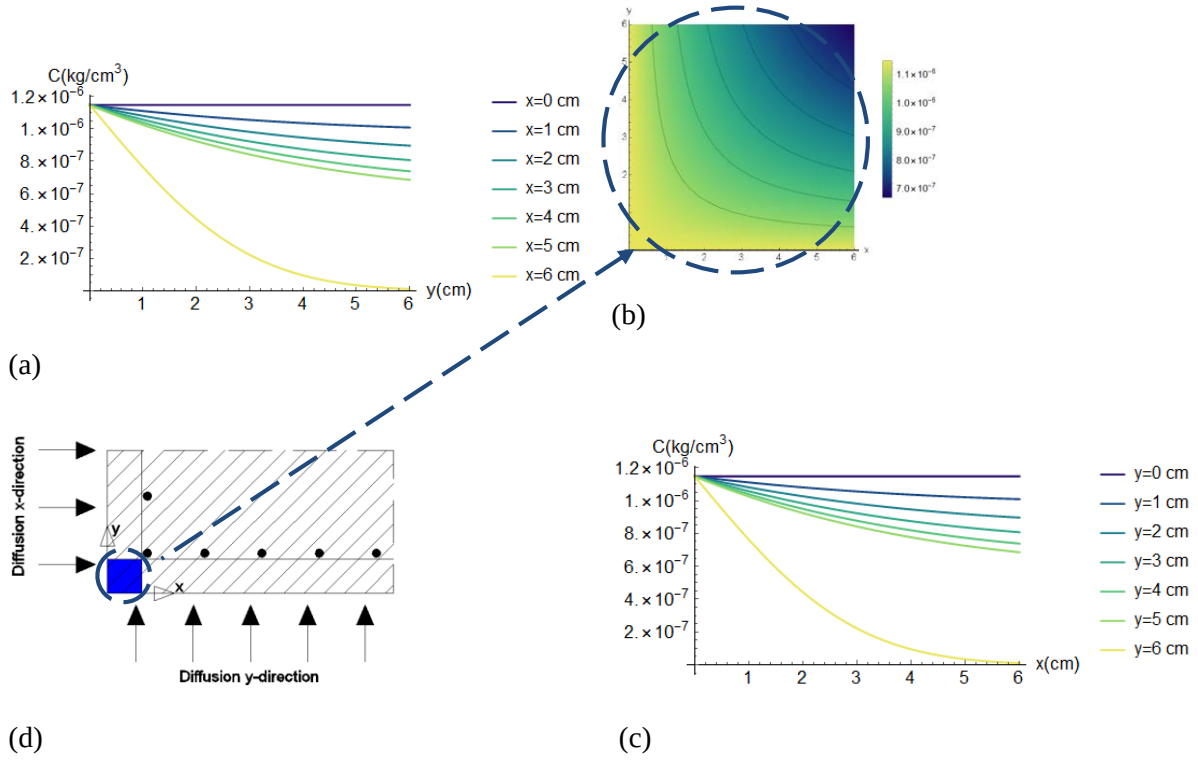

Figure 9. Numerical solution of the C(x,y,t) for $f_D(x,y,t)$ constant (a,b,c). Example of a RC beam (d). Curves vary regarding to the adopted range, for $t_m = 2\pi$ years: {0 ≤ y ≤ 6 cm, with steps dy = 1 cm} and {0 ≤ x ≤ 6 cm, with steps dx = 1 cm}. Data refer to I scenario.

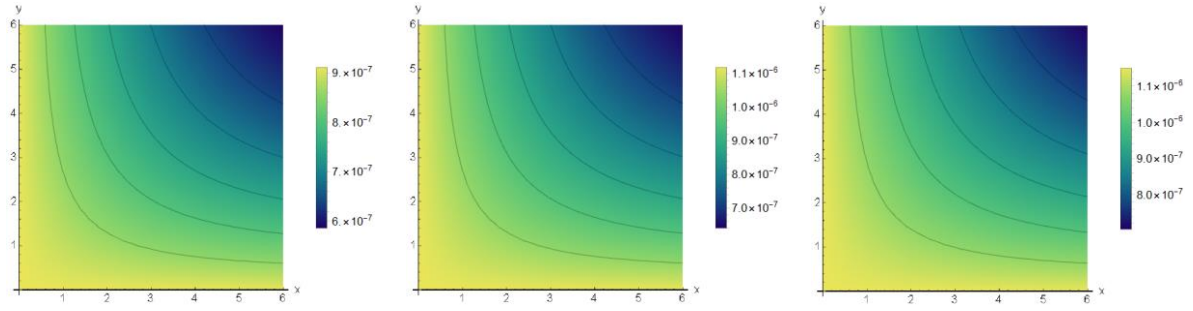

(a) tm = 1 year (b) tm = 3 years (c) tm = 12 years

Figure 10. Numerical solution of the C(x,y,t) with f_D(x,y,t) constant and equal to 1.0 for tm = 1 year (a), tm = 3 years (b) and tm = 12 years (c).

Table 6 shows the results of the analysis and a comparison between 2D and 3D solutions. The chloride concentration is evaluated at the steel bar position inside the concrete element, i.e. x = 6 cm in 2D analysis and x = y = 6 cm in 3D analysis. As expected, the chloride concentration in 3D analysis is greater than in 2D analysis (deviation is > 1.0). This is because the chloride diffusion comes, in 3D, from two different directions, providing a better representation of the ion ingress.

Table 6 - Comparison of both models.

Chloride content	2D	3D	Deviation (3D/2D)
C(i = 6, t = 1)	5.0×10^{-7} kg/cm^3	5.9×10^{-7} kg/cm^3	1.18
C(i = 6, t = 3)	5.1×10^{-7} kg/cm^3	6.5×10^{-7} kg/cm^3	1.27
C(i = 6, t = 6)	5.2×10^{-7} kg/cm^3	6.9×10^{-7} kg/cm^3	1.32
C(i = 6, t = 12)	5.4×10^{-7} kg/cm^{3*}	7.2×10^{-7} kg/cm^3	1.33

Note: i = x, for 2D analysis. i = x and y, for 3D analysis. * = Value not plotted.

6 Overall discussions

Fick's II law expressed by Eq. (2) considering $D_{cl,i}$ non-constant is an equation hard to be solved because the problem is non-linear. This disadvantage makes this model less attractive in practice. For this reason, the analytical solution given by Eq. (6) is usually used. The model expressed in Eq. (6) is obtained by adopting afore-mentioned hypothesis, which are rarely satisfied because:

(1) The material and dimensional properties of the concrete are heterogeneous. The heterogeneous nature of the microstructure of the hardened cement paste plays a significant role in the corrosion and diffusion of chlorides, which occur spatially over any exposed surface;

(2) The hypothesis of water saturated occurs in many real-world cases due to the limited thickness of the concrete cover (depending on the size and boundary conditions it is generally less than 100 mm in

actual engineering). However, the chloride concentration at non-saturated (or partially saturated) condition is higher than saturated state (Homan et al. (2016));

(3) The hypothesis of chloride concentration at external surface as uniform and constant may be to apply when there is no frequent washing by rain or other chloride-free water. Chloride ingress mainly depends on the drying-wetting cycles. However, this is difficult to establish it *a priori*;

(4) Considering D_{cl} constant, the chloride diffusion does not account the dependency of the time of several factors that have been described. In this sense, an analysis in the t-domain is necessary;

(5) The complete phenomenon is more complex: (i) the chloride penetration process driven by the concentration gradient is not the only mechanism for the chloride ingress into concrete. It exists, for example, the diffusion/reacting coupled conditions and the influence of the stresses. The surface chloride concentration in compressive zone is higher than that in tensile zone; this is due to the restrain effect of compressive stress and chloride binding in concrete (Fu et al. (2015)); (ii) this paper did not consider the influence of initial defects, which has a greater influence on the corrosion induced stress distribution in concrete cover (Zhang et al. (2017)). In this sense, the fabrication process is also an important factor. About the probabilistic models, using more sophisticated stochastic models improves the result precision (output), but does not change the observed trend (input). Here MCS and FORM approaches have been used.

MCS is an iterative simulation technique used to evaluate functions by several random variables (10×10^6). For every sample, each random variable is assigned a deterministic value from which a several random numbers are generated. The results are treated as a distribution and are statistically determined. Moreover, MCS provides directly the t-variant failure probability. A very good agreement was achieved with DI and FORM. Finally, in order to evaluate the quality of the results (poor, fair or good estimation) and their practicability is necessary to associate it to a specific RC structure. Adaptation measures for new/existing structures may be made depending of the effectiveness, cost and practicability (E = Easy. M = Medium. D = Difficult). For example: surface treatments (E/M depending on the surface position), several layers of mortar at external surface (E/M depending on the surface position), thickness of protective layer (E/M depending on the surface position), extra design cover (M/D), increase concrete durability (E), injection of additives (E), galvanised steel reinforcement (E) for new structures and (D) for existing structures (Bastidas-Arteaga et al. (2013)).

These adaptation strategies will have varying degrees of effectiveness and cost considering the location, timing and extent. Some will require regular maintenance over the life of the structure, such as surface treatments.

For this reason, a probabilistic-based approach is needed to assess the optimal adaptation to execute. It is preferable to use strategies during design and construction rather than in-service, as the latter will be much costlier in terms of direct or/and indirect costs.

7 Conclusions

The main conclusions can be summarized as explained below:

- In this analysis, the LS function is written as the difference between the time for corrosion initiation t_R and the structural lifetime expected in design t_a as $G(X) = t_R(X) - t_a$. The parameter t_R is estimated by using a probabilistic approach as MCS and FORM. In this sense, a new method and several deterministic and probabilistic data have been estimated (Table 2 and 3) to perform the analysis. These data have been collected by literature as quoted and they have been readjusted in order to carry out a more appropriate analysis. The expected values and their standard deviation in the scenario I are for DI ~ N(14.11, 4.68), FORM ~ N(14.87, 4.21) and MCS ~ N(14.87, 5.20). The μ_{tR} and σ_{tR} for the scenarios II and III are higher of 39% and 51-71% with respect to scenario I. In this sense, these three scenarios show the importance of the temperature variation and C_f. Finally, the probability of failure is calculated in an interval 0 – 50 years, showing a good calibration among the methods in an interval 5 – 20 years.
- A comparison between a constant diffusivity and generic diffusivity is carried out by introducing a generic function $f_D(x,t)$. This it is possible by developing a numerical solution with defined boundary conditions. In this way it is possible to simulate different trend of a single particle of chloride ion correlated to an external loading. This analysis can better quantify a minor/major accumulation of ions chloride. Results show that a constant D_{cl} can under- over-estimates the diffusivity, thus the chloride content in the structures. Results show that the chloride ions content, varying in the time, can assume lower values than for constant diffusivity. Here D_{cl} ranges between 1.1×10^{-7} kg/cm^3 at x = 0 cm and 6.0×10^{-6} kg/cm^3 at x = 6 cm.
- A comparison of the chloride ions concentration C thought a 2D and 3D model is carried out. A 3D model provides more accurate results because considers the chloride flux for various directions; however, as explained, in this analysis the influence of the ∇C variation is not considered. Results show that, at x = 6 cm, C in 2D analysis is lesser of about 78% than C in 3D analysis; this is because the chloride diffusion in 3D comes from two different directions, therefore it reaches a higher value. This comparison is possible by a numerical analysis as proposed.

Acknowledgements

The first author acknowledges the Itecons Institute, Portugal, for the Wolfram Mathematica license and University of Coimbra (UC), Portugal, to pay the rights (when applicable) to completely download all papers in the references. The study was funded by Support Program for Foreign Students of Doctorate (PAEDEX) and Ibero-American University Postgraduate Association (AUIP) (reference number: 3.224.803.003.569).

References

Al-Kutti WA, Rahman MK, Shazali MA, Baluch MH (2014) Enhancement in chloride diffusivity due to flexural damage in reinforced concrete beams. Journal of Materials in Civil Engineering 26: 658-667, DOI: https://ascelibrary.org/doi/10.1061/%28ASCE%29MT.1943-5533.0000836

Andrade C (2002) Concepts on the chloride diffusion coefficient. In: Third RILEM workshop on testing and modelling the chloride ingress into concrete, 9-10 September 2002, Madrid, Spain.

Apostolopoulos CA, Papadakis VG (2008) Consequences of steel corrosion on the ductility properties of reinforcement bar. Construction and Building Materials 22: 2316-2324, DOI: https://www.sciencedirect.com/science/article/pii/S0950061807002401

Bastidas-Arteaga E, Chateauneuf A, Sánchez-Silva M, Bressolette P, Schoefs F (2011) A comprehensive probabilistic model of chloride ingress in unsaturated concrete. Engineering Structures 33: 720-730, DOI: https://www.sciencedirect.com/science/article/pii/S0141029610004281

Bastidas-Arteaga E, Schoefs F, Stewart MG, Wang X (2013) Influence of global warning on durability of corroding RC structures: a probabilistic approach. Engineering Structures 51: 259-266, DOI: https://www.sciencedirect.com/science/article/pii/S0141029613000217

Bažant ZP, Najjar LJ (1972) Nonlinear water diffusion in nonsaturated concrete. Matériaux et Constructions 5(25): 3-20, DOI: https://link.springer.com/article/10.1007/BF02479073

Ben-Fraj A, Bonnet S, Khelidj A (2012) New approach for coupled chloride/moisture transport in non-saturated concrete with and without slag. Construction and Building Materials 35: 761–771, DOI: https://doi.org/10.1016/j.conbuildmat.2012.04.106

Bentz DP, Detwiler RJ, Garboczi EJ, Halamickova P, Schwartz LM (1997) Multi-scale modelling of the diffusivity of mortar and concrete. Proceedings of Chloride Penetration into Concrete, RILEM 1997: 1-6.

Capozucca R (1995) Damage to reinforced concrete due to reinforcement corrosion. Construction and Building Materials 9(5): 295-303, DOI: https://www.sciencedirect.com/science/article/pii/095006189500033C

Carrara P, De Lorenzis L, Bentz DP (2016) Chloride diffusivity in hardened cement paste from microscale analyses and accounting for binding effects. Model. Simul. Mat. Sci. Eng. 24:1-44, DOI: https://doi.org/10.1088/0965-0393/24/6/065009.

Chen W, Zhang J, Zhang J (2013) A variable-order time-fractional derivative model for chloride ions sub-diffusion in concrete structures. Fract. Calc. Appl. Anal. 16: 76-92, DOI: https://doi.org/10.2478/s13540-013-0006-y.

Da Costa A, Fenaux M, Fernández J, Sánchez E, Moragues A (2013) Modelling of chloride penetration into non-saturated concrete: case study application for real marine offshore structures. Construction and Building Materials 43: 217-224, DOI: https://www.sciencedirect.com/science/article/pii/S0950061813001141

Damrongwiriyanupap N, Limkatanyu S, Xi Y (2015) A thermo-hygro-coupled model for chloride penetration in concrete structures. Hind. Publis. Corp. 2015: 1-10, DOI: http://dx.doi.org/10.1155/2015/682940

El Hassan J, Bressolette P, Chateauneuf A, El Tawil K (2010) Reliability-based assessment of the effect of climatic conditions on the corrosion of RC structures subject to chloride ingress. Engineering Structures 32: 3279-3287, DOI: https://www.sciencedirect.com/science/article/pii/S0141029610002579

Fan WJ, Wang XY (2015) Prediction of Chloride Penetration into Hardening Concrete. Hind. Publis. Corp. 2015: 1-8, DOI: http://dx.doi.org/10.1155/2015/616980

Fu C, Jin X, Jin N (2010) Modeling of chloride ions diffusion in cracked concrete. In: Earth and Space 2010: Engineering, Science, Construction, and Operations in Challenging Environments 3579-3589, 14-17 March, Honolulu, Hawaii, USA.

Fu C, Jin X, Ye H, Jin N (2015) Theoretical and experimental investigation of loading effects on chloride diffusion in saturated concrete. Journal of Advanced Concrete Technology 13:30-43, DOI: https://www.jstage.jst.go.jp/article/jact/13/1/13_30/_article/-char/en

Halamickova P, Detwiler RJ, Bentz DP, Garboczi EJ (1995) Water permeability and chloride ion diffusion in Portland cement mortars: relationship to sand content and critical pore diameter. Cement and Concrete Research 25(4): 790-802, DOI: https://www.sciencedirect.com/science/article/pii/000888469500069O

Hariri-Ardebili MA (2018) Risk, reliability, resilience (R^3) and beyond in dam engineering: A state-of-the-art review. International Journal of Disaster Risk Reduction 31: 806-831, DOI: https://www.sciencedirect.com/science/article/pii/S2212420918306307

Homan L, Ababneh AN, Xi Y (2016) The effect of moisture transport on chloride penetration in concrete. Construction and Building Materials 125: 1189-1195, DOI: https://www.sciencedirect.com/science/article/pii/S0950061816313873?via%3Dihub

Ishida T, Iqbal PON, Anh HTL (2009) Modeling of chloride diffusivity coupled with non-linear binding capacity in sound and cracked concrete. Cem. Conc. Resea. 39: 913-923, DOI: https://doi.org/10.1016/j.cemconres.2009.07.014

Kim YY, Lee BJ, Kwon SJ (2014) Evaluation technique of chloride penetration using apparent diffusion coefficient and neural network algorithm. Adv. Mat. Sci. Eng. 2014: 1-13, DOI: http://dx.doi.org/10.1155/2014/647243.

Kong JS, Ababneh AN, Frangopol DM, Xi Y (2002) Reliability analysis of chloride penetration in saturated concrete. Prob. Eng. Mech. 17: 305-315, DOI: https://koreauniv.pure.elsevier.com/en/publications/reliability-analysis-of-chloride-penetration-in-saturated-concret

Lizarazo-Marriaga J, Claisse P (2011) Modelling chloride penetration in concrete using electrical voltage and current approaches. Materials Research 14(1): 31-38, DOI: https://www.scielo.br/scielo.php?script=sci_arttext&pid=S1516-14392011000100008&lng=en&tlng=en

Malheiro R, Meira G, Lima M, Perazzo N (2011) Influence of mortar rendering on chloride penetration into concrete structures. Cement & Concrete Composites 33: 233-239, DOI: https://www.sciencedirect.com/science/article/pii/S0958946510001897

Meira GR, Andrade MC, Padaratz IJ, Alonso MC, Borba JC (2006) Measurements and modelling of marine salt transportation and deposition in a tropical region in Brazil. Atmospheric Environment 40: 5596-5607, DOI: https://www.sciencedirect.com/science/article/pii/S1352231006004444

Michel A, Solgaard AOS, Pease BJ, Geiker MR, Stang H, Olesen JF (2013) Experimental investigation of the relation between damage at the concrete-steel interface and initiation of reinforcement corrosion

in plain and fibre reinforced concrete. Corrosion Science 77: 308-321, DOI: https://www.sciencedirect.com/science/article/pii/S0010938X13003867

Mien TV, Stitmannaithum B, Nawa T (2009) Simulation of chloride penetration into concrete structures subjected to both cyclic flexural loads and tidal effects. Comp. Conc. 6: 421-435, DOI: https://doi.org/10.12989/cac.2009.6.5.421.

Morga M, Marano GC (2015) Chloride penetration in circular concrete columns. International Journal of Concrete Structures and Materials 9: 173-183, DOI: https://link.springer.com/article/10.1007%2Fs40069-014-0095-y

Nguyer PT, Bastidas-Arteaga E, Amiri O, El Soueidy CP (2017) An efficient chloride ingress model for long-term lifetime assessment of reinforcement concrete structures under realistic climate and exposure conditions. International Journal of Concrete Structures and Materials 11(2): 199-213, DOI: https://link.springer.com/article/10.1007/s40069-017-0185-8

Nogueira CG, Leonel ED, Coda HB (2012) Probabilistic failure modelling of reinforced concrete structures subjected to chloride penetration. International Journal of Advanced Structural Engineering 4: 10-23, DOI: https://link.springer.com/article/10.1186/2008-6695-4-10

Oliveira HL, Chateauneuf A, Leonel ED (2018) Probabilistic mechanical modelling of concrete creep based on the boundary element method. Advances in Structural Engineering 00(0): 1-12, DOI: https://journals.sagepub.com/doi/abs/10.1177/1369433218788088

Ortega NF, Robles SI (2016) Assessment of residual life of concrete structures affected by reinforcement corrosion. HBRC Journal 12: 114-122, DOI: https://www.sciencedirect.com/science/article/pii/S168740481400090X

Pang L, Li Q (2016) Service life prediction of RC structures in marine environment using long term chloride ingress data: Comparison between exposure trials and real structure surveys. Construction and Building Materials 113: 979-987, DOI: https://www.sciencedirect.com/science/article/pii/S0950061816304603

Park S, Choi Y (2012) Influence of curing-form material on the chloride penetration of off-shore concrete. International Journal of Concrete Structures and Materials 6: 251-256, DOI: https://link.springer.com/article/10.1007/s40069-012-0026-8

Pellizzer GP (2015) Mechanical and probabilistic analysis of reinforcement corrosion of reinforced concrete structures subjected to chlorides penetration. Mater Dissertation, School of Engineering of São Carlos, University of São Paulo, Brazil.

Pellizzer GP, Leonel ED (2015) Avaliação da integridade mecânica de estruturas em concreto armado submetidas à corrosão de armaduras: abordagem via método dos elementos finitos, mecânica do dano e lei de Fick. In: Proceedings of the XXXVI Latin-American Congress on Computational Methods in Engineering, CILAMCE 2015, 22-25 November 2015, Rio de Janeiro, Brazil.

Pellizzer GP, Leonel ED, Nogueira CG (2015) Influence of reinforcement's corrosion into hyperstatic reinforced concrete beams: a probabilistic failure scenarios analysis. Ibracon Structures and Materials Journal 8(4): 479-490, DOI: https://www.scielo.br/scielo.php?script=sci_arttext&pid=S1983-41952015000400479&lng=en&tlng=en

Pellizzer GP, Leonel ED, Nogueira CG (2018) Numerical approach about the effect of the corrosion on the mechanical capacity of the reinforced concrete beams considering material nonlinear models. Ibracon Structures and Materials Journal 11(7): 26-51, DOI: https://www.scielo.br/scielo.php?script=sci_arttext&pid=S1983-41952018000100026

Rahimi A, Gehlen C (2018) Semi-probabilistic approach to the service life design of reinforced concrete structures under chloride attack. Beton- und Stahlbetonbau 113: 13-21, DOI: 10.1002/best.201700062

Rosenblatt M (1952) Remarks on a multivariate transformation. The Annals of Mathematical Statistics 23: 470-472.

Silva CA, Guimarães ATC (2014) Evaluation of the diffusion model considering the variation in time of the chloride content of the concrete surface. Matéria 19: 81–93, DOI: https://www.scielo.br/scielo.php?pid=S1517-70762014000200081&script=sci_abstract

Stewart MG, Mullard JA (2007) Spatial time-dependent reliability analysis of corrosion damage and the timing of first repair for RC structures. Engineering Structures 29: 1457-1464, DOI: https://www.sciencedirect.com/science/article/pii/S0141029606003798

Sun YM, Liang MT, Chang TP (2012) Time/depth dependent diffusion and chemical reaction model of chloride transportation in concrete. App. Math. Mod. 36: 1114-1122, DOI: https://doi.org/10.1016/j.apm.2011.07.053.

Suo Q, Stewart MG (2009) Corrosion cracking prediction updating of deteriorating RC structures using inspection information. Reliability Engineering and System Safety 94: 1340-1348, DOI: https://www.sciencedirect.com/science/article/pii/S0951832009000556

Wang Q, Sun W, Guo L, Gu C, Zong J (2018) Modeling chloride diffusion coefficient of steel fiber reinforced concrete under bending load. Advances in Civil Engineering 2018: 1-6, DOI: https://www.hindawi.com/journals/ace/2018/3789214/

Wolfram Mathematica (2017) Version 11 Student Edition, Wolfram Research, Inc.

Xie Y, Guan K, Zhan L, Wang Q (2016) Mechanical behavior and chloride penetration of precracked reinforced concrete beams with externally bonded CFRP exposed to marine environment. International Journal of Polymer Science 2016: 1-8, DOI: https://www.hindawi.com/journals/ijps/2016/1790585/

Yuan C, Li Y, Chen X, Wang W (2015) Effect of reinforced concrete cracking on chloride ion penetration. MATEC Web of Conference 22: 1-8, DOI: https://www.matec-conferences.org/articles/matecconf/abs/2015/03/matecconf_iceta2015_04026/matecconf_iceta2015_04026.html

Zacchei E, Molina JL (2018) Shape optimization of double-arch dams by using parameters obtained through Bayesian estimators. Iranian Journal of Science and Technology, Transactions of Civil Engineering 2018: 1-14, DOI: https://link.springer.com/article/10.1007/s40996-018-0223-z

Zacchei E, Nogueira CG (2019) Chloride diffusion assessment in RC structures considering the stress-strain sate effects and crack width influences. Construction and Building Materials 201: 100-109, DOI: https://www.sciencedirect.com/science/article/pii/S0950061818331544

Zhang R, Castel A, François R (2010) Concrete cover cracking with reinforcement corrosion of RC beam during chloride-induced corrosion process. Cement and Concrete Research 40: 415-425, DOI: https://www.sciencedirect.com/science/article/pii/S0008884609002798

Zhang SF, Lu CH, Liu RG (2011) Experimental determination of chloride penetration in cracked concrete beams. Procedia Engineering 24: 380-384, DOI: https://www.sciencedirect.com/science/article/pii/S1877705811055135

Zhang X, Li M, Tang L, Memon SA, Ma G, Xing F, Sun H (2017) Corrosion induced stress field and cracking time of reinforced concrete with initial defects: analytical modeling and experimental

investigation. Corrosion Science 120: 158-170, DOI: https://www.sciencedirect.com/science/article/pii/S0010938X17300859

Zofia S, Adam Z (2013) Theoretical model and experimental tests on chloride diffusion and migration processes in concrete. Proc. Eng. 57: 1121-1130, DOI: https://doi.org/10.1016/j.proeng.2013.04.141

Gmail

Enrico Zacchei <enricozacchei@gmail.com>

KSCE-D-20-01242 - KSCE: Submission Confirmation for Probabilistic-based analysis of time corrosion initiation in RC structures considering the fluctuation of chloride ions influenced by external actions: a comparison between analytical and numerical 2D and 3D approaches

Editorial Office <em@editorialmanager.com> 12 luglio 2020 10:17
Rispondi a: Editorial Office <ejournal@ksce.or.kr>
A: Enrico Zacchei <enricozacchei@gmail.com>

Dear Dr. Zacchei,

Your submission entitled "Probabilistic-based analysis of time corrosion initiation in RC structures considering the fluctuation of chloride ions influenced by external actions: a comparison between analytical and numerical 2D and 3D approaches" has been received by journal KSCE Journal of Civil Engineering

The submission id is: KSCE-D-20-01242
Please refer to this number in any future correspondence.

You will be able to check on the progress of your paper by logging on to Editorial Manager as an author. The URL is https://www.editorialmanager.com/ksce/.

Your manuscript will be given a reference number once an Editor has been assigned.

Thank you for submitting your work to this journal.

Kind regards,

Editorial Office
KSCE Journal of Civil Engineering

As a result of the significant disruption that is being caused by the COVID-19 pandemic we are very aware that many researchers will have difficulty in meeting the timelines associated with our peer review process during normal times. Please do let us know if you need additional time. Our systems will continue to remind you of the original timelines but we intend to be highly flexible at this time.

This letter contains confidential information, is for your own use, and should not be forwarded to third parties.

Recipients of this email are registered users within the Editorial Manager database for this journal. We will keep your information on file to use in the process of submitting, evaluating and publishing a manuscript. For more information on how we use your personal details please see our privacy policy at https://www.springernature.com/production-privacy-policy. If you no longer wish to receive messages from this journal or you have questions regarding database management, please contact the Publication Office at the link below.

In compliance with data protection regulations, you may request that we remove your personal registration details at any time. (Use the following URL: https://www.editorialmanager.com/ksce/login.asp?a=r). Please contact the publication office if you have any questions.